TU Delft

Delft University of Technology

Developing Solid Oxide F uel Cell Based Power Plant For Water Treatment Plants Experimental and System Modelling Studies

Saadabadi, S.A.

DOI
10.4233/uuid:780a2f7f-b96a-4a55-928c-4ea8cc8fdfe5

Publication date
2021

Document Version
Final published version

Citation (APA)
Saadabadi, S. A. (2021). *Developing Solid Oxide F uel Cell Based Power Plant For Water Treatment Plants: Experimental and System Modelling Studies*. [Dissertation (TU Delft), Delft University of Technology]. https://doi.org/10.4233/uuid:780a2f7f-b96a-4a55-928c-4ea8cc8fdfe5

Important note
To cite this publication, please use the final published version (if applicable).
Please check the document version above.

Copyright
Other than for strictly personal use, it is not permitted to download, forward or distribute the text or part of it, without the consent of the author(s) and/or copyright holder(s), unless the work is under an open content license such as Creative Commons.

Takedown policy
Please contact us and provide details if you believe this document breaches copyrights.
We will remove access to the work immediately and investigate your claim.

This work is downloaded from Delft University of Technology.
For technical reasons the number of authors shown on this cover page is limited to a maximum of 10.

Developing Solid Oxide Fuel Cell Based Power Plant For Water Treatment Plants

Experimental and System Modelling Studies

Seyed Ali Saadabadi

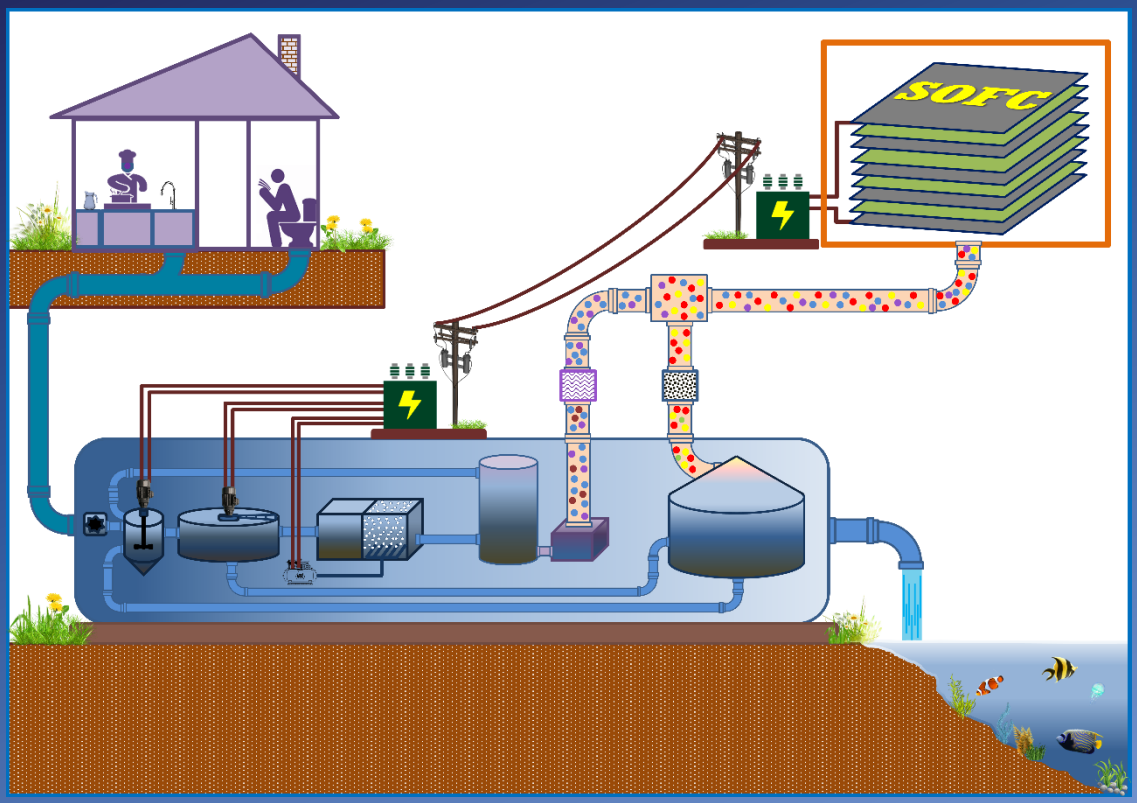

Developing Solid Oxide Fuel Cell Based Power Plants For Water Treatment Plants

Experimental and System Modelling Studies

Seyed Ali Saadabadi

Department of Process & Energy
Delft University of Technology
The Netherlands

Developing Solid Oxide Fuel Cell Based Power Plants For Water Treatment Plants

Experimental and System Modelling Studies

Proefschrift

ter verkrijging van de graad van doctor
aan de Technische Universiteit Delft,
op gezag van de Rector Magnificus Prof. dr. ir. T.H.J.J. van der Hagen
voorzitter van het College voor Promoties,
in het openbaar te verdedigen op woensdag 31 maart 2021 om 10.00 uur

door
Seyed Ali SAADABADI

Master of Science in Mechanical Engineering
Islamic Azad University of Tehran, Iran
geboren te Neyshabour, Iran.

Dit proefschrift is goedgekeurd door de promotoren:

Samenstelling promotiecommissie:

Rector Magnificus	voorzitter
Prof. dr. ir. P. V. Aravind	Technische Universiteit Delft, promotor
Prof. dr. ir. B. J. Boersma	Technische Universiteit Delft, promotor
Onafhankelijke leden:	
Prof. dr. A.J.M. van Wijk	Technische Universiteit Delft (The Netherlands)
Prof. dr. ir. M. van der Kreuk	Technische Universiteit Delft (The Netherlands)
Prof. dr. ir. M. Santarelli	Polytechnic University of Turin (Italy)
Prof. dr. ir. M. A. van den Broek	University of Groningen (The Netherlands)
Overig lid:	
Dr. ir. R.E.F. Lindeboom	Technische Universiteit Delft (The Netherlands)

Printed by: Ipskamp printing

Cover design by: S.Ali Saadabadi

Copyright © 2020 by S. Ali. Saadabadi

ISBN: 978-94-6421-290-7

An electronic version of this dissertation is available at

http://repository.tudelft.nl/.

To my dear Family

Summary

Fossil fuels are currently the primary source for electrical power generation, which subsequently increases the rate of greenhouse gas (CO_2, CH_4) emission. It has been agreed at the Climate Change Conference 2015 in Paris (COP21) to reduce greenhouse gas emissions in order to limit the global temperature increase to less than 2°C compared to pre-industrial era temperature. The GHG (Greenhouse Gas) effect is mostly attributed to methane and carbon dioxide emissions into the atmosphere. In order to reduce the use of fossil fuels and their negative impact on the environment, renewable energy resources have been receiving much attention in recent years. Sanitation systems, centralized Wastewater Treatment Plants (WWTPs) and organic waste digesters give an ample opportunity for resource recovery to produce biogas that contains mainly methane and carbon dioxide. The low conversion efficiency of conventional energy conversion devices like internal combustion engines and turbines prevents biogas from reaching its full potential as over 50% of chemical energy is dissipated.

Wastewater treatment is a developed technology from human health and environmental-friendliness points of view. However, from energy aspects, it is still an energy-intensive process step. Wastewaters might contain significant amounts of organic matter and nutrient (nitrogen and phosphorus) compounds. The chemical energy in domestic wastewater is approximately 3.8 $kWh.m^{-3}$ based on theoretical Chemical Oxygen Demand (COD) of 1 kg m^{-3}. At wastewater treatment plants (WWTPs), collecting and treating wastewater streams need a considerable amount of electricity (0.5 kWh m^{-3}) to reach an acceptable quality of discharge requirements. In a conventional WWTP, nitrogen is removed through nitrification, and biodegradable organic matter is converted to methane in anaerobic digestion.

The energy demand at WWTPs could be partially offset by an efficient recovery of nutrient and organic matter from the wastewater stream. Biogas production is an important technology widely applied in Europe. Biogas can be converted to energy through thermal conversion with combined heat and power (CHP) plants. However, the electrical efficiency of the system is limited to 25-30%. In parallel, nitrogen can be removed from wastewater and converted and stored in the form

of an ammonia-water mixture from ammonium-rich streams after anaerobic digestion.

Solid oxide fuel cell (SOFC) is an energy conversion device that directly converts chemical energy into electrical energy based on electrochemical reactions. SOFC can operate with different types of fuels, especially unconventional or renewable fuels. The efficiency of SOFC is higher compared to conventional combustion-based processes. Therefore, the sustainability of WWTPs can be improved first by a recovery of nutrient and organic material from the wastewater stream and then, replacing the inefficient combustion process with an efficient high-temperature electrochemical reaction in SOFC. Due to the modularity of SOFC, this can be used for a wide range of biogas production capacities at WWTPs. However, the development of SOFC is still facing many challenges, and a better understanding of the constraints is needed.

This dissertation aims to provide design concepts and thermodynamic system analysis for the biogas-ammonia fuelled SOFC system at wastewater treatment plants with a focus on achieving a safe operating condition and high electrical efficiencies. Thereupon, extended experimental studies have been conducted in this work on biogas dry and combined reforming. Moreover, the influence of mixing ammonia-water to biogas in SOFC has been experimentally investigated. After indicating the safe operating condition of biogas-ammonia fuelled SOFC, system modelling studies have been carried out in order to design an efficient conceptual biogas-ammonia fuelled SOFC system at wastewater treatment plants. Additionally, a complete biogas SOFC pilot system consists of a gas cleaning unit and an external gas processing system has been designed. The dissertation comprises of three main parts:

Experimental study of the biogas-ammonia fuelled SOFCs:

Chapter 3 investigates the internal dry reforming (IDR) of biogas on a commercial Ni-GDC cell, which focuses on the effect of CO_2 concentration, current density (CD), the operating temperature on cell performance. The best performance is identified based on maximum power production and minimum cell degradation. Moreover, methane reforming is studied at different current densities and operating temperatures.

Chapter 4 presents the obtained experimental data for aqueous ammonia fuelled SOFC in a single cell level. The cell performance is studied by using an ammonia-water mixture with 14 mol.% ammonia. These results are used to model an ammonia-SOFC system in Cycle Tempo. It is assumed that aqueous ammonia is produced through struvite precipitation at the WWTP.

Chapter 5 gives a further evaluation of the performance of SOFCs fuelled with biogas and aqueous ammonia mixture. First biogas internal combined reforming is investigated. The minimum required H_2O/CH_4 to prevent carbon deposition on

the anode surface is determined at operating temperature of 850°C. Moreover, methane conversion is studied at different operating current densities.

System modelling study of the biogas-ammonia fuelled SOFCs:

Cycle Tempo is a software developed at the Delft University of Technology to evaluate power cycles thermodynamically. In chapter 4, the aqueous ammonia fuelled SOFC system is developed in such a way that required heat for the struvite decomposition is partially supplied by the SOFC. The net energy and exergy efficiencies is investigated. This system is optimized by integrating a heat pump assisted distillation tower to increase the ammonia concentration to 90 mol.%. The last section of chapter 5, presents a Cycle-Tempo biogas-ammonia fuelled SOFC system based on internal methane reforming. The safe operating condition is determined based on the experimental results obtained with the single-cell experiments. The net electrical system efficiency of biogas-ammonia fuelled SOFC is determined.

Design a conceptual SOFC pilot plant fuelled with recovered methane

Chapter 6 presents a conceptual design of a 4-kW biogas SOFC system (steady state thermodynamic off-design model) consists of a gas cleaning unit (GCU) with an external gas processing unit. Traces of H_2S (10 ppmv) have been found in the recovered methane from groundwater. First, A series of experiments is conducted to clean the gas with iron oxide (Fe_2O_3), which is one of the by-products of the groundwater treatment plant and the H_2S adsorption capacity of iron oxide is determined. Subsequently, the influence of steam concentration on the SOFC performance is investigated in a single cell test fuelled with the recovered methane gas. Then, a modelling study is conducted in order to design an SOFC system based on the most suitable fuel processing method. The net electrical efficiency of the recovered methane fuelled (50% methane) system with a catalytic partial oxidation gas processing unit (CPOX) is studied. Effect of adding a CO_2 recovery process on the system efficiency is investigated.

The conclusions and recommendations are described, and future work is proposed in Chapter 7. Experimental studies have shown the feasibility of using the dry reforming technique to reform methane in the biogas-SOFC system. However, some extra CO_2 is required for obtaining a safe operating condition. The current density plays a vital role in suppressing carbon deposition. However, further experimental studies in operating SOFC stack is required. System modelling studies for both ammonia and biogas-ammonia mixture fuels illustrate that these are promising fuels for SOFC systems, whereas the electrical system efficiencies are as high as 50% for either of them.

Samenvatting

Fossiele brandstoffen zijn momenteel de belangrijkste bron van elektriciteitsopwekking, waardoor de uitstoot van broeikasgassen (CO_2, CH_4) toeneemt. Op de Climate Change Conference 2015 in Parijs (COP21) is afgesproken om de uitstoot van broeikasgassen te verminderen om de wereldwijde temperatuurstijging te beperken tot minder dan 2 °C in vergelijking met de temperatuur uit het pre-industriële tijdperk. Het broeikasgaseffect wordt voornamelijk toegeschreven aan de uitstoot van methaan en kooldioxide in de atmosfeer. Om het gebruik van fossiele brandstoffen en hun negatieve impact op het milieu te verminderen, hebben hernieuwbare energiebronnen de afgelopen jaren veel aandacht gekregen. Sanitaire systemen, gecentraliseerde afvalwaterzuiveringsinstallaties (Wastewater Treatment Plants, WWTPs) en vergisters voor organisch afval bieden volop gelegenheid om grondstoffen terug te winnen voor de productie van biogas, dat voornamelijk methaan en kooldioxide bevat. De lage efficiëntie van conventionele energieconversieapparatuur, zoals verbrandingsmotoren en turbines, verhindert dat biogas zijn volledige potentieel bereikt, aangezien meer dan 50% van de chemische energie wordt gedissipeerd.

Afvalwaterbehandeling is vanuit het oogpunt van menselijke gezondheid en milieuvriendelijkheid een uitontwikkelde technologie. Energetisch gezien is het echter nog steeds een energie-intensieve processtap. Afvalwater kan aanzienlijke hoeveelheden organisch materiaal en nutriënten (stikstof en fosfor) bevatten. De chemische energie in huishoudelijk afvalwater is ongeveer 3,8 $kWh.m^{-3}$ gebaseerd op een theoretisch chemisch zuurstofverbruik (Chemical Oxygen Demand, COD) van 1 $kg.m^{-3}$. Bij afvalwaterzuiveringsinstallaties (WWTPs) is voor het verzamelen en behandelen van afvalwaterstromen een aanzienlijke hoeveelheid elektriciteit nodig (0,5 $kWh.m^{-3}$) om een aanvaardbare kwaliteit voor lozingseisen te bereiken. In een conventionele WWTPs wordt stikstof verwijderd door nitrificatie en wordt biologisch afbreekbare organische stof omgezet in methaan middels anaerobe vergisting.

De energievraag op WWTPs kan gedeeltelijk worden opgevangen door een efficiënte terugwinning van nutriënten en organisch materiaal uit de afvalwaterstroom. Biogasproductie is een belangrijke technologie die op grote schaal wordt toegepast in Europa. Biogas kan worden omgezet in energie door thermische conversie met warmtekrachtkoppeling (combined heat and power, CHP). Het elektrische rendement van het systeem is echter beperkt tot 25-30%.

Tegelijkertijd kan stikstof uit het afvalwater worden verwijderd en na anaerobe vergisting worden omgezet en opgeslagen in de vorm van een ammoniak-watermengsel uit ammoniumrijke stromen.

De vaste-oxide brandstofcel (Solid oxide fuel cell, SOFC) is een technologie die chemische energie direct omzet in elektrische energie op basis van elektrochemische reacties. SOFC kan werken met verschillende soorten brandstoffen, in het bijzonder onconventionele of hernieuwbare brandstoffen. De efficiëntie van SOFC is hoger in vergelijking met conventionele op verbranding gebaseerde processen. Daarom kan de duurzaamheid van WWTPs worden verbeterd door eerst nutriënten en organisch materiaal uit de afvalwaterstroom terug te winnen en vervolgens het inefficiënte verbrandingsproces te vervangen door een efficiënte elektrochemische reactie op hoge temperatuur in SOFC. Door de modulariteit van SOFC kan deze worden ingezet voor een breed scala aan biogasproductiecapaciteiten op WWTPs. De ontwikkeling van de SOFC staat echter nog voor veel uitdagingen, en een beter begrip van de beperkingen is nodig.

Dit proefschrift heeft tot doel ontwerpconcepten en thermodynamische systeemanalyse te bieden voor het biobrandstof-SOFC-systeem in afvalwaterzuiveringsinstallaties, met een focus op het bereiken van een veilige bedrijfsomstandigheid en hoge elektrische efficiëntie. Vervolgens zijn in dit werk uitgebreide experimentele studies uitgevoerd naar droge en gecombineerde reformering van biogas. Bovendien is de invloed van het mengen van waterige ammoniak tot biogas in SOFC experimenteel onderzocht. Na het aangeven van de veilige bedrijfstoestand van met biogas-ammoniak gestookte SOFC, zijn systeemmodelleringsstudies uitgevoerd om een efficiënt conceptueel biobrandstof-SOFC-systeem te ontwerpen bij afvalwaterzuiveringsinstallaties. Daarnaast bestaat een compleet biogas SOFC pilot-systeem uit een gasreinigingsunit en is een extern gasverwerkingssysteem ontworpen. Het proefschrift bestaat uit drie delen:

Experimentele studie van de op biogas-ammoniak gevoede SOFC's:

Hoofdstuk 3 onderzoekt de interne droge reforming (internal dry reforming, IDR) van biogas op een commerciële Ni-GDC-cel, waarbij de nadruk ligt op het effect van CO_2-concentratie, stroomdichtheid (current density, CD), de bedrijfstemperatuur op celprestaties. De beste prestatie wordt bepaald op basis van maximale stroomproductie en minimale celafbraak. Bovendien wordt methaanreforming bestudeerd bij verschillende stroomdichtheden en bedrijfstemperaturen.

Hoofdstuk 4 presenteert de verkregen experimentele gegevens voor waterige ammoniakgevoede SOFC in een enkele cel. De celprestaties worden bestudeerd door een ammoniak-watermengsel met 14 mol.% ammoniak te gebruiken. Deze resultaten worden gebruikt om een ammoniak-SOFC-systeem te modelleren in Cycle Tempo. Aangenomen wordt dat waterige ammoniak wordt geproduceerd door struvietprecipitatie op de WWTP.Hoofdstuk 5 geeft een verdere evaluatie

van de prestaties van SOFC's die worden gevoed met biogas en een waterig ammoniakmengsel. Eest is interne gecombineerde reformering van biogas wordt onderzocht. De minimaal vereiste H_2O/CH_4 om koolstofafzetting op het anode-oppervlak te voorkomen, wordt bepaald bij een bedrijfstemperatuur van 850 °C. Bovendien wordt methaanconversie bestudeerd bij verschillende bedrijfsstroomdichtheden.

Systeemmodelleringstudie van de op biogas-ammoniak gestookte SOFC's:

Cycle-Tempo is software ontwikkeld aan de Technische Universiteit Delft om stroomcycli thermodynamisch te evalueren. In hoofdstuk 4 is het waterige ammoniakgestookte SOFC-systeem zo ontwikkeld dat de benodigde warmte voor de struvietafbraak gedeeltelijk wordt geleverd door de SOFC. De netto energie- en exergie-efficiëntie wordt onderzocht. Dit systeem is geoptimaliseerd door de integratie van een door een warmtepomp ondersteunde destillatietoren om de ammoniakconcentratie te verhogen tot 90 mol.%. Het laatste deel van hoofdstuk 5 presenteert een Cycle-Tempo biogas-ammoniak aangedreven SOFC-systeem op basis van interne methaanreforming (internal methane reforming). De veilige bedrijfsomstandigheden worden bepaald op basis van de experimentele resultaten die zijn verkregen met experimenten op een enkele cel. Het netto rendement van het elektrische.

Contents

List of Figures

List of Tables

Nomenclature

Abbreviations:

AD	Anaerobic Digestion
AGR	Anode Gas Recirculation
APU	Auxiliary Power Unit
ASC	Anode Supported Cell
ASR	Area Specific Resistance
ATR	Autothermal reaction Reformer
BoP	Balance of Plant
CD	Current Density
CEM	Controlled Evaporation and Mixing
CFD	Computational Fluid Dynamics
CHP	Combined Heat and Power
CCHP	Combined cooling, heating and power
CNT	Carbon Nanotube
COD	Chemical Oxygen Demand
CPOX	Catalytic Partial Oxidation
CSTR	Continuous Stirred Tank Reactor
DIR	Direct Internal Reforming
DO	Dissolved Oxygen
DTGA	Derivative Thermogravimetric Analysis
DWTP	Drinking water treatment plant
EIS	Electrochemical Impedance Spectroscopy
ESC	Electrolyte Supported Cell
GC	Gas Chromatography
GDC	Gadolinium Doped Ceria
GHG	Greenhouse Gas
GT	Gas Turbine
hrs	Hours
IC	Internal Combustion
IDR	Internal Dry Reforming
LHV	Lower Heating Value
LSM	Lanthanum Strontium Manganite
MAP	Magnesium Ammonium Phosphate
MBR	Membrane Bioreactor
MCFC	Molten-Carbonate Fuel Cell
MFC	Mass Flow Meter
MHP	Magnesium Hydrogen Phosphate

ms	milliseconds
MSR	Methane Steam Reforming
OCP	Open circuit potential
OCV	Open Circuit Voltage
P	Partial pressure
POX	Partial Oxidation
ppm	Parts Per Million
RWGS	Reverse Water-Gas Shift
SC	Steam to Carbon ratio
ScSZ	Scandia Stabilized Zirconia
SOFC	Solid Oxide Fuel Cell
TA	Total Nitrogen
TAN	Total Ammonia Nitrogen
TGA	Thermogravimetric Analysis
TOC	Theoretical open circuit
TPB	Triple Phase Boundary
UASB	Up-flow Anaerobic Sludge Blanket
UBF	Up-flow blanket filter
V	Potential
VOC	volatile organic compound
VS	Volatile Solid
WAS	Waste Activated Sludge
WGS	Water-Gas Shift
WWTP	Wastewater Treatment Plant
YSZ	Yttria-Stabilized Zirconia

Greek letters:

σ	Standard deviation
λ	Excess air value
γ	Mole fraction
Ω	Ohmic resistance
η	Ohmic resistance
ρ	Density (kg m^{-3})
U_f	Fuel utilization factor

Roman Symbols:

A	Area (m^2)
c_p	Heat capacity (J mol^{-1} K^{-1})
E	Potential (V)
F	Faraday constant (C mol^{-1})
ΔG^0	Change of standard Gibbs free energy (kJ mol^{-1})
ΔH^0	Enthalpy change, (kJ mol^{-1})
I	Current (A)
n	Number of electrons participating in the electrochemical reactions (-)
P	Power (W)

Po_2	Equilibrium oxygen partial pressure
R	Universal gas constant (J/mol.K)
T	Temperature (°C)
U_f	fuel utilization (%)
V_{cell}	Cell voltage (V)
V_{Nernst}	Nernst voltage (V)
X_{CH4}	Methane conversion (%)
Y_i	mole fraction of gas species i (-)

Subscripts:

act	Activation
ano	Anode
act	Activation polarization
cat	Cathode
conc	Concentration resistance
e	Electric power
eff	Efficiency
in	Inlet
ohmic	Ohmic resistance
out	Outlet
rev	Reversible
s	Solid

Chapter 1
Introduction

This chapter presents the aim of this dissertation within the scope of the biogas-ammonia fed Solid Oxide Fuel Cell system. The specific research questions and the outline of the dissertation are presented.

1.1 Overview

Fossil fuels are currently the primary source for electrical power generation, which subsequently increases the rate of greenhouse gas (GHG) emission including, carbon dioxide (CO_2) and methane (CH_4) [1]. It has been agreed at the Climate Change Conference 2015 in Paris (COP21) to reduce greenhouse gas emissions and limit the global temperature increase to less than 2°C compared to pre-industrial era temperature [2]. In order to reduce the use of fossil fuels and their negative impact on the environment, using fossil fuels should be gradually replaced by renewable fuels. Renewable energy resources have been receiving much attention in recent years, especially from organic and human wastes [3].

Wastewater treatment is crucial due to sanitation requirements which helps keeping the preserving water resources clean. Major wastewater contaminants include phosphates, nitrogen compounds, and organic matter. These contaminants should be removed in sanitation systems in centralized Wastewater Treatment Plants (WWTPs) [4].

Major issues in WWTPs are associated with the waste production (concentrated sludge in aerobic WWTP), energy consumption, GHG emissions (CH_4 and CO_2), and NOx emission. Conventional aerobic digestion is the most typically used nitrogen removal process. The aerobic wastewater treatment process requires electrical energy for aeration with a low capital cost. However, the operation costs are high due to the energy demand for pumping oxygen through wastewater [5]. The energy required for this process might be compensated by the chemical energy contained in the organic matter of the wastewater [6]. However, the WWTP needs to be equipped by additional facilities.

Anaerobic Digestion (AD) of waste activated sludge (after the primary treatment) is a complementary technique in WWTPs in order to break down biodegradable material in the absence of oxygen. Biogas (CH_4-CO_2 gas mixture) is produced in the AD reactor, and separated digested solids can be utilized in agriculture as fertilizer (Fig. 1-1). AD has been known for a long time [7]. The earliest reporting of biogas use is for heating water in Persia (16th century). The first modern digestion plant was developed in India in 1859. The technology was further developed and is currently being used to generate electricity in the MW range in industrialized countries like Germany [7].

Produced biogas is typically used in conventional energy conversion devices such as gas boiler, gas turbine or internal combustion (IC) engine technologies used in combined heat and power (CHP) systems. Exergy analyses of these conventional combustion systems has shown that the total efficiency is generally below 50%, because the low concentration of methane in the outlet gas [8, 9]. Using electrochemical conversion devices like fuel cells could help to make the system

more efficient and sustainable since high efficiency electrical power and high temperature heat can be generated.

Fuel cells are energy conversion devices that can produce electrical power directly through the electrochemical reaction of fuels. Hydrogen is the primary fuel for fuel cells. Fuel cells are modular (scalable), which implies that cells can be stacked to produce power in various ranges for small house applications (500 W system), up to power plant size (few MW systems). Recently, proton-exchange membrane (PEM) fuel cells, operating at low temperature (80°C), are commercially used in the automotive industry fuelled with pure hydrogen.

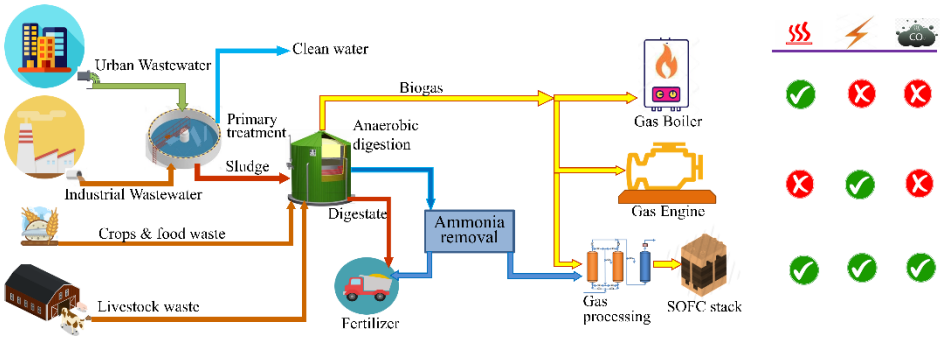

Figure 1-1: Biogas-ammonia production from WWTP and using in different energy conversion devices.

There are different types of Fuel Cells. The low-temperature fuel cells like PEM fuel cell can also be applied for power generation in WWTP but, produced biogas must be converted to pure hydrogen gas as a fuel, and extensive gas cleaning is essential, which leads to a costly system [10]. Other types of high-temperature fuel cells like Molten-Carbonate Fuel Cell (MCFC) can also be used [11], but the electrolyte is corrosive (lifetime issues), and an extra CO_2 flow is required for the cathode side, which is not always available [12, 13]. Solid oxide fuel cell (SOFC) is a type of high operating-temperature fuel cell which is more fuel flexible. SOFC seems a promising candidate for biogas fuelled fuel cell for stationary integrated power plants, and it is also an appropriate option for auxiliary power units (APU) in vehicles [14]. SOFCs are more fuel-flexible in comparison to IC engines and the low operating-temperature fuel cells. Latest developments in SOFC shows that this technology is mature enough to be integrated and developed as a commercializing full-scale SOFC system. For instance, natural gas-fuelled fuel cell is used as a reliable power supplier in the data centres in silicon valley, USA.

There are several advantages in replacing the IC gas engine with SOFCs in WWTPs. The efficiency of SOFCs is much higher than IC engines (especially for small system sizes) [15]. In SOFCs, carbon monoxide (CO) can also directly (electrochemically) reacts with oxygen and generates electricity. So, different types of fuels, such as renewable syngas fuel, biogas, ammonia, and conventional

hydrocarbon fuels like natural gas (after fuel processing) can be used in SOFCs. For instance, in WWTPs in addition to biogas, ammonium from wastewater can also be converted in the form of ammonia (after anaerobic digestion) and used as a fuel in SOFC (Fig. 1-1). Moreover, the presence of CO_2 is helpful for reforming the methane in biogas [16, 17].

Due to the high operating-temperature of SOFC stack, high-quality waste heat is available at the outlet of the stack. The operating temperature of SOFCs is in the range of 650°C to 900°C. In SOFC systems, the temperature of anode and cathode outlet flows are in the range of operating temperature. Generally, the heat is used in the pre-heating of anode and cathode inlet flows. In most cases of SOFC systems, there is still high-quality waste heat available to be used in a bottoming cycle. For instance, in WWTPs, this heat can be used in thermal pre-treatment of wastewater stream or an ammonia removal process, which decreases the energy demand of WWTPs.

Some obstacles should be tackled in developing SOFC stacks. Fuel cells are more expensive than conventional energy conversion devices due to the materials and the manufacturing process. But, in the last decades, developing new materials, new manufacturing methods and mass production of fuel cells brought down the general costs. Nevertheless, the knowledge of using SOFC in different systems is being developed for different fuels and various system operating conditions.

However, biogas conditioning is still challenging. Biogas conditioning includes the biogas cleaning and an appropriate biogas reforming. In order to prevent carbon deposition and nickel oxidation in the biogas-SOFC system, the operating conditions, including temperature, the current density, the amount, and the type of reforming agent should be precisely controlled for different cell materials. Moreover, mixing ammonia to biogas also might influence on biogas reforming, which makes it more complicated.

The system configuration also should be optimized to get maximum output power efficiency. The system efficiency can be improved by minimizing the exergy loss of the system, for instance, replacing the external fuel reformer by an internal reforming or designing an anode/cathode gas recirculation system for the SOFC system. A comprehensive review of potential and challenges in applying biogas-ammonia fuelled SOFC system is presented in chapter 2 of this dissertation.

Overall, integrating a SOFC system in WWTP can promote the self-sustainability of the plant by covering around 30% of the WWTP electrical consumption [18]. This can be improved further improved by optimizing the wastewater treatment processes [19]. This might help develop small-scale WWTPs in remote areas where the electricity grid is not available, which improves the sanitation and quality of life of people. In the large scale WWTPs, the SOFC system integration can reduce the carbon footprint of the sanitation system by providing power and

heat integration can help in reducing the waste remained after the treatment process.

1.2 Motivation and Objective of this Dissertation

Developing an SOFC-based power plant in waste/drinking water treatment plants is the focus of this dissertation. Produced biogas and recovered ammonia from wastewater treatment processes can be utilized in the SOFCs. Power generated in the SOFC system compensates some of the electrical demands of the plant. Additionally, the excess heat generated in the SOFC system can be used in the wastewater treatment processes. This helps to improve the sustainability of waste/drinking water treatment plants.

First, experimental studies are required to identify the safe operating conditions of biogas-ammonia fuelled SOFCs. In biogas-SOFC, there is an opportunity to reform methane and crack ammonia inside the SOFC due to the presence of nickel (as an active catalyst) in the anodes, and it has not been understood well. One of the advantages of internal reforming and cracking is that the waste heat from the electrochemical reactions (of H2 and CO) can drive highly endothermic reforming and cracking reactions. This leads to a decrease in the required cooling of the cell, which typically is achieved through a high cathode airflow. So, using the internal reforming method and ammonia cracking improve system efficiency. However, the risk of carbon deposition increases and the concentration of reforming agents should be carefully controlled. Specifically, in terms of internal methane reforming, this might cause thermal stress due to the highly endothermic reforming reactions and the exothermic electrochemical reactions. Therefore, the required amount of reforming agents should be determined precisely based on operating conditions like temperature and current density.

The cell material also can influence on internal reforming of fuel in SOFCs. Nickel-Gadolinium doped ceria (Ni-GDC) as an anode has advantages in comparison to commonly used Nickel-Yttria stabilized zirconia (Ni-YSZ) anodes [20]. For instance, Ni-GDC cell has better performance under methane dry reforming and higher tolerance levels of H_2S contamination due to a higher electronic conductivity and oxygen vacancies [21]. Some experimental and system modelling studies have been carried out to evaluate the biogas fuelled SOFC for different catalyst materials. However, operating SOFC under internal biogas reforming conditions has required further experimental investigations, especially for Ni-GDC anode. Moreover, to the best knowledge of the author, the influence of ammonia cracking on biogas internal reforming is not investigated, neither experimentally nor in system modelling.

Then, after identifying the performance of SOFC (single-cell level) with biogas-ammonia (internal reforming/cracking in the Ni-GDC cell), system modelling studies are required. The system modelling studies should be carried out to

determine the system configuration for biogas, ammonia, and mixture fuels. System modelling study used to design an integrated SOFC system, including the fuel processing and integration to the fuel production units in waste/drinking water treatment plants. Moreover, system modelling assesses system performance, including energy and exergy efficiencies. Exergy analysis of the integrated system is applied to optimize the system configuration and maximize the system's energy efficiency in waste/drinking water treatment plants. The exergy analysis determines the exergy destruction in different SOFC system components, including the SOFC stack.

Based on the motivation and concepts presented in the previous sections, the main research targets for this work have been listed below:

- To experimentally investigate biogas internal dry reforming and determining the extra amount of CO_2 required to prevent carbon deposition in Ni-GDC electrolyte supported single cell.
- To experimentally evaluate the internal ammonia cracking in aqueous ammonia fuelled SOFC and investigate the influence of steam concentration (in aqueous ammonia) on the cell performance. additionally, to design an ammonia SOFC system integrated with an ammonia removal (precipitation) process.
- Experimental study of biogas internal combined (dry and steam) reforming is carried out to identify the safe operating condition in terms of operating temperature and current density. Additionally, to investigate the influence of ammonia cracking on methane reforming.
- Conceptual design and thermodynamic assessment of a biogas SOFC system in an existing drinking water treatment plant (using steady-state models), including design of a low-temperature gas cleaning unit, optimized a biogas processing method and CO_2 capture unit.

1.3 Thesis Scope Outline

Experimental studies are necessary and very important for the development of the SOFC systems. A better understanding of the biogas internal reforming is essential to improve the SOFC system performance in terms of safe operation and maximizing power generation. Moreover, the influence of ammonia cracking on methane reforming has not been investigated, which is essential for the design of biogas-ammonia fuelled SOFC systems. Modelling work can give an overall preview of the system performance, and gives suggestions to the system design, such as identifying a proper reforming method based on the type of fuel. The structure of this dissertation is illustrated in Fig. 1-2.

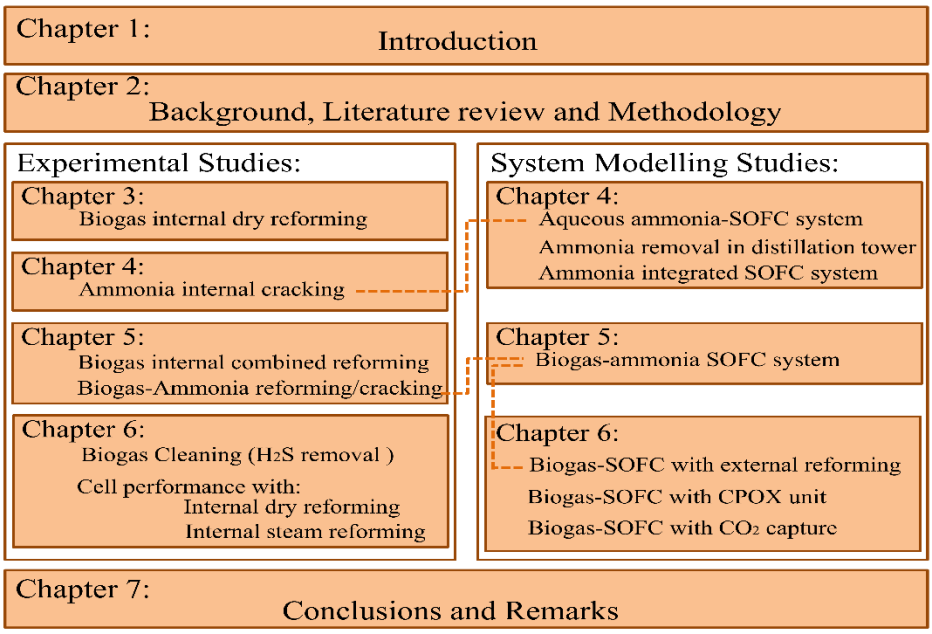

Figure 1-2: Overview of the structure of this dissertation.

Chapter 2 presents the background, technologies evolved in SOFCs and a literature review associated with biogas internal reforming in experimental research and system modelling.

Chapter 3 investigates the operation of biogas Fuelled SOFC under internal dry reforming conditions to identify the precise amount of extra CO_2 required for methane (CH_4) reforming based on operating conditions and prevent carbon deposition on the anode surface of a Ni-GDC anode supported cell.

Chapter 4 identifies the feasibility of the integration of ammonia recovery (precipitation) process with an SOFC system and operates fuel cell with aqueous ammonia. The SOFC performance is experimentally evaluated with ammonia-water mixture with different ammonia concentrations (14 to 90 mol.%). The system modelling study is carried out to assess the exergy and energy efficiencies of the system. With this system, the heat demand of struvite decomposition is supplied by the SOFC stack and an afterburner.

Chapter 5 gives a further evaluation of the performance of SOFCs fuelled with biogas-ammonia mixture. First, the biogas combined (dry and steam) reforming is studied in order to identify the amount of steam required to prevent carbon deposition. Subsequently, the influence of ammonia cracking on methane reforming and the impact of this on the cell performance is evaluated. Finally, a biogas-ammonia fed SOFC system is developed in order to assess the system energy and exergy efficiencies.

Chapter 6 presents a conceptual design of a biogas-SOFC system to be replaced the existing 500 kW gas engine at a groundwater treatment plant in Spannenburg, the Netherlands. A gas cleaning unit is designed to remove the H_2S traces in CH_4-rich recovered gas. Different types of gas processing units are evaluated to maximize the energy efficiency of this integrated system. Moreover, the impact of adding a CO_2 capture unit on the system efficiency is investigated for this system.

The conclusions and recommendations are described, and future works are proposed in Chapter 7 of this dissertation.

Chapter 2

Biogas-ammonia fuelled Solid Oxide Fuel Cell: Potential and constraints

This chapter presents a literature review on the process of power generation by biogas-ammonia fuelled SOFC in the wastewater treatment plants, discusses operational issues and assesses the efficiency of integrated anaerobic digestion-SOFC systems. First, the theory and working principle of SOFC and anaerobic digestion are explained. Subsequently, biogas production from different waste sources is reviewed, and the impact of pre-treatment and digestion conditions on biogas production and quality are evaluated. Afterwards, integrated biogas-SOFC technology is described, including fuel processing, reforming and operating challenges. Biogas-SOFC modelling studies at different levels like, cell, stack and system are reviewed and efficiency of integrated systems with different equipment is considered. Finally, the performances of some biogas-SOFC pilot-plants are evaluated, and techno-economic aspects of Anaerobic Digestion-SOFC integrated system (AD-SOFC) are assessed.

Parts of this chapter have been published in Journal of Renewable Energy (134 (2019) 194-214)

2.1. Background

Anaerobic Digestion (AD) is used worldwide for treating organic waste and wastewater. Biogas produced can be converted using conventional energy conversion devices to provide energy efficient, integrated waste solutions. Typically, the electrical conversion-efficiency of these devices is 30-40% and is lowered due to biogas utilization instead of high pure refined natural gas. The Solid Oxide Fuel Cell (SOFC) as an alternative device offers high (50-60%) electrical efficiency with low emissions (CO_2, NO_x) and high temperature residual heat. The high quality residual heat from SOFCs could be used to improve biogas production through thermal pre-treatment of the substrate for anaerobic digestion. This chapter discusses the advantages and challenges of integrated AD-SOFC systems against the most recent scientific and practical developments in the AD and SOFC domain. First, the biogas production process and its influence on the composition and level of contaminants in biogas are explained. Subsequently, the potential of various biogas cleaning techniques is discussed in order to remove contaminants that threaten stable and long-term SOFC operation. Since SOFCs utilize H_2 and/or CO as fuel, possibilities for internal and external reforming are explained in detail. Special attention is given to biogas dry reforming in which CO_2 naturally present in the biogas is utilized effectively in the reforming. A detailed discussion on the choice of SOFC materials is presented, with a focus on biogas internal reforming. Various integrated SOFC system models with multiple configurations are also reviewed indicating the overall efficiencies. Some biogas SOFC pilot-plants are described and discussed to conclude with the techno-economic aspects of biogas SOFC systems.

Torrijos has reported on the state of biogas production in Europe and the anticipated future market [22]. Germany and Italy are leading countries in Europe in terms of number of anaerobic digestion plants. Biogas production in France and UK is growing fast especially from landfill and sewage. In the Netherlands, the idea of the NEW (energy & raw materials) Factory has been introduced. In this concept, wastewater is considered as a resource of nutrients, energy and clean water [23]. In the Amsterdam-west WWTP, approximately 25000 m3/day of biogas is produced, and that is used in Combined Heat and Power (CHP) units with electrical net efficiency of maximum 30%. The environmental benefit of this plant is considerable as it avoids 3200 ton CO2-eq/year [24]. It will be possible to increase the net efficiency to 50% or more if a high efficiency energy conversion device is used instead of the CHP unit.

Generally, the produced biogas consists of different gas compositions at different ranges as shown in Table 2-2. Typically, protein degradation results in the additional formation of NH_3 and H_2S that appear as constituents for biogas. The water vapour in the biogas follows Raoult's law and is fully dependent on the bioreactor temperature.

Table 2-1: General biogas composition [25, 26]

Substances	Symbol	Range (%)	Average (%)
Methane	CH4	35 – 75	60
Carbon dioxide	CO2	25 – 50	35
Nitrogen	N2	0.01 – 17	1
Hydrogen sulphide	H2S	0.01-2	35 ppm
Ammonia	NH3	0.01-3.5 ppm	1 ppm
Water vapour *	H20	3.1	3.1

* (T=25°C, standard pressure)

The application of biogas as a fuel to high efficiency energy conversion devices like fuel cells, especially Solid Oxide Fuel Cell (SOFC) has been reported for stationary applications. SOFCs are modular, silent, low-emission and vibration free devices that generate electrical power by electrochemical reactions [10]. Moreover, the high-temperature operation gives an opportunity to use the heat for co-generation or bottoming cycles and enables high exergy efficiencies [27]. However, there are still challenges with operating SOFCs that need to overcome the hurdles to emerge as a widely implemented technology.

2.2. Working principle of Solid Oxide Fuel Cells

The Solid Oxide Fuel Cell converts the chemical energy of a fuel into the electrical energy through electrochemical reactions. The SOFC is composed of three major layers. A dense layer of ceramic called solid electrolyte is sandwiched between two electrodes (anode and cathode). The anode and cathode are made out of specific porous conducting material. Electrochemical reactions are driven by the difference in oxygen partial pressure across the electrolyte. SOFCs operate at high temperatures in the range of 500-1000°C to enable oxygen ion transport through the solid electrolyte and they are suitable for long-term stationary applications [10]. Generally, at high temperature, oxygen at the cathode is reduced to oxygen ions and is transferred through the electrolyte. The oxygen ions react with fuel at Triple Phase Boundary (TPB) where the fuel gases H_2 and CO (gas phase), electrolyte (ionic phase) and electrode (electronic phase) meet. A thin layer helps to increase the ions flow and decreases the ohmic losses and resistance [10]. Electrochemical reaction of hydrogen at the anode (Eq. 2-1) and oxygen at the cathode (Eq. (2)) sides are shown below:

$$H_2 + O^{2-} \rightarrow H_2O + 2e^- \quad (2\text{-}1)$$

$$\tfrac{1}{2}O_2 + 2e^- \rightarrow O^{2-} \quad (2\text{-}2)$$

$$H_2 + \tfrac{1}{2}O_2 \rightarrow H_2O \quad (2\text{-}3)$$

The ideal fuel for fuel cells is hydrogen, but because of complications in hydrogen production, storage and associated costs, alternative fuels are widely

considered. Oxidation of carbon monoxide in SOFCs can also take place at the anode by free oxygen ions as shown in Eq. (2-4).

$$CO + O^{2-} \rightarrow CO_2 + 2e^- \qquad (2\text{-}4)$$

However, the effective diffusion coefficient for the larger CO molecules is lower than for the smaller H_2 molecules. As a result, slower CO diffusion and larger concentration variation have been observed in the porous layer, which results in a slower CO electrochemical oxidation in comparison to H_2 [28, 29]. It is also observed that the polarisation resistance with hydrogen is less than with carbon monoxide in nickel and ceria pattern anode SOFCs [30]. A poor performance of CO fed Ni-YSZ anode SOFC has been observed by Costa-Nunes et al. [31]. This can be improved by using the Cu–CeO_2–YSZ anode instead of conventional anodes.

In case of having a fuel mixture of CO, H_2 and some steam or carbon dioxide, Water Gas Shift (WGS) reaction (Eq. (2-5)) is considered to occur simultaneously.

$$CO + H_2O \rightarrow H_2 + CO_2 \qquad (2\text{-}5)$$

In addition to the type of fuel gas, other conditions such as temperature, pressure and local gas concentrations affect fuel cell performance. The theoretical reversible Potential (E_{rev}) of the SOFCs can be calculated using the Nernst equation:

$$E_{rev} = \frac{RT}{nF} \ln\left(\frac{P_{O_2} cathode}{P_{O_2} anode}\right) \qquad (2\text{-}6)$$

Where R is the universal gas constant, T is the absolute temperature (K), n is the number of electrons transferred for each mole of oxygen, for which is n=4, and F is the Faraday's constant (96485 C/mol). The actual voltage of the operating cell is always lower than the theoretical Nernst value due to various losses (overpotential). These include ohmic overpotential (η_{Ohmic}), charge-transfer (activation) overpotential (η_{Act}), and diffusion (concentration) overpotential (η_{Conc}) [32]. Hence, the actual cell potential can be calculated using the following equation:

$$V = E_{rev} - \eta_{Ohmic} - \eta_{Act} - \eta_{Conc} \qquad (2\text{-}7)$$

Methane-containing fuels such as syngas and biogas are potential fuels for SOFCs. The power generation from biogas-SOFC is considerably high, even when the methane in biogas is below the value that normal combustion could occur [33]. Methane in biogas can be converted into hydrogen and carbon

monoxide through the reforming reaction and at high concentration of hydrogen, good performance of SOFC is realized. Despite the possibility of biogas reforming, power density (power/active area of cell) achieved by biogas fuelled SOFC is lower than hydrogen fuelled ones. For instance, Girona et al. [34] investigated the performance of biogas (CH_4/CO_2=1) fed SOFC. The Open Circuit Voltage (OCV) was 0.99 V, which was lower than for a humidified hydrogen fuelled SOFC (1.07 V). The obtained power density for hydrogen and biogas fuelled SOFC at the same current density and fuel utilization (30%) were 207 and 245 mW/cm^2, respectively. Hence, biogas reforming plays an important role in SOFCs performance and needs to be investigated in detail.

2.3. Anaerobic Digestion

AD is the most promising technology for intensive biodegradation of organic matter [4, 35]. Based on recent studies and specified development guidelines, biogas production using anaerobic digestion has a bright future [36-39]. Lettinga has discovered that capacity of an anaerobic reactor can be enhanced by the specific design of Up-flow Anaerobic Sludge Blanket (UASB) and up to 97 % of Chemical Oxygen Demand (COD) removal can be achieved [40].

It can be applied to different treatment plant sizes. For instance, Rajendran et al. [41] assessed the feasibility of biogas production from household waste. In large-scale municipal WWTPs, after primary and secondary treatment of the sewage and sludge separation, activated sludge is conveyed into the anaerobic bioreactor to reduce sludge volume, stabilize the sludge and produce biogas. During the anaerobic digestion process, organic compounds are converted into methane by a mixed community of bacteria and archaea. First, the complex particulate organic matter is disintegrated by physico-chemical processes that enhance the accessibility by the enzymes excreted by the microbial community in the second step, the hydrolysis. The enzymatic hydrolysis process produces amino acids, sugars and fatty acids that can be taken up into the microbial cells. Depending on the waste stream composition, proteins and carbohydrates are the dominant (more than 60%) constituents of the total organic matter [42]. At that point, the involved microorganisms use these intermediates for their metabolic respiration which results in the formation of short chain fatty acids like propionic and butyric acid in the acidogenesis step. Subsequently, this leads to the production of acetic acid, carbon dioxide and hydrogen by the acetogenic bacteria in the acetogenesis step. Finally, hydrogenotrophic and aceticlastic methanogenic archaea convert these products into methane in the methanogenesis step [43, 44]. The whole process is shown in Fig. 2-1.

The potential of methane production mainly depends on the quantity and characteristics of the organic matter in the waste stream. The degradable organic material can be estimated by the Bio Methane Potential and Chemical Oxidation

Demand (COD) in the waste stream [45]. Different types of anaerobic bioreactors have been investigated including Completely Stirred Tank Reactors (CSTR), UASB, Expanded Granular Sludge Bed (EGSB), internal circulation process, etc.

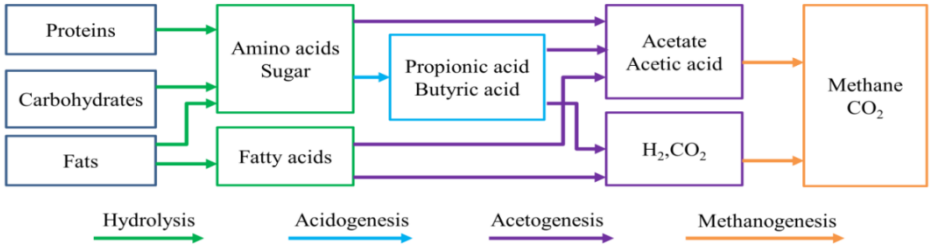

Figure 2-1: The simplified process of Anaerobic Digestion [46]

2.4. Towards integrated Anaerobic Digesters - SOFCs

2.4.1. Conventional use of biogas at WWTPs

In wastewater treatment plants, IC engines might be utilized to generate electrical power and heat from the biogas produced. In Fig. 2-2, a schematic block diagram is shown for the energy production process based on anaerobic digestion. The energy demand in WWTPs is mainly accounted for the thermal pre-treatment and mechanical processes. Mechanical processes demand electrical power and consist of three parts: aeration, mixing and, pumping. Innovative waste activated sludge digestion technology such as thermal/chemical process can improve the efficiency of systems because of higher sludge degradation and thus results in higher biogas yield. For pre-treatment of waste, heat is required. Based on the energy conversion device, different gas processing steps are needed. For instance, in order to burn biogas in a boiler, IC engine or gas turbine, only desulfurization is required. However, advanced biogas upgrading is needed for converting biogas into a storable fuel or for grid injection. In these cases, the partial pressure of methane should be increased to reach the natural gas quality. Then it is stored in high-pressure tanks (200 bars) [47]. Also for fuel cell applications, advanced gas processing is required depending on the type of fuel cell. The energy requirement for biogas production and processing can be supplied by the energy conversion device.

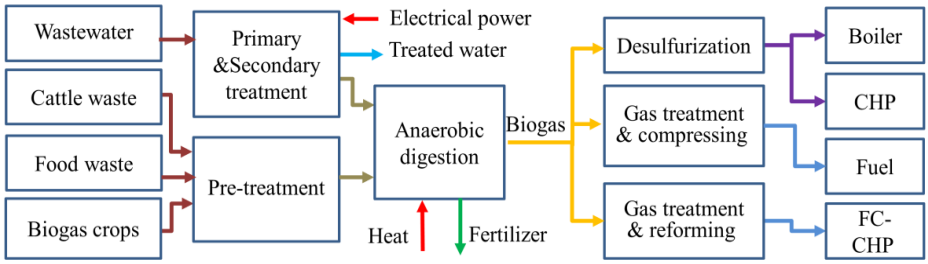

Figure 2-2: Simplified schematic of energy generation from different types of organic waste and biogas crops

At the WWTP, heat is used for several processes and the quality of heat determines how it can be used. In this article deals with low (less than 60°C) and medium (range from 60 to 180°C) temperature. High temperature heat is also sometimes used to incinerate contaminated activated sludge, but this usually happens after transport of the sludge to a sludge incineration facility [48].

2.4.2. Low temperature heat demand in digesters

Digesters can theoretically be operated under psychrophilic (10-20 °C), mesophilic (30-37 °C) and thermophilic (50-60°C) conditions. Too rapid changes in temperature can cause damage to the microorganisms and subsequently reduce reactor performance [49, 50]. With seasonal temperature variations, the digester temperature could be reduced by reduced temperatures in the incoming substrate as well as heat losses to the environment. Accordingly, microbial biogas generation, which is temperature dependent, could vary as the season changes [51]. Keeping the temperature constant is therefore crucial for stable methane production [52]. For northern European climate, municipal sewage is usually treated aerobically, because the concentration of organic matter (COD) is too low for anaerobic treatment to generate sufficient methane to sustain the operational temperature upon combustion in a CHP. As a consequence, only more concentrated streams like manure or concentrated primary and/or secondary sewage sludge contain sufficient energy to be digested under mesophilic or thermophilic conditions [53].

2.4.3. Medium temperature heat demand in digesters

In order to accelerate the solubilization of organic matter (hydrolysis stage) and improve methane production inside the anaerobic digester, several pre-treatment techniques can be applied [54] (Fig. 2-2). The main improvement in performance can be achieved by increasing the surface area of the organic matter, such that enzymes excreted by the microbes can attach to the biodegradable organic matter. Many studies have been carried out to evaluate the effect of different types of pre-

treatment on methane production, such as thermal, mechanical (ultrasound and high pressure) and chemical with oxidation (mainly ozonation) [42, 55]. In the review article, Hendriks and Zeeman [56], revealed that thermal pre-treatment is the most commonly used technique in practice for anaerobic digestion of cellulose, hemicellulose, and lignin.

Carbohydrates, proteins, and lipids in the waste streams such as waste activated sludge, fruit and vegetable waste should be degraded, but the cell wall protects the complex polymers from the enzymatic hydrolysis. Thermal pre-treatment in the medium temperature (range from 60°C to 180°C) helps to destroy the cell walls and opens up the cell content for enzymatic biological degradation. Furthermore, thermal pre-treatment reduces the required retention time as hydrolysis is often the rate limiting biological step. Bougrier et al. [57] assessed thermal pre-treatment for five different types of sludge samples at different temperatures for 30 minutes retention time. At pre-treatment temperature below 200°C, the COD solubilization ($COD_{soluble}/COD_{total}$) increases linearly with temperature and this increase of solubilization fraction is more considerable for temperatures higher than 130°C. Moreover, the results showed that thermal pre-treatment between 135°C and 190°C does not have a substantial influence on the methane content of biogas. Perez-Elvira et al. [58] evaluated the thermal pre-treatment of mixed fresh and hydrolysed sludge at 170°C and it has been observed that biogas production improved (with 40% higher VS removal) even at shorter retention time. To heat up the sludge generally heat exchangers or direct steam is utilized.

Alvareza and Liden [59] evaluated biogas production at three different low temperature ranges for a hydraulic residence time of 30 days. Biogas production improves by increasing digestion temperature with immediate responses. Climent et al. [60] claimed that time and temperature have the same effect on biogas production. Different kinds of treatments were studied and a 50% improvement of biogas production was observed at low temperature thermal treatment. However, they conclude that methane production does not improve by increasing the pre-treatment time more than 24 hours. Qiao et al. [61] observed that thermal pre-treatment significantly increases the biogas generation for municipal sewage sludge in comparison to other waste sources and it is reported that the highest biogas production takes place on the first day of 14 days retention time. Appels et al. [62] studied the effect of low temperature thermal treatment on biogas production and compared biogas production after thermal treatment at 70°C and 90°C for one hour. The results exposed that only 20°C temperature rise can

increase biogas production considerably. Gonzalez-Fernandez et al. [63] observed double methane yield with thermal pre-treatment of sludge at 90°C in comparison to 70°C. Up to 48% anaerobic biodegradability has been achieved at this temperature while the rate of methane production during the first 8 days was much higher than during the rest of the 25 days experimental period. The exposure time is also a very important factor in thermal pre-treatment. Passos et al. [64] studied thermal treatment of microalgae at lower temperatures (55°C to 95°C) at different exposure times (5 to 15 hours) and reported that methane production improves by 62% after increasing temperature to 95°C compared to untreated. It states that increasing pre-treatment process from 10 to 15 hours just slightly increases methane production for all temperatures studied. Some more references are shown in Table 2-2.

Table 2-2: Influence of thermal pre-treatment on methane production for different primary sludge and waste activated sludge.

Anaerobic digestion	Retention Time (Days)	Thermal treatment	Results (increase in CH_4 production/convertibility)	Reference
CSTR	15	175° C, 30 min	62 % (COD based)	[65]
CSTR	5	175°C, 60 min	100 % (COD based)	[66]
Batch	-	70°C, 7 days	26 % (VS based)	[67]
Batch	7	121°C, 30 min	32 % (WAS based)	[68]
CSTR	20	170°C, 60 min	61 % (COD based)	[69]
Batch	10	80°C, 30min	18.5% (SCOD based)	[70]
Batch	10	70°C, 9 h	30 % (COD based)	[71]
Batch	13	70°C, 2 days	48 % (COD based)	[72]
Batch	-	30°C, 30 min	50.8 % (COD based)	[73]
thermophilic batch	35	120°C, 30 min	53% (COD based)	[74]
Batch	20	175°C, 60 min	34.8% methane increase	[75]

2.4.4. Future use in Solid Oxide Fuel Cells

Banks et al. [76] have conducted a long-term experiment on a biogas fuelled IC-CHP system (195 kW). A thermal pre-treatment system was used at 70°C and the generated biogas was fed to an IC engine. The overall electrical conversion efficiency was 32% for CHP system and 53% of the heat was recovered, and the total recoverable energy per wet tonne of food waste was almost 405 kWh. Lübken et al. [77] developed a model to evaluate the energy balance of AD while it is self-heating at different operating conditions. The results show that the energy production during a year is much higher than the energy consumed during the entire year, however, during the winter, energy consumption (because of radiation losses) increases dramatically. Bohn et al. [78] evaluated the energy balance of

AD at low temperature farm-scale system. They found that the optimum methane yield and energy production would be achieved at 30°C (digestion temperature) and 60% net energy efficiency. Berglund and Borjesson [79] found that, in Sweden, using raw materials with high water content decreases the net power generation but, the energy demand for AD (including waste collection, transportation, electricity and heating requirements) ranges between 20% and 40% of the overall energy production. The energy balance of different biogas production methods (single and co-digestion of multiple feedstock) have been evaluated by Martina Poschl et al. [80]. It is indicated that energy input to output ratio can change from 10.5% to 64% for single feedstock digestion (mesophilic) and energy input largely depends on the type of waste materials. The Energy balance can be negative for municipal solid waste feedstock when transportation distances are more than 425 km.

Bouallagui et al. [81] evaluated the net energy production of AD at three different low temperature levels. Energy consumption at the highest temperature (thermophilic process) was about 41% higher than medium temperature (mesophilic process) AD, however increased biogas production compensates the energy consumption and net energy production is almost double at the highest temperature. Also, due to the faster kinetics at thermophilic temperature, the tank volume can be smaller. Hence, anaerobic digestion of all kind of wastes results in positive energy production and thermal pre-treatment even at low temperatures can improve biogas production and consequently energy efficiency of the system, regardless of the type of energy conversion device. Thermal pre-treatment indeed is useful in enhancing biogas production. In spite of a varying temperature range reported in the literature for thermal pre-treatment, it can be seen that heat available from SOFC or bottoming cycles could be possibly used for thermal pre-treatment offering an opportunity for efficiency improvement. Fig. 2-3 depicts a simplified energy flow diagram for an AD-SOFC integrated system. It is assumed that part of the organic substrate is not converted into biogas and there is heat loss from the AD tank. The electricity generated can be used for wastewater treatment process and high temperature outlet gas is conveyed to an afterburner. Heat generated in the afterburner can be used in wastewater treatment process, more specifically for thermal pre-treatment of the organic waste.

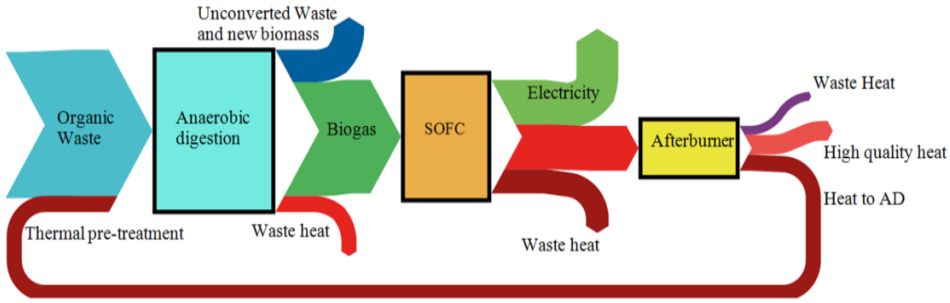

Figure 2-3: A simplified energy flow diagram of AD-SOFC system.

2.5. Biogas contaminants and fuel processing

The composition of anaerobic digester gas can vary naturally due to the digestion conditions and feed wastes. At low concentrations of methane, the IC engine efficiency declines considerably [8, 82]. Bari [83] recommended to reduce the carbon dioxide in biogas with at least 10% to improve biogas combustion in diesel engine. When using biogas containing more than 40% CO_2, the IC engine performance severely declines. Porpatham et al. [84] suggested adding 10% hydrogen to biogas to improve the performance of spark ignition engine. They concluded that this does not affect NOx production. Also, ammonia in biogas increases the NOx production in an IC engine [85]. Hence, using devices that can tolerate high CO_2 concentrations and reduce NOx emissions would be preferable. The SOFC has these desirable features.

Biogas is therefore a promising fuel for SOFCs [86] as neither carbon dioxide nor vapour have to be removed. However, raw biogas often contains considerable quantities of undesirable trace compounds such as hydrogen sulfide (H_2S) and siloxanes that can cause SOFC degradation already at very low concentrations. Additionally, ammonia (NH_3) is also known as a contaminant in conventional CHP systems, which causes a gradual erosion and corrosion on Balance of Plant (BoP) components. Hence, biogas cleaning for such contaminants is a crucial step [87]. The amount of these contaminants varies widely depending on the biogas production unit operating conditions and raw feedstock composition [88]. In the following subsections, the effects of the most important trace contaminants on system performance are discussed.

2.5.1. Hydrogen Sulfide

The majority of wastewaters contain sulfate, and during anaerobic treatment, sulfate is reduced to sulfide by sulfate reducing bacteria. Sulfate reducing bacteria compete for substrate with methanogenic microorganisms, which results in less methane and the presence of highly undesirable hydrogen sulfide (H_2S) [89, 90]. Hydrogen sulfide is a flammable, malodorous, poisonous and colourless gas that

is heavier than air. This gas is converted to environmentally hazardous compounds such as sulphur dioxide (SO_2) and sulfuric acid (H_2SO_4). H_2S is also a corrosive gas that could form concentrated sulphuric acid, depending on humidity, oxygen concentration and presence of biofilm and can thereby destroy pipe lines and other metal equipment. In general, many types of gas utilization units can tolerate H_2S levels between 100 and 3,000 ppm and for expensive equipment such as CHP systems, H_2S levels below 250 ppm and water vapour removal are recommended [86]. Numerous studies have been carried out in order to investigate the H_2S removal for different applications [91-97].

The effect of H_2S on SOFC performance has been addressed in several studies. In nickel-based anode SOFCs, H_2S poisons the anode by converting Ni to Ni-sulfide that forms large, dense metal sulfide particles on the anode surface. This leads to a reduction in the three phase boundaries and degradation in the electrochemical activity [98]. However, SOFC is considered the most tolerant fuel cell type to H_2S impurities [99]. According to experiments conducted by Norheim et al. [100], at a high level of H_2S impurities (>20 ppm), a reduction of SOFC performance has been observed with a Ni-YSZ anode supported cell. This reduction in the cell performance was depending up on the cell material as well as operating temperature and found to be reversible after H_2S removal from the fuel gas. Aguilar et al. [101] studied SOFC performance on H_2S containing fuel for Strontium doped Lanthanum Vanadate (LSV) anode and observed no considerable deterioration if the fuel contained less than 5% H_2S. Indeed, electrochemical oxidation of H_2S was more active compared to hydrogen fuel for the LSV anode. Sasaki et al. [102] have analysed H_2S poisoning of SOFC with different cell materials (Yttria-Stabilized Zirconia (YSZ) and Scandia-Stabilized Zirconia (ScSZ)) with respect to impurity concentration, operational temperature, and fuel composition. The results showed that a considerable voltage drop for higher than 5 ppm H_2S poisoning occurred. Sulfur tolerance was better for the cell with ScSZ in the anodes. Appari et al. [103] concluded that poisoning at high temperature in Ni based anode (packed bed reactor) can be easily reversed just by removal of H_2S from the feed stream. Zhang et al. [104] investigated the impact of sulfur poisoning on operational behaviour of different SOFC anodes (Ni/YSZ and Ni/GDC (Gadolinium Doped Ceria)). Results indicated that Ni/GDC cermet (ceramic–metallic composite) anode has a better performance during the exposure to H_2S-containing hydrogen fuels, which is likely associated with the mixed ionic and electronic conductivity of the GDC phase. Mahato et al. [32] state that better performance of Ni–GDC anodes is associated with their mixed ionic and electronic-conductivity and also with the adsorption of hydrogen on GDC. Therefore, even though the Ni surface is covered by sulfur, GDC can still prepare the required conditions for the electrochemical reactions. Da Silva and Heck [105] studied the thermodynamics of sulfur poisoning in SOFCs to identify the effect of H_2S on operating parameters such as current density. At fuel utilizations (U_f)

lower than 90%, increasing current density slightly increases the interaction of sulfur with Ni. So, understanding sulfur poisoning and increasing the sulfur tolerance are important for commercialization of SOFCs.

Shiratori et al. [106] studied the feasibility of biogas direct fuelled SOFCs by using a Ni–ScSZ cermet as the anode. They observed a 9% voltage drop and 40% decline in methane conversion rate in a 1 ppm H_2S poisoning test that was conducted under operation conditions of 200 mA/cm^2 current density and a temperature of 1000°C. Ouweltjes et al. [21] studied the influence of sulfur contaminant (2-9 ppm) on the Ni-GDC cell fed with biosyngas. Results illustrate that sulfur largely affects the internal methane reforming however, the influence was negligible for the oxidation of hydrogen and carbon monoxide. Papurello et al. [107] have used Na–X zeolites fixed bed reactor followed by a ZnO guard bed to remove H_2S from a simulated biogas contaminated with 30 ppmv H_2S, and the concentration of H_2S decreased to 0.07 ppmv for an extended test period (250 hrs). Further studies on H_2S tolerance with biogas in operating SOFCs are highly recommended

2.5.2. Siloxane

Siloxanes are a group of silicon (Si)-bearing molecules that are used in cleaning, cosmetics, defoamer products and deodorants, and are generally found in wastewater treatment plants and landfills [108, 109]. According to literature, D4 and D5 are the most abundant among the different siloxanes detected in biogas samples (Table 2-3). During the combustion of biogas at high temperature, silicon dioxide (SiO_2) forms. The size of SiO_2 particles ranges between 40 and 70 nm and the particles occur as fibrous dusts that are categorized as nanoparticles, and considered to be toxic to human health [108]. Ajhar et al. [110] have done a thorough study on siloxane removal from biogas. A pre-drying step is proposed before using activated carbon for the gas produced from sewage sludge. Removing Siloxanes and H_2S can be done simultaneously through activated carbon.

Table 2-3: Volatile methyl siloxanes in biogas [111]

Abbreviation	Compound	Formula	Molar mass (g/mol)
D4	Octamethylcyclotetrasiloxane	$C_8H_{24}O_4Si_4$	297
D5	Decamethylcyclopentasiloxane	$C_{10}H_{30}O_5Si_5$	371

Schweigkofler and Niessner [112] reported that apart from activated charcoal, silica gel has shown high adsorption capacities for siloxanes. It is also advised to use a Fe-based adsorbent (meadow ore) bed. It can bring down siloxane concentration by 75%. Yu et al. [113] have evaluated different types of activated carbon for siloxane adsorption and a range of 1.7nm to 3 nm pores diameter has been suggested as the optimum pore size. Finocchio et al. [113] assessed a variety

of siloxane purification solids and it was observed that activated carbon is the most efficient sorbent. Recently, Gislon et al. [114] have conducted experiments to achieve a purified biogas with less than 1 ppm siloxane. It is suggested to use activated carbon with a larger specific surface area.

In addition to siloxane removal from biogas, a few studies have also been carried out to assess the performance of SOFCs with siloxane containing fuels. Siloxane causes fatal degradation of cell performance even at ppm levels. Solid SiO_2 is formed within porous cermet anodes and near the top surface anode layer [98]. Haga et al. [115] evaluated the effect of siloxane on the performance of SOFC and they concluded that the cell voltage declines gradually at 10 ppm siloxane contaminant at different temperatures due to SiO_2 precipitated on the top surface of the anode. Sasaki et al. [98] have investigated different impurities such as chlorine, siloxane, phosphorus, and boron. A tentative concentration threshold of impurities has been defined for a humidified hydrogen fuelled SOFC, which is 2ppm for siloxane (D5). Madi et al. [116] assessed the impact of siloxane on Ni-YSZ anode SOFCs by conducting Electrochemical Impedance Spectroscopy (EIS) tests. Adding siloxane to the fuel stream resulted in an increase in required activation energy and this is attributed to a decrease in the active triple phase boundary area. Haga et al. [117] evaluated the poisoning of Ni–ScSZ cermet anodes by various fuel impurities such as H_2S, CH_3SH, COS, Cl_2, and siloxane. Experimental studies were conducted for 10 ppm siloxane (D5) in 3%-humidified H_2 at 800, 900 and 1000 °C. The degradation was attributed to SiO_2 that was precipitated near the top surface of the porous anode and reduces TPB areas.

Arespacochaga et al. [118] suggested three steps for biogas treatment for SOFC applications. First, H_2S removal by a regenerable iron-based adsorbent unit, secondly trace components removal such as siloxanes by an activated carbon unit and the third step, to use a biogas drying unit to remove moisture.

2.5.3. Ammonia

Ammonia (NH_3) is the second most important contaminant present in biogas considering IC engine applications. It is corrosive and during the combustion process, slightly increases the NOx emissions [119]. Also, this water soluble gas can be a threat to aquatic plants and animals if present in high concentrations (more than 1 mg $NH_3\,L^{-1}$) [120]. Generally, in WWTPs, ammonia and oxidized nitrogen are removed through the conventional aerobic energy-intensive activated sludge process. Moreover, ammonia has shown to be inhibiting methane production in a concentration range of 1-2 g NH_3-N L^{-1} [121]. Several energy consuming physicochemical methods can be applied to remove ammonia, such as air stripping and chemical precipitation [122-125]. However, for conventional biogas energy conversion devices like IC engines, the ammonia concentration in biogas (gas phase) needs to be reduced to very low ppm level [126], which is highly energy intensive[127].

Unlike for IC engines, ammonia is considered as a fuel for SOFCs. Due to the high temperature operation, ammonia is cracked into nitrogen and hydrogen molecules. Electrical power is then subsequently produced by the electrochemical oxidation of H_2 (Eq. (2-3))[128]. Recently, the use of ammonia as a fuel for SOFC has been drawing attention as ammonia is an easily storable, efficient hydrogen carrier[129-131]. For Ammonia, endothermic cracking reaction starts at 405°C with simultaneous evolution of nitrogen and hydrogen. Complete conversion of ammonia occurs at 590°C following Eq. (2-8). No undesirable nitrogen oxides are formed on the nickel cermet anode [132].

$$NH_3 \rightarrow \frac{3}{2}H_2 + \frac{1}{2}N_2 \quad , \quad \Delta H^0_{298} = 46.22 \ {}^{kJ}/_{mol} \qquad (2\text{-}8)$$

Results indicate that Ni-based catalyst is appropriate to promote ammonia cracking, similar to methane reforming [133]. The performance of the nickel cermet SOFC has been evaluated under various conditions at a temperature range of 700°C -900°C, and results showed a considerable performance in comparison to pure hydrogen fuel [134]. Note that ammonia is also considered as a biogas contaminant in IC engine applications, whereas it can be potentially used as a fuel in SOFC systems [135]. This opens up opportunities for removing ammonia directly from the digesters and to use it in SOFCs. The energy requirement for nitrification/denitrification depends on the Nitrogen concentration of the wastewater (1.224 MJ/m^3 of wastewater (roughly 24.5 MJ/kg-N) for small scale plant). This can then be significantly reduced by extracting ammonia after primary treatment of wastewater stream [136]. The removed ammonia can be used as a fuel for SOFCs. Overall energy efficiency of 81.1% and electrical efficiency of 69.3% have been reported for an ammonia fuelled SOFC-gas turbine integrated system which is equal to 15.1 MJ/kg-NH_3 overall and 12.8 MJ/kg-NH_3 electrical power based on the ammonia LHV [137]. On the other hand, it should be considered that the electrical energy demand for ammonia recovery from WWTP is roughly equal to 11.2 MJ/Kg-N [138, 139]. Therefore, an energy consuming process can be converted into an energy-positive one.

2.6. Biogas conversion

As mentioned before, biogas is predominantly methane and direct electrochemical oxidation of methane is much slower than H_2 and CO, thus only methane reforming is considered in this article [140, 141]. The reforming can be achieved either internally using SOFCs or externally using a catalytic (pre) reformer. The three major methods for methane conversion are steam reforming, Partial Oxidation (POX), and dry reforming. Also, there are mixed methods such as Autothermal Reforming (ATR) (mixed steam reforming and methane POX).

2.6.1. Steam reforming

Most studies only consider steam as a reforming agent for methane reforming in SOFCs. This method also has been proposed for methane reforming of natural gas and syngas [142]. Methane is reformed by direct steam injection at high temperature through the reaction shown in Eq. (2-9). The Methane Steam Reforming (MSR) reaction is a highly endothermic reaction that can take place either inside or outside SOFCs. As it can be seen in steam reforming reaction, one mole of steam is required to reform one mole of methane. The carbon monoxide generated can also react with the remaining steam and produces more hydrogen through the exothermic WGS reaction (Eq. (2-10)). Ni present in the SOFC anode is also a good catalyst for the WGS reaction [31].

$$CH_4 + H_2O \leftrightarrow 3H_2 + CO \quad , \quad \Delta H^0_{298} = 206.3 \ {}^{kJ}/_{mol} \qquad (2\text{-}9)$$

$$CO + H_2O \leftrightarrow H_2 + CO_2 \quad , \quad \Delta H^0_{298} = -41.1 \ {}^{kJ}/_{mol} \qquad (2\text{-}10)$$

Steam reforming is a well-established technique, although, from a thermodynamic point of view, the chance of carbon deposition is still high at low steam to carbon ratios [143]. High temperature and a high steam/carbon ratio are favourable conditions for steam reforming [144]. This process is considerably endothermic and a heat source has to be used. Moreover, steam generation is highly energy consuming. Therefore, determining a minimum steam/carbon ratio is crucial. On the other hand, a high amount of steam is required to avoid carbon deposition. In literature, a variety of steam/carbon ratios have been proposed at different operating conditions to guarantee safe operation and improve the exergy efficiency of SOFCs. However, direct internal reforming in operating SOFCs is not well understood and much focus is now on improving catalyst materials for the same [145].

2.6.2. Partial Oxidation (POX)

Methane conversion can also be carried out through one of the simple partial oxidation reactions which are shown in following equations. Oxygen from the air can also be used as a reforming agent [146].

$$CH_4 + \tfrac{1}{2}O_2 \leftrightarrow 2H_2 + CO \quad , \quad \Delta H^0_{298} = -44 \ {}^{kJ}/_{mol} \qquad (2\text{-}11)$$

$$CH_4 + O_2 \leftrightarrow 2H_2 + CO_2 \quad , \quad \Delta H^0_{298} = -322 \ {}^{kJ}/_{mol} \qquad (2\text{-}12)$$

$$CH_4 + 2O_2 \leftrightarrow 2H_2O + CO_2 \quad , \quad \Delta H^0_{298} = -803.03 \ {}^{kJ}/_{mol} \qquad (2\text{-}13)$$

The products of Eq. (2-11) can be directly fed into the SOFC. This reaction is slightly exothermic and the generated heat increases the temperature of the fuel so that the required fuel pre-heating is also done through this reaction. If more oxygen is available, partial oxidation goes through the Eq. (2-12). This reaction is much more exothermic. Required steam for steam reforming can be produced by increasing the available oxygen as in Eq. (2-13). This reaction is largely exothermic and sufficient heat is generated to heat the SOFC inlet fuel. These reactions can take place in a Catalytic Partial Oxidation (CPOX) unit outside of SOFC. On the other hand, in these reactions hydrogen yield is much lower in comparison to the steam reforming. A ratio of one to one for the air to biogas ratio has been suggested to avoid carbon deposition at 800°C in an operating SOFC, and the voltage stability was improved. However, re-oxidation of Ni metal catalyst has been observed and optimization of air dosage must be carried out [147]. Additionally, due to the presence of nitrogen in the air and fuel mixture, the partial pressure of hydrogen in the fuel is low which leads to a lower voltage in SOFC.

2.6.3. Dry reforming

Apart from steam, carbon dioxide also can be considered as an agent for methane reforming [146]. This type of reforming is known as dry reforming. Biogas consists of two greenhouse gases: CH_4 and CO_2. Therefore, dry reforming is the most interesting type of reforming for biogas processing because one gas component (CO_2) is utilized to reform the other one (CH_4). Meanwhile, the generated gas mixture can be applied as a fuel for SOFCs. Additionally, in case of carbon deposition, the presence of CO_2 in biogas has a beneficial effect on SOFC operation, because CO_2 can fairly remove carbon deposition by gasification of carbon [148]. Nevertheless, the dry reforming reaction is highly endothermic and needs a high operating temperature (800-1000°C) to obtain a high conversion rate of methane [149]. This reaction is shown in Eq. (2-14). In the case of direct internal reforming, this endothermic reaction causes a sharp temperature gradient at the entrance of the fuel channel inside SOFCs, which can result in cell cracking [150]. Moreover, hydrogen generated from the dry reforming reaction can react with the remaining CO_2 and produce CO which is also a fuel for SOFCs [151].

$$CH_4 + CO_2 \leftrightarrow 2H_2 + 2CO \quad , \quad \Delta H^0_{298} = 247.3 \ {}^{kJ}/_{mol} \tag{2-14}$$

$$H_2 + CO_2 \leftrightarrow H_2O + CO \quad , \quad \Delta H^0_{298} = 41.1 \ {}^{kJ}/_{mol} \tag{2-15}$$

While high temperatures are required for the fast kinetics of methane reforming, Reverse Water-Gas Shift (RWGS) is slightly endothermic and high temperature is in favour of CO production. So, the partial pressure of CO is higher than the partial pressure of H_2 in the reformed gas [152]. This leads to some

problems such as carbon deposition on the anode, delamination of anode and finally deactivation of anode catalyst [153].

Generally, CH_4/CO_2 molar fraction in actual biogas is between 1.2 to 1.9 [154]. So, the CO_2 in biogas is insufficient to completely reform the methane into hydrogen and carbon monoxide. The required CO_2 for dry reforming can be supplied from other processes for instance, from the exhaust gas of the activated sludge process [155] or by partial recirculation of the anode exhaust flow [156]. Otherwise, extra reforming agent is required which can be the steam (Eq. (2-9)). The required steam can be produced from different sources for instance, a steam generator or the hydrogen electrochemical reaction (Eq. (2-1)) on the anode side. Lanzini and Leone [157] have suggested adding 1.2 mole of CO_2 to each mole of biogas to achieve a stable voltage. An equimolar CH_4/CO_2 feed gas composition is recommended by Yentekakis et al. [158] to maximize the electrical power output of SOFC, whereas Xu et al. [159] proposed a CO_2/CH_4 ratio of 1.3 as an optimum gas composition for dry reforming. On the other hand, it has also been reported that adding CO_2 to general biogas composition increases the ohmic resistance of the cell [160].

Shiratori et al. [147] have used real and simulated biogas for SOFC, focusing on poisoning by contaminants, fluctuation in biogas composition, and carbon deposition. In spite of theoretical predictions of carbon deposition with a ternary diagram, no carbon deposition was observed for the simulated biogas. It is claimed that by drawing current, methane conversion was promoted. On the other hand, severe carbon deposition took place during the long term experiment with actual biogas. Staniforth and Ormerod [161] have studied the impact of methane partial pressures on operating SOFC performance with a low methane concentration (15 mol.%). Power production was high enough while carbon deposition was inevitable. They have found that at methane mole fraction of 0.45 the obtained power is the maximum corresponding to the high partial pressure of H_2 and CO through internal dry reforming. Santarelli et al. [162] have investigated internal dry reforming of biogas on a tubular (Ni-YSZ anode supported) SOFC stack with different extra moles of CO_2, corresponding to CH_4/CO_2 ratios of 0.43, 0.32, and 0.25. Performance maps of the SOFC for a wide range of current densities under different fuel flow rates have been determined. It has been reported that dry reforming is more effective for CH_4/CO_2 of 0.43. Guerra et al. [163] have assessed dry reforming on Ni/YSZ catalyst. Different parameters such as temperature, residence time and CH_4/CO_2 ratio have been studied to optimize the performance of a biogas SOFC. A range of $0.5< CH_4/CO_2 <0.75$ has been suggested to obtain a high methane conversion and to prevent carbon deposition. Also, it is shown that reforming reactions are fast and temperature-dependent. It is also observed that at an appropriate residence time, reaching equilibrium condition is possible even at an intermediate temperature of 800°C. Thermodynamic equilibrium of biogas (60% CH_4 and 40% CO_2) with air (21% O_2) were calculated and shown in Fig. 2-

4. At 750°C the carbon deposition disappears and at 800°C all methane reformed to hydrogen and carbon monoxide. However, the challenges in maintaining appropriate gas composition and temperature gradients across large-area SOFC stacks make it difficult to get all hydrocarbon fuels reformed by the internal reforming [164].

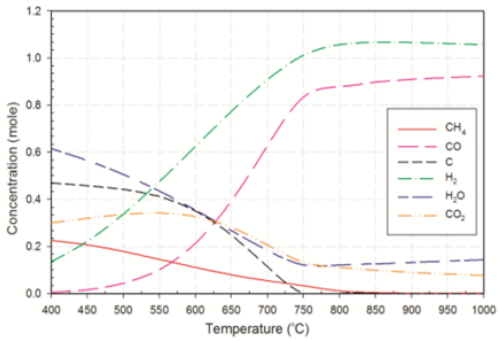

Figure 2-4: Thermodynamic equilibrium concentrations (moles) in the temperature range 400–1000°C at 1 atm for mixed biogas and air.

2.6.4. Combined reforming

Steam and dry methane reforming are endothermic whereas the partial oxidation is an exothermic reaction that can produce the required heat for reforming or preheating the fuel gases. Therefore, combined reforming is a good opportunity to optimize SOFC performance. The required steam for methane reforming can be produced by fuel oxidation in a Catalytic Partial Oxidation (CPOX) unit. With Autothermal Reforming (ATR), the POX and MSR take place in a reactor by feeding the hydrocarbon with both steam and air. Ahmed and Krumpelt [165] found that ATR is capable of achieving higher reforming efficiencies in comparison to steam reforming whereas the hydrogen partial pressure in steam reforming is higher. However, it is difficult to control all operational parameters such as the O/C ratio to produce a hydrogen rich fuel for SOFC.

Lanzini and Leone [157] investigated bio-methane and bio-hydrogen fuelled SOFC with different additional oxidation and reforming agents such as air, steam, and CO_2. A carbon formation boundary diagram is proposed for different reforming agents. The results showed that from a power production perspective, the best reforming agent is steam, for which the obtained overall stack electrical efficiency was 41%. Piroonlerkgul et al. [166] compared different biogas reforming agents (steam, air, and combined steam/air) for different plant configurations. The results illustrate that increasing the concentration of reforming agents decreases the electrical efficiency. However, they state that steam is the most appropriate reforming agent. Papurello et al. [107] have

investigated combined reforming in external reformer at space velocities (the volumetric flow rate entering the reactor divided by the reactor volume) as high as 150000 h^{-1}. Methane conversion for dry reforming at 800°C was reported to be about 47%. A further increase in conversion by 21% was observed with the addition of steam (H_2O/CH_4=1.2). Addition of small amounts of oxygen (O_2/CH_4=0.12) has been shown to increase the methane conversion to about 78%.

Van Herle et al. [167] illustrated the variation of electrical efficiency for an SOFC stack with different CO_2 fractions of air mixed biogas. In a developed model, when the oxygen to methane ratio and fuel utilization were kept constant (O_2/CH_4= 0.35, U_f=0.8), fuel gas composition with rich carbon dioxide (60% CO_2/40% CH_4) was determined as an optimum in order to maximize the electrical power production. Takahashi et al. [150] have used air to partially oxidize methane in biogas on Ni–ScSZ and Ni–YSZ anodes. They observed that additional air can decrease the temperature gradient that is generated because of endothermic dry reforming reaction. On the other hand, the methane conversion rate decreases. Because of the short residence time, no difference was observed for these two anodes. Optimum air/biogas mixing ratio was found to be 0.7 for biogas-SOFC whereas CH_4/CO_2=1.5 for biogas at 800°C. However, it is proposed by Takahashi that the air/biogas ratio be higher than 1 to obtain a homogeneous temperature at the fuel channel of SOFC.

Leone et al. [168] have conducted a series of experiments for biogas-SOFC single cell. A Ni-YSZ cermet (ceramic-metallic) anode supported SOFC was used with a biogas composition that possibly could lead to carbon formation. A fast voltage drop has been observed. So, a steam to carbon ratio of 0.5 has been proposed to avoid carbon formation. However, it has also been observed that adding steam to biogas results in a reduction in the current density obtained [28]. Shin-Kua Ray et al. [149] evaluated the combined steam and dry methane reforming on Ni catalyst. They observed that CO_2/H_2O ratio influences the methane reforming because Ni shows a better catalytic activity for steam in comparison with CO_2. This ratio is more effective at lower temperatures (<973 K).

As mentioned in this section, there are different methods for biogas reforming and based on the availability of reforming agents and conditions, an appropriate method should be selected. Partial oxidation of biogas is one of the simpler techniques, however, the exergy efficiency of the process is low due to the direct oxidation of methane. Furthermore, there remains a possibility of re-oxidation of anode due to high oxygen partial pressures in the fuel gas. Biogas combined (steam/dry) reforming is a more established technology with several experimental studies carried out in the past. Dry reforming is more environmental-friendly and less expensive, however slow kinetics, high thermal stresses, risk of carbon deposition and limited experimental investigations make this method not very

attractive. The optimal method for methane conversion in biogas-SOFC remains not well understood. Moreover, there are several challenges that should be handled for the continuous operation of biogas fed SOFC systems. The next section gives a comprehensive overview of these challenges.

2.7. Operational challenges for biogas fuelled SOFC

Using biogas fuelled SOFC as an energy conversion device offers multiple advantages, but there are many challenges that should be tackled to make sure that the fuel cell operates under safe conditions. This section elaborates on the main operating challenges encountered with biogas fuelled fuel cells with review of proposed solutions.

2.7.1. Direct Internal Reforming

Steam and dry methane reforming reactions (Eq. (2-9) and (2-15)) are considerably endothermic and a heat source is needed to run the external reformer reactions. On the other hand, electrochemical reactions (Eq. (2-1) or (2-4)) which take place in SOFCs is significantly exothermic and hence controlling the temperature is a challenge. In the case of Direct Internal Reforming (DIR), these reactions take place simultaneously in SOFC. Therefore, DIR reduces the electrical power required for cooling down the SOFC stacks compared to hydrogen fuelled ones [147]. Applying DIR makes the system compact and cost-effective. A possible drawback of DIR is the additional thermal stresses in cells because of the sharp temperature drop due to the endothermic reforming at the entrance of the fuel channel in SOFC stacks.

The complex interaction between reforming, POX, WGS and electrochemical reactions determine the local heat production in SOFCs. Therefore, it is crucial to know the reforming reaction kinetics for operating SOFCs. Methane steam reforming kinetics for catalytic external reforming have been extensively investigated and some experimental studies on the kinetics of internal methane steam reforming especially, in Ni based anodes have been reported [169]. Only a few studies have tried to illustrate the dry reforming reaction mechanism and associated kinetics [162, 170].

Gokon et al. [171] studied the dry reforming kinetics for a low temperature SOFC (600°C -700°C). The catalytically activated metallic foam absorber such as Ru/Al_2O_3 catalyst on a Ni–Cr–Al alloy foam has been used for different CH_4/CO_2 ratios. Langmuir–Hinshelwood has been found as the best kinetic model to predict the methane reforming reaction rate. The power law rate equation has also been used to evaluate the reforming kinetics for different temperatures and partial pressure of fuel components. The results have indicated that Ni/La-Co(3%wt)/ Al_2O_3 catalyst has the highest activity in reforming and highest activation energy (99.4 kJ/mol). Laosiripojana and Assabumrungratb [152] have reported that for a

ceria (CeO_2) catalyst material (with highly mobile oxygen vacancies) the dry reforming rates are almost equal to the steam reforming rate for the same methane partial pressure. Moreover, the same reaction mechanism for methane and dry reforming is proposed. Ceria (CeO_2) has a good potential for indirect internal reforming in SOFCs and the disadvantages are the low specific surface area and catalyst deactivation because of thermal sintering. Using CeO_2, which has a large surface area, improves the performance of this catalyst. Hecht et al. [172] investigated the elementary heterogeneous chemical kinetics of dry, steam and mixed reforming of a Ni-YSZ SOFC with an anode supported cell. They found that at low current density, the reaction tends toward equilibrium.

Brus et al. [173] have analysed the thermodynamics of carbon deposition in SOFCs with combined steam and dry reforming. A numerical model has been developed to study the kinetics of reforming. With a small additional amount of steam, SOFC can operate in the safe region of coking, however high CO cocentration in the fuel decreases the overall efficiency of SOFC. Kinetics of mixed steam and CO_2 reforming of methane in a fixed-bed reactor have been assessed over $Ni/La/Al_2O_3$ based catalyst by Park et al [174].

Meng [28] has developed a numerical model to test the effect of steam addition to biogas for different operating conditions. Especially the gas composition through the fuel channel has been studied as well as the impact of current density. The results show that for a mixture of biogas and steam, despite a reduction in total current density, the local current density slightly increases toward the downstream direction. This shows that using a long fuel channel has a beneficial effect on the operation of biogas SOFC. It was observed that the rate of dry reforming is higher at the inlet and decreases significantly along the fuel channel. WGSR rate was negative at the inlet for pure biogas due to a lack of water. Also, a large temperature drop is observed from inlet to outlet due to all endothermic reactions. Furthermore, some studies have been dedicated to investigate the reforming kinetics in external reformers (catalytic CO_2 reforming). These studies mostly focused on the kinetics of steam and combined methane reforming and more studies are still needed to investigate the kinetics of biogas SOFC dry reforming. Furthermore, in case of having ammonia mixed with biogas fuel, the influence of ammonia cracking on methane reforming also needs to be investigated.

2.7.2. SOFC materials

SOFC consist of an electrolyte, electrodes (cathode and anode), interconnect (metal or ceramic) and inactive thermal insulator. Materials should be chosen in order to reduce losses, for instance, lowering electric resistance of the electrodes, contact resistance associated with interfaces, and lowering ionic resistance of electrolytes. Moreover, high operating temperatures with SOFCs lead to several

materials problems, which include interfacial diffusion between electrolyte and electrode materials, thermal instability, mechanical and thermal stresses because of the difference in the thermal expansion coefficients for different components. Decreasing the operational temperatures would bring considerable cost benefits. Zirconia doped with 8 to 10 mole % yttria (yttria-stabilized Zirconia (YSZ)) is still the most effective electrolyte for the high-temperature SOFC, although several others have been investigated, for instance, ceria and lanthanum materials [10]. The catalytic effect of anodes is also important when fuel reforming is needed.

One of the advantages of SOFCs is being fuel flexible. In literature, it is found that many reported studies evaluated the influence of material for different types of fuels and for different operating temperature on biogas-fuelled SOFC catalysts. Also, surface modifications were proposed to suppress carbon deposition and sulphur poisoning [175]. For fuels with short carbon chain, the catalytic reactions of fuel reforming mainly take place at a very thin layer of the catalyst. Therefore, choosing an appropriate catalyst based on the gas composition is crucial [144].

The anode has a porous structure that should transfer the fuel to the TPB rapidly. SOFC's anode is usually made of a metallic nickel cermet with a supporting structure of YSZ (e.g., Ni–YSZ and Ni-GDC). Lanzini and Leone [157] have studied Ni-YSZ anode supported cell (ASC) and Ni-GDC electrolyte supported cell (ESC) SOFC at 800°C for current densities of 0.5 A/cm^2 and 0.3 A/cm^2, respectively. Because of thicker anode, ASC (600 µm) showed a better performance in comparison with a 40 µm GDC (ESC) cell with respect to methane internal reforming.

Sumi et al. [29] compared Ni-YSZ and Ni-ScSZ (Scandia Stabilized Zirconia) for steam and dry methane reforming. The results illustrate that generally cell degradation rate is higher with Ni-YSZ for both dry and steam reforming. Contrary, Takahashi et al. [150] showed that the performance of cell with Ni-YSZ anodes is similar to Ni–ScSZ for biogas dry reforming whereas ScSZ is a better ion conductor. In terms of methane steam reforming the Ni-YSZ cermet anode has a better performance compared to Ni-ScSZ. However, the carbon deposition rate is significantly higher for Ni–YSZ than Ni–ScSZ [176]. The comparison of these two experimental studies shows that the selection of reforming agent can influence the behaviour of anodes. Ke et al [177] investigated the Ni/ScSZ anode for methane fuelled SOFC at high temperature and low steam partial pressure (3%). They observed that steam enrichment on the Ni surface for Ni/ScSZ cermet anode is higher than YSZ, which leads to lower carbon deposition on Ni/ScSZ.

A combined catalyst layer with a conventional Ni-based anode (4-layer coated) has been suggested by Cheekatamarla et al. [178]. Internal reforming has been studied for different fuels including biogas for a tubular SOFC. Complete methane

conversion has been observed at 700°C. Extra air has been used to assist dry reforming in such a way that O_2/C ratio was 0.1.

Trimm [179] has investigated the impact of doping Ni with a small amount of metals, like Bismuth, on carbon deposition which is significantly effective to reduce carbon formation on the nickel surface. Horita et al. [180] investigated metal/oxide interfaces of anodes, YSZ and YDC (Y_2O_3-doped CeO_2) substrates combined with different Ni and Au electrodes. Ni is more active than Au for methane decomposition and carbon deposition. However, using YDC substrate decreases carbon deposition on the Ni surface and it is associated with hydrogen ionization and transportation capability. Alipour et al. [181] have studied Ni/Al_2O_3 catalyst with the addition of alkaline salts such as MgO, CaO, and BaO. Results show that MgO is the best aid material to promote catalytic activity and suppress carbon deposition for a wide range of gas compositions. Other materials such as copper and lanthanum also have been reported as active anode metals for the direct introduction of large hydrocarbon fuels [182]. Gorte et al. [183] have reviewed different Cu-based anodes. The results show that Cu-cermet anodes have the potential to be used for direct oxidation of carbon fuels whereas they do not have the coking issue of Ni-based anodes. However, long term cell operation with such anodes is yet to be demonstrated. More investigations have to be carried out on biogas-SOFC materials in order to improve the methane conversion, durability of fuel cell and to decrease the material costs.

2.7.3. Carbon deposition

For SOFC operating on biogas, one of the major challenges is to prevent carbon deposition. The gas equilibrium calculation for general biogas (60% methane, 40% CO_2) shows that carbon deposition might occur in the SOFC over a large range of SOFC operating temperatures [157]. Carbon deposition on the active area of the cell reduces the performance and durability and in the worst case, it causes a local thermal stress, which can lead to cell cracks and delamination. Ni is a good catalyst for hydrocarbon reforming reactions. In addition, it also actively promotes carbon deposition on the anode surface. The chance of getting carbon deposition depends on the fuel composition, operating conditions and anodes used in the SOFC. The risk of carbon deposition is much higher in dry reforming on Ni-based anodes due to higher C/H ratio in comparison with steam reforming [152].

Operating parameters such as temperature, current density, and fuel utilization should be regulated in order to avoid carbon deposition. Carbon deposition mainly occurs due to: i) methane cracking at high temperature (Eq. (2-16)) in absence of other reforming agents such as steam and CO_2 [29], and ii) reduction of carbon monoxide or disproportionation (Eq. (2-17)) for high partial pressure of CO and CH_4 at low temperature.

Because the CO_2 partial pressure in biogas is not sufficient, always extra CO_2 or steam is required. Additionally, steam can remove carbon through an endothermic reaction (Eq. (2-18)) [184].

$$CH_4 \leftrightarrow 2H_2 + C_s \quad , \quad \Delta H^0_{298} = 75.6\ {}^{kJ}/_{mol} \tag{2-16}$$

$$CO \leftrightarrow CO_2 + C_s \quad , \quad \Delta H^0_{298} = -173\ {}^{kJ}/_{mol} \tag{2-17}$$

$$H_2O + C_s \leftrightarrow H_2 + CO \quad , \quad \Delta H^0_{298} = 131\ {}^{kJ}/_{mol} \tag{2-18}$$

The steam required can also be produced by the electrochemical reaction of hydrogen (Eq. (2-3)), RWGS reaction or using an external steam generator. Choosing a proper fuel gas composition is essential. Moreover, at high current density, electrochemical reaction rate increases and, as a result, the production of steam and carbon dioxide increases, which reduces the possibility of carbon deposition [163].

In the ternary C-H-O diagram, the theoretical boundaries of carbon deposition and NiO formation can be indicated based on thermodynamic equilibrium calculations at different reaction temperatures and gas compositions. The status of biogas (60% CH_4 and 40% CO_2) is shown in ternary diagram (Fig. 2-5) and located at carbon deposition region at all temperatures as high as 1000°C. Adding steam, CO_2 or oxygen can move the inlet gas composition towards the safe region.

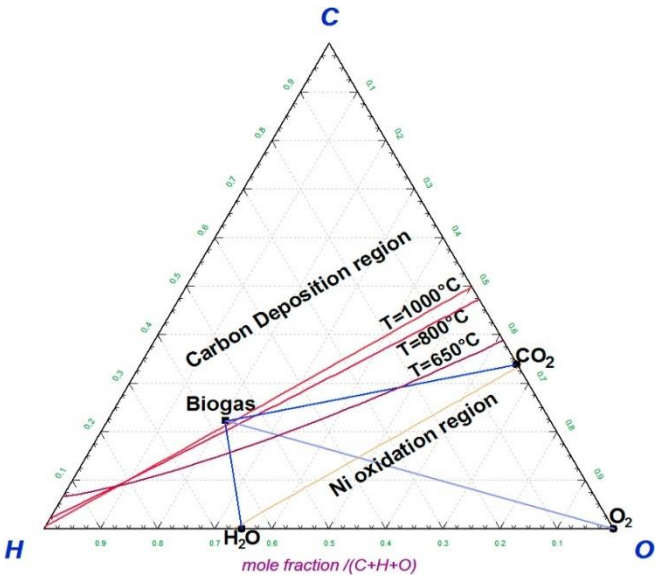

Figure 2-5: Carbon deposition limits in a C-H-O ternary diagram calculated at different temperatures and under 1 atm.

Kuhn and Kesler [185, 186] have investigated carbon deposition thresholds on Ni-based anode under different operation conditions and different gas compositions. First, based on thermodynamic equilibrium calculations, increasing fuel utilization can decrease the likelihood of carbon deposition. The presented experimental studies at 700°C agreed with thermodynamic equilibrium calculations on nickel cermet anode. However, for lower temperatures (600°C), a modified Gibbs free energy for carbon formation has been proposed. Moreover, the influence of Steam to Carbon ratio (SC) and Current Density (CD) on carbon deposition have been investigated. The minimum SC was found to be 1.18 at 700°C to prevent coking.

Girona et al. [187] have determined appropriate operating conditions for biogas fed SOFC. The experimental studies were conducted at constant temperature with two gas compositions (with additional CO_2 and steam to biogas) at open circuit voltage (OCV) and operating at 120 mA/cm^2. A scenario has been proposed for carbon deposition. During the first hours, it is suggested that a film of carbon could form, which leads to degradation. It has also been observed that after a few hours, carbon precipitates germinate and nickel surface becomes active again.

Lanzini and Leone [157] have investigated carbon deposition on anode and electrolyte supported cells for pure biogas fed SOFC at high current density. With a 12-hour SOFC operation, the cell voltage is shown to decrease by 7 and 14% for ASC and ESC, respectively. It is proposed that carbon deposition leads to nickel re-oxidation due to a lack of H_2 and CO on the anode side [188]. To avoid carbon formation for a CH_4-rich-biogas (CH_4/CO_2=2), the amount of required air is determined by thermodynamic calculations (0.2102 mole O_2/mole biogas) and 98.2% methane conversion has been obtained at 800°C. Based on the equilibrium calculation, it has been suggested that operation above 740°C is safe to prevent carbon deposition for CH_4-rich biogas (60% CH_4) composition. Nevertheless, in the absence of extra reforming agents, the chance of coking increases due to local temperature gradient and the non-homogenous gas distribution through the cells. Therefore, thermodynamic calculations cannot guarantee a safe operating condition [163].

An alternative way to avoid carbon deposition is the use of a novel anode obtained by adding other metals to the conventional Ni based anode. Such an approach has been reported by using Cu and CeO_2 in the anode [34]. Cerium oxide or ceria is an important material for hydrocarbons fuelled SOFCs which has highly mobile oxygen vacancies [152, 177]. Pillai et al. [160] evaluated the impact of combining a porous barrier layer on the anode for dry reforming and partial oxidation of methane. They concluded that the barrier layer inhibits the flux of CO_2 and H_2O from the anode to the fuel channel and increases the concentration of reforming agents close to the anode. High current density leads to the production of enough CO_2 and steam on the surface of anode to prevent carbon

deposition. This barrier layer reduces the required current density. It can be observed from Fig. 2-5, that under higher current load the gas composition moves towards a higher partial pressure of oxygen, which is located in the non-carbon deposition region.

2.7.4. Nickel re-oxidation

As mentioned in the previous sections, Ni based anode is one of the preferred materials for hydrocarbon fuelled SOFC due to high catalytic activity. However, there exists a risk of nickel re-oxidation. Due to the lack of fuel gas (high fuel utilization) at high temperatures, oxygen ions that pass through the electrolyte might react with nickel in the anode. Also, if air enters to the anode side because of sealing failure or control of fuel composition, nickel re-oxidation might take place (see Fig. 2-5). Nickel re-oxidation leads to volume expansion and consequently cell or sealing fracture. It is argued that increasing the porosity of the materials could improve the tolerance of expansion due to Ni re-oxidation [189]. Ettler et al. [190] reviewed literature about Ni reoxidation cycles and concluded that 20-25% of the Nickel reoxidation does not lead to electrolyte cracking at 800°C and at lower temperature, the risk is lower. Pihlatie et al. [191] studied the kinetics of nickel re-oxidation on Ni-YSZ anode with intermediate and high temperature SOFCs. Different activation energies and models are proposed for the reduction and oxidation reactions at different operating temperatures. No generation of porosity was observed at low temperature [192]. Vedasri et al. [193] have studied the NiO formation during the cooling procedure of Ni/YSZ anode-supported stack from 800°C to 600°C. A cooling rate of 3°C/min has been suggested to minimize the expansion due to Ni oxidation and prevent cell cracking. The mechanism of Ni re-oxidation for biogas fuelled SOFC has not been elucidated. However, results from other fuels show that increasing the operating temperature to values typical for biogas SOFCs, increases the chance of Ni re-oxidation and these aspects need to be studied more [194].

2.8. Technical evaluation of biogas SOFC performance

So far, the influence of different operating parameters on the solid oxide single cell has been discussed, but as a power generation unit, stacks are generally employed. Due to the cost and risk of stack damages, SOFC modelling is crucial because, to some extent, the effect of operating parameters can be evaluated. Additionally, the energy and exergy efficiency of the stack and integrated systems can be evaluated under various conditions.

2.8.1. Biogas-SOFC stack and system modelling

To evaluate the energy efficiency of biogas fuelled SOFC system, a comprehensive model of the SOFC stack is a useful tool. It is difficult to achieve

100% internal reforming of fuel in SOFC [164], as the fuel utilization should be maintained less than 100% in order to avoid the risk of nickel oxidation. Therefore, the anode exhaust gas always contains some fuel gases and hence the outlet gas should be combusted in a device (i.e. an afterburner). In this section, some studies on biogas-SOFC stack steady state modelling will be reviewed, which are focused on different types of reforming.

A mathematical model of methane reforming reactions (based on heterogeneous reactions) has been developed by Santarelli et al. [162]. This model can predict the gas composition profile along the fuel channel for a biogas fed tubular SOFC stack (with a Ni-YSZ anode supported cell) at different fuel utilization. The model has been experimentally validated. The results show a good performance of SOFC under direct dry reforming of biogas and high methane conversion through the fuel channel. Biogas direct steam reforming has also been investigated with SC: 0.47 at 800°C. Results show the higher effectiveness of steam reforming in comparison with dry reforming due to the kinetically faster reaction and higher H_2 production. Lanzini et al. [195] have developed a model to evaluate the performance of a biogas fuelled tubular SOFC. The model, neglects dry reforming because of lack of dry reforming kinetic data, is experimentally validated. Maximum electrical efficiency was less than 30% due to the low conversion of methane even for low CH_4/CO_2 ratio of 0.5 at 800°C.

A direct internal reforming model has been developed by Wongchanapai et al. [196] in order to study the combined steam, dry reforming and partial oxidation. First, fuel oxidation is considered to generate heat, steam and carbon dioxide for endothermic steam and dry methane reforming reactions. Then WGS reaction is taken into account to convert CO to hydrogen. The reaction rates of partial oxidation and steam reforming have been calculated. However, detailed kinetics of the dry reforming reaction is not explicitly included in calculations.

An energy balance model has been developed for a biogas fuelled SOFC co-generator system by Van Herle et al. [167]. The influence of various parameters such as the fuel inlet composition, stack temperature and current density, have been investigated. Air with a ratio of 1:1 is used in this study for converting methane. The obtained electrical and thermal efficiencies based on Lower Heating Values (LHVs) were 33.8 and 57.6%, respectively. The results also show that using a pressurized system decreases the electrical and thermal efficiency, despite the fact that the single cell voltage might increase by 50-100 mV in the operating system. A small SOFC stack has been modelled by Membrez and Bucheli [197]. Mixed biogas/air fuels with different excess air value (λ) were studied. Thermodynamic equilibrium has been considered to estimate the likelihood of carbon deposition at the operating temperature. Electrical and thermal efficiencies were 38.2 and 46%, respectively. The heat generated from exhaust gas,

afterburner and stack have been used for pre-heating the fuel and air, and domestic hot water.

Van Herle et al. [16] have developed a model for a 100 kW biogas-SOFC system. This model was developed to investigate the performance of the complete SOFC system with steam reforming and POX. For steam reforming, the minimum required steam/carbon ratio of 0.5 had been chosen based on thermodynamic calculations and considering a safety factor. Obtained electrical efficiency was 48.7%. Generated heat in SOFC and after-burner was used for pre-heating and fuel reforming. System electrical efficiency decreased to 43% for partial oxidation due to fuel consumption (λ=4.5). In this case, oxygen to carbon ratio was 0.3 and thermal efficiency of the system was above 46%, which was 6% higher than steam-reformed biogas system. Piroonlerkgul et al [166] have developed a model to thermodynamically analyse the performance of SOFC with combined biogas reforming. The model was validated by conducting experiments with various inlet gas (CH_4–CO–H_2 mixtures). The required steam and air for biogas reforming have been calculated at different temperatures. They concluded that the smaller concentration of CO_2 in the biogas is an advantage that reduces the energy losses from the system exhaust gas. Most modelling studies have hitherto investigated the sensitivity of steam and oxygen to the methane reforming reaction, however, the influence of CO_2 partial pressures has never been reported. This is highly encouraged as a future research activity.

2.8.2. Integrated system modelling

SOFCs have some additional advantages in comparison with other types of fuel cells. Operating temperature of SOFC is high and this allows using the residual heat in co-generation cycles. Higher system efficiency can be achieved by CHP generation. In a CHP system, the exhaust gas from fuel cell, which contains unconverted methane and hydrogen, can be transferred to downstream devices, such as after-burner, gas and steam turbine in order to generate heat or mechanical power. The generated heat/power can be used for different purposes. For instance, raising the temperature of anaerobic digestion increases methane production in an anaerobic bio-reactor [198, 199]. The overall thermal and electrical efficiency of SOFC integrated system (with gas or steam turbine) can reach up to 90% at proper conditions and optimum system configuration [200].

System design can be evaluated by calculating the system efficiency and this can be further improved by integration. However, the integration depends on the application requirements and limitations. Zhang et al. [201] reviewed different SOFC integration strategies (with different types of fuels) that include applying various designs of the Gas Turbine (GT) with pressurized, non-pressurized SOFC,

indirect thermal coupling and fuel coupling. Moreover, three different configurations of SOFC with gas–cooled nuclear reactor cycle, gasification cycle and humidified air turbine cycle were reviewed.

Piroonlerkgul et al. [166] investigated the performance of different configurations of biogas fed SOFC. In addition to dry reforming with CO_2 present in the biogas, different reforming agents, including steam, air and mixed reforming were used. Thermodynamic equilibrium has been assumed to calculate the gas compositions. Use of afterburner, steam turbine and Anode Gas Recirculation (AGR) has been made for enhancing the efficiency with the different configurations. The overall electrical efficiency is around 55% (LHV based) for combined steam/dry reforming. The results of the second configuration (air-fed biogas-SOFC system) showed that both power density and overall efficiency decline with increasing the air content. Generally, the electrical efficiency of the integrated system decreases with increasing amount of reforming agents. However, these results illustrate that high electrical efficiency (59%) can be achieved with a new approach while residual heat from afterburner is used for fuel processing (reformer and steam generator). Wongchanapai et al. [196] have used a model to study a combined SOFC with a Micro Gas Turbine (MGT) fed by biogas. The influences of SOFC and MGT operating parameters have been studied. The results show that the SOFC efficiency is higher when steam is used as a reforming agent instead of partial oxidation. High fuel utilization improves the SOFC generated electrical power, but extra fuel is needed to produce the required heat. Total system efficiency of 69.7% has been achieved for a high fuel utilization (U_f=0.90). The decline in electrical power production of SOFC has been observed for high amounts of air (as a methane conversion agent). It has been compensated by MGT and it has been shown that the air/steam ratio has a minor effect on electrical power production.

Farhad et al. [156] have developed three different configurations for biogas-SOFC with different fuel processing. In the first model, anode gas recirculation is considered. All fuel streams are assumed to be in thermodynamic equilibrium at the operating temperature. According to the modelling calculations, the minimum AGR flow to prevent carbon deposition is a function of fuel utilization. For instance, it is equal to 63% of SOFC inlet flow at 80% fuel utilization. The maximum electrical efficiency (42.4%) is achieved with anode exhaust recirculation system. However, the maximum CHP efficiency (80%) is obtained in the system that works under partial oxidation of biogas, however, the maximum

exergy destruction took place with this system and the largest share was by the air heater.

Tjaden et al. [202] investigated the performance of a small-scale (25 kW_{elec}) biogas fed SOFC, focusing on developing appropriate gas cleaning and reforming units. Autothermal reforming has been proposed according to biogas composition. Additional steam and oxygen required are determined in order to achieve a zero heat duty for an external reformer (the required heat has been supplied by methane partial oxidation). Operating voltage and U_f sensitivity analysis have been carried out to evaluate the influence of SOFC operating conditions on system efficiency. The results show that applying direct internal reforming considerably increases the total efficiency and slightly the electrical efficiency. The maximum electrical efficiency achieved under steam reforming and at the optimum condition was 50.65%. However, the system costs under partial oxidation reforming were expected to be the lowest due to the lowest required cell active area for the same power production.

A cycle-tempo model has been also developed within our research team by Patel et al. [203] to evaluate a fuel cell gas turbine system with different fuels including methane. It is proposed that by using only 20% of steam along with methane can avoid carbon deposition due to the use of AGR. Further, it concluded that there is always enough steam from the electrochemical reaction of fuels in the proposed system to prevent carbon deposition. The reported energy and exergy efficiencies of methane-SOFC system are 78.3% and 75.5%, respectively.

2.8.3. CFD modelling

Computational Fluid Dynamic (CFD) models are helpful tools to predict temperature, pressure and species distribution in biogas fed SOFCs. In CFD models the transport equations (mass, energy, species, and momentum) are coupled to the electrochemistry equations. The CFD model can estimate the extent of electrochemical reaction through the fuel channel and accordingly, local temperature, gas composition, and current density can be calculated. Considerable research work have been carried out on internal steam methane reforming simulation compared to methane dry reforming [204-207].

A quasi-two-dimensional numerical simulation has been developed by Nishino et al. [208] to study a tubular biogas fed SOFC. The feed tube was considered as a reformer for biogas. Fuel gas has been varied with different methane partial pressures while SC ratio is changed in a range between 2 to 4. Methane dry reforming is only implicitly included in this model because it does not need to be explicitly specified since both steam and dry methane reforming reactions are considered to be mechanistically equivalent. When methane Concentration in

biogas is higher than 40%, methane is completely reformed for all the steam to carbon ratios due to enough catalyst material in the feed tube (1 gr/cm^3). The results of this study are helpful for thermal management of indirect biogas reforming. The cell voltage reduces with a decrease in the methane partial pressure in biogas under a current density of 400 mA/cm^2, which is attributed to the decrease in the electromotive force.

A three-dimensional CFD simulation has been developed for a Ni-YSZ anode planar SOFC fuelled by biogas/steam mixtures. This study investigated the location of increased thermal stresses and the likelihood of solid carbon deposition [209]. Results demonstrate that equimolar CH_4/CO_2 biogas improves the cell performance and carbon deposition possibility is higher for methane-rich mixtures. Nevertheless, major coking has not been observed under closed circuit operation because of the electro-oxidation reactions of carbon. The coking possibility is greater in the anode/gas phase interface. The maximum power production has been achieved for equimolar CH_4/CO_2 biogas with just 10% steam and increasing the steam concentration leads to power losses.

Elizalde-Blancas et al.[210] have developed a numerical model to assess the influence of actual biogas composition on the performance of an anode supported button cell. The inlet gas composition has been determined based on the equilibrium composition of biogas at 800°C. Simultaneous oxidation of hydrogen and carbon monoxide has been considered in this study. Internal reforming has been modelled using two reactions, MSR and WGSR. In contrast, Ogura and Wakamatsu [211] only considered methane dry reforming and reverse WGSR to calculated temperature and concentration of gas species distributions along the fuel channel. A paper-structured catalyst is used to overcome the problem of local cooling due to the direct biogas reforming. The results of three-dimensional temperature profiles have been validated by experimental measurements for both cases of homogeneous and functionally-graded paper structure catalysts. This model has been extended for a three-cell-stack. Distribution of temperature is more homogeneous for this stack, which improves the durability.

2.9. Implementation of Biogas SOFCs

2.9.1. Latest developments in pilot and demo-scale implementation

Fuel cell technology is moving from research and prototype demonstration to the industrial demonstration. The technology is being developed for a broad range of power generation applications [212]. Several demonstrations for hydrogen and natural gas fuelled SOFC have been carried out [213-218], however only a few have been dedicated to biogas-SOFCs.

In the Biocell project (for pilot plants in Barcelona), biogas from a WWTP has been used in two types of fuel cell [219]. The first one is PEMFC that requires

external cleaning and reforming. Biogas has also been injected directly into an SOFC after cleaning process. The cleaning system consists of four steps. Biotricking filter with the live bacteria has been used for desulphurization. Supplementary purification was carried out by iron oxide, activated carbon and dryer to completely remove H_2S and halogenated compounds. Siloxanes have been reduced to 0.1 $mgSi/Nm^3$ (less than 0.1 ppm) as well. This pilot plant is designed for 2.8 kW_{elec}. Electrical and thermal efficiencies for the SOFC pilot plant were 24.2 and 39.4%, respectively, which are much higher than that for PEMFC pilot plant [220].

A part of SOFCOM demonstration project (DEMO 1 Torino, Italy) is dedicated to investigate the high efficiency combined cooling, heating and power (CCHP) based biogas fuelled SOFC [221]. Moreover, the influence of the fuel contaminants and biogas processing on the SOFC is studied. For minimizing emissions, the possibility of CO_2 separation from the anode exhaust gases is examined [222]. Achievements of this project will be used in the DEMOSOFC project that is known as the first European industrial biogas-SOFC [223]. Three SOFC modules will be utilized to generate a total of 175 kW of electrical power and 90 kW of thermal energy. An electrical efficiency of 53% is expected. The project is planned to run until the end of 2020.

The objective of the BioZEG pilot plant is to develop a zero emission hydrogen station based on local renewable sources [224]. An upgrading gas system produces biomethane from biogas (municipal waste landfill). Through a sorption enhanced reforming (steam reforming) hydrogen is produced and CO_2 capture is carried out by a solid CaO-based sorbent. Hydrogen is sent to a 20 kW_{elec} SOFC stack. The generated heat in the SOFC is used for the CO_2 absorbent regenerating. Bloom Energy is an SOFC manufacturer who develops SOFC units that can deliver a power of 210 kW with natural gas or biogas [225]. The net electrical efficiency is claimed to be in a range of 52-60%. The system is called as “carbon neutral” on direct-biogas.

Besides biogas, ammonium and phosphate are also the products of WWTPs that should be recovered in order to prevent their returning to the surface water. As mentioned in section 4.3, ammonia removal can be replaced by ammonia recovery and subsequently ammonia can be used in an SOFC. This concept changes an electricity-consuming process step to an energy -producing process step. Moreover, ammonia recovery from AD may increase methane production by alleviating the inhibition by dissolved NH3. Hemmes et al. [226] proposed an innovative technique to integrate the purification of wastewater with the power generation by SOFC. Ammonia and phosphate are removed in the form of struvite $MgNH_4PO_4 \cdot 6H_2O$, and subsequent decomposition of the struvite to release ammonia. The released ammonia can be fed to an SOFC. Results show that this process is more cost-effective than conventional nitrogen removal process. The

first pilot plant of this concept has been initiated by DHV at Waterboard Hunze en Aa's in the Netherlands. There are on-going multiple projects and research activities at Delft University of Technology aimed at the development of integrated waste to energy SOFC systems. The objective of LOTUS project is to develop an advanced wastewater treatment technologies at a selected location in New Delhi and use produced biogas in SOFC [227]. A similar project at "TU Delft Global Initiative" focuses on biogas-SOFC energy system for rural energy supply [228]. The N2kWh project aims to develop a pilot installation using biogas and recovered nitrogen from manure and urine/reject water in an SOFC [229].

2.9.2. Techno-economic evaluation of the biogas-SOFC system

With the ongoing implementation of pilot and demonstration scale biogas-SOFC systems, it becomes possible to assess the economic feasibility of biogas SOFCs. There are two important challenges: 1) the economics of the gas cleaning unit, as supplying clean biogas for SOFC increases the gas cleaning cost, and 2) the cost of SOFC itself. Techno-economic characterization of the biogas-SOFC system can be helpful in order to illustrate the obstacles from an economic point of view.

Pipatmanomai et al. [230] carried out an economic evaluation of biogas to electricity system. This system primarily consists of an H_2S gas cleaning unit and a modified IC engine (1.6 kW) coupled with electric generator. In this work, H_2S removal has been focussed and a 2% KI (potassium iodide) - impregnated activated carbon adsorption is used for this purpose. It is mentioned that this method of H_2S removal increases the removal efficiency to 100%. Mainly operating cost of H_2S removal unit increases the payback period from 4 (without H_2S removal) to almost 8 years. Electricity price and governmental subsidy play important roles in the payback period, as without subsidy the payback period can go up to 11 years.

Papadias et al. [231] carried out an investigation on an integrated system. Adding AD-SOFC system to an existing waste water treatment (WWT) plant could yield positive values of internal rate of return on investment (IRR) at average electricity prices. This could compete with other options for using biogas to generate electricity. There is an uncertainty in the SOFC-CHP equipment capital costs, but the normalized cost is in the range of \$3600-4000 kW^{-1}. The economic analysis of biogas production shows that the cost of electricity is about 10.5 c\$/kWh (for a conventional plant generating 300 kW_e). The cost of gas clean-up represents roughly 20% of the cost of electricity. The H_2S (iron oxide bed) and siloxanes (carbon bed) removal processes contribute most to the cost.

Trendewicz and Braun [15] carried out a techno-economic investigation on an integrated SOFC-CHP plant with WWTP in 2013. The results show that the electricity price is competitive with other grid price roughly 5-8 c\$/kW h. The

estimated costs for the whole system could be between 3590 and 5780 $/kW for large and small scale plant respectively. In order to analyse the performance of the Biogas-SOFC plant, an Aspen Plus model has been developed with a gas cleaning unit.

Further investigations are highly encouraged to assess the economic feasibility of biogas-SOFC system, especially techno-economic evaluation of AD-SOFC integrated system with thermal pre-treatment. Moreover, it is recommended to assess the concept of producing ammonia as a fuel from the techno-economic point of view in WWTPs. Ammonia separation increases the operating and capital cost of WWTP while on the other hand, there is an advantage of using ammonia as a fuel in SOFCs.

2.10. Nitrogen removal by conventional techniques

Conventional biological treatment like aerobic digestion is most typically used nitrogen removal processes in wastewater treatment plants due to lower capital costs and fewer operational problems [5]. However, the operating costs are high due to the high amount of dissolved oxygen (DO) demand, which is the most essential parameter in the aerobic digestion process. The DO concentrations generally range between 0.5 to 2.0 mg/L_{water}, based on type of influent and aeration conditions [225, 232] and makes total aeration energy demands very high. The energy requirement for wastewater treatment based on the treatment method can reach to 15.2 MJ/m^3 while 53% of that is attributed to aeration [233].

In 18 and 19th-century, several processes were investigated to treat the digester liquid with nitrification/denitrification by the addition of organic carbon sources. These processes are based on biological transformation of ammonia to nitrate. Denitrification occurs during the anoxic period and nitrification takes place during the aerobic period. Through the biological nitrogen removal, first organic nitrogen converts to ammonium ($NH4^+$). Then, ammonium reacts with oxygen to produce nitrite ($NO2^-$) which is followed by oxidizing of nitrite to nitrate ($NO3^-$) during the nitrification process. Finally, produced nitrate converts to nitrogen by heterotrophic bacteria through nitrification process in presence of external carbon source determined by biochemical oxygen demand (BOD). Oxygen demand for complete nitrification of ammonium is 4.57 g O_2/g N [234]. Additionally, some amount of alkalinity is required for nitrification reactions. It is also claimed that 4 mg/l of DO is sufficient to achieve a sustainable nitrification. Electricity demand for the nitrification (aeration) is 17 MJ/kg N [139] which can be about 70–80% of the total energy demand of a municipal WWTP [235].

In the late 90s, anaerobic ammonium oxidation (anammox) process was introduced. Strous et al. [236] claim that this process can significantly reduce the aeration energy demands and requires no organic carbon source. However, nitrogen removal through an advanced Sharon/Anammox process still requires a considerable amount of power (14 MJ/kg N) [237]. Even with applying new nitrogen removal techniques such as using anaerobic membrane bioreactors, electrical energy required is still high and energy requirement of around 18.3 MJ/kg-N (considering a TAN of 100 mg/l) is reported in literature [238]. On the other hand, there is an alternative approach to convert nitrogen to ammonia in order to use it for different applications.

A conventional wastewater treatment plant is shown in Fig. 2-6.The concentration of organic compounds and nutrients in wastewater stream is increased through primary and secondary sewage treatment. The activated sludge stream is more suitable for use in the waste-to-energy strategy [9]. Activated sludge is conveyed to the anaerobic digester where biogas is produced from organic materials. The concentration of ammonia/ammonium is high in the influent stream to anaerobic digestion (AD). Moreover, ammonia concentration also increases during the AD process. Ammonia removal is essential because high ammonia concentration (4-5 gr NH_3-N/l) is an inhibitor of methanogenic bacteria [89, 239]. The level of toxicity depends on AD conditions such as temperature, pH, retention time and concentration of organic and inorganic compounds inside the anaerobic digester [240]. Furthermore, removing ammonia from AD also decrease the DO demand in aeration due to the low concentration of ammonia in recirculated water stream [237]. This reduces the energy demand during aeration process.

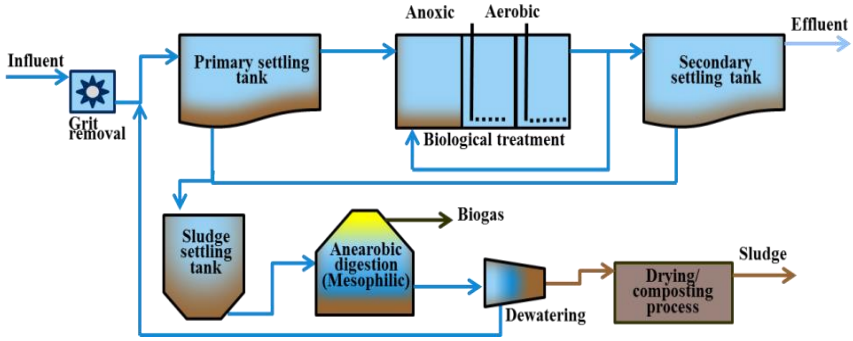

Figure 2-6: Conventional wastewater treatment plant including nitrogen removal process (aeration) and anaerobic digestion.

Several studies have been carried out on nitrogen removal/recovery processes like direct stripping either with air or with biogas [241, 242], ion exchange [243], electrodeionization [244], pre-treatment by microwave radiation [245], electrodialysis and pre-evaporation (hydrophobic) for a wide range of total nitrogen (TA) concentration and different wastewater resources [246-248]. For instance, energy demand for ammonia removal through the air stripping process is around 40-50 MJ/kg N [237]. Luther et al. [249] have investigated ammonia recovery from human urine (with a high concentration of ammonium) by electrochemical cell. The electrical power demands for different concentration of ammonium are shown in Table 2-4. It should be noted that during this process, some amount of hydrogen is produced which is worth approximately 15.5 MJ/kg N and decreases the overall energy demand for ammonia recovery. This study is focused on the chemical precipitation process for ammonia recovery with heat generated from an SOFC stack.

Table 2-4: Ammonia extraction from synthetic and undiluted human urine using an electrochemical cell.

Ammonium concentration flux (gN/m^2d)	Current efficiency (%)	Electrical power demand (MJ/kg N)
384 ± 8	61±1	43
275 ± 5	55±1	47

2.10.1. Precipitation process

Generally, the Ammonia-Nitrogen (NH_3-N) and Ammonium-Nitrogen (NH_4^+-N) concentration is moderately low in the wastewater stream (roughly 50 mg/l) [250]. But, the concentration is higher after primary wastewater treatment. Struvite precipitation is one of the interesting methods for ammonia recovery when the concentration of ammonium is in the range of 0.1 to 5 g N/l [251]. Magnesium ammonium phosphate (MAP) so-called struvite, is crystallized by adding magnesium ion to wastewater in order to gradually increase the pH level Eq. (2-19). To achieve high-purity struvite, it is recommended to raise the pH value to 9.0-9.5 [252, 253]. Struvite crystals are formed inside the reactor with an average size of 42 to 80 µm [237].

$$Mg^{2+} + NH_4^+ + PO_4^{3-} + 6H_2O \rightarrow MgNH_4Po_4.6H_2O \quad (2\text{-}19)$$

Next, in the decomposition reactor, the struvite crystals can be decomposed into magnesium hydrogen phosphate (MHP) and ammonia Eq. (2-20) by absorbing

heat. Struvite is thermodynamically unstable and dehydration starts just above the room temperature [254]. Sarkar [255] found that the maximum decomposition takes place at 106°C based on the results from derivative thermogravimetric analysis (DTGA). The remained MHP is returned to the crystallization reactor to react with ammonium from the wastewater stream again (Fig. 2-7).

$$Struvite + Heat \rightarrow NH_3 + 6H_2O + MHP \quad (2\text{-}20)$$

This method is known as a cost-effective technique in comparison to aeration of elemental nitrogen gas in conventional WWTPs [237]. Energy demands of struvite production are estimated around 9.3 MJ kg^{-1}N electricity (5.6 MJ kg^{-1}N for the process itself). Other energies including the energy need for production of magnesium and phosphorus at the beginning of the process is not considered [139].

Theoretically, the stream released from the pyrolysis of struvite contains an ammonia-water mixture with 14.3 mol.% (13.6 mass%) ratio of ammonia. The decomposition stage of the struvite needs around 2650 kJ/kg of produced stream (See Appendix). Moreover, phosphorus reduction is also another advantage of this method and phosphate can be recovered from struvite decomposition. Phosphate is a limited source in the environment and essential material in the food industry which is also used as a fertilizer. Schematic of ammonia production from wastewater influent is shown in Fig. 2-7.

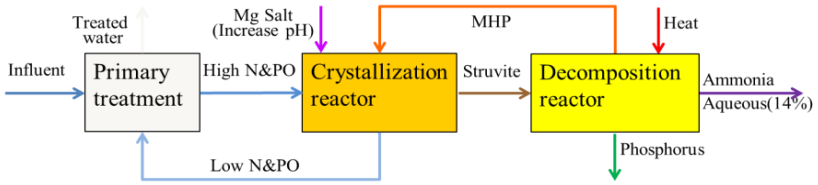

Figure 2-7: Scheme of struvite precipitation process.

2.10.2. Increasing ammonia concentration

Regarding the ammonia production process from struvite, the ammonia concentration would be 14.3 mol.% (based on the stoichiometric ratio shown by Eq. (2-20)). In the previous section, the ammonia-SOFC system efficiency has been evaluated with respect to the struvite decomposition process. There is a possibility to increase the ammonia concentration in the inlet stream by applying the distillation method. Thus, it is interesting to investigate whether increasing ammonia concentration improves net system efficiency.

Distillation is a physical separation process that used to remove components from a liquid phase by selective boiling and condensation. The liquid stream is being brought in contact with a gas stream in each stage (tray) inside a distillation tower [256]. A distillation tower can be used to supply an ammonia-water mixture, rich in ammonia, to be fed to the SOFC. The process was found to be effective while the nitrogen discharge regulations (concerning the ammonia left in the waste-water) are met.

Separation of the less volatile components concentrate in the liquid phase (in this case water), and the more volatile one (ammonia) can be accomplished by using multiple stages in series with a reflux ratio between stages [256]. However, in practice, specifically for ammonia-water mixture, there are limits to the number of stages, the reflux ratio and ideal stages in this process [256]. First, the ammonium-water mixture (in vapour phase) is fed from the bottom stage of the distillation tower. Because of high temperature, the gasified mixture rises through the packed column, and this mixture is condensed at the top of the tower. A larger ammonia Concentration is achieved after condensation of vapour in top of the distillation tower. Then, based on the reflux ratio, part of the condensed mixture flows back into the distillation tower, and flow with high ammonia concentration discharges. Typically reboiler is used to provide heat to the bottom of distillation towers, however, in this case, because of the high temperature of the flow from the struvite decomposition reactor (106°C), the presence of a reboiler is not required for the distillation tower in this system. For more information and details regarding the distillation tower, refer to Ref. [256-258].

A simplified ammonia recovery model (based on distillation) has been developed using Aspen plus software to determine energy consumption through the distillation process. Various reflux ratios have been applied to increase the ammonia concentration (Table 2-5).

Table 2-5: Ammonia recovery results from Aspen plus distillation tower model (without reboiler equipment).

Influent Temp.(°C)	Reflux Ratio	Top stream (vapour)			Condenser Heat Duty		Bottom stream (liquid)	
		Ammonia concentration	Temperature (°C)	Flow rate (kg/s)	(kcal/s)	(MW)	flow rate (kg/s)	Ammonia (ppm)
106	5,3	90 %	50	1.46	-4,7 E+03	-19.7	8,54	2340
106	3,4	60 %	76	2.18	-4,3 E+03	-18.0	7,82	1923
106	1,3	30 %	90	4,32	-3,14E+03	-13.1	5.68	1763

Increasing the reflux ratio increases the ammonia concentration in the vapour stream from the top of the distillation tower. The reflux ratios have been varied to change the ammonia concentration from 14% to 30, 60 and 90 mol.%. Results show that it is possible to obtain a high concentration of ammonia (90%) with only 5 (theoretical) stripping stages. The outlet liquid stream still contains a small

amount of ammonia (0.2 %), but it is still too high to be released to receiving waters. This stream should flow back to the wastewater treatment cycle. The temperature of the bottom streams (liquid) mentioned in Table 2-5 is 96°C for all the three cases. This stream can be circulated in a heat exchanger to increase the temperature of ammonia-rich flow (top stream in distillation tower).

Ammonia water vapour with 30 mol.% ammonia can be condensed and stored in closed containers at atmospheric pressure and ambient temperature. Storage of ammonia in the liquid phase is desirable for transportation, and this limits possible exposure to the environment [131]. In section 6.3, the operation of an SOFC system with different ammonia concentrations, including 30% ammonia, will be studied.

The vapour stream in a distillation tower should be cooled down further to achieve higher ammonia concentrations. For instance, an ammonia concentration of 90% can be obtained by decreasing the vapour stream temperature to 50°C. Heat duties of the condenser for different reflux ratios are illustrated in Table 2-5. Low-temperature water is used to fulfil the cooling in the condenser of the distillation tower. A heat pump is used to decrease the temperature of circulation water. In the next section, integration of the struvite decomposition reactor, heat pump and distillation tower are explained.

2.11. Final remarks

SOFC systems bring a good opportunity for future applications because of high efficiencies, fuel flexibility, and environmental friendliness aspects compared to the conventional IC engine based CHP approach. Biogas as a renewable fuel is well-matched with SOFC systems, despite the fluctuation of methane partial pressure in biogas. The high quality residual heat from the SOFC can improve the biogas production by thermal pre-treatment of sludge. This increases the overall system efficiency. Due to the possibility of biogas production in small scales and modularity of SOFC stacks, there is no size limitation for these integrated systems unlike for the traditional biogas applications. This advantage can increase the implementation in rural off-grid situations. Latest developments show that the biogas-SOFC is reaching a mature technology status, but several challenges should still be solved before the commencement of commercializing full-scale biogas-SOFC systems.

One of the most essential challenges is the durability of operation with respect to contaminants in biogas. Several experiments have been conducted to understand the tolerance of contaminants on SOFCs. Some contradictory results have been reported which show the necessity of further investigations. Moreover, biogas reforming is influenced by contaminants and this also depends on the type of reforming agents. Internal dry reforming is the most interesting reforming reaction for biogas-SOFC operation, due to the existence of CO_2 (reforming agent)

and CH_4 (fuel) in biogas. But, methane dry reforming is not understood as much as steam reforming. For instance, only a very few studies have focused on the kinetics of internal dry reforming. Also, there is no comprehensive investigation on the effect of contaminants like H_2S on dry reforming reaction. On the other hand, it has been proven that depending on cell materials, the performance can be fully recovered after removing contaminants when the initial contaminant concentration was low. Regarding the biogas-SOFC anode, high electronic conductivity, high methane conversion and low carbon deposition and degradation are favourable. In contrary to Ni cermet anodes, there are only a few experimental investigations carried out on ceria based anodes containing Cu, Pt, Au and Ag anodes in biogas-SOFC, but these show promising results.

Experimental studies have shown the feasibility of using dry reforming to reform methane in biogas. However, the results have not been achieved in complete system experiments and generally steam reforming and partial oxidation have been applied in order to prevent carbon deposition. Anode gas recirculation is an alternative to avoid the use of additional reforming agents. Integrated system modelling (steady-state) investigations have been performed on biogas-SOFC with AGR but, to the best of the knowledge of the authors, there have been no experimental studies reported on biogas-SOFC with AGR system. There have also been some modelling studies on biogas-SOFC stacks with combined reforming/ATR, however, without considering the influence of the dry methane reforming reaction. Moreover, developing biogas-SOFC dynamic models is also highly encouraged in order to predict the performance and limitations of biogas-SOFC system operating under different electrical power demands.

Nowadays, the cost of SOFC stacks seems a major barrier for further development of biogas-SOFC systems. Based on the material investigations and new manufacturing techniques, the SOFC costs are expected to come down to some extent in the near future. High efficiencies of biogas SOFC systems, make such systems capable of competing with conventional power generation devices. However, without subsidy and governmental support, it is difficult to make the biogas-SOFC system commercially viable, unless the SOFC costs come down significantly. Integration of SOFC with gas or steam turbine shows very high efficiencies and might be an interesting approach for the development of Biogas-SOFC systems. On the other hand, there is no investigation carried out specifically on the efficiency of complete AD-SOFC integrated system (considering thermal pre-treatment) regarding the optimum heat to power ratio for such a system. Additionally, investigating the use of ammonia (from WWTP) mixed with biogas for SOFC presents an interesting option to promote the self-sustainability of WWTPs. Despite all these challenges, some demo projects show the feasibility of implementing the biogas-SOFC systems.

Chapter 3

Biogas Internal Dry Reforming in SOFC

In this chapter, Internal dry reforming (IDR) of methane for biogas fed solid oxide fuel cell (SOFC) applications has been experimentally investigated on planar Ni-GDC (cermet anode) electrolyte supported cells. This study focuses on the effect of CO_2 concentration, current density, operating temperature, and residence time on internal methane dry reforming. A single cell is fed with different CH_4/CO_2 mixture ratios between 0.6 and 1.5. Extra CO_2 recovered from carbon capture plants can be utilized here as a reforming agent. The I-V characterization curves are recorded at different operating conditions in order to determine the best electrochemical performance while the power production is maximized, and carbon deposition is suppressed. The outlet gas from the anode channel is analysed by a micro gas chromatograph to investigate methane conversion inside the anode fuel channel and understand its influence on the cell performance.

This chapter has been published in Journal of Energy Science & engineering (2021).

3.1. Introduction

Waste to energy conversion is one of the most important technology to improve sustainability as it simultaneously reduces the fossil fuel consumption and greenhouse gas emission. High concentration of nutrients in wastewater streams is interesting for energy recovery [259]. Waste stream contains organic compounds that can be converted to biogas through anaerobic digestion (AD) process [260]. Biogas consists of methane, carbon dioxide and traces of contaminants like hydrogen sulphide and volatile organic compounds (VOCs) [118, 261]. Biogas produced is commonly flared in conventional wastewater treatment plants (WWTPs) hence increasing greenhouse gas emissions[262]. For the large scale WWTPs, an internal combustion (IC) engine can be used to produce heat and power simultaneously in combined heat and power (CHP) systems [82]. Based on AD conditions and the source of the wastewater stream, the concentration of methane is in the range of 50-70 mol.% and this might be different for different seasons due to different ambient temperatures [9, 167]. High concentration of CO_2 brings down the energy density of biogas which leads to power de-rating of biogas fuelled IC engine [263]. Moreover, fluctuation of methane concentration also influences the IC engine performance and NOx emission is significantly high at high combustion temperature [85].

Replacing the IC engine with Solid Oxide Fuel cell (SOFC) can improve the power production and makes the whole system more sustainable in terms of energy efficiency and emission levels [264]. SOFCs are more efficient and fuel flexible in comparison to IC engines [15]. However, biogas should be reformed to a hydrogen-rich gas either internally or externally for a biogas-SOFC system [220]. SOFC can tolerate high concentration of CO_2 because this is not a toxic gas for SOFCs. Additionally, it aids methane dry reforming reaction at high operating-temperatures [265]. The R ratio is defined as the partial pressure of CH_4 to CO_2 ($R=CH_4/CO_2$) and indicates the amount of dry reforming agent (CO_2) present in the biogas. The R ratio may change at different biogas production conditions. On the other hand, concentrations of H_2S and other contaminants such as siloxanes in biogas should be reduced to a few ppm levels (even less than 0.5 ppm) [98]. High concentration of contaminants has an influence on the electrochemical performance and increases the cell degradation rate. Using a gas cleaning unit is essential for biogas-SOFC systems [202, 266].

Internal reforming is more efficient and cost-effective method in comparison with external reforming [267, 268]. Generated heat through the electrochemical reactions of fuel is used for the endothermic reforming reactions, which decrease the cooling demand of SOFC stack. However, some challenges such as slow kinetics, high thermal stresses and risk of carbon deposition make this a complex method [174]. There are relatively few research studies on biogas fuelled SOFCs specifically operating under internal reforming conditions, with limited experimental investigations on dry reforming [269].

Shiratori et al. [147] have used actual biogas (with R fluctuating between 1.4 and 1.9) and simulated biogas (R=1.5) fuels for Ni-ScSZ button cell. No carbon deposition was observed for the simulated biogas under a current density of 2000 $A.m^{-2}$ whereas, severe carbon deposition took place during the long-term experiment with actual biogas. Lanzini and Leone [157] have recommended using an extra 1.2 mole of CO_2 to each mole of biogas (R=0.55) in order to achieve a stable voltage in biogas dry reforming for Ni-GDC (ceramic–metallic composite) electrolyte supported cell (ESC) at a current density of 3000 $A.m^{-2}$. The same experiment has been conducted for a Ni-YSZ anode supported cell (ASC) and the operating condition with R=0.67 at a current density of 5000 $A.m^{-2}$ has been advised. An equimolar CH_4/CO_2 feed gas composition (R=1) is recommended by Yentekakis et al. [158] to maximize the electrical power output for Ni-YSZ and Ni-GDC SOFC at 875 and 700°C, respectively. This maximum power is achieved at a cell voltage of 0.450 V. In this study, a non-commercial cell was designed with an electrolyte tube with a thin film coated inside (anode) and outside (cathode) of the tube. On the other hand, a negligible carbon deposition has been observed by Goula et al. [270] for the methane dry reforming experiments with R>1.0 performed for a Ni-YSZ anode supported cell in open circuit voltage (OCV) condition at 800°C. The stability (stable voltage at constant current density) of an ASC with Ni-YSZ anode was studied for rich-methane biogas (R=3.0) [160]. The stability was improved by increasing the CO_2 concentration by 20% and the operating CD to 16000 $A.m^{-2}$. It has also been reported that adding CO_2 to general biogas composition decreases the operating voltage of the cell which results in reduced system efficiency [160]. Staniforth and Ormerod [161] have studied the impact of methane concentrations on the performance of a small tubular SOFC with Ni-YSZ anode. They found that at a methane concentration of 45% (R=0.82), the obtained power was maximum corresponding to the high concentration of H_2 and CO through internal dry reforming at 850°C. Direct internal dry reforming of biogas in a tubular (Ni-YSZ anode) SOFC was

performed with different R ratios of 0.43, 0.32, and 0.25 where the number of moles of CO_2 was varied. Performance maps of the SOFC for a wide range of current densities under different fuel flow rates were determined. It is claimed that dry reforming is more effective for an R value of 0.43 [162]. The results of these experimental studies are summarised in Table 3-1.

Table 3-1: Overview of some of experimental studies on internal dry reforming of biogas in SOFC

Cell anodes	***Temperature (°C)***	***Cell type/size***	***Current density /Voltage***	***Fuel***	***Ref.***
Ni-ScSZ (ASC)	800	Button cell	5000 & 2000 ($A.m^{-2}$) 2000 ($A.m^{-2}$)	Actual biogas Simulated (R=1.5)	[147]
Ni-GDC (ESC) Ni-YSZ (ASC)	850	Circular cell (D=80mm)	3000 ($A.m^{-2}$) 5000 ($A.m^{-2}$)	R=0.55 R=0.67	[157]
Ni-YSZ Ni-GDC	875 700	non-commercial	0.45 V 0.45 V	R=1.0	[158]
Ni-YSZ	875	Button cell (non-commercial)	1300 ($A.m^{-2}$)	R=1.0	[270]
Ni–YSZ (ASC)	800	Button cell	4000-16000 ($A.m^{-2}$)	R=3.0	[160]
Ni-YSZ	850	Tubular cell	0.7 V	R=0.82	[161]
Ni/YSZ (ASC)	800	Tubular cell	1600 ($A.m^{-2}$)	R=0.43	[162]
Ni(Au)-GDC	600-640	Tubular cell	Up to 2000 ($A.m^{-2}$)	R=1.0	[271]
Ni-YSZ (ASC)	800	Circular cell (D=56 mm)	1600($A.m^{-2}$)-0.6 V	R=1 with 6% humidity	[34]

There are also some studies carried out to evaluate the effect of CO_2 partial pressure on dry reforming reaction for different catalysts. Xu et al. [159] proposed an R ratio of 0.77 as an optimum gas composition for dry reforming over a Ni–Co bimetallic catalyst. It is claimed that a higher amount of CO_2 is not beneficial in preventing gradual catalyst deactivation and it might increase the risk of Ni re-oxidation [272]. Guerra et al. [163] have assessed dry reforming on Ni/YSZ catalyst. A range of $0.5< R<0.75$ has been suggested to obtain a high methane conversion and prevent carbon deposition. These contradictory recommendations

for operating SOFC under internal biogas reforming conditions have shown that further experimental investigations are required, especially for the Ni-GDC anode.

Ni-GDC as an anode has certain advantages when used in the biogas-SOFC system. This type of SOFC anode shows better performance under methane dry reforming in comparison to Ni-YSZ anode because of its higher ionic and electronic conductivity [20]. Also, Ni-GDC can tolerate higher levels of H_2S contamination (2 ppm) which can be present at the outlet of the biogas gas cleaning unit (GCU) [21]. Zhang et al. [104] examined the impact of sulphur poisoning on the operational behaviour of Ni-YSZ and Ni-GDC cermet anodes. The results revealed that Ni/GDC cermet anode exhibited better electrochemical performance during the exposure to H_2S-containing gas. The GDC can still support the electrochemical reactions while the Ni surface is blocked due to H_2S poisoning. This is attributed to mixed ionic-electronic conductivity and better hydrogen adsorption on the anode surface [32]. It is also observed that sulphur poisoning is slower during dry methane reforming in comparison with steam methane reforming [273, 274].

The objective of this research is to experimentally explore the influence of the SOFC operating conditions on direct internal dry reforming and the electrochemical performance of cell. The experimental study with a commercial Ni-GDC anode, electrolyte supported cell is conducted at different operating temperatures (800-900 °C). The impact of fluctuation of CH_4/CO_2 ratio (due to the biogas production conditions) on the methane reforming and the cell electrochemical performance is studied. Additionally, the influence of the current density in suppressing carbon deposition, which is predicted through the thermochemical equilibrium calculations, is evaluated. The relatively long-term experimental study presented here investigates the optimum and safe operating conditions in terms of both power production and in preventing carbon deposition.

3.2. Thermodynamic approach of dry reforming

The carbon deposition threshold can be predicted by thermodynamic calculations at equilibrium condition. Thus, the C–H–O ternary diagram for different gas compositions with different CH_4/CO_2 molar ratios (R) and operating temperatures have been illustrated in Fig. 3-1. Increasing the operating temperature and concentration of CO_2 can decrease the risk of carbon deposition. The (●) points in Fig. 3-1 show the fuel cell operating condition at open circuit (assuming no oxygen transfers from cathode to anode). At closed-circuit operating conditions,

oxygen ions transfer through the electrolyte layer. Steam and carbon dioxide are produced on the anode side due to the electrochemical reactions of hydrogen and carbon monoxide. These products can again contribute to the methane reforming reactions (Eq. (2-9) and (2-14)). This can prevent carbon deposition to some extent (■ points in Fig. 3-1). The concentration of transferred oxygen ions is indicated based on the operating current. The influence of increasing current density on carbon deposition for biogas (R≥1.0) is also shown in Fig. 3-1. It is also claimed that carbon formation under operating condition (high current density) can be hydrogenated and removed from anode surface [275].

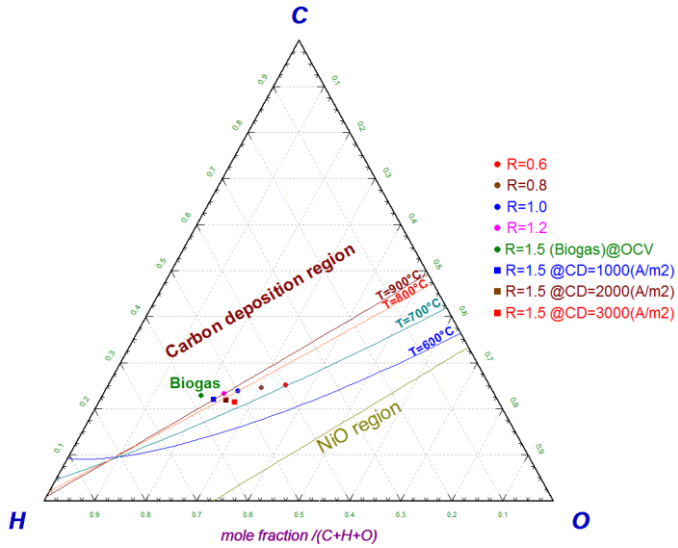

Figure 3-1: Carbon deposition limits in a C-H-O ternary diagram based on equilibrium calculated at atmospheric pressure.

However, there are two issues that should be addressed for the internal methane dry reforming in SOFC under closed-circuit operating condition. The first major issue is that the kinetics of IDR are not very well known and very little attention has been paid to the role of CO_2 on methane conversion in the biogas fuelled SOFCs [195]. Chemical equilibrium condition might not be completely achieved inside the anode fuel channel because of the low residence time in contact with catalyst [162]. Understanding the kinetics of dry reforming can also help in suppressing thermal stress on the cell surface [276]. The second issue is attributed to the uniform distribution of fuel gas, steam and CO_2 (generated through electrochemical reaction) on the anode surface. It should be considered that the distribution of current density is not uniform along the fuel channel inside the SOFC and increasing rapidly from the inlet of fuel channel, reaching to maximum

in the middle and then decreasing again at the outlet [277]. Therefore, the risk of carbon deposition increases significantly at the inlet of fuel channel. Experimental studies have shown the feasibility of IDR for Ni-YSZ anode with a high concentration of H_2O in fuel gas (SC >1.5) [278]. However, there is no agreement on additional CO_2 required for a safe long-term operation. Moreover, the relative importance of current density is still debated and should be experimentally investigated [157-159, 270].

3.3. Experimental

3.3.1. Set up and Cell specifications

Experimental research is adopted to investigate the feasibility of biogas internal dry reforming in an operational SOFC. A schematic of the experimental test bench is shown in Fig. 3-2. Simulated gas is prepared by mixing the required gases stored in gas cylinders and the CH_4/CO_2 ratio (R) is adjusted by using mass flow controllers (MFC). The total flow rate of simulated gas for anode fuel is 1000 $Nml.min^{-1}$ and for the cathode side, air is simulated by mixing 1200 $Nml.min^{-1}$ nitrogen and 320 $Nml.min^{-1}$ oxygen. The anode inlet gas is preheated (by trace heating) to 120°C. Simulated air is also preheated inside the alumina tube which is exposed to the furnace electrical heaters and the off-gas is vented out to the environment. The anode outlet is also trace heated (130°C) in order to prevent steam condensation inside the pipe.

In this experimental study, the composition of the anode outlet gas is analysed to calculate the methane conversion. A gas chromatograph (Agilent 490 micro-GC) device is used for this purpose. The anode outlet gas should be dried for this analysis in micro-GC columns (Molsieve 5A and PoraPLOT U). First, the anode outlet gas is bubbled through a steam condenser unit in order to remove steam and cooled down to the ambient temperature. It is then dried further in a silica gel bottle. A gas sample is then automatically taken by the Micro-GC for analysis and the composition of the gas (dry based) is determined. It is considered that the silica gel adsorbs CO_2 at the beginning of the test and saturation time has been noted for sampling. A mass flow meter (MFM) is used for an indicative measurement of the flow rate of outlet gas to assess the gas leakage in this setup. All electrochemical measurements, including the current-voltage (I-V) characterization are performed in the potentiostatic control mode by an electronic impedance spectroscopy (EIS) device (Gamry FC-350). EIS measurements are also performed periodically in Galvanostatic mode to examine the electrochemical performance of the cell at different operating conditions.

Commercial planar Ni-GDC electrolyte-supported cells (ESC) manufactured by H.C Starck are used to conduct the experimental investigation on IDR at atmospheric pressure. This square cell consists of a 35 µm thick NiO-GDC (NiGd0.1Ce0.9O1.95) anode, 100 µm YSZ electrolyte and a 40 µm LSM ($La_{1-x}Sr_xMnO_{3-\delta}$) cathode. The anode activated area is 81 cm^2 with about 57% wt. NiO and 23 wt.% cerium oxide. The cell is placed between two alumina blocks and the gas tightness is achieved with a ceramic sheet in the anode side and a mica (thermiculite) sheet in the cathode side. To ensure the gas sealing, extra weight is added on the top of the block as shown in Fig. 3-2. Anode off gas flow rate can be measured by an MFM. Comparison of the anode flow rate and the expected flow rate (after reforming) shows the gas tightness of sealing. The expected flow rate of the anode can be calculated based on the nitrogen balance and equilibrium calculation (with FactSage software). Current collectors for the anode and cathode sides are nickel and platinum meshes, respectively. The cell temperature is measured with a k-type thermocouple, placed inside the anode block and very close (2 mm) to the anode surface.

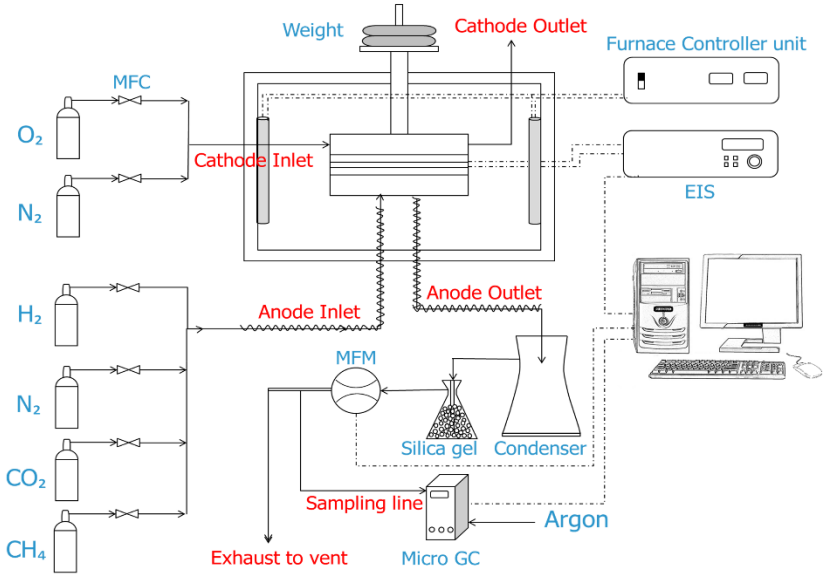

Figure 3-2: Schematic of the experimental test bench.

3.3.2. Experimental method

After preparing the setup, the furnace is heated up to 1000°C with a ramp rate of 40°C/hr while nitrogen is fed into the anode and cathode sides. After stabilization of the cell temperature at 950°C, the Nickel oxide in the anode is reduced to Nickel by hydrogen while simulated air is fed to the cathode. In this procedure, the concentration of hydrogen is gradually increased from 2% to 100% during 4 hours operation. At the beginning of the test, pure hydrogen was fed to the cell and an I-V characterization test was performed as a reference and the area specific resistance (ASR) was calculated around 1.5 $\Omega.cm^2$ at high current densities (1000 $A.m^{-2} \leq CD \leq 2500\ A.m^{-2}$). The anode off gas flow rate measured by the MFM showed that less than 10% hydrogen leakage takes place inside the setup (including the cell holder block, pipes and the steam condenser).

Based on SOFC stack operating temperature in commercial systems, the experiments are carried out at three different cell temperature ranges, 900, 850 and 800 °C. Since the heaters are positioned close to the four furnace walls and the cell holder is placed at its centre, the cell temperature is around 60°C less than the furnace set point temperature. In these experiments, the furnace temperature is adjusted to obtain the desired operating temperature (900/850/800) with biogas fuelled in equimolar ratio (R=1.0) at open circuit and the furnace temperature is kept constant for each operating temperature. The cell is fed with CH_4, CO_2 and N_2 mixtures with different R (CH_4/CO_2) ratios. This ratio is varied between 0.6 to 1.5 to simulate both methane-rich and poor biogas. When the R ratio is 1.5, the gas composition is similar both CO_2 predominant and CH_4 predominant biogas. When the R ratio is 1.5, the gas composition is similar to the real biogas with 60% methane concentration. Changing the gas composition through R values of 0.6 to 1.5 resulted in a change in cell temperature by ±5°C in comparison to the biogas fed with equimolar composition. This is because of the change in the rate of the endothermic methane reforming reactions.

For different gas compositions, the flow rate of the main fuel (CH_4) and the total flow rate of fuel are kept constant in order to cancel the influence of residence time (Table 3-2). So, the N_2 gas is added to the biogas gas composition as an inert gas. Considering the geometry of the fuel channels of the ceramic block in the anode side and the porosity of the current collector (φ=0.5), the residence time was 410 milliseconds according to the total flow rate of 1000 $Nml.min^{-1}$.

Table 3-2: Anode inlet gas compositions for a total flow of 1000 Nml.min^{-1}

Gas composition	CH_4(%)	CO_2(%)	N_2(%)	Total flow rate (Nml.min^{-1})	R	O/C
A	30	50	20	1000	0.6	1.25
B	30	37.5	32.5	1000	0.8	1.11
C	30	30	40	1000	1.0	1.00
D	30	25	45	1000	1.2	0.91
E	30	20	50	1000	1.5	0.80

The I-V characterizations were performed from OCV to 0.6 V with a rate of 30 mA.s^{-1}. All EIS measurements are carried out in the frequency range from 100 Hz to 0.1 Hz. In order to understand the influence of methane conversion on cell electrochemical performance, the anode off-gas was analysed at OCV and under specific current densities between 500 and 2000 A.m^{-2} with a current density interval of 500 A.m^{-2}. The methane conversion (X_{CH4}) is calculated based on the carbon balance of outlet gas composition at different current densities. Based on the methane (dry and steam) reforming reactions, one mole of methane produces in total four moles of CO and H_2. The H_2/CO ratio changes based on the operating condition due to the contribution of the RWGS reaction. Therefore, the methane conversion is calculated by the following equations [171].

$$X_{CH_4} = \frac{0.5\ Y_{CO}}{Y_{CH_4} + 0.5\ Y_{CO}} \qquad (3\text{-}1)$$

Where Y_i is the mole fraction of gas species *i*. It is important to mention that the concentration of the outlet gas was measured when the operating conditions (the cell voltage and the cell temperature) were stabilised. The gas composition at the outlet was sampled and analysed every 4 minutes. This condition is obtained after 4 hours of operating the cell at a certain gas composition, current density and cell temperature.

3.4. Results and Discussion

In order to understand the influence of the CO_2 concentration on biogas fed SOFC, Nernst voltage for different gas compositions has been calculated based on equilibrium conditions. The Nernst voltages for various inlet gases at 850°C are shown in Fig. 3-3a. The Nernst voltage decreases with increasing the CO_2 concentration in the fuel (decreasing the R ratio). Adding CO_2 dilutes the fuel and the concentration of H_2 in the reformed gas decreases, which is shown in Fig. 3-3b. Although the concentration of fuel for SOFC (H_2 and CO) in the reformed gas

is higher with lower R ratios (Fig. 3-3b), the Nernst voltage is lower. This attributed to the high concentration of hydrogen and higher H2/CO ratios for the higher R ratios, as it is illustrated in Fig. 3-3a. When the R ratio is more than one (equimolar CH_4/CO_2), the hydrogen partial pressure is higher than the CO.

The methane conversion at the equilibrium condition of 850°C is calculated by Eq. (3-1). Methane conversion is higher than 96% for all gas compositions (Fig. 3-3c) and it is above 99.7% when the R ratio is 0.6. Nevertheless, it is not possible to operate an SOFC for a long-term operation at open circuit condition due to the carbon deposition for gas composition with low CO_2 concentrations ($R \geq 1.0$), as shown in Fig. 3-3c based on the equilibrium condition.

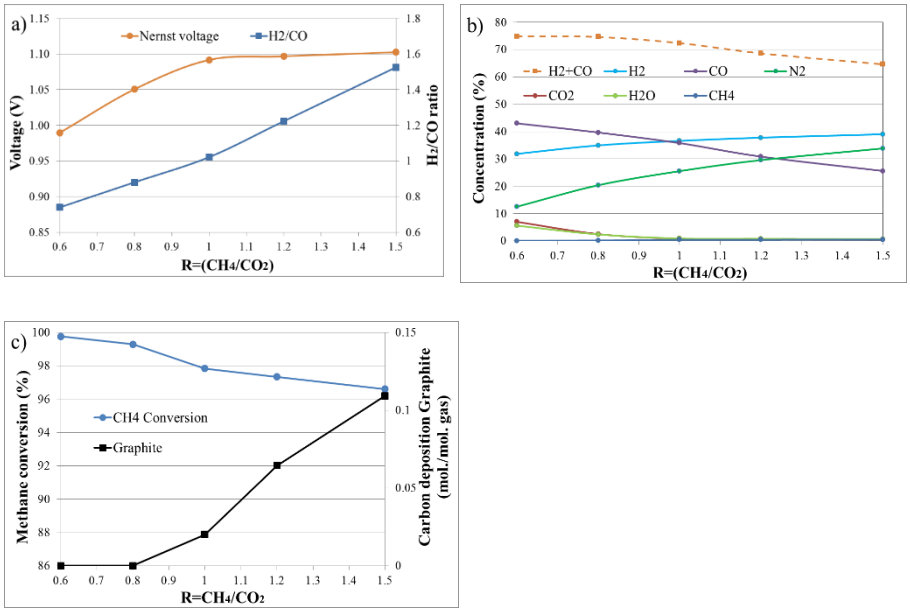

Figure 3-3: Equilibrium calculations at 850°C for different biogas compositions, a) Nernst voltage and H2/CO ratio, b) reformed gas compositions, c) methane conversion and carbon deposition at open circuit voltage.

3.4.1. Influence of gas composition

Biogas-dry reforming experiments with various R ratios are conducted according to gas compositions in Table 3-2. First, the influence of gas composition on the performance of the cell has been investigated at 900°C. These tests have been conducted for a short period of time (around a half an hour) for each gas composition and repeated at 850 and 800°C as well.

The I-V characteristics for different gas compositions ($0.6 \leq R \leq 1.5$) at 850°C (the oven temperature) have been illustrated in Fig. 3-4a. Results show that in short term experiments, increasing the CO_2 concentration decreases the cell voltage for all current density ranges, as it is expected based on the thermodynamic calculations presented in Fig. 3-3a. The OCV for gas composition with high concentration of CO_2 (R=0.6) was higher (around 20 mV) than the calculated Nernst voltage shown in Fig. 3-3a. This is attributed to the lower cell temperature (840°C), because of the higher partial pressure of CO_2 in biogas. The voltage difference between OCV and calculated Nernst voltage decreases (to a few mV) with decreasing the CO_2 concentration ($R \geq 1$). However, the ASR of the cell for all gas compositions was the same and with this short-term operation, there was no major degradation and increase of the cell resistance.

I-V characteristic with pure H_2 fuel is also shown in Fig. 3-4a as a reference. The ASR was slightly less for this test due to a higher cell operating temperature (858°C) and lower activation overpotential because of higher hydrogen concentration in the anode. Moreover, a relative low concentration resistance was observed because of the small molecular size of the H_2 fuel. The cell efficiency for the H_2 fed cell at the current density of 2000 $A.m^{-2}$, was 63% (E=0.81 V) and for the cell operating with the gas composition of R=1.0 was 58.3% (E=0.75 V).

The I-P characteristics are calculated for different gas compositions based on the results of the I-V characteristics and illustrated in Fig. 3-4b. The power density decreases with increasing CO_2 concentrations. The power density of the cell fuelled with gas composition C (R=1.0) is around 19% less than the hydrogen fuelled one at a cell voltage of 0.7 V. This implies that the active area of the cells should be 19% more than the hydrogen fuelled one to generate the same power.

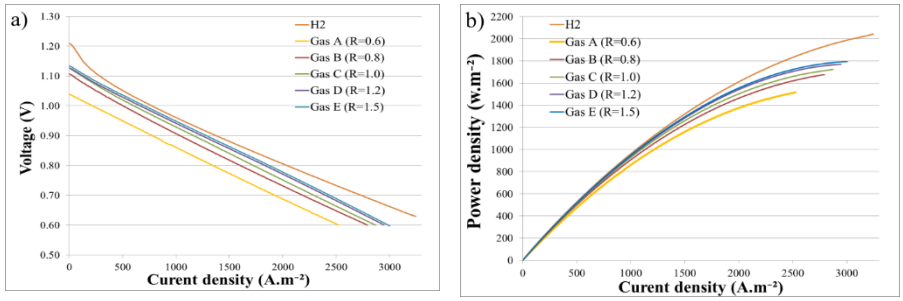

Figure 3-4: Influence of gas composition on the cell performance at different current densities at 850°C (a) the cell voltage, (b) the power density.

After I-V characterizations for different gas compositions, methane conversion has been studied for different R ratios at 850°C. Methane conversion at different current densities has been calculated based on analysed outlet gas compositions in order to understand the influence of the gas composition and the operating conditions on methane conversion. Considering the configuration of the setup, it takes one hour for each gas composition and current density to achieve stabilisation, both in terms of the cell voltage and the gas compositions at the outlet. These tests have been conducted at current densities of 500 to 2000 $A.m^{-2}$ with an interval of 500 $A.m^{-2}$ since carbon deposition is predicted for gas composition E (biogas with R=1.5) at OCV according to chemical equilibrium (see Fig. 3-1).

Methane conversion is calculated by Eq. (3-1) and shown in Fig. 3-5a. Methane conversion increases by increasing CO_2 concentration at closed circuit conditions. However, at high current densities, the methane conversion are above 95% of all gas compositions. For instance, methane conversion for gas compositions with $R \leq 1$ was the same at current density of 2000 $A.m^{-2}$ and increasing the CO_2 concentration does not influence on the methane conversion rate. Analysis of the outlet gas shows that H_2 concentration at high current densities is higher (Fig. 3-5b). Results are in agreement with equilibrium calculations shown in Fig. 3-3a. For simulated biogas composition (Gas E), the methane conversion is increased by 25% when the current density is increased to 2000 A. m^{-2}.

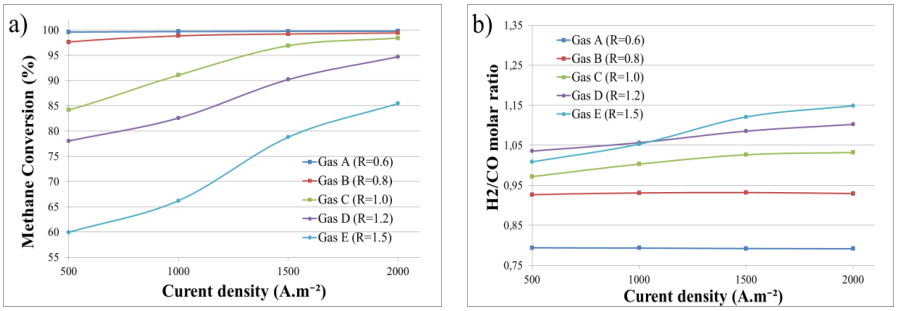

Figure 3-5: Influence of gas composition and current density on (a) methane conversion (b) H2/CO molar ratio at 850°C.

It is claimed that the methane conversion is maximised for gas composition with R=1.0 for a tubular cell [271] whereas, in this study, higher methane conversion is achieved with higher CO2 concentration ($R \leq 1$) at open and closed circuit conditions. During these tests, it is observed that rapidly changing the operating

conditions increases the rate of cell degradation (dropping the cell voltage at a constant current density). This might be because of the thermal stress, which is due to endothermic (steam and dry reforming) reforming reactions and the exothermic electrochemical reactions.

3.4.2. Cell degradation tests

During the short term methane conversion tests in the previous section, it is noticed that the cell performance was degraded (cell voltage decreased at a constant current density) specifically for gas compositions D and E, with R>1. In this section, cell degradation is investigated with a new cell placed inside the ceramic block. The test is conducted for all gas compositions mentioned in Table 3-2 at a current density of 2000 $A.m^{-2}$ and around 850°C (at constant furnace temperature). These conditions have been selected since biogas-SOFC stacks are commonly operated in this range of temperature (800<T<850°C) and the cell voltage (0.6<V<0.8). First, a reference test has been conducted with H_2/N_2 mixture with equivalent hydrogen (1200 $Nml.min^{-1}$) similar to the biogas composition (CH_4:300 $Nml.min^{-1}$). The cell degradation with dry hydrogen at the current density of 2000 $A.m^{-2}$ has been monitored for 24 hrs (see Fig. 3-6a). The cell voltage is measured every 5 seconds. The cell temperature at this current density increased to 860°C and the cell degradation with this gas composition is attributed to normal ageing of the anode (see Table 3). After measurement of the cell degradation rate with H_2, the cell is then fed with gas composition A at the same current density for 25 hours. Due to the endothermic reaction of methane reforming, the cell temperature decreased to 840°C which took approximately one hour to get it stabilised. The I-V and EIS measurements (at the current density of 2000 $A.m^{-2}$) were conducted when the cell voltage stabilized. After roughly every 24 hrs of operation at current density of 2000 $A.m^{-2}$, the measurements were repeated in order to evaluate the cell electrochemical performance. Before changing the gas compositions to gas composition B, the experiment was continued by feeding dry hydrogen for 12 hrs at the same current density in order to recover the cell electrochemical performance in case of a minor amount of carbon deposition (Fig 3-6a). I-V measurements were performed at the beginning and the end of each step. The same procedure at the current density of 2000 $A.m^{-2}$ was applied for all gas compositions mentioned in Table 3-2.

To the best of our knowledge, this is the first time that the cell voltage degradation under different dry reforming conditions (CO_2 concentration) has been reported as shown in Fig. 3-6. It is important to mention that the I-V and EIS tests

performed during the degradation experiments change the cell voltage. These parts of the experiment have not been shown in Fig. 3-6.

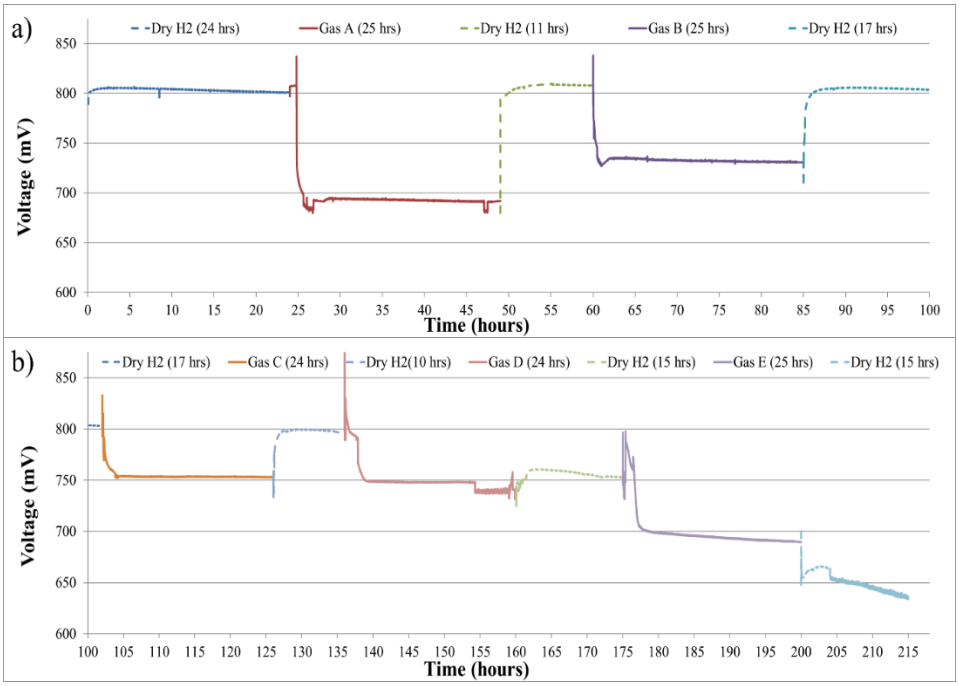

Figure 3-6: Cell stability testing results under hydrogen and various biogas compositions (a) Gas composition A, B (b) Gas composition C, D and E, at a current density of 2000 $A.m^{-2}$ and 850°C.

During this experiment, the temperature of the furnace is kept constant. The cell temperature is higher with hydrogen in comparison to biogas fuels. The cell temperature drops due to the endothermic reforming reaction on the anode surface. The cell temperature influences the cell resistance and methane reforming. After changing the inlet fuel, it takes roughly one hour to reach a stable cell voltage. Different degradation rates were observed for different gas compositions (Table 3-3). Cell voltage fluctuation was observed for all gas compositions which was negligible (±1 mV) for gas composition *C* and *D* (only first 20 hours). The voltage fluctuation for gas compositions might be because of steam condensation in the anode outlet which causes a pressure gradient at the anode outlet pipe. The cell electrochemical performance was partially recovered after using H_2/N_2 gas mixture for gas composition *A*, *B* and *C*. It should be noted that the part of the cell degradation is because of normal cell aging. For instance, the degradation rate (extrapolation of the short-term experiment) for hydrogen fuelled cell was 0.125

V in 1000 hours. The cell voltage fluctuation for gas composition *D* was significant only at the end of the test period. The cell voltage suddenly dropped by 12 mV and started fluctuating. Changing the inlet gas composition to H_2/N_2 gas mixture could not improve the cell performance, however, the voltage stopped fluctuating after changing the gas composition to H_2/N_2 gas mixture. The cell voltage declined to 0.755 V with this gas mixture and dropped by 40 mV in comparison with the same gas composition before feeding composition *D*. In case of gas composition *E* (simulated biogas with 40% CO_2), the voltage fluctuation was not observed (less than ±3 mV) but, a continuous degradation rate occurred which was dramatically higher than other gas compositions.

The I-V characteristics for different gas compositions at the beginning and at the end of each period (see Fig. 3-6) have been illustrated in Fig. 3-7. For gas composition *A* with R=0.6, negligible cell degradation was observed and the I-V curves before and after feeding gas composition *A* were identical (see Fig. 3-7a). The cell degradation for gas composition *B* (R=0.8) for 25 hrs test at similar conditions was minor as it is shown in Fig. 3-7a. In comparison with the cell voltage at initial phase, at high current densities, the cell voltage at the end of the 25-hour operation was only 10 mV lower than at the beginning of the test with the gas composition *B*. Subsequently, for gas composition *C* with equimolar CH_4 and CO_2, the cell degradation is in the same order of that for Gas *B* (though slightly lower) which is attributed to normal cell ageing. The cell voltage at open circuit for the final I-V curve of gas composition *C* is slightly (3 mV) higher than the initial one (Fig. 3-7a), this might be because of a small amount of carbon deposition, which was reversible and did not influence on the cell performance during the long term experiment. The ASR of the cell operating with different gas compositions is calculated based on the I-V curve measurements at the beginning of each test and shown in Table 3-3. The higher area specific resistance (ASR) for gas composition D and E, could be related to the lower concentration of H_2 and CO in the reformed gas.

As discussed at the beginning of this subsection, a sudden cell degradation was observed for gas D after 20 hrs operation under the current density of 2000 $A.m^{-2}$. The influence of voltage fluctuation (with a tendency to decrease the voltage) is also visible on the I-V characterisation after relatively long term experiment (see Fig. 3-7b). The current density achieved at 0.6 V was 250 $A.m^{-2}$ less than the beginning of the long term test. In the case of gas composition E (simulated biogas), the voltage fluctuation of ±5 mV was observed during the whole

experiment period. The degradation at the end of this experiment was also in the same order of degradation for gas composition D. Increasing the cell voltage at open circuit after the 25 hrs experiment for gas compositions D and E might be because of the solid carbon oxidation at the high operating temperature which is generated during the relatively long term test. This is more visible in gas composition E in Fig. 3-7b.

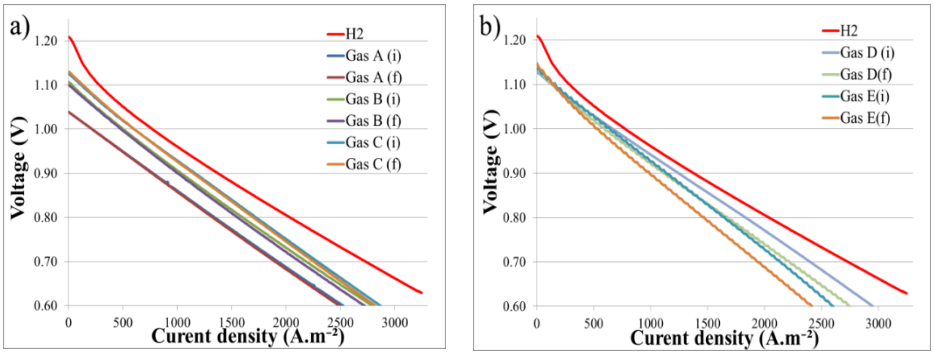

Figure 3-7: The I-V characteristics, for the cell stability test under hydrogen and various biogas (0.6<R<1.5) (a) Gas composition A, B and C (b) Gas composition D and E, at 850◦C (i: Initial, f: Final).

Table 3-3: Cell degradation rates and ASR for different biogas compositions under current density of 2000 A m^{-2} at 850°C.

Gas compositions	Hydrogen	Gas A	Gas B	Gas C	Gas D	Gas E
Degradation rates (V/1000 hr)	0.125	0.16	0.16	0.14	0.625	0.630
ASR ($\Omega.cm^2$)	1.52	1.71	1.73	1.74	1.76	1.98

Fig. 3-8 shows measured electrochemical impedance spectra (EIS) for gas compositions with various R ratios measured between 100 and 0.1 Hz, before and after relatively long term experiments, operated at 850°C. A constant steady current density of 2000 $A.m^{-2}$ was imposed in all EIS measurements. The intercept with the real axis at high frequency in the left-side of Nyquist arcs corresponds to the purely ohmic resistance of the cell. The low frequency in the right-side is activation and mass transfer losses due to the gas conversion, diffusion and oxidation through the electrodes. Carbon deposition causes a gradual filling of the anode porosity, which depresses the charge transfer process and results in higher losses. In Fig. 3-8, the shape of arcs showed only minor changes by varying the

fuel composition. Low-frequency experimental data were found to be slightly noisy, which is because of the gas transport limitation.

Decreasing the CO_2 concentration in the fuel gas increases the cell temperature due to less endothermic dry reforming. This leads to a higher electrolyte cell ionic conductivity, and the Nyquist curve shift to the left at high-frequencies (Fig. 3-8a). This should be mentioned that the cell temperature increases (roughly 5°C) by decreasing CO_2 concentration from gas composition A to B. The ohmic resistance is higher for gas compositions D and E. This could be because of the lower methane conversion and lower H_2 and CO concentrations (as already shown in Fig. 3-5a) at the current density of 2000 $A.m^{-2}$.

After relatively long-term experiments, the high-frequency intercept shifts to the right for all gas compositions, meaning higher resistance, which is negligible for gas composition A, B and C (Fig. 3-8a). This is partially attributed to normal cell aging for the gas compositions with R ≤1.0. The cell resistance increases dramatically after the relatively long-term experiment for gas compositions D and E (Fig. 3-8b). This is mainly attributed to cell degradation due to carbon deposition. A gradual filling of the anode porosity impacts the charge transfer process and results in higher losses in low frequency. This results in a decrease in the active triple phase boundary (TPB) area. The formation of carbon fibers can result in the removal of Ni particles from the electrode. This occurs when the nickel catalyst is physically lifted from the electrode by its attachment to the growing carbon fibers. Ni delamination reduces the electrolyte ionic conductivity and thereby increases the cell ohmic resistance, as observed in Fig. 3-8b.

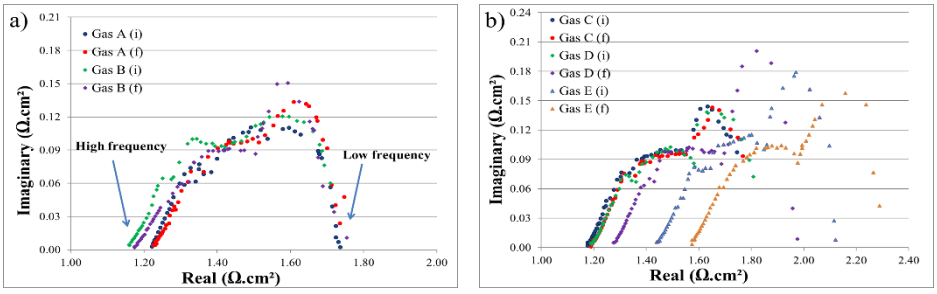

Figure 3-8: The EIS measurements, for the cell stability tests under various biogas compositions (0.6<R<1.5) (a) Gas composition A, B (b) Gas composition C, D and E, under current density of 2000 $A.m^{-2}$ at 850°C.

After this long term experiment, the furnace was cooled down, and the cell was taken out of the furnace. Anode delamination and nickel re-oxidation were observed on the anode surface close to the fuel inlet (Fig. 3-9). Carbon deposition occurred at the fuel inlet when R>1, although a safe operation was predicted based on chemical equilibrium calculations at a current density of 2000 $A.m^{-2}$ (Fig. 3-1). This is in agreement with the findings of Baldinelli et al. [194] and Yong Jiao et al. [279].

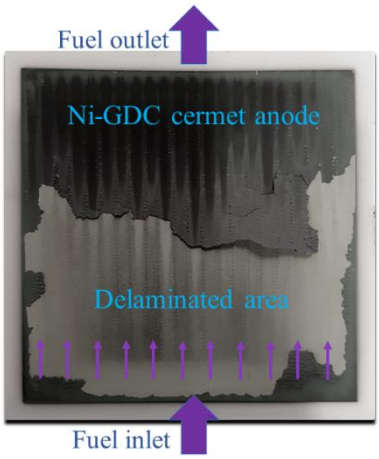

Figure 3-9: A photo of the anode side of cell operated under biogas internal dry reforming with various biogas compositions (0.6<R<1.5) after the long term experiment.

3.4.3. Influence of cell temperature

In order to evaluate the influence of operating temperature on cell electrochemical performance, the same I-V and methane conversion measurements have been conducted for gas composition *C* (with equimolar CH_4 and CO_2) at different current densities at 900 and 800°C as well. This gas composition is selected because the produced power was maximum during the degradation test (See Fig. 3-6). The methane conversion of gas composition *C* at the chemical equilibrium condition (at 850°C) is around 98%. Decreasing the cell temperature, substantially decreases the methane conversion [280]. After obtaining a stable performance of SOFC fuelled by gas composition *C*, the methane conversion for this gas composition at different current densities has been investigated at different operating temperatures and illustrated in Fig. 3-10a. At OCV, the methane conversion increases by 23% by increasing the operating temperature from 800 to 900°C . However, at high current densities (2000 $A.m^{-2}$), the difference is

negligible, around 5%. This shows that a high methane conversion (97%) is achieved at the operating of 850°C and high current density (2000 A.m^2), and a further increase in operating temperature is not required to obtain a high methane conversion.

The H_2/CO ratio of the outlet gas for different operating temperatures is shown in Fig. 3-10b. At OCV (when there is no steam produced through the electrochemical reaction of hydrogen), the H_2/CO ratio is less than one for all operating temperatures. Increasing the operating temperature more than 850°C (at OCV) promotes the methane reforming, but this does not improve the H_2/CO ratio any more as it is observed in Fig. 3-10b.

At a low operating temperature (800°C), the H_2/CO ratio increases by increasing the current density. However, increasing the current density does not affect the H_2/CO ratio for the cell operating at 900°C and current densities above 1000 A. m^{-2}. At this temperature, the methane reforming is already high, and increasing the current density does not change the methane reforming (see Fig. 3-10a).

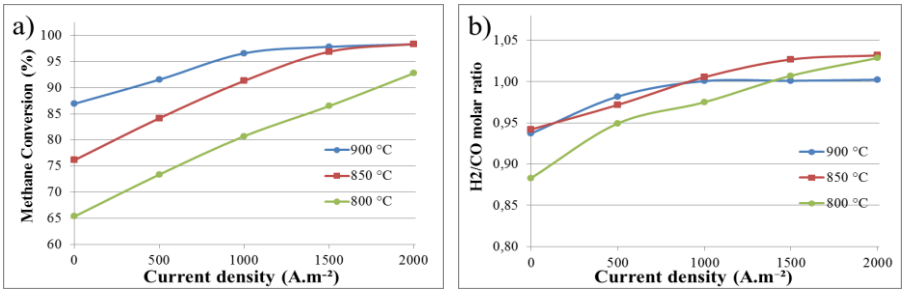

Figure 3-10: Influence of operating temperature on (a) methane reforming (b) H2/CO ratio for gas composition C (R=1).

Moreover, the cell temperature also influences the cell electrochemical performance which increases the conductivity of the cell electrolyte, and this reduces the ohmic losses within the cell [10]. At higher operating temperatures, higher current densities can be achieved with the same gas composition. Impact of the cell temperature on the performance of the cell fed with gas composition *C* has been shown in Fig. 3-11.

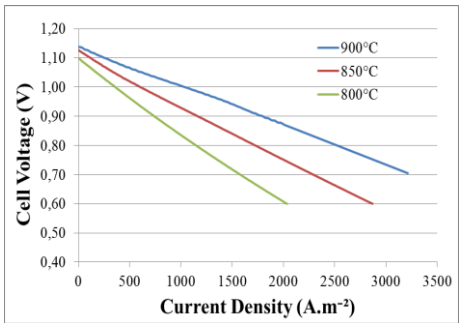

Figure 3-11: The I-V characteristics, influence of operating temperature on the cell performance for gas composition C.

For hydrogen fed SOFCs, the OCV is commonly lower at a higher operating temperature, according to the Nernst equation. However, for biogas fuelled SOFC, the OCV at higher operating temperature is higher. This is because of a higher rate of methane dry reforming and a higher concentration of H_2 and CO. It should be emphasised that operation at high temperature (above 900°C) increases the ageing (degradation) rate of electrolyte due to loss of ionic conductivity [281, 282]. Thus, it is not advised to increase the cell temperature even though a higher current density can be achieved. Moreover, for SOFC stacks, cell sealing is more challenging at high operating temperature.

3.4.4. Influence of residence time

In this section, the influence of residence time on methane conversion and electrochemical performance of cell was investigated. These experiments were conducted for gas composition *C* with different inlet flow rates (20% higher and lower than reference test) and residence time (Table 3-4) at 850°C and different current densities.

Table 3-4: Anode inlet gas compositions and inlet flow rate for different residence times at 850°C.

Gas composition	CH_4 (%)	CO_2 (%)	N_2 (%)	R	Total flow rate ($Nml.min^{-1}$)	U_f (@ 2000 $A.m^{-2}$)	Residence time (ms)
C-1	30	30	40	1	800	0.24	512
C-2	30	30	40	1	1000	0.19	410
C-3	30	30	40	1	1200	0.16	340

The outlet gas composition (dry based) was analysed by the Micro GC. Increasing the residence time by decreasing the total flow rate increases the methane conversion as shown in Fig. 3-12. Decreasing the residence time from 512

milliseconds *(C-1)* to 410 milliseconds *(C-2)* does not impact on methane conversion dramatically. However, decreasing the residence time to 340 milliseconds *(C-3)* decreases the methane conversion by roughly 5%, which is also in the same range for high and low current densities. Results showed that using a longer residence time (*C-1*) can slightly promote the methane conversion, however this is limited by fuel utilization (U_f). It is advised to keep the overall U_f around 80% in the SOFC stack operation.

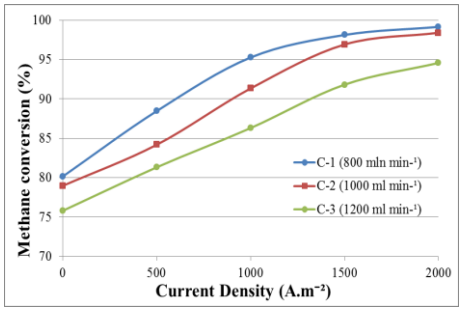

Figure 3-12: Influence of residence time and current density on methane conversion at 850°C.

The I-V measurements of this gas composition with different flow rates (different residence times) have been illustrated in Fig. 3-13. Higher cell voltage and higher current density have been achieved with longer residence time due to a higher methane conversion. However, the difference is negligible. In these experiments at a current density of 2000 $A.m^{-2}$, the fuel utilization was around 19% at a methane flow rate of 300 $Nml.min^{-1}$ (C-2). Decreasing the fuel utilization by increasing the inlet flow rate, can decrease the cell voltage and power production at higher current densities due to decreasing the methane conversion rate. This has not been seen in this experiment since the residence time was long enough for these gas compositions.

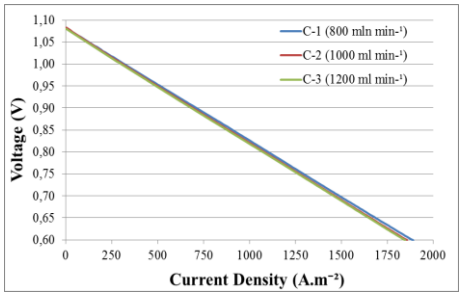

Figure 3-13: The I-V characteristics, influence of operating temperature on the cell performance.

3.5. Conclusions

Internal dry reforming of biogas in electrolyte supported solid oxide fuel cell, with a Ni-GDC anode has been studied at different operating conditions. After preliminary thermochemical equilibrium prediction of carbon deposition for specific gas compositions and conditions, experimental investigations were conducted. The final goal was to determine the minimum amount of extra CO_2 gas required to obtain maximum power density at stable cell performance (in comparison to hydrogen-fuelled one) and at the same time prevent carbon deposition.

Complete characterization of biogas-SOFC with different CH_4/CO_2 molar ratios ($0.6<R<1.5$) has been performed for short term studies in order to understand the influence of CO_2 concentration and current density on methane conversion. Methane conversion increases by increasing CO_2 concentration. Steam produced through an electrochemical reaction of hydrogen impacts the methane reforming when $R\geq1$ and the methane conversions are above 95% of all gas compositions at a current density of 2000 $A.m^{-2}$. However, a high degradation rate has been observed with simulated biogas (with 60 mol.% methane) fed, due to carbon deposition at 850°C. In this experiment, carbon deposition led to an anode Ni re-oxidation and delamination of the cell surface close to the fuel inlet. Furthermore, the results showed that changing the residence time does not significantly influence methane conversion at 850°C. This implies that the kinetics of the reforming reactions is fast enough for the internal reforming of methane.

Continuous, relatively long-term performance (more than 215 hrs) under a current density of 2000 $A.m^{-2}$ has been conducted for gas compositions with different CO_2 concentrations. This represents the novelty of this research on direct dry reforming of methane with a Ni-GDC anode (with a commercial cell size). Stable cell performance (in terms of voltage decrease at constant current density) has been achieved when $R\leq1$ and carbon deposition observed when $R>1$. The best performance has been achieved with $R=1$ since the degradation was minimum and power production was maximized. With this R ratio, complete methane reforming (above 97%) occurred at a current density of 2000 $A.m^{-2}$ and the highest H_2/CO molar ratio achieved in comparison to SOFC fuelled with safe operating condition ($R\leq1$). However, biogas-fuelled SOFC system's power density is around 19% less than hydrogen-fuelled one, and this should be considered while designing the biogas-SOFC system.

Chapter 4

Developing Ammonia fuelled SOFC System

An initial objective of this chapter is to identify the feasibility of integration of the ammonia recovery process (precipitation) from the wastewater treatment plant with SOFC. An experimental study is conducted on a single commercial Ni-GDC electrolyte supported cell with the ammonia-water mixture as a fuel. The cell performance is assessed for different ammonia mole fraction at 800°C. Subsequently, system modelling is carried out to evaluate the ammonia-SOFC system efficiency in such a way that the ammonia-water mixture (with low ammonia concentration) is used as a fuel, and the generated heat is applied in the ammonia recovery process. Then, this system is optimized to improve the system efficiency by increasing the ammonia concentration before feeding to SOFC and evaluate the performance of the developed model thermodynamically.

This chapter has been published in Journal of Fuel Cells (20-2 (2020), P. 143-157)

4.1. Introduction

To decrease the rate of greenhouse gas emissions, the usage of conventional energy resources should be replaced by alternative renewable sources. Recently, energy recovery from wastewater streams has received more attention [259, 283, 284]. Raising the quality of discharge water and nutrient removal increases the energy costs of wastewater treatment, which is dominated by the conversion and elimination of nitrogen and phosphorus [285]. Efforts have been made to promote sustainability of the overall sewage treatment and change the wastewater treatment plants (WWTPs) to a net energy producer process [9, 285-288].

Sewage water contains a wide variety of contaminants, such as excess nutrients and organic compounds. Nitrogen is one of the major pollutants in wastewater stream that can cause eutrophication (overly enriched water with minerals and nutrients) [289]. Nitrogen in wastewater stream is in the form of organic nitrogen and ammonium nitrogen. Part of ammonia (NH_3) present in the wastewater can be ionised (NH_4^+) and deionised again (to NH_3). The concentration of ammonia in wastewater can be identified by the total ammonia nitrogen (TAN) value. Excessive nitrogen decreases dissolved oxygen levels of the receiving waters and cause toxicity to the aquatic organisms. Hence, the removal of nitrogen from wastewaters is crucial to reduce harmful effects on the environment [290]. Based on the pH level and temperature, ammonia toxicity has been reported at concentrations ranging from 0.53 to 22.8 mg/L [291]. Strict regulations for nitrogen discharge from the municipal WWTP leads to significant energy and material costs [290]. There are various techniques like nitrification and denitrification [225, 234, 292, 293] to extract nitrogen from the wastewater stream and thereby return it to the atmosphere. Another method is to accumulate nitrogen in the form of ammonia and then remove it from the wastewater stream. Adding an ammonia removal process in WWTP makes the N-removal process more efficient and economical by reducing the needed areas and volumes of the nitrogen removal step [290].

The accumulated ammonia can be recovered through the struvite precipitation process as this technique certainly possesses some remarkable advantages like reducing the electricity required for nitrogen removal and chemical usages for chemical phosphorus removal [226, 237, 290]. Generally, recovered ammonia from WWTP is used as a fertilizer. However, ammonia is considered as a carbon-free fuel, which helps in reducing carbon dioxide emissions. Ammonia can be used as a promising fuel due to its high hydrogen density, less flammability, and well-known infrastructures associated with transportation and storage (Table 4-1) [294]. The only drawback of ammonia is its toxicity but can be detected easily due to its strong odour. The concentration of ammonia produced from a precipitation process is as low as 14.3% molar or 13.6% mass fraction (the rest is water vapour). Ammonia-water mixture with such a low concentration of

ammonia is not a suitable fuel for conventional energy conversion device like an internal combustion engine. Efficient energy conversion methods such as oxidation of ammonia in the fuel cell can improve energy recovery and reduce the emissions. An energy content comparison and properties of conventional fuels are shown in Table 4-1.

Table 4-1: Ammonia in comparison with other conventional fuels (in liquid phase).

Fuel	Density (kg/L)	LHV (MJ/kg)	LHV (MJ/L)	H_2 Density (kg H_2/L)
Hydrogen	0.07	120.1	8.4	0.070
Ammonia	0.76	18.6	14.1	0.136
Methane	0.47	50.1	23.3	0.116
Gasoline	0.70	42.5	29.8	0.110

Fuel cells provide an opportunity to develop thermodynamic systems that generate electricity on the basis of electrochemical reactions. SOFCs are modular, silent, low-emission and vibration free energy conversion devices. The fuel cells have already been used in different power generation systems, and very high electrical efficiencies (above 60%) have been reported [9]. Even though hydrogen is the most commonly used fuel, SOFC itself can convert chemical energy from a variety of fuels, like hydrocarbon fuels and ammonia [10]. In SOFC application, internal ammonia cracking is observed due to its high operating temperature (650°C-900°C) [131, 134]. Fuel cell-based combined heat and power (CHP) system enhances high system energy and exergy efficiency. Moreover, operating at high-temperature allows using the heat in co-generation or bottoming cycle [203]. In an integrated ammonia-SOFC system with struvite precipitation process, the generated heat can be used in the decomposition of struvite. However, to the best of the authors' knowledge, the operation of ammonia fed SOFC with low concentrations of ammonia has not been investigated.

4.2. Ammonia Production and Nitrogen Removal

The main industrial procedure for ammonia production is the Haber–Bosch process. Ammonia is produced through the reaction of H_2 and N_2 under high temperatures and pressures. The energy demand (mostly electricity) of this process is in a range of 28-166 MJ/kg NH_3 and releases 1.92-3.82 Kg CO_2/Kg NH_3 [295-297], which is significantly higher than the low heating value (LHV) of ammonia (see Table 4-1). However, ammonia can be produced from nitrogen-rich sources through some minimal carbon footprint techniques. For instance, several biological and physicochemical treatment techniques have been considered and developed to remove nitrogen from wastewater streams [298].

Ammonia can be recovered through a struvite precipitation process in the form of an ammonia-water mixture (with 14 mol.% ammonia) and used as a carbon-free

fuel. The ammonia removal through the precipitation process is expalned in chapter 2 (section 9).

4.3. Ammonia- fuelled SOFC

4.3.1. Background

Ammonia recovered as a hydrogen carrier fuel can be cracked to hydrogen at high temperature. Ammonia cracking reaction is endothermic and starts at 405°C Eq. (4-1) and complete conversion of the ammonia takes place at 590°C [132]. The normal operating temperature of SOFC is in the range of 650 to 850°C. So, ammonia cracking can take place inside the SOFC.

$$NH_3 \rightarrow \frac{3}{2}H_2 + \frac{1}{2}N_2 \quad , \quad \Delta H^0_{298} = 46.22 \ {}^{kJ}/_{mol} \qquad (4\text{-}1)$$

A lot of studies have been carried out on the thermal decomposition of ammonia with different catalysts [299]. Chellappa et al. [300] have investigated the kinetics of ammonia cracking over a Ni-Pt/Al_2O_3 catalyst at a diverse range of temperatures. The reaction rate was first order with respect to ammonia partial pressure at the temperature between 524 and 690°C.

$$r = k_0 \exp\left(-\frac{E_a}{R.T}\right) P_{NH_3} \qquad (4\text{-}2)$$

The activation energy (E_a) of ammonia cracking is found to be about 196.2 kJ/mol. The coefficient k_0 has been determined as 4.0×10^{15} for Eq. (4-2) [299]. Conducted experiments on different kind of electrolytes and anodes of SOFCs indicate that Ni-based anode is a proper catalytic material for ammonia cracking and more than 90% ammonia cracking can be achieved for ammonia-SOFC at a high temperature around 800°C [131, 301, 302]. An ammonia cracking of 99.996% has been reported for a Ni-YSZ (Yttria-stabilized zirconia) anode at 800°C, which is close to the equilibrium composition [303]. Many studies have been conducted to assess the direct ammonia-fuelled SOFCs potential [131, 299, 303, 304]. Experimental studies illustrate that the performance of the SOFC running on ammonia is close to hydrogen-fuelled one [305-307]. Comparable cell performances are reported on ammonia in comparison to humidified hydrogen when operated at a higher temperature (roughly around 800°C) [134, 303, 308, 309]. Furthermore, a better SOFC system performance is reported due to less cooling required for ammonia-SOFC stacks [303].

Additionally, by using ammonia as an alternative fuel for SOFC, NO_x formation can be prevented because of the low-temperature reaction in comparison with typical combustion devices [310]. Generally, in ammonia-fed SOFC studies, it was assumed that the partial oxidation reaction forming NO is energetically less

favourable. Later, investigations show that the NO_x concentrations in the SOFC off-gas are negligible [307, 311].

Ammonia-SOFC modelling studies have been conducted for different operating conditions. Farhad and Hamdullahpur [312] proposed a conceptual design of a portable ammonia-fuelled SOFC system. The results predicted through the simulation system confirm that the first-law efficiency of 41.1% is achievable with the system operating at a cell voltage of 0.73 V and fuel utilization of 80%. Rokni [313] has developed a hybrid system for different types of fuel, like ammonia by a general energy system simulation tool. The obtained system efficiency for the ammonia fuelled SOFC was around 58%, the lowest value among different types of fuel. However, it is found that energy efficiency is not decreasing by lowering the SOFC operating temperature. Baniasadi and Dincer [314] have studied an ammonia-SOFC system with SOFC-H^+ technology for vehicular applications. They have focused on energy and exergy analyse of this system by varying fuel utilization and current density. An energy efficiency of 42% is achieved in this system operating at 700 °C fuelled with ammonia at a current density of 1400 A/m^2 and fuel utilization of 80%. Patel et al. [203] have found total exergy efficiency of 69.8% for a high-temperature SOFC-GT system fed with ammonia at a cell voltage of 0.78 V and cell resistance of $5.0x10^{-5}$ $\Omega.m^2$ (at 950°C). Results show that 55.1% of the exergy is converted to electrical power in the SOCF stack.

4.3.2. Experimental method

So far, many studies only focused on using high concentrations of ammonia or hydrogen ammonia-mixture for SOFC [203, 312, 315], however, as mentioned, the concentration of ammonia from the struvite decomposition reactor is as low as 14 mol.% (based on the stoichiometric ratio) and the rest is water vapour. If the ammonia concentration in the fuel mixture decreases, the hydrogen concentration of ammonia cracking decreases as well. This leads to a low hydrogen partial pressure in fuel gas flow, which reduces the cell reversible potential. The performance of ammonia-SOFC with low concentration has not been comprehensively studied.

A series of experiments have been conducted to evaluate the performance of SOFC with different ammonia-water mixtures at 800°C. The schematic of the setup used is shown in Fig. 4-1. A commercial Ni/GDC electrolyte-supported cells (ESC) with an activated area of 81 cm^2 is used in this experiment. Inlet gas composition is supplied from gas bottles, and the flow rate and the ratio of the ammonia-water mixture are adjusted by using mass flow controllers (MFC) and the controlled evaporation and mixing (CEM) system. The anode inlet gas is preheated (trace heating) to prevent steam condensation inside the pipe. For the cathode side, the air is simulated by mixing 1200 $Nml.min^{-1}$ nitrogen and 320

Nml.min^{-1} oxygen. The current-voltage (I-V) characterization is performed in the potentiostatic control mode by an electronic impedance spectroscopy (EIS) device (Gamry FC-350). The outlet gas (dry based) composition can be analysed by a micro gas chromatography (GC) device (Agilent 490). The outlet gas can be sampled at the outlet of the fuel cell ceramic block, and the concentration of ammonia can be measured by a Dräger sampling tube. The cell temperature is measured with a k-type thermocouple placed very close to the anode side.

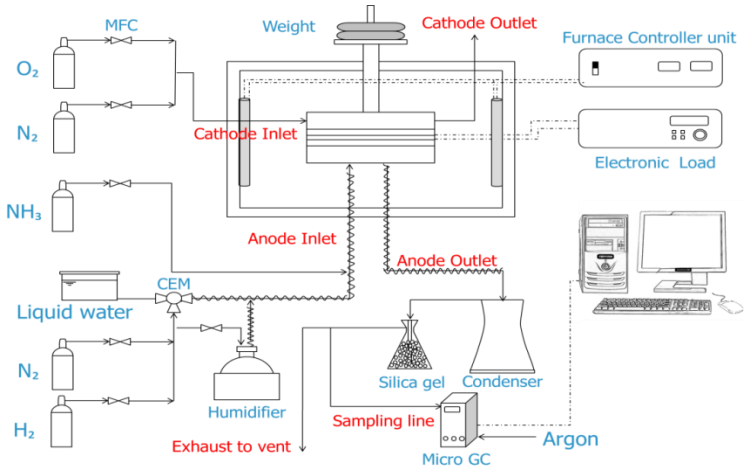

Figure 4-1: Schematic of the experimental test station.

4.3.3. Experimental results

4.3.3.1. Ammonia cracking

After the cell reduction process with the hydrogen-nitrogen mixture, a mixture of ammonia (200 NmL. min^{-1}) and nitrogen (600 NmL. min^{-1} as carrier gas) is used to check the feasibility of ammonia cracking inside the fuel cell block (cell holder) itself. The outlet gas from the anode channel is analysed by micro GC. The same test is conducted with an equivalent amount of hydrogen and nitrogen (300 and 700 NmL. min^{-1} H_2 and N_2, respectively). The results of the micro GC show that the H_2/N_2 ratio of the outlet gas for both ammonia and hydrogen fuelled SOFC are 0.39. This implies that ammonia is completely cracked into nitrogen and hydrogen at 800°C in this setup. The concentration of ammonia at the outlet also measured by a Dräger sampling tube and it was less than 0.4%

4.3.3.2. Ammonia in comparison to Hydrogen

Subsequently, ammonia is used as a fuel (350 NmL. min^{-1}). The polarization curve of this test is shown in Fig. 4-2. Then, an equivalent amount of hydrogen

and nitrogen (525 and 175 NmL. min^{-1} H_2 and N_2, respectively) are fed to SOFC. The performance of the cell with ammonia fuel is comparable with hydrogen/nitrogen mixture fuel. For both tests, the oven temperature was constant but, the cell temperature is slightly lower (around 7°C) with ammonia fuel due to the endothermic reaction of ammonia cracking which causes higher cell ohmic resistance for Ammonia-fed SOFC. This is in agreement with results reported by Cinti et al. [302].

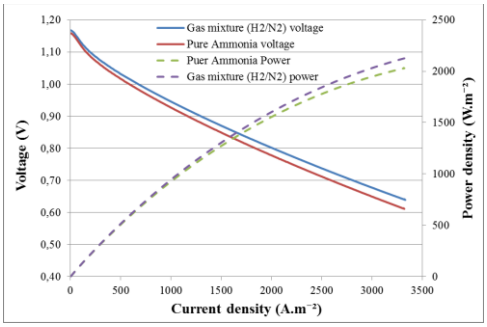

Figure 4-2: Polarization (I-V) curves for an SOFC fuelled with ammonia and hydrogen/nitrogen mixture at 800°C.

4.3.3.3. Ammonia-water mixture

Various ammonia-water mixtures are used to evaluate the influence of steam concentration on cell performance. The total flow rate and ammonia flow (for the anode) are 1000 NmL. min^{-1} and 200 NmL. min^{-1}, respectively. A fuel utilization of 56% achieved in the test with ammonia at a current density of 3000 $A.m^{-2}$. The oven temperature was constant for all gas compositions. The polarization (I-V) curves of these gas compositions have been shown in Fig. 4-3. Low concentration of steam (15%) is provided by a humidifier, and higher steam concentrations are supplied by a controlled evaporation and mixing (CEM) system. The nitrogen gas stream is required to carry steam before mixing with the ammonia stream. Results show the possibility of operating SOFC with a high concentration of steam at 0.7 V and 800°C. These are the conditions that will be used in the system modelling section of this study. Increasing ammonia concentration increases obtained current density. The area specific resistance (ASR) is in the order of $1.1x10^{-4}$ $\Omega.m^2$.

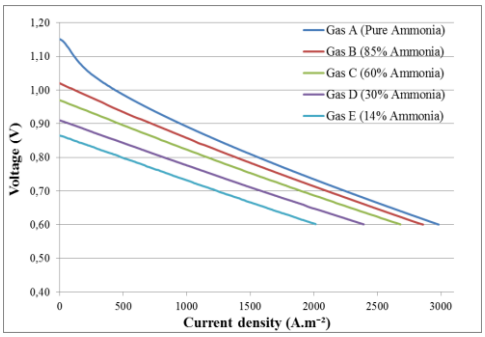

Figure 4-3: Polarization (I-V) curves for an SOFC fuelled ammonia-water mixture with different ammonia concentration.

4.4. Ammonia-SOFC system modelling

4.4.1. Thermodynamic analysis and modelling approach

Exergy analysis can be employed to improve the energy efficiency of systems by minimizing of irreversibilities. For instance, electrochemical oxidation is more reversible in comparison with the combustion process. System optimization can also be carried out by improving system configuration in order to decrease the irreversibilities. Based on works reported in the literature, there are some studies on SOFC system modelling with different system configurations and types of fuels [203, 315, 316]. A cycle-tempo model has been developed by H. Patel et al. [203] to evaluate an SOFC-gas turbine system with different fuels, including ammonia. It is claimed that the energy efficiency of ammonia fed SOFC is higher than hydrogen, but the exergy efficiency is slightly lower. The highest exergy destruction is attributed to the fuel cell itself and exergy losses in the cold sink is almost the same for all types of fuels.

This study analyses the energy and exergy efficiency (LHV based) of an integrated power generation system based on an ammonia fed SOFC in which ammonia is produced through the decomposition of struvite. The influence of individual components on the overall system efficiency is evaluated by the exergy analysis. The system performance is improved by the optimization of operating conditions. It is aimed to convert an energy consuming process step (nitrogen removal in WWTP) to an energy-producing process step.

4.4.2. System description

After the primary wastewater treatment process, effluent with a high concentration of nitrogen is conveyed to the crystallization reactor. Struvite is extracted from the sludge stream in this reactor and carried to the decomposition reactor. Ground struvite is heated up in this reactor where the ammonia-water mixture is evaporated, and the MHP is sent back to the crystallization reactor. Ammonia

water mixture can be condensed and stored in a vessel, or the vapour can be conveyed directly to the SOFC as a fuel. Potential contaminants and particles in the ammonia-water vapour stream can be removed by using a filter before entering the SOFC stack. Since the fuel utilization is set in the range of 80%, an afterburner is used to burn the remaining hydrogen gas in anode exhaust. The heat generated from the electrochemical reaction of fuel in SOFC and burning hydrogen in the afterburner can be used for the struvite decomposition process. The flow diagram (Fig. 4-4) shows a simplified integrated system of the ammonia precipitation process with ammonia fuelled SOFC. The operating temperature would be between 700°C to 850°C because at a higher temperature (up to 950°C) trace of NO_x (0.5 ppm) has been observed [317].

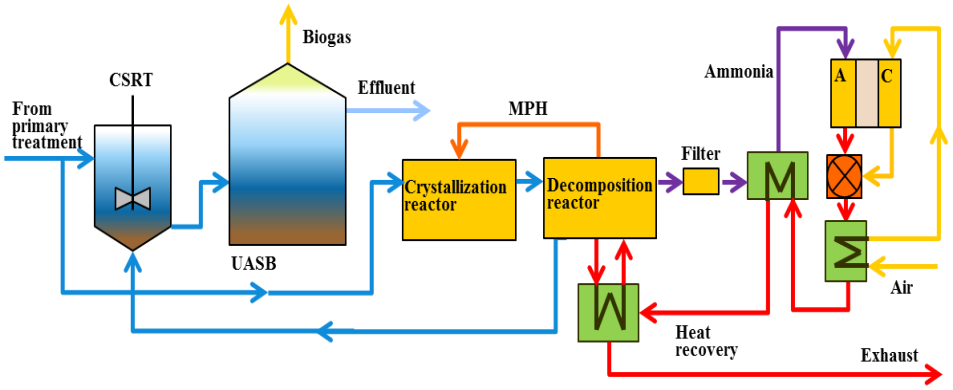

Figure 4-4: A simplified layout for implementation of ammonia precipitation process in WWTPs with SOFC.

4.4.3. Model description

Cycle Tempo is a software developed at Delft University of Technology to thermodynamically evaluate power cycles (including fuel cell systems). Equilibrium calculations are employed to calculate the fluid properties and energy production/consumption in each apparatus. Calculation methods employed and detailed information pertaining this is explained in detail in the manual of this software [299]. Mass and energy balance equations are used to calculate mass flow in each apparatus. The airflow for the cathode side is calculated based on the cooling requirement of the SOFC stack. It should be mentioned that the system efficiency is calculated based on absorbed energy, the LHV of the ammonia-water-mixture. The filter (after the decomposition reactor) is not included in the system modelling as it has no influence on the thermodynamics of the system. Some of the major input parameters used in the model have been illustrated in Table 4-2.

Table 4-2: Input parameters for ammonia-SOFC system model in Cycle Tempo.

Parameter		Value
Cell operating temperature		750-800 °C
Cell operating voltage		0.6-0.75 V
Fuel utilization (per-pass utilization)		76-80%
Cell resistance		$1.0\times10^{-4}\ \Omega.m^{-2}$
Current density		1400-2200 $A.m^{-2}$
SOFC temperatures:	Inlet	650-680 °C
	Outlet	775 °C
	Operating (reaction)	800 °C
Compressor:	Isentropic efficiency	75%
	Mechanical efficiency	98%
Pressure drops:	Fuel Cell	0.005 bar
	Heat Exchanger	0.025 bar

This Ammonia-SOFC integrated system is operating at atmospheric pressure. The cell resistance is set $1.0\times10^{-4}\ \Omega/m^2$ at a cell temperature of 800°C. This is in agreement with the cell resistance reported in the literature at this operating temperature and also measured in section 3 of this study [317]. Aqueous ammonia with 13 mass % ammonia (14 mol.%) in water with a flow rate of 10 kg/s is assumed as SOFC fuel. First, ammonia and air flows are preheated in heat exchangers (Fig.4-5) and then mixed with the anode and cathode gas recirculation flows, respectively. The overall fuel utilization (based on fresh fuel in pipe #101) is fixed. However, the per pass fuel utilization (based on fuel used in the stack) can change based on the anode and cathode gas recirculation ratios. These ratios are determined based on the outlet temperatures of the fuel and air in the heat exchanger #405 and #403, respectively. Increasing the temperature of the fuel in pipe #104 decreases the gas recirculation ratio for the anode side and results in increasing the per pass fuel utilization. The temperature of fuel at the inlet of the SOFC stack reaches to 675 °C. The temperature for air (cathode side) is set to 650 °C. The fuel cell exhaust still includes some hydrogen gas (U_f=80%) which can be burnt in a catalytic afterburner (apparatus 301). Then, the flue gas is passed through heat exchangers to preheat inlet streams, air flow for the cathode side and ammonia-steam mixture flow for the anode side. This leads to better heat recovery and a decrease in thermal stress inside the SOFC. Ammonia cracking takes place inside the fuel cell. All heat exchangers are assumed to be in counter-flow configuration. There is still residual heat, which can be used in the struvite decomposition process (See Appendix). A heat sink is considered to simulate the decomposition reactor in the struvite precipitation process. Air circulation is used to transfer heat from flue gas to the decomposition reactor. It appeared that the outlet flue gas temperature of the heat exchanger (407) is high enough to avoid condensation of water-vapour in this heat exchanger.

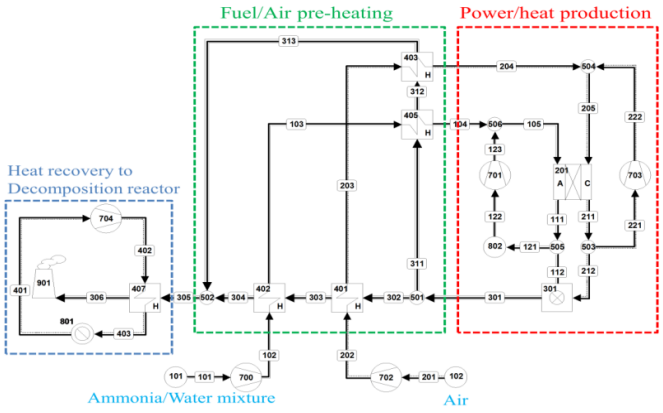

Figure 4-5: Simplified Ammonia-SOFC system model in Cycle Tempo with ammonia decomposition reactor.

4.5. Modelling results and discussions

4.5.1. Operating with low ammonia concentration

As a first step, ammonia water mixture with an ammonia concentration of 14 mol.% is used as a fuel for this model. The experimental results show the feasibility of using low concentration ammonia as a fuel for operating an SOFC. Results from computations showed that the fuel cell produces 12.42 MW electrical power at 0.66 V cell voltage and a current density of 1500 A/m^2, which is in line with experimental results (Fig. 4-3). The overall fuel utilization (based on fresh fuel injected into the system) is set at 83%, while the per-pass utilization obtained is less than 79.1%.

In this system, the fuel and air exhausts from the SOFC stack are partially recirculated to the stack and mixed with preheated fuel and air respectively. Because of this, system efficiency increases by increasing the overall fuel and air utilization. The recycle ratio is the ratio of recirculated flow back to the SOFC from the outlet flow. The fuel and air recirculation ratios are 0.12 and 0.66, respectively. The oxygen utilization (per-pass) is roughly 50%. Due to the cooling effect of the water vapour in the fuel, the cooling requirements by the air are less (compared to a system fuelled with hydrogen) which increases the oxygen utilisation. On the other hand, the air recirculation reduces the oxygen-utilisation per-pass. The electrical energy requirements for compressors are 6 and 32.3 kW for anode gas and air recirculation, respectively. Ammonia gas completely cracks inside the SOFC stack, and there is still hydrogen in the anode off-gas stream. Hydrogen combustion takes place in the afterburner with low air-fuel ratios (λ=1.5). With this system configuration, the net energy efficiency achieved is 48.5%, and the exergy efficiency is 39%. Operating the ammonia-SOFC system

in these conditions provides 12.35 MW heat for struvite decomposition reactor, which is not sufficient for producing 10 kg/s of ammonia-water fuel. The remaining heat demand for struvite decomposition (14.15 MW) can be supplied from biogas combustion produced in an anaerobic digestion reactor [9]. This brings the overall efficiency (including struvite decomposition) to 31.8% (based on ammonia and biogas LHV values).

Energy/exergy losses in this system are attributed to the irreversibilities in heat exchangers, mixing nodes, fuel cell and afterburner (combustor). Most exergy loss takes place in the fuel cell, heat exchangers, especially in apparatus 401, 402 and 407 due to high-temperature differences between the flows. The exergy efficiency of SOFC stack ($W/(Ex_{in}-Ex_{out})$) in this system is 81 %, while 9.2% of total exergy destruction occurs in the fuel cell stack. On the other hand, a high concentration of nitrogen and steam in the inlet fuel stream declines the air requirement for the cathode side. Decreasing air requirements increases the exergy efficiency of the system. The heat from out flow can still be used for other processes since the temperature is around 90°C, for instance, in the thermal pre-treatment of sludge for anaerobic digestion. Exergy destruction of the ammonia-SOFC system has been shown in Fig. 4-6. The high amount of exergy loss (15.7%) to the stack (the exhaust, apparatus #901) should be decreased to make this system more efficient. Part of the exergy flow (4.3 MW for 12.35 MW_{th}) is delivered to the struvite decomposition reactor for the precipitation process. In spite of low ammonia concentration, the energy and exergy efficiencies of this system are comparable with results reported in the literature [312, 314].

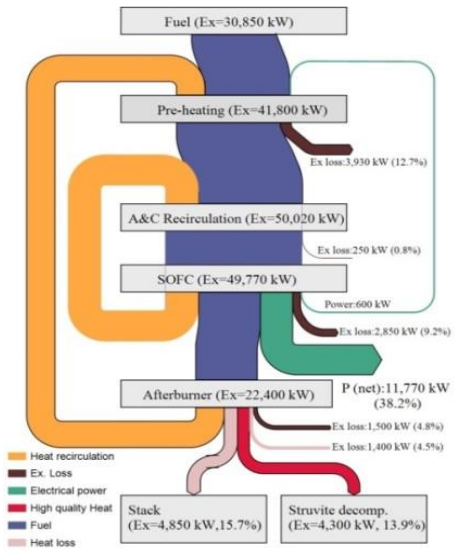

Figure 4-6: Distribution of Exergy losses in Ammonia-SOFC model with ammonia concentration of 14 mol.%.

4.5.2. Increasing ammonia concentration

The ammonia production process from struvite, the ammonia concentration would be 14.3 mol.% (based on the stoichiometric ratio). In the previous section of this chapter, the ammonia-SOFC system efficiency has been evaluated with respect to the struvite decomposition process. As it is explained in chapter 2, after struvite decomposition, the ammonia concentration can be increased in a distillation tower. Thus, it is interesting to investigate whether increasing ammonia concentration improves net system efficiency.

4.5.2.1. Heat pump assisted distillation tower

The vapour stream of the distillation tower needs to be cooled down in the condenser of distillation tower (#1 in Fig. 4-7). For instance, with a reflux ratio of 5.3, the condenser heat duty is 19.7 MW at the condenser temperature of 50°C. On the other hand, heat is required for the decomposition of struvite in the precipitation process. Using a heat pump between condenser and reboiler (in the distillation tower) is already investigated [318]. In this study, a subsystem is designed to transfer heat from the condenser of the distillation tower to the struvite decomposition reactor of the precipitation process. The schematic of this system is shown in Fig. 4-7.

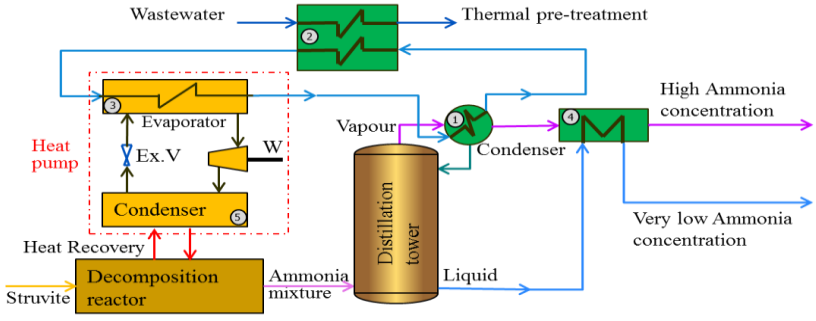

Figure 4-7: Schematic of ammonia flow from struvite decomposition process with heat pump assisted distillation tower.

In order to simulate the heat pump assisted distillation tower, a Cycle Tempo model is developed (Fig. 4-8). A water cycle is required to transfer heat from the condenser of the distillation tower to the evaporator of the heat pump. Then, heat is transferred to the decomposition reactor by this heat pump, whereas pure ammonia is used as a refrigerant [319]. The condenser of the distillation tower is modelled as a heat source (apparatus 301 in Fig. 4-8). The model calculates all flow rates required for heat transmission.. For instance, the water flow rate is 195 kg/s in pipe 301. In heat exchanger 103, 100 kg/s of wastewater is heated up to 35°C, which transfers around 8.4 MW heat. In the evaporator (heat exchanger 204 in Fig. 4-8), about 11.5 MW heat is transferred to the condenser of the heat pump.

A compressor is needed to increase the ammonia pressure to 42 bar and the temperature to 191 °C. The coefficient of performance (COP) of 3.2 is calculated and, 3.6 MW electrical power is required for the compressor. In the condenser, 15.0 MW heat is transferred to the struvite decomposition reactor. The pressure decreases to 5.5 bar in the expansion valve. The ammonia-rich flow from distillation tower is heated up again to 90°C with hot water from the bottom stream of the distillation tower (in heat exchanger #4). In section 5.3, the influence of the ammonia concentration on the SOFC system will be investigated.

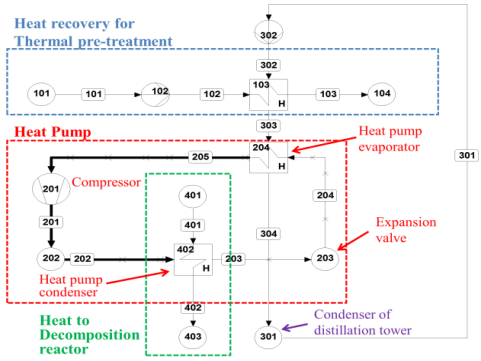

Figure 4-8: Modelling of a heat pump assisted distillation tower with cooling cycle on Cycle Tempo software.

The main assumptions for the Cycle Tempo model are presented in Table 4-3. The outlet temperature of the wastewater (35°C) is considered to be high enough for a low-temperature thermal pre-treatment (mesophilic condition) of sludge for anaerobic digestion [9]. The circulation air with a temperature of 90°C is provided to heat the struvite (heat exchanger 402 in Fig. 4-8), and struvite heats up further with flue gas from the SOFC system. Produced ammonia is used in the same SOFC system with minor modifications. With a higher concentration of ammonia, a higher current density in the SOFC can be achieved.

Table 4-3: Assumptions of heat pump assisted distillation tower model.

Parameter		Value
Condenser of distillation tower:	Vapour outlet	50 °C
	Water outlet	40 °C
Heat Ex. #103 (Fig. 4-8):	Circulation water outlet	30 °C
	Wastewater inlet temp.	15 °C
	Wastewater outlet temp.	35 °C
Compressor:	Isentropic efficiency	75%
	Mechanical efficiency	95%
Pumps:	Mechanical efficiency	80%
Pressure drop:	Heat exchanger	0.1 bar

4.5.3. SOFC operating with high ammonia concentration

In the previous section, an ammonia recovery system with a heat pump assisted distillation tower has been explained. In this section, the influence of ammonia concentration on the performance of an ammonia-SOFC system is assessed. Various ammonia concentrations, along with specified fuel flow rates (see Table 4-4) have been used for the same ammonia-SOFC model developed for a fuel stream with an ammonia concentration of 14 mol.%. The amount of ammonia in the fuel streams (1.33 kg/s) has been kept constant for the model with different ammonia concentrations, and the fuel flow rates have been changed accordingly. Because of different flow rates and the temperature of fuel stream, the LHV of the fuel is slightly different, although the mass flow rate of ammonia is constant for different cases. The cell resistance is kept constant for different models. The cell voltage is calculated by the model accordingly. Minor modifications (such as overall fuel utilization and anode/cathode recirculation ratios) are required to optimize the system operation in terms of power generation, for different ammonia concentrations. Results of Cycle-Tempo modelling have been summarized in Table 4-4. Increasing the ammonia concentration from 14% to 30 mol.% increases energy and exergy efficiencies. The performance of the developed system shows an excellent potential to be used for aqueous ammonia (ammonium hydroxide liquid fuel) with roughly 28% ammonia by mass (30 mol.%). With further increasing the ammonia concentration, energy efficiency (LHV-based) of the system relatively increases.

Table 4-4: Ammonia-SOFC system results with different ammonia concentration in Cycle Tempo.

Fuel stream		Cell Voltage (V)	CD (Am^{-2})	Overall Uf (%)	λ	Power density (kWm^{-2})	Energy generation		Net Efficiency	
Ammonia (mol.%)	Flow rate (kg/s)						Power (MW)	Heat (MW)	Energy (%)	Exergy (%)
14%	10.0	0.67	1450	82	1.5	0.97	12.42	12.35	48.5	39.0
30%	4,62	0.67	1600	84	4.1	1.10	12.91	11.20	50.7	45.0
60%	2,27	0.67	1950	87	5.7	1.32	13.20	11.28	51.8	47.9
90%	1,49	0.67	2150	89	8.6	1.44	13.51	11.48	53.1	50.9

Since the concentration of ammonia is increased to 90%, the fuel flow rate decreases to 1.49 kg/s. The Nernst voltage for the highest ammonia concentration (90%) is 1.09 V, and higher current density and higher fuel utilization are achievable (Fig. 4-3). This leads to increasing the SOFC power production (13.50 MW) at higher fuel utilization (89%), current density (2150 A/m^2) and higher cell voltage (0.67 V) in comparison with a system operating on low ammonia concentration. Moreover, the power density of the SOFC stack increases significantly by 48% (Table 4-4). Per-pass fuel utilization still has been kept around 80%. On the other hand, low steam concentration in the fuel increases

required air (14.9 kg/s) for cooling the SOFC stack, and this increases lambda in the afterburner (λ=8.6). The heat generated in the SOFC and afterburner can be partially transferred to the struvite decomposition reactor at a very high temperature (610 °C). However, in comparison with the lower concentrations, less heat is delivered to the decomposition reactor (11.48 MW). The temperature of the flue gas stream to the environment is 60°C. This temperature is lower than the flue gas temperature for other cases because of the low concentration of water in the system, and this makes the system more efficient. The ammonia-SOFC system net energy efficiency is 53.1%.

Exergy destruction of the ammonia-SOFC system fed with a high concentration of ammonia (90 mol.%) is shown in Fig. 4-9. Due to the lower fuel flow rate, the exergy input, in this case, is slightly lower (26.54 MW). Exergy destructions take place in all components, mostly in the fuel cell with 11.5%, and heat exchangers in the fuel/air preheating process with 8.3%. Exergy losses in the afterburner are 3.2%, which is attributed to the high fuel utilization in the SOFC fuelled with rich-ammonia gas. Only 2.1% of fuel exergy is transferred to the cold sink, and this makes the system more efficient compared to system fuelled with lower ammonia concentrations since 14.6% of the fuel exergy is transferred to the decomposition reactor. The total exergy efficiency of this system, including the exergy of heat transferred to the struvite decomposition reactor, is 65.5%.

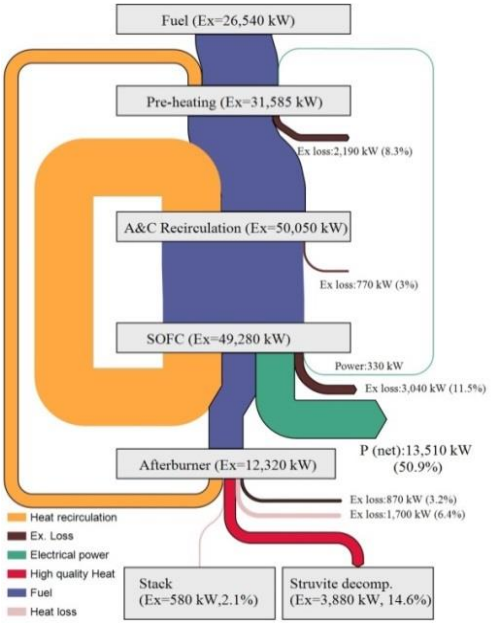

Figure 4-9: Distribution of Exergy losses in Ammonia-SOFC model with ammonia concentration of 90 mol.%.

The achieved exergy efficiency of 50.9% is comparable with the result of SOFC-GT system with exergy efficiency of 55.1% [203], despite lower ammonia concentration in the fuel (90 mol.%), lower operating temperature, higher cell resistance ($1.0x10^{-4}$ $\Omega.m^2$) and lower operating voltage (0.67 V). In comparison with hydrogen, an ammonia fed SOFC needs less cooling as the generated heat is partially used for the ammonia cracking reaction inside the fuel cell stack.

4.5.4. Integrated System

Finally, the energy balance of the ammonia-SOFC system, integrated with a heat pump assisted distillation tower and precipitation process is investigated in this section. The SOFC supplies part of the struvite decomposition heat demand and the heat pump provides the rest. A heat pump is applied to extract heat from the condenser of the distillation tower. SOFC also provides electrical power for the compressor of the heat pump. Meanwhile, the heat required for thermal pre-treatment (35°C) of 100 kg/s of wastewater sludge is supplied (8.4 MW). This integration makes the system sustainable since there is still net electrical power generated by the SOFC (9.9 MW_E). The energy balance flow diagram of this system is illustrated in Fig. 4-10. The net electrical efficiency of this system (including energy demand of the heat pump assisted distillation tower) is 39% based on ammonia LHV (18.6 MJ/kg) of the ammonia-water mixture.

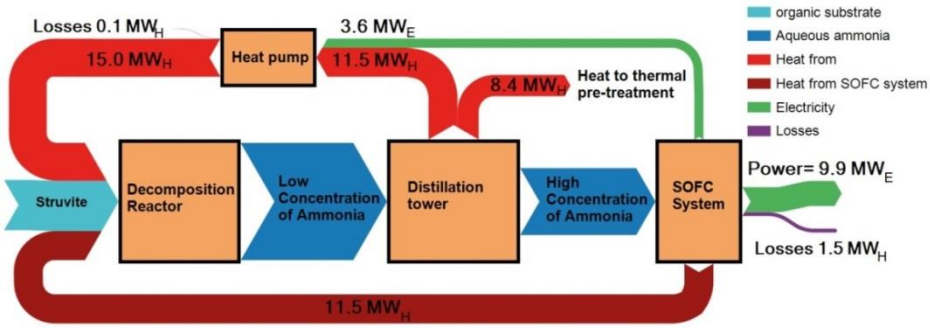

Figure 4-10: Energy balance flow diagram of Ammonia-SOFC model and heat pump assisted distillation tower with ammonia concentration of 90 mol.%.

4.6. Conclusions

Nitrogen removal from wastewater treatment is known as an energy-intensive process. Struvite precipitation is one of the methods of nutrient (Phosphorus and nitrogen) removal in wastewater. Struvite can be decomposed to ammonia water mixture by heating at (an optimum temperature of 106°C). The concentration of produced aqueous ammonia in this process is very low (14.3 mol.%) but, can be used as a fuel in an SOFC system. Feasibility of operating an SOFC with different

concentration of ammonia is investigated by conducting experiments at 800°C. Ammonia is fully cracked inside the SOFC at this operating temperature. Subsequently, a model incorporating a fuel cell with ammonia recovery (precipitation) process is developed. The energy and exergy efficiencies of this system were 48.5% and 39% respectively. However, in this system, the required heat for struvite decomposition could not be generated by the SOFC system (stack and afterburner).

To make the system more sustainable and efficient, the concentration of ammonia in the fuel stream is shown to be increased by integrating a distillation tower to the system and decreasing the temperature of the ammonia-water stream. A heat pump is coupled with the distillation tower to satisfy the heat duty of the condenser of the distillation tower and reduce the temperature of the outlet stream. The higher concentration of ammonia improves ammonia-SOFC system efficiency. The heat pump and SOFC system supply the heat required for struvite decomposition reactor (see Fig. 4-7). The net energy and exergy efficiencies of ammonia-SOFC system operating with an aqueous solution of ammonia (90% ammonia mole fraction) are 53.1% and 49.6% respectively. The net energy efficiency of the integrated SOFC system with heat pump assisted distillation tower is around 39% (ammonia LHV-based). After assessment of the ammonia-SOFC system, the next step would be the evaluation of a SOFC system with an ammonia-biogas mixture as a fuel. Sustainability of conventional WWTP can be improved by applying SOFC as a heat and power generation device.

4.7. Appendix: Heat usage calculation

Based on the thermogravimetric analysis (TGA) measurements, it is possible to determine the heat required for the decomposition of struvite. The Q600 unit from TGA instruments measures the temperature rise due to the heating of the furnace of the sample and a reference. The temperature difference (ΔT) between the two is used to determine the net heat flow into or out of the sample during the experiment. While no transitions take place in the sample, the sample temperature will track the reference temperature. This ΔT signal is then used to calculate the heat flow for the reaction. Endothermic reactions such as melting and evaporation will result in a negative heat flow curve, whereas exothermic reactions such as oxidation will result in a positive heat flow curve. Three distinct struvite samples (20-30 mg) with different free water concentrations have been tested. First, the oven is closed, and nitrogen is purged for around 20 minutes to provide an inert environment. The oven is heated up to 80°C and kept at that temperature for about 20 minutes to release most of the free water. Then, TGA experiments are conducted in a range of from 80 °C to 160°C with a ramp of $1°C.min^{-1}$. Results show that the struvite samples lose their water and ammonia simultaneously during decomposition. Most of the water and the ammonia is evaporated around

90 °C, and it is observed that weight loss is less significant after 110°C. As an example, combined graphs for a struvite sample (with maximum water Concentration) are shown in Fig. 4-11 with the weight loss per minute, the heat

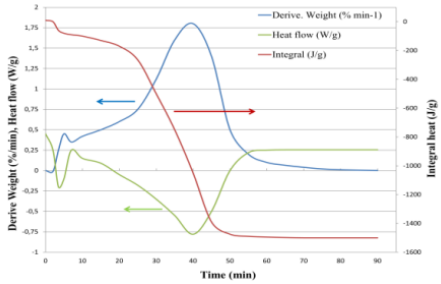

flow and the integrated heat flow during the experiment.

Figure 4-11: Integrated heat flow for evaporating ammonia water mixture in struvite decomposition reactor.

Struvite samples (with different free water concentrations) demonstrate a negative heat flow, between 1000 kJ/kg to 1500 kJ/kg, in comparison to the reference. In this study, it is assumed that the heat required for struvite decomposition is 1350 kJ/kg. Based on decomposition reaction Eq. (2-20), 1 kg struvite decomposes into 510 grams of ammonia water vapour and 490 gram of MHP. Therefore, the heat required for producing ammonia-water mixture is 2650 kJ/kg. This is higher than the heat of vaporization of water (2000 kJ/kg). Moreover, it is seen that concentrations of struvite did not change due to heating, and there was no sulphur-containing compound in the vapour stream (which is hazardous for SOFC).

Chapter 5

Developing Biogas-Ammonia fuelled SOFC system

This chapter aims to explore the potential of using biogas-ammonia mixture from WWTP as a fuel for a SOFC in order to convert an energy-consuming process step (nitrification-denitrification) into an energy-producing process step. The focus is also on direct internal biogas reforming, and ammonia cracking when biogas-ammonia mixture is fed to SOFCs at different operating conditions. To the best knowledge of the present study's authors, this is the first experimental investigation of using biogas and ammonia-water mixture together in SOFCs

5.1. Introduction

Wastewater treatment is a well-developed environmental-friendly technology to effectively remove contaminants and convert the wastewater into an effluent that can be returned to the surface water. However, the treatment process is energy-intensive. At wastewater treatment plants (WWTPs), collecting and treating wastewater streams need a considerable amount of electricity (0.5 kWh m^{-3}) to reach an acceptable quality of discharge requirements [320]. Wastewaters might contain significant amounts of organic matter and nutrients (nitrogen and phosphorus) compounds. The chemical energy in domestic wastewater with theoretical Chemical Oxygen Demand (COD) of 1.0 $kg.m^{-3}$ is approximately 3.8 $kWh.m^{-3}$ [321]. In conventional WWTPs, biodegradable organic matter is converted to methane in an anaerobic digestion process, and nitrogen is removed through nitrification. The required energy for the nitrification process (aeration) is more than 50% of the total energy demand of WWTPs [322].

The energy demand at WWTPs can be offset by efficient nutrient and organic matter recovery from wastewater stream and utilization in energy conversion devices [9]. Biogas production is an important technology widely applied in Europe. Produced biogas is currently converted to bio-methane or used in the reciprocating engine-based combined heat and power (CHP) systems [260]. However, the system's electrical efficiency is limited to 22-30% [82, 323]. In parallel, total ammoniacal nitrogen (TAN), can be recovered from ammonium-rich wastewater streams and converted and stored in the form of aqueous ammonia. In WWTPs, the ammonium concentration in the waste sludge stream (after secondary sewage treatment, anaerobic digestion, and dewatering) might increase to 400-8000 mg $L^{-1}$of NH_4^+-N, [244].

The electrical efficiency of SOFC systems is higher than the conventional combustion-based CHP systems, with lower atmospheric emissions [15, 324]. Moreover, the operation and maintenance costs of SOFCs are expected to be less than the IC engines-CHP systems [325]. Operating SOFCs with renewable fuels, including biogas, ammonia, and ammonia-steam mixture, have already been reported separately at different operating conditions [294, 326]. Due to the modularity of SOFCs, they can be used for a wide range of biogas production capacities at WWTPs. Therefore, WWTPs could be made environmentally friendlier by i) recovery of nutrient and organic materials from wastewater streams and ii) replacing the inefficient combustion systems with electrochemical fuel oxidation in SOFCs.

This study explores the potential of using biogas-aqueous ammonia mixture recovered from WWTP in a SOFC system. This helps to convert an energy-consuming process (nitrification-denitrification) into an energy-producing process. The focus is on the direct internal biogas reforming and ammonia cracking (simultaneously) in a single planar Ni-GDC commercialized SOFC at different operating conditions. To the best knowledge of the authors, this study presents the first experimental investigation of using biogas and ammonia-steam mixture in SOFCs. A series of experiments were conducted to investigate the methane conversion with combined (steam and dry) reforming to determine the minimum steam required for preventing carbon deposition in biogas fuelled SOFCs. Then, the influence of adding ammonia on the methane reforming is studied for a biogas fuelled SOFC with extra steam added for reforming. Subsequently, different ammonia-steam mixtures (with different ammonia concentrations) are mixed with biogas and SOFC experiments were carried out to determine the safe operating conditions. Finally, the effect of mixing aqueous ammonia to biogas and its influence on SOFC power density is studied.

5.2. Process description

5.2.1. Biogas production and Ammonia recovery

Biomethanation is a natural biochemical process that decomposes biodegradable organic matter in habitats such as swamps, peat bogs, lakes. Anaerobic digestion (AD) is a technique to control bio-methanation in a closed reactor. Thick sludge with rich-biodegradable matter from primary and secondary treatment processes at WWTP can be collected in an AD reactor, and up to 90% of the chemical energy of organic matter can be recovered (Figure 5-1) [327]. The degradable organic material in the waste stream can be estimated by the chemical oxidation demand (COD), which typically varies between 20-800 $mgr.L^{-1}$ for influent of municipal WWTPs [328-330]. The COD can be increased up to 18 $gr.L^{-1}$ for activated sludge and fed into the AD reactor [331-333]. The overall process of anaerobic digestion has been explained in chapter 3 of this thesis. The products are biogas and organic sludge, which are generally used as fuel and fertilizer, respectively.

Biogas composition from the AD process consists of approximately 50-75% CH_4 and 30-50% CO_2 with undesirable trace compounds such as hydrogen sulphide (H_2S) and siloxanes. Siloxanes (D-4 and D-5) are generally found more in produced biogas from landfills [9, 334]. The amount of contaminants depends on the AD operating conditions and raw feedstock composition [88]. The primary

contaminant in the produced biogas from the waste stream in municipal WWTPs is H2S, ranging from 10 to 1200 ppm [231]. In general applications, such as the balance of plants (BoPs) of CHP systems, it is advised to keep the H_2S levels below 250 ppm [86]. Hence, for biogas with very high H_2S concentration, integrating a gas cleaning unit to CHP systems is essential.

The major source of nitrogen in municipal wastewater is human urine. The concentration of nitrogen in the wastewater stream is commonly around 40-60 mg of $N.L^{-1}$. This is also presented by total ammonia nitrogen (TAN) concentration, which is the total amount of nitrogen in the forms of NH_3 and NH_4^+ in the wastewater stream. The TAN concentrations can be much higher in the industrial and dairy waste streams [250, 335]. If nitrogen is discharged into the environment in the form of ammonium, it causes eutrophication of water resources [289]. In conventional WWTPs, aerobic digestion is the most typically used method for nitrogen removal. However, the operation costs are high due to the high amount of dissolved oxygen (DO) demand, while the N_2O emissions are also significant [232, 336]. The efficiency of this process has been improved over recent decades by converting nitrate to nitrogen gas with nitrification/denitrification or anaerobic ammonium oxidation (anammox) techniques [139, 225, 337]. The energy demand is substantially decreased by applying these technologies [235].

The ammonia/ammonium concentration in the wastewater stream is increased through primary, secondary sewage treatment and the AD process. Due to the high concentration of ammonium, the effluent is suitable for nitrogen recovery. However, in practice, ammonia recovery is not considered in most WWTPs. The major issue with TAN removal processes is that these processes are generally neither economically nor environmentally friendly.

It has been tried to optimize TAN removal techniques by using chemicals and electrical power for different wastewater resources. For instance, ammonia recovery from human urine has been investigated by Luther et al. [249] using an electrochemical cell with an electrical power demand of 43 MJ kg^{-1} of N_2 for a wastewater stream with an ammonium concentration of 384 gN $m^{-2}d^{-1}$. Van Linden et al. [338] have used a bipolar membrane electrodialysis to recover ammonia avoiding the use of chemicals. An ammonia removal efficiency of 91% was achieved from feed water with an initial NH_4^+ concentration of 1.5 g L^{-1}. In this method, the electrical power demand of 19 MJ kg^{-1} of N_2 is required. There are also some nitrogen recovery techniques, such as using zeolite based separation (ion exchanger) [243] and struvite precipitation process [248]. Ammonia is

commonly used as a fertilizer. Recently, it has gained more attention as a carbon-free fuel. However, ammonia has a high ignition resistance in internal combustion engine applications, and a high concentration of ammonia and NO_x have been observed in the exhaust gas [339].

In this study, ammonia recovery from the struvite precipitation process is considered to be applied in developing a biogas-ammonia fuelled SOFC in WWTPs. The struvite precipitation process is an interesting technique for ammonia recovery from a rich ammonium stream (range between 0.1 to 5 $gr.Nl^{-1}$) [249]. Struvite is a phosphate mineral (Magnesium Ammonium Phosphate (MAP)) in the wastewater stream. By adding a magnesium ion to wastewater, the pH level gradually increases, and struvite is crystallized (See chapter 4). Then, struvite crystals are formed and accumulated inside a fluidized bed reactor [226].

By heating struvite in a decomposition reactor, the struvite crystals can be decomposed into magnesium hydrogen phosphate (MHP) and ammonia mixed with water vapour (explain in chapter 4). The produced MHP is recycled to the crystallization reactor to produce more struvite. Phosphate is also another by-product of this process (Figure 5-1).

The integration of the struvite precipitation process into a conventional WWTP with an anaerobic digestion reactor is shown in Figure 5-1 [226, 340]. The sludge streams from primary and secondary treatment steps are mixed with the effluent from the sludge dewatering process. The nitrogen and phosphate concentrations of this stream are very high and are suitable for ammonia recovery. This stream is conveyed to a fluidized bed reactor (crystallization) to produce struvite (red dashed block in Figure 5-1). Then, struvite is heated (at above 100°C) in the decomposition reactor, and aqueous ammonia with 14.6 % molar fraction is produced (based on the stoichiometric ratio). In the decomposition reactor, struvite is heated (at above 100°C), and aqueous ammonia with 14.6 mol.% molar fraction is produced based on the stoichiometric ratio [252]. The ammonia produced by the struvite precipitation process is relatively clean, but the water vapour concentration is as high as 85.4 mol.% [341]. The recovered aqueous ammonia can be stored at ambient temperature and atmospheric pressure. There is still a possibility of increasing the ammonia concentration to 25 mol.% by applying an enrichment technique like distillation and storing it at the same condition [256, 341].

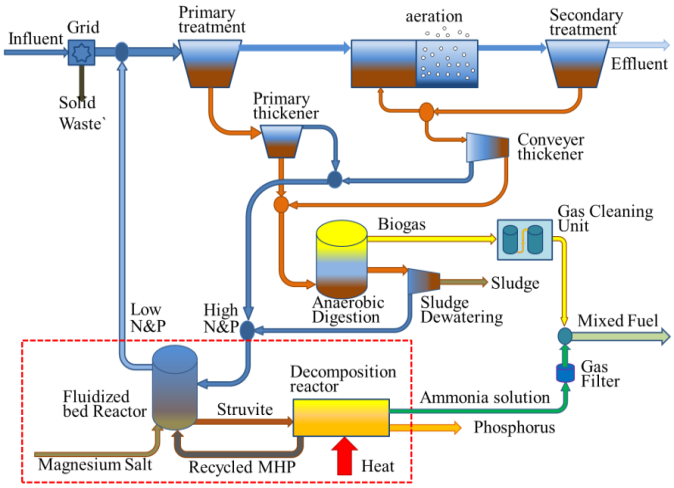

Figure 5-1: Process scheme of conventional WWTP integrated with AD and struvite precipitation process

The quality of organic matter in wastewater stream impacts the amounts of biogas (methane) production and recovered ammonia in WWTPs. The ammonia to methane ratio can be estimated by measuring the COD and NH_4-N concentrations in the wastewater influent. For instance, the COD to NH_4-N ratio in wastewater stream after the SHARON® process is around 3.3 at Dokhaven WWTP in Rotterdam, Netherlands [342]. Considering the COD recovery efficiency of 55% in the AD reactor and an ammonia recovery efficiency of 80% through the precipitation process, an NH_3 to CH_4 ratio of 0.45 can be achieved in this WWPT [343].

5.2.2. SOFC integration in WWTP

The sustainability of WWTPs can be improved by using the SOFC system as an energy conversion device instead of the commonly used thermal conversion devices like internal combustion engines. There are several advantages, i) SOFCs offer high electrical efficiency (50-60%) and high overall efficiency (80-90%), ii) the NOx emissions are negligible, iii) SOFCs are modular and can be integrated with different WWPT capacities, iv) SOFCs are more fuel flexible and can be operated with low quality (diluted) fuels such as biogas with a low methane concentrations (50 mol. %) or ammonia-steam mixture with a low ammonia concentration (15 mol.%) [310]. However, in terms of contaminants present in the fuel stream, SOFCs are more delicate in comparison to combustion-based CHP systems. Therefore, a comprehensive gas cleaning unit is required to reduce the

level of contaminants (H_2S, HCl, and siloxane) at levels below the tolerance limits [98]. Moreover, after cleaning, the methane in biogas needs to be converted to H_2/CO rich-gas either internally or externally to obtain a more effective, stable, and durable SOFC performance.

5.2.2.1. Biogas Fuelled SOFC

Biogas is a promising fuel for SOFCs, which is shown in several research report [9]. In a biogas SOFC system at WWTPs, biogas should first be cleaned. Either physisorption or chemisorption may dominate biogas desulphurisation process, which is commonly carried out at ambient temperature. Synthesized adsorbent materials like activated carbon are commonly used for H_2S removal [344]. The removal of siloxanes from biogas may be attempted in adsorption in solid materials at low temperatures. The most practical techniques are using activated carbons, silica and zeolites, and polymeric resins [9, 334].

Because of the high operating temperature of SOFC and the existence of catalyst in the anode, like nickel, it is possible to reform methane inside the SOFC. In the internal reforming, the heat required for the reforming reaction is provided by the oxidation reaction of H_2 and CO and the cooling demand of the SOFC stack is reduced. Moreover, the steam required for the methane reforming reaction is minimized due to the produced steam [345]. Therefore, the internal reforming method helps SOFCs to be more efficient. On the other hand, internal reforming might cause thermal stress due to the highly endothermic methane reaction, leading to anode deactivation, degradation, and in the worst cases, anode delamination and cell cracking [346].

The major disadvantage of the internal reforming technique is the risk of solid carbon formation on the anode surface. This is due to catalysts like nickel, which has shown a good activity for carbon formation [9]. The amount of reforming agent should be precisely determined based on the anode type, fuel and SOFC operating conditions to prevent the carbon deposition. In the biogas fuelled SOFC, the concentration of CO_2 in biogas is less than methane concentration and in the range of 40 mol.%, and it is not enough for complete conversion of methane. Therefore, an additional reforming agent (like steam) might still be required [147].

Attempts to investigate biogas internal reforming in SOFC have been reported in literature. Madi et al. [347] studied the performance of biogas fuelled SOFC short stack (with Ni-YSZ anode supported cell) with steam to carbon S/C ratio between 2.0 to 2.5. A degradation rate of 1.4% per 1000h has been observed for biogas

fuelled SOFC with S/C of 2.5 at an operating temperature of 750°C and under a current density of 2700 $A.m^{-2}$. Moreover, it is assumed that CO_2 only dilutes the fuel, and the influence of CO_2 on the stack performance was investigated. No significant effect on the cell voltage has been observed. The internal steam and dry reforming in SOFCs with Ni-YSZ and Ni-ScSZ anodes fuelled with H_2, CO and CO_2 gas mixtures have been investigated by Sumi et al. [29]. The Ni-ScSZ cell with an S/C of 0.5 showed a better performance and durability at an operating temperature of 1000°C. However, methane cracking has been observed, which leads to Amorphous carbon formation.

Lanzini and Leone [157] have investigated different biogas reforming methods for a Ni-GDC (ceramic-metallic composite) electrolyte supported cell (ESC). A better cell performance (in terms of the cell voltage) was achieved with steam reforming conditions compared to dry reforming and partial oxidation. It is recommended to add an extra 0.9 mole of steam to each mole of biogas (or S/C=1.5) to achieve a stable voltage at a current density of 3000 $A.m^{-2}$ at 850°C. A similar experiment was also conducted for a Ni-YSZ anode supported cell (ASC) with S/C=1.2 at a current density of 5000 A m^{-2} and showed a better cell performance than the ESC type because of the presence of more Ni-catalyst and a larger cell active area.

Madi et al. [278] studied the feasibility of internal biogas reforming for Ni-YSZ anode with steam concentrations in the range of 0.58 <S/C <2.32. Results showed that the cell voltage degradation is because of carbon deposition on the anode's active sites. It was partially reversible for S/C >1.5 at an operating temperature of 800°C and a current density of 3000 $A.m^{-2}$. Girona et al. [34] studied the impact of steam concentrations (0.12<S/C<2) over Ni-YSZ cermet anode fuelled with a humidified CO_2-rich biogas (CH_4/CO_2=1 and with 6 mol.% steam) at an operating temperature of 800°C. It was observed that a current density above 2600 $A.m^{-2}$ is required to prevent carbon deposition on the anode. However, the results of a biogas-SOFC system modelling study by Lackey et al. [326] illustrated that the system's electrical efficiency with S/C of 2.0 is higher than S/C of 1.0. This was due to the higher H_2 partial pressure in the reformed gas.

Results from different research groups showed that further experimental investigations are required, especially for Ni-GDC anodes. Using Ni-GDC anodes has several advantages in biogas fed-SOFCs, such as the higher electronic conductivity [20] and tolerance of H_2S contamination [104].

5.2.2.2. Ammonia fuelled SOFC

In contrary to IC engines, ammonia-steam mixture is considered a fuel for SOFCs [304]. Ammonia is cracked into nitrogen and hydrogen inside the SOFCs due to the high operating temperature of SOFCs (>650 °C). Complete ammonia cracking (Eq. 2-8) has been reported at 590 °C [132]. The ammonia cracking reaction is an endothermic reaction. Nickel, is considered as good catalyst for ammonia cracking. [348].

Dekker [317] has experimentally studied ammonia fuelled SOFCs, and performance was comparable to H_2 fuelled SOFCs. The cell voltage degradation rate of the cell during 3000 hrs was lower than 1% /1000 hrs. It is claimed that ammonia must be cracked directly at the inlet of the anode. The results illustrate that the electrical efficiency of SOFC can be 13% higher compared to H_2 fuelled one. This is due to the cooling effect of the endothermic ammonia cracking reaction, which consumes a fraction of the produced heat by the exothermic electrochemical reaction of H_2. This reduces the cooling demand of the SOFC stack, which increases the SOFC system efficiency. Similar results have been achieved by Liu et al. [349] with Ni-SSZ anode at different operating temperatures. However, in the SOFC-WWTP applications, the concentration of recovered ammonia from various waste resources is generally low [226, 338]. Only a few experimental studies focusing on the operation of ammonia concentrations were reported in literature. Saadabadi et al. [341] have investigated the performance of SOFC fuelled with ammonia-steam mixture (with various ammonia-water mixtures), recovered from struvite decomposition in WWTP. The power density of SOFC fuelled with aqueous ammonia with 14 mol.% ammonia was 33% less than the ammonia fuelled ones.

5.2.2.3. Biogas-Ammonia fuelled SOFC

Among the different fuels that have been considered for the SOFC systems, the biogas-ammonia mixture recovered from WWTP has not been thoroughly investigated [350, 351]. As mentioned, the concentration of ammonia recovered through the precipitation process is relatively low (≤14% molar) and diluted in water. On the other hand, for biogas reforming in SOFC systems, additional steam is required to prevent carbon deposition. This steam required can be supplied by adding the ammonia-steam mixture and biogas and use the mixture as a fuel in SOFC systems (Figure 5-2). However, in order to optimize the SOFC system performance and methane reforming, these two fuel streams should be mixed in an appropriate ratio. The minimum steam concentration required to prevent carbon deposition should be determined based on

the SOFC operating condition. High steam partial pressures in the fuel stream reduces the cell voltage, leading to low SOFC system efficiency. Moreover, due to the simultaneous NH_3 cracking in SOFC, the concentration of H_2 increases, impacting the methane reforming and has not been experimentally investigated (Figure 5-2). From the thermodynamic point of view, increasing the H_2 concentration reduces carbon deposition risk and increases the cell operating voltage [351]. Further experimental studies are required to come up with optimal strategies for ammonia-biogas processing for SOFC systems connected to WWTPs.

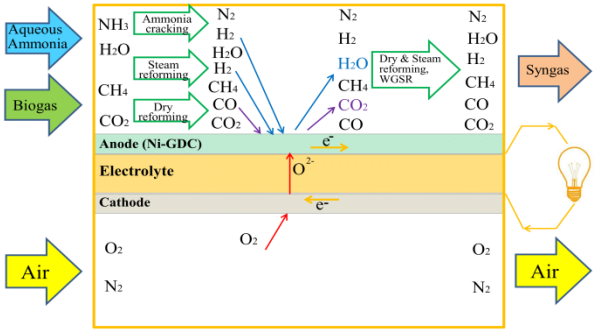

Figure 5-2: Biogas-Ammonia internal fuel processing in SOFC application

A simplified ammonia-steam-biogas fed SOFC system (in WWTPs) is presented in Figure 5-3. First, H_2S is removed in a gas cleaning unit (GCU) operating at ambient temperature. The cleaned biogas is mixed with the aqueous ammonia (in gas phase) after struvite decomposition. Subsequently, the mixed gas is preheated and fed to the SOFC stack. Ammonia cracking and methane reforming take place inside the SOFC stack and produce an H_2 and CO rich gas stream (Figure 5-2). After electrical power generation in the SOFC stack, the remaining H_2 and CO in the SOFC exhaust syngas are catalytically burned in an afterburner. The heat generated in the afterburner is used for pre-heating the air and fuel streams to above 650 °C. The remaining heat can be used in the struvite precipitation process (Figure 5-3).

The steam concentration should be adjusted to prevent carbon deposition. This should be controlled based on the operating current density and the temperature of the SOFC stack. The risk of carbon deposition in the anode can be roughly estimated by calculating O/C (Eq. (5-1)) and S/C (Eq. (5-2)) ratios. S/C and O/C ratio can be adjusted by changing the mixing ratio of the ammonia-steam and biogas streams (Figure 5-3).

$$O/C = \frac{2\times[CO_2]+[H_2O]}{[CH_4]+[CO_2]} \quad (5\text{-}1)$$

$$S/C = \frac{[H_2O]}{[CH_4]} \quad (5\text{-}2)$$

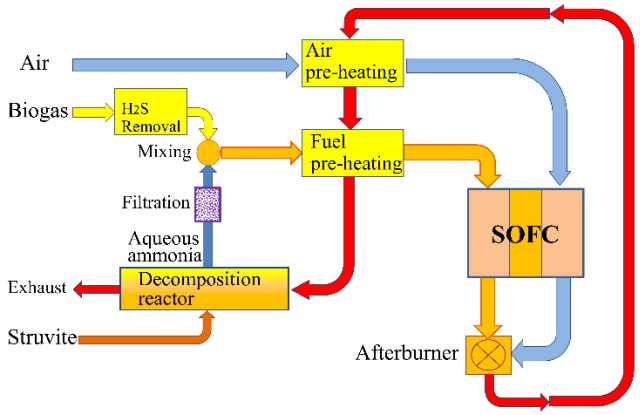

Figure 5-3: A simplified Biogas-Ammonia fuelled SOFC system integration and heat management.

5.3. Thermodynamic calculation

The carbon deposition threshold can be predicted based on chemical equilibrium calculations for different operating conditions and shown in a C–H–O ternary diagram (Fig. 3-4). The thermodynamic calculations help to identify the carbon deposition region based on the SOFC operating temperatures and fuel composition. The concentrations of C, H, and O elements in the fuel gas composition determine the operating point's location in the ternary diagram (Fig. 5-4). As shown in Fig. 5-4, using biogas (60% CH_4, 40% CO_2) in SOFC leads to carbon deposition at open-circuit voltage even at high operating temperatures like 850°C. Increasing the H and O concentrations by adding H_2O, NH_3, and CO_2 shifts the operating point toward the safe operating region.

In biogas fed SOFCs, steam is commonly considered as a reforming agent to prevent carbon deposition. In general, S/C ratios, in excess of 0.50 are expected to help to avoid carbon deposition at an operating temperature of 850°C, (as

indicated in equilibrium calculations). This S/C ratio corresponds to an O/C ratio of 1.10. The influence of increasing the steam concentration (O/C) in the C–H–O ternary diagram is shown in Fig. 5-4 with the (●) points.

Mixing ammonia-steam with biogas also increases the S/C and O/C ratios. This takes the fuel mix to the carbon-free region in the ternary diagram (at the given conditions). Steam in ammonia-steam mixture contributes to methane reforming. Hydrogen produced from ammonia cracking, increases the hydrogen concentration in the reformed fuel. The influence of mixing ammonia-steam with biogas is shown in the ternary diagram in Fig. 5-4 with the (■) points.

It is assumed that ammonia-steam with a composition of 25 mol.% ammonia and 75mol.% of water is mixed with biogas. The ammonia to steam (A/S) ratio for this ammonia-steam mixture is 0.33 (Eq. (5-3)). In this study, the ammonia to methane mixing ratio (A/C) is defined (Eq. (5-4)). This helps to explore the influence of the mixing ratio of ammonia-steam to biogas on methane reforming and SOFC performance. Increasing the A/C ratio results in different O/C ratios, and this also shifts the operating condition to the bottom left side in the ternary diagram (Fig. 5-4). For instance, by increasing the ammonia-steam flow, which increases the A/C ratio from 0.17 to 0.27, the O/C increased from 1.1 to 1.28, the blue and green (■) points, respectively (Fig. 5-4).

$$A/S = \frac{[NH_3]}{[H_2O]} \tag{5-3}$$

$$A/C = \frac{[NH_3]}{[CH_4]} \tag{5-4}$$

It should be emphasised that these results are with the SOFCs operating at OCV. While it might be different in practice as several studies have reported significant deviations between the equilibrium calculations results and experimentally measured values [352]. Experimental studies are hence required to identify the safe operating point at different operating conditions. Increasing the current density of SOFC also influences the operating conditions by increasing oxygen concentration in the anode, resulting in suppressing carbon formation [275].

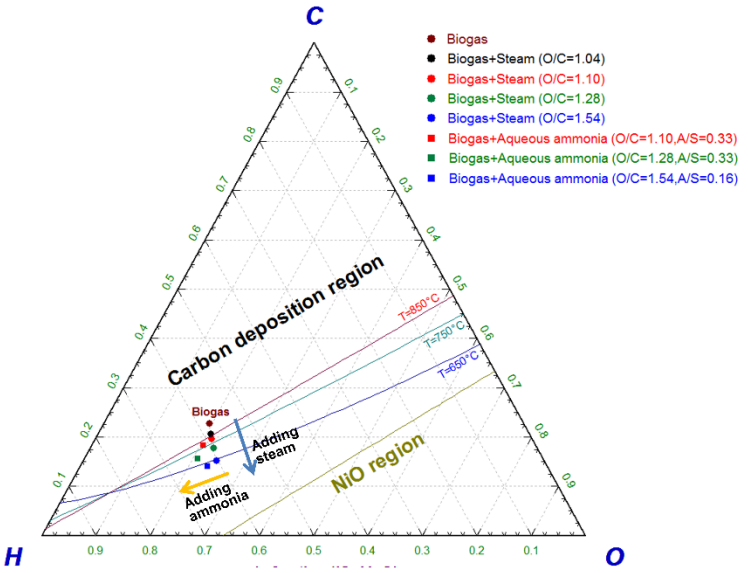

Fig. 5-4: Carbon deposition limits in a C-H-O ternary diagram based on equilibrium calculated at atmospheric pressure.

5.4. Experiment

5.4.1. Set up and Cell specifications

These experiments are conducted using biogas-ammonia fuel mixture for SOFCs with an electrolyte supported cell (ESC) with Ni-GDC anode. The experiments are planned so as to identify safe operating conditions for SOFCs with internal methane reforming and to investigate the influence of ammonia on the methane reforming and cell performance. A commercial planar (square) cell manufactured by H.C Starck is used with an active area of 81 cm^2. The anode consists of 57 wt.% NiO and 23 wt.% cerium oxide (NiGd0.1 Ce0.9 O1.95) with a thickness of 35 µm. The cell electrolyte is YSZ with a thickness of 100 µm, and the cathode is made of a 40 µm LSM ($La_{1-x}Sr_xMnO_{3-\delta}$) layer. An alumina block is used to hold the cell inside the furnace. A mica (thermiculite) sheet and ceramic sealants are used in the cathode and anode sides, respectively. Platinum and nickel meshes are used for current collectors' cathode and anode sides, respectively.

A schematic of the experimental test bench is illustrated in Figure 5-5. Gas mixtures are composed of different gas cylinders, and the gas flow rates are controlled by using mass flow controllers (MFCs). This helps to adjust the gas compositions hence the variables such as the O/C and A/S ratios. Steam is injected into the fuel stream with a controlled evaporation and mixing (CEM) system. An

online software (FLUIDAT) developed by the Bronkhorst High-Tech B.V is used to set the CEM mixing temperature based on the required steam partial pressure at the SOFC inlet. The fuel pipe is trace heated and increases the fuel temperature to 120°C at the SOFC block's inlet. Ammonia and CO_2 are injected at different points of the inlet pipe (Figure 5-5) in order to prevent ammonium carbamate (NH_2COONH_4) formation, which is a spontaneous reaction in dry gas at ambient temperature and pressure. The anode outlet pipe is also heated to 130°C to prevent steam condensation inside the outlet pipe. Simulated air is provided to the cathode side of the SOFC by mixing 1200 $Nml.min^{-1}$ nitrogen and 320 $Nml.min^{-1}$ oxygen. Air is preheated at the cathode alumina tube inlet, which is placed inside the SOFC furnace.

The exhaust gas of the SOFC is dried by passing the gas through a bubbled condenser and silica gel (Figure 5-5). This gas is then analysed by a micro gas chromatograph (micro-GC) to calculate the methane conversion. The micro-GC (Agilent 490) is equipped with a thermal conductivity detector with a Molsieve 5A and a PoraPLOTU column. The CO_2 in the anode exhaust gas can also be absorbed in silica gel [353]. Therefore, the measurements were conducted after the CO_2 saturation of the silica gel. The cell performance is evaluated by performing electrochemical current-voltage (I-V) characterization in the potentiostatic control mode by a Gamry FC-350 device.

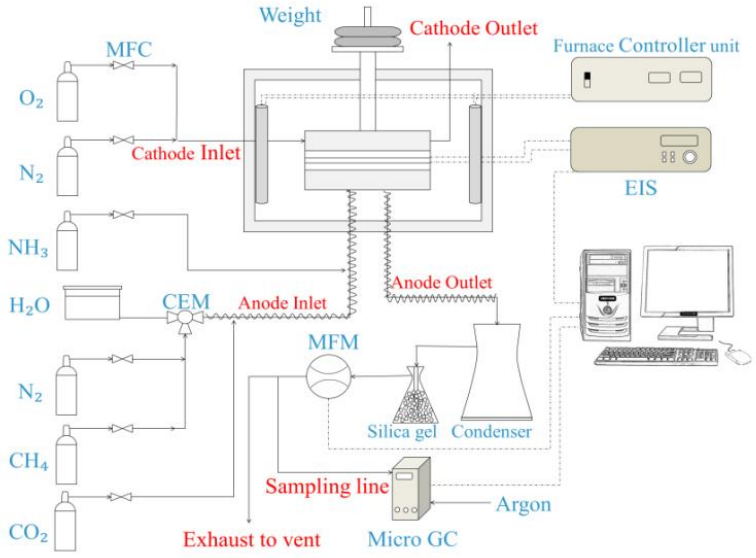

Figure 5-5: Schematic of the experimental test bench.

5.4.2. Experimental method

The furnace is heated up to 1000°C with a ramp of 40°C/hr, while nitrogen is fed into anode and cathode sides. When the cell temperature is stabilized at 950°C, the nickel oxide (anode) is reduced to nickel by gradually increasing the hydrogen concentration in the anode and providing simulated air to the cathode side. After cell reduction, the cell temperature is reduced to 850 °C for conducting the internal methane reforming experiments with different gas compositions. After the cell voltage stabilization, the I-V characterization test was performed with pure hydrogen as a reference test.

The experimental study's approach was to first identify the influence of steam concentration without mixing ammonia. Biogas with a fixed gas composition (60% CH_4 and 40% CO_2) was mixed with steam with different S/C ratios in the range of 0.4 to 1.23 (according to the O/C ratios between 1.04 to 1.54). The methane flow rate and the total flow rate of the fuel mix were kept constant for all gas compositions (Table 5-1). This is to avoid any potential of the fuel residence time effect fuel reactions. Nitrogen gas (as an inert gas) was added to the gas composition to keep the total flow rate at 1000 $Nml.min^{-1}$.

Table 5-1: Anode inlet gas compositions for combined reforming experiments.

Gas composition	CH_4 (%)	CO_2 (%)	NH_3 (%)	H_2O (%)	H_2 (%)	N_2 (%)	Total flow rate ($Nml.min^{-1}$)	S/C	O/C
A	-	-	-	18	78	4	1500	max	max
B	30	20	-	12	-	38	1000	0.4	1.04
C	30	20	-	15	-	35	1000	0.5	1.10
D	30	20	-	18	-	32	1000	0.6	1.16
E	30	20	-	24	-	26	1000	0.8	1.28
F	30	20	-	36.9	-	13.1	1000	1.23	1.54

Subsequently, the influence of mixing aqueous ammonia on the methane reforming is experimentally investigated. First, the influence of internal ammonia cracking on the methane reforming was studied. The ammonia concentration is increased by up to 8% at a constant S/C ratio of 0.6 (O/C=1.16) within three gas compositions of *G*, *H*, and *I* (see Figure 5-6). The A/C ratio also increases from 0.1 to 0.27. The A/C ratio of 0.1 (Gas composition *G*) represents the fuel mix of biogas and ammonia-steam with 14 mol.% ammonia concentration, obtained through struvite decomposition in WWTPs. The A/C ratio of 0.27 (Gas composition *I*) represents the biogas and ammonium hydroxide mix (commercially available) with 30 mol.% ammonia (Table 5-2).

Afterward, the influence of increasing steam concentration in the presence of ammonia is studied by increasing steam concentration from 15% to 37% in gas compositions *J*, *H*, *K* and *L*, while the ammonia concentration is constant (6%) (see Table 5-2). This implies that the ammonia concentration in ammonia-steam mixture increased from 14% to 30%, while the ammonia to methane ratio is constant A/C=0.2 (See Figure 5-6). The results indicated whether increasing the concentration of ammonia in the aqueous solution influence the performance of SOFC.

Finally, the influence of the biogas and ammonia-steam mixing ratio is investigated to identify the optimum mixing ratio maximum power generation. This is investigated by conducting experiments with gas compositions of *M*, *H* and *N*, with a constant ammonia concentration (25%) in the ammonia-steam with A/S=0.33. In these gas compositions, the ammonia to methane ratio (A/C) increases from 0.17 to 0.27. Accordingly, S/C increases from 0.5 to 0.8. The gas composition matrix for these four sets of experiments is shown in Figure 5-6.

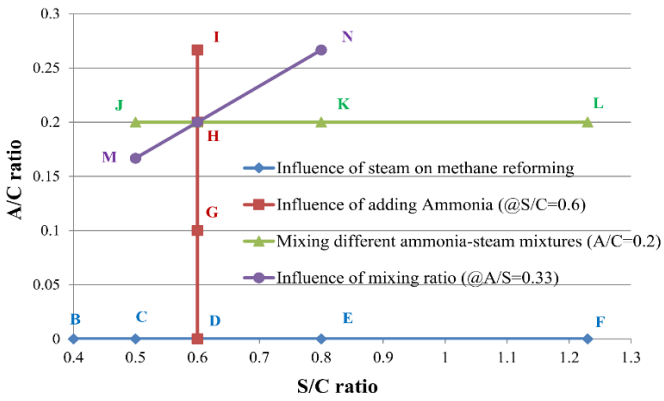

Figure 5-6: The experiment gas composition matrix.

Table 5-2: Anode inlet gas compositions for ammonia biogas mixture with different ratios

Gas compositions	CH_4 (%)	CO_2 (%)	NH_3 (%)	H_2O (%)	N_2 (%)	Total flow ($ml.min^{-1}$)	S/C	O/C	A/C	A/S
G	30	20	3	18	29	1000	**0.60**	**1.16**	0.10	0.17
H	30	20	6	18	26	1000	**0.60**	**1.16**	**0.20**	**0.33**
I	30	20	8	18	24	1000	**0.60**	**1.16**	0.27	0.44
J	30	20	6	15	29	1000	0.50	1.10	**0.20**	0.40
K	30	20	6	24	20	1000	0.80	1.28	**0.20**	0.25
L	30	20	6	37	7	1000	1.23	1.54	**0.20**	0.16
M	30	20	5	15	30	1000	0.50	1.10	0.17	**0.33**
N	30	20	8	24	18	1000	0.80	1.28	0.27	**0.33**

The methane conversion (X_{CH4}) is calculated based on the carbon balance of outlet gas composition at different current densities using Eq. (5-5). In this equation, *Yi* is the mole fraction of gas species *i* measured by Micro-GC at the SOFC outlet [171].

$$X_{CH_4} = \frac{0.5\ Y_{CO}}{Y_{CH_4} + 0.5\ Y_{CO}} \qquad (5\text{-}5)$$

5.5. Results and discussions

A reference test with humidified hydrogen was conducted at the beginning. As shown in Table 5-1, the methane flow rate of 300 N ml.min^{-1} was considered for reforming experiments. Therefore, an equivalent amount of hydrogen (1200 Nml.min^{-1}) has been considered for the reference test (assuming that one mole of methane can produce in total four moles of H_2 and CO through either steam or dry reforming reactions). The steam flow rate was 240 Nml.min^{-1}, similar to the gas composition D with 18% humidity (the S/C ratio of 0.6) as shown in Table 5-1.

After cell voltage stabilization, the cell performance was characterized by an I-V measurement and illustrated in Figure 5-7. At a cell voltage of 0.67 V, a current density of 3200 A.m^{-2} was achieved, which was the maximum achievable current density with the Gamry FC-350 device. The area specific resistance (ASR) was calculated around 1.0 Ω.cm^2 at high current densities (>1000 A m^{-2}).

5.5.1. Influence of S/C ratio on biogas combined reforming

First, initial biogas combined reforming experiments have been carried out with various S/C ratios according to the proposed gas compositions in Table 5-1. As shown in Fig. 5-4, based on equilibrium calculation, carbon deposition is predicted when the cell operates with gas composition *B* with an O/C ratio of 1.04 (S/C=0.4). These experiments started with the gas composition *F* with a higher S/C ratio because of the safer operating conditions with high S/C ratios (gas compositions *F* to *B*). The influence of steam concentration and current density on the internal methane reforming have been investigated at 850°C.

The cell performance has been evaluated by recording the I-V characteristics with different S/C ratios and compared the results with the results from reference test with humidified hydrogen in Figure 5-7a. Results showed that decreasing the steam concentration (S/C ratio) increases the cell voltage at open circuit. The OCV of the cell fuelled with the humidified H_2 was less than the cell fuelled with gas

composition *D*, while the steam flow rate is the same (Table 5-1). This is attributed to a lower local operating cell temperature (840°C) due to endothermic reactions of methane reforming on the anode. A lower operating temperature causes a higher cell voltage at open circuit. However, lower operating temperature increases the ohmic resistance. Therefore, the hydrogen-fuelled cell voltage at high current densities (CD>2500 $A.m^2$) is higher than the biogas fuelled one (Figure 5-7a).

For the gas composition *B* with the S/C ratio of 0.4, the cell voltage suddenly dropped by increasing CD (Figure 5-7a). The main reason is attributed to the carbon deposition as predicted by the equilibrium calculations (see Fig. 5-4). The cell area specific resistance (ASR) for the gas composition C (S/C=0.5, O/C=1.1) is higher than other gas compositions with higher steam concentrations. This might be because of a local carbon deposition on the anode surface, which blocks the micro-pores impacting the cell performance. This was not predicted with the ternary diagram in Fig. 5-4. Accumulation of solid carbon during long-term operation with gas composition C might cause the anode's deactivation.

The cell performance with gas compositions *E* and *D* were assessed with a relatively longer 12-hour test with I-V measurements. The I-V measurements with these two gas compositions at the beginning of the test (i) and after the 12-hour test (f) have been illustrated in Figure 5-7b. The cell performances were quite stable with these two gas compositions, and no cell voltage degradation was observed. The I-V curves before and after feeding these gas compositions were identical.

The OCV was around 40 mV higher for gas composition *D* (S/C=0.6) in comparison to gas composition *E* (S/C=0.8) because of a lower steam concentration. However, the ASR (slope of the I-V curve) for the gas composition *D* was slightly higher than the gas composition *E*. This might be because of the normal cell aging since the test with gas composition *D* was carried out after the gas composition *E*.

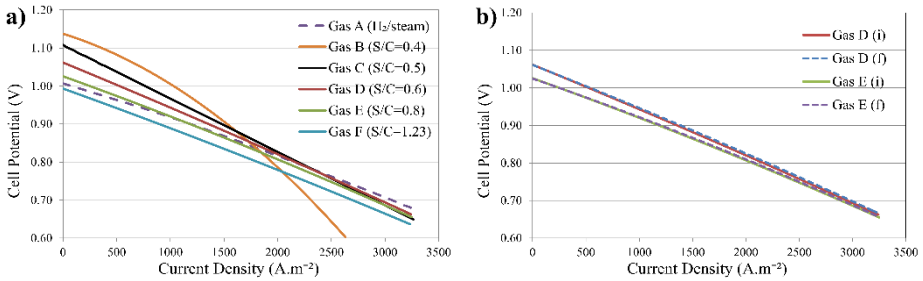

Figure 5-7: The I-V characterizations (a) for different gas compositions at 850°C (b) for gas composition D and E, initial (i) and final (f) after 12 hours experiment.

The methane conversion rate was investigated for gas compositions *C* to *F* for the cell operation at OCV, CD of 500 and 1000 A.m^{-2}. The methane conversion calculations were carried out when the cell temperature, voltage, and anode off-gas composition were stabilized. Based on the experience with the fuel flow rate and configuration of this setup, at least one-hour system stabilization time was considered for each CD, and a longer stabilization time (more than two hours) was considered when the gas compositions were changed. The results have been illustrated in Figure 5-8.

Based on this section's results, the optimum S/C of 0.6 is required for a Ni-GDC anode to prevent carbon deposition, obtain high methane conversion (above 95% at open circuit), and maximizing the cell's power density. This is similar to the results achieved by Sumi et al. [29] that a Ni-ScSZ cell was operated with an S/C of 0.5 at 1000°C. However, the identified optimum S/C ratio in this study is less than S/C ratio suggested by Madi et al. [278] with the S/C of 1.5 operating a Ni-YSZ anode at a current density of 3000 A.m^{-2}and 800°C. The achieved CDs in this study were comparable with the CDs obtained in other experimental studies with electrolyte supported cells [34, 278].

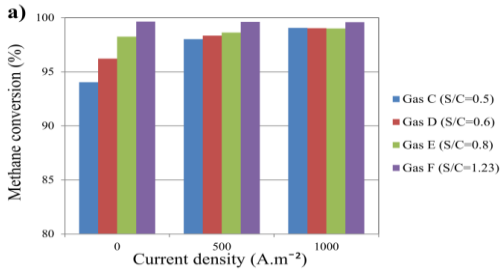

Figure 5-8: Influence of S/C ratio and applied current density on methane conversion at 850°C.

5.5.2. Influence of ammonia on biogas combined reforming

In ammonia-steam-biogas fuelled SOFCs, ammonia cracks first due to the low ammonia cracking temperature in comparison to the typical biogas reforming reactions. This suddenly increases the hydrogen concentration at the anode inlet and can influence the methane reforming reactions, and the cell voltage. In this section, the influence of ammonia cracking on the methane reforming reactions was experimentally investigated. This experiment was carried out with a constant S/C ratio of 0.6 (O/C=1.16) based on the result of the safe operating condition from the previous section. The influence of ammonia concentration was studied with three gas compositions *G*, *H* and *I*, with ammonia concentrations of 3%, 6%, and 8%. The cell performance was compared to the gas composition *D* in the absence of ammonia as a reference (Figure 5-6).

After the cell performance stabilization, the SOFC anode off-gas was analysed for different gas compositions. Results showed that the methane conversion was not significantly influenced by increasing ammonia concentration, as shown in Figure 5-9a. It increased by 1% by adding 3 mol.% of ammonia, and a further increase of ammonia concentration did not affect the methane conversion. Adding ammonia had another impact on the off-gas composition. Increasing the ammonia concentration decreased the CO_2 concentration, as shown in Figure 5-9a.

The composition of the anode off-gas has been analysed under different current densities as well. The H_2/CO ratio of the off-gas was calculated and shown in Figure 5-9b. The H_2/CO ratio was increased by increasing ammonia concentration due to hydrogen production through the ammonia cracking process. However, this ratio was not influenced by increasing the current densities.

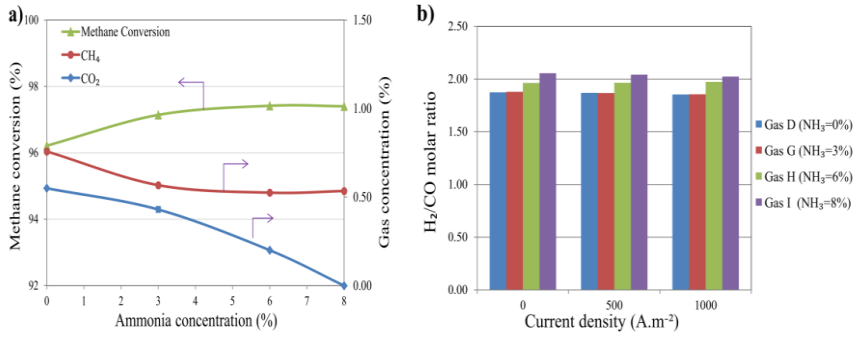

Figure 5-9: Influence of ammonia cracking on (a) methane conversion (b) current density (c) H_2/CO ratio at 850°C.

The I-V measurements were carried out for gas compositions *D*, *G*, *H* and *I*, to evaluate the influence of adding ammonia to the fuel on the SOFC performance (Figure 5-10a). These tests have been conducted for a short period (around 1 hour) for each gas composition when the cell temperature was stabilized. Results showed that adding NH_3 to biogas (with S/C=0.6) slightly increases the cell voltage at open circuit (Figure 5-10a). Increasing ammonia concentration increases the H_2 concentration. Increasing ammonia concentration decreases the cell operating temperature slightly (<5 °C) due to the endothermic internal ammonia cracking in the anode. Decreasing the cell temperature increases the OCV. On the other hand, decreasing the cell operating temperature leads to a higher cell ohmic resistance, which decreases the cell voltage at high CDs.

However, increasing the H_2 concentration by adding ammonia is more effective at high CDs, as illustrated in Figure 5-10a. Higher CDs were achieved by increasing the ammonia concentration at the cell voltage of 0.6 V. The results showed that by mixing 8% of ammonia to the biogas (with S/C=0.6), the power density of the SOFC increased by 10% (Figure 5-10b).

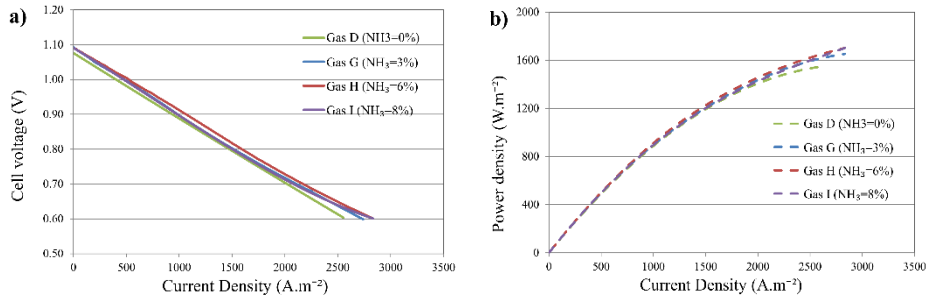

Figure 5-10: The I-V characterizations (a) and the I-P characterizations (b) for different gas compositions at 850°C.

5.5.3. Influence of ammonia concentration of ammonia-steam mixture

The concentration of ammonia in ammonia-steam can vary based on the effectiveness of ammonia recovery process. The ammonia concentration recovered from the struvite precipitation process (in WWTP) can be around 14%. However, ammonia concentration can be increased to 30% and still stored at ambient temperature and atmospheric pressure. In this section, the influence of ammonia concentration (in ammonia-steam mixture) on the biogas processing is investigated. It is assumed that the ammonia removal efficiency in WWTP is

constant. So, the ammonia concentration in the gas mixture was kept constant (6%), and steam concentration was varied between 15% to 37% (see Table 5-2).

Using ammonia-steam mixture with a higher water concentration improves the methane conversion at open circuit, as shown in Figure 5-11a. However, the influence of increasing the S/C ratio on the methane conversion was negligible when the S/C ≥0.8. Operating the cell at a higher current density improves the methane concentration for fuels with the S/C ≤ 0.8. The methane conversion for all gas composition at CD of 1000 $A.m^{-2}$ is around 99 mol.%. Therefore, to achieve a high methane conversion rate (> 98 mol.%) for a SOFC operation under high current densities (>1000 $A.m^{-2}$), an S/C ratio of 0.6 is sufficient.

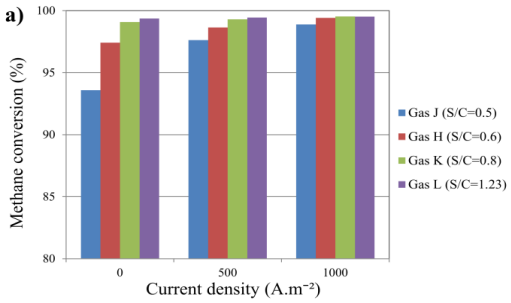

Figure 5-11: Influence of steam concentration and applied current density on methane conversion of ammonia-biogas mixture at 850°C.

The cell performance for this series of experiments was assessed by performing the I-V measurements (Figure 5-12a). The results showed that increasing the steam concentration decreases the cell voltage both at open circuit and when operating at high CDs. The results showed that mixing the ammonia-steam with a higher ammonia concentration of 30% (gas composition *J*) increases the OCV by 90 mV in comparison to the mixed biogas with ammonia-steam mixture with 14 mol.% ammonia (gas composition *L*). The maximum CD (at 0.60 V) obtained by gas composition *J* was 250 $A.m^{-2}$ higher than gas composition *L*. This increased the achieved power density by 15% with the gas composition *J* in comparison to gas composition *L*. Therefore, increasing the ammonia concentration in ammonia-steam mixture helps to increase the power density of the SOFC system connected with WWTPs. At the same time, the S/C ratio of the biogas and ammonia-steam mixture should be kept higher than 0.5 to prevent carbon deposition.

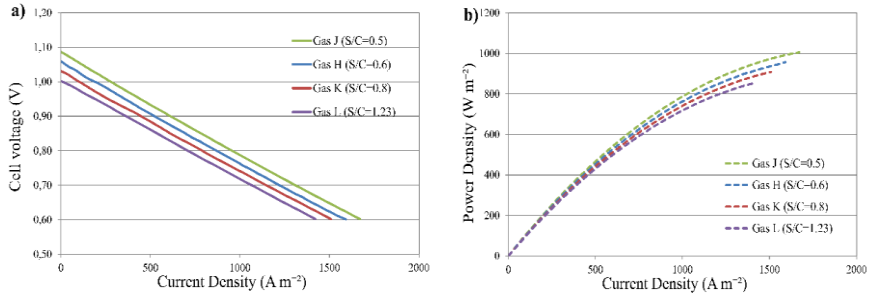

Figure 5-12: The I-V characterizations (a) and the I-P characterizations (b) for different gas compositions with a constant ammonia concentration (6 mol.%) at 850°C

5.5.4. Effect of mixing ratio of aqueous ammonia and biogas

Finally, the influence of adding ammonia aqueous (with 25 mol.% ammonia concentration) to biogas stream is investigated in order to identify an optimal mixing ratio. This maximizes the power density of SOFC while carbon deposition is prevented. A series of experiments was conducted with gas compositions of *M* and *N* and compared with the gas composition *H*. In these gas compositions, the ammonia concentration in ammonia-steam mixture was 25%, and the ammonia/water ratio was kept constant (A/S= 0.33). In contrast, the ammonia to methane ratio (A/C) increased from 0.17 to 0.27 (according to the S/C ratio between 0.5 to 0.8).

Increasing the ammonia-steam to biogas ratio simultaneously increased the ammonia and steam concentrations in the anode inlet. As expected (based on the previous series of experiments), increasing the ammonia-steam concentration increases the methane conversion rate slightly, as shown in Figure 5-13a. The methane conversion with gas composition *M* (A/C ratio of 0.17) was less than 95% at open circuit. Increasing the CD to 1000 $A.m^{-2}$ increases the methane conversion to more than 98%. In contrast, this was more than 98% at open circuit for the gas composition *N* with an A/C ratio of 0.27.

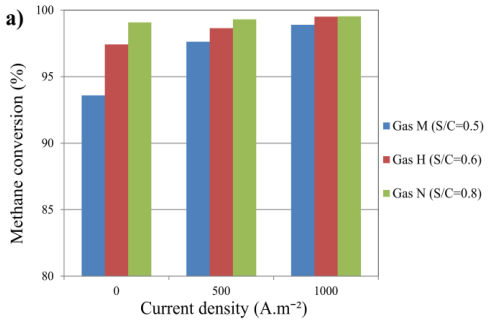

Figure 5-13: Influence of steam concentration and applied current density on methane conversion of ammonia-biogas mixture at 850°C.

The I-V measurements were applied to evaluate the impact of mixing ammonia-steam and biogas ratio on the SOFC performance and shown in Figure 5-14. As expected, increasing the ammonia-steam to biogas mixing ratio decreases the cell voltage, although the ammonia concentration rises. This is due to a higher concentration of water in the ammonia-steam mixture. By increasing the A/C ratio from 0.17 to 0.27, the OCV decreases from 1.09 to 1.03 V (Figure 5-14a). The ohmic resistance (ASR) for all three gas compositions is the same. The maximum obtained CD (at 0.6 V) decreased by 10%, as shown in Figure 5-14a. Therefore, when the A/S ratio is constant in ammonia-steam mixture, increasing the ammonia-steam to biogas ratio decreased the achieved CD and the SOFC power density (Figure 5-14b). However, it is essential to keep the S/C ratio in the fuel mixture above 0.5 to prevent carbon deposition.

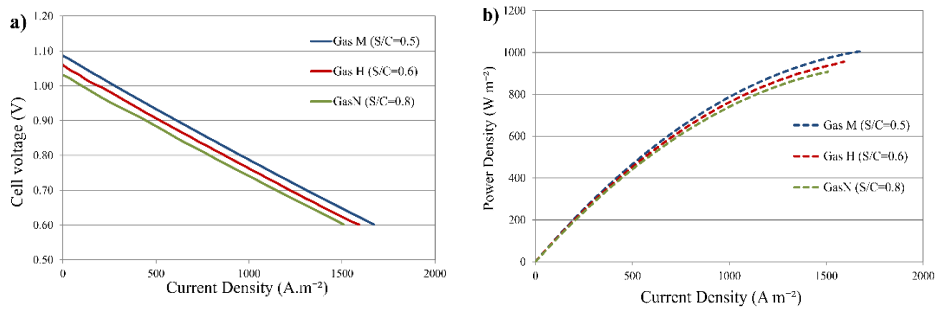

Figure 5-14: The I-V characterizations (a) and the I-P characterizations (b) for different mixing ratio of ammonia-steam and biogas at 850°C

5.6. System modelling study

As explained in the previous section (Fig. 5-1), biogas from anaerobic digestion and aqueous ammonia from the struvite precipitation process can be mixed and used in a SOFC stack. The results of experimental studies showed that biogas-ammonia fuelled SOFCs could be operated safely with the conversion of both methane and ammonia unaffected. Biogas direct internal reforming and ammonia cracking take place in SOFC. In this section, the SOFC system operation fuelled with the ammonia-biogas mixture is assessed by thermodynamic system modelling.

5.6.1. Model description

To evaluate the efficiency of the biogas-ammonia fuelled SOFC system, a Cycle-Tempo model is developed. This system is similar to the system developed in chapter 4, and a similar set of assumptions has been used (Table 4-2). Mass and energy balance equations are used to calculate mass flow in each apparatus. In this section, we describe a system model and its performance with three different types of fuels.

It is assumed that ammonia is stored in liquid phase at ambient temperature and atmospheric pressure. In this system, the aqueous ammonia should be evaporated and mixed with the biogas produced in the anaerobic digester reactor and cleaned in a gas cleaning unit. Then, the fuel is preheated to 650°C in two steps by two heat exchangers. The fuel utilization of the SOFC stack is set to 85%. The operating temperature of this SOFC stack is 825°C, and the flue gas temperature is 775°C at the outlet of the stack. An afterburner is used to burn the remaining fuel catalytically. The Flue gas goes through the heat exchangers to preheat the fuel and air (for the cathode side). The airflow for the cathode side is calculated based on the cooling requirement of the SOFC stack. Cathode gas recirculation is considered in this system to decrease the exergy losses. The air is heated up to 450° C in two steps. Then, mixed with the cathode air and the temperature increases up to 600° C. The system efficiency is calculated based on the LHV of the ammonia-biogas-mixture.

After preheating fuel and air, there is still high-quality heat (580°C) available to be used in the bottoming cycle. In this system, three processes, including an ammonia decomposition (in precipitation process), wastewater thermal pre-treatment, and ammonia evaporation processes, have been considered. Airflow is used to transfer heat in the heat exchangers of these three processes.

In the appendix of chapter 4, the required heat for ammonia removal in a decomposition reactor has been reported for three different samples of struvite. The results showed that 2650 kJ heat is required to produce one kg of ammonia-water vapour (with an ammonia concentration 0f 13 wt.% or 14 mol.%) in the decomposition reactor of the precipitation process. A heat sink (apparatus #801) represents the decomposition reactor in the Cycle-Tempo model, and the required heat is determined based on the flow rate of aqueous ammonia (the system fuel).

After the decomposition reactor, the heat is used to evaporate the aqueous ammonia. This is carried out within two heat exchangers. The first one (apparatus #408) increases the temperature of aqueous ammonia to the saturation temperature, and the second one (apparatus #407) is an evaporator. Then, the airflow temperature is still high enough to be used in thermal pre-treatment of wastewater streams. The temperature of wastewater increases from 15°C to 35° C in the heat exchanger (#409). This wastewater stream is transferred to an anaerobic digestion reactor to promote biogas production. This system is shown in Figure 5-15.

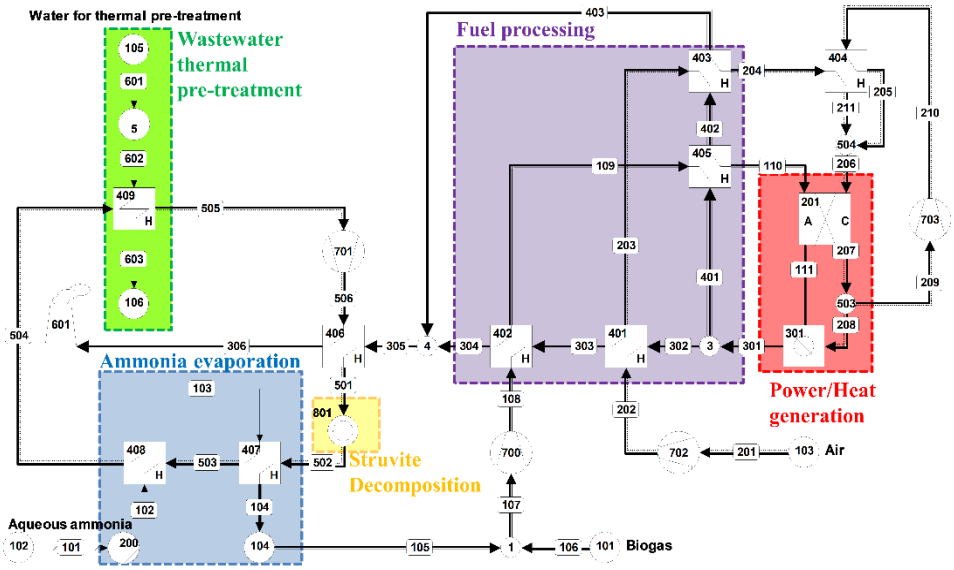

Figure 5-15: The Cycle.Tempo system configuration for biogas-ammonia fuelled SOFC system.

5.6.2. Modelling approach

The system has been explained in the previous section. This system is used to study three different scenarios with different fuels' mixtures. The reference model

is developed based on the mixture of aqueous ammonia and biogas similar to the Gas composition *G* in the experimental study section, and shown in Table 5-3.

Two more gas compositions are also selected for the system modelling study. In the gas composition *L*, it is assumed that the mixture ratio is different while the ammonia concentration in aqueous ammonia is kept constant (14 mol.%). This results in a higher steam concentration in the fuel, and the O/C ratio increases to 1.23. This implies that the ammonia removal is more efficient with this gas composition than the reference gas composition (gas composition *G*), and the ratio of NH_3/CH_4 is increased to 0.2 in the gas mixture. Additionally, the system performance fuelled with aqueous ammonia with an ammonia concentration of 25 mol.% is also studied. With gas composition *H*, the O/C ratio is similar to gas composition *G*.

Table 5-3: Gas compositions of ammonia biogas mixture with different ratios.

Gas composition	[NH_3] in aqueous ammonia	$\frac{O}{C}$	$\frac{NH_3}{CH_4}$	$\frac{H_3O}{CH_4}$	Aqueous Ammonia wt.%	Biogas wt.%
G (reference)	14 mol.%	1.16	0.10	0.60	21.95	78.05
L	14 mol.%	1.54	0.20	1.23	36.01	63.99
H	25 mol.%	1.16	0.20	0.60	23.85	76.15

For these three different gas compositions, the operating parameters such as fuel utilization, cell resistance, and the cell area are set the same. Operation parameters for the SOFC stack and the balance of plant components have been shown in the following table.

Table 5-4: Input parameters for ammonia-SOFC system model in Cycle Tempo.

Parameter			**Value**
Fuel utilization			85 %
Cell resistance			$1.0\times10^{-4}\ \Omega.m^{-2}$
Fuel flow rate			1 kg S^{-1}
Cells area			5000 m^2
SOFC operating temperatures:			
	Cell operating temperature:		825 °C
	Anode	Inlet:	650 °C
		Outlet:	775 °C
	Cathode	Inlet:	625 °C
		Outlet:	775 °C
Compressor:		Isentropic efficiency:	75%
		Mechanical efficiency:	98%
Pressure drops:		Fuel Cell:	0.005 bar
		Heat Exchanger	0.025 bar

The heat required for the decomposition reactor (Figure 5-15) is determined based on the ammonia flow rate and, based on the experimental results, is around 19.49 kJ/kg of ammonia. Moreover, the flow rate of aqueous ammonia and ammonia concentration affect the required heat for heating and evaporation of the aqueous ammonia stream. Since the fuel flow rate was constant, the cell area is determined in such a way that at Uf of 85% and cell resistance of 1.0×10-4 $\Omega.m^2$, the cell voltage is around 0.7. This cell voltage is in line with experimental results.

5.6.3. System modelling results

5.6.3.1. Reference model with aqueous Ammonia (14 mol.%)

First, as a reference, the system's operation fuelled with gas composition *G* is studied. The fuel mixture ratio (aqueous ammonia/biogas) is 0.43 to satisfy the O/C ratio of 1.16. The power generated in this system is 8.06 MW at a cell voltage of 0.689 V, a current density of 2340 $A.m^{-2}$, and overall fuel utilization of 85%. The air recirculation for this system is considered around 51%, resulting in around 28% oxygen utilization.

Methane is completely reformed to hydrogen and CO. The concentration of steam and CO_2 at the SOFC stack outlet are 53% and 32%, respectively. As fuel utilization of is set to 85%, the exhaust gas contains 8.6% and 5.2% of Hydrogen and CO, respectively. The Flue gas is catalytically burned in an afterburner by mixing air from the cathode side of the SOFC stack. The air to fuel ratio is (λ=) 7.2. The temperature of flue gas increases to 980°C. After pre-heating the fuel and air in two different steps, the temperature of flue gas decreases to 550 °C. The heat is transferred to the loop for heating struvite and wastewater stream by heat exchanger #406. The flue gas is cooled down to 100°C and released into the environment. The concentrations of steam and CO_2 in the exhaust gas are 13.6 % and 7.7 %, respectively. There are no traces of methane, hydrogen, and CO in the exhaust.

As mentioned in the previous section, the rest of the heat is used in a bottoming cycle with three different processes. The heat required in the struvite decomposition reactor for ammonia production is around 580 kW to produce aqueous ammonia (14 mol.%) with a flow rate of 0.22 kg. s^{-1}. The airflow at 530 °C supplies the required heat. Then, 560 kW heat is transferred to the aqueous ammonia in two heat exchangers. In the first heat exchanger, the fuel stream is heated up to 60.5°C (saturation temperature). Then the aqueous ammonia is evaporated in the second heat exchanger, which increases the temperature to

95.9 °C. Moreover, around 4880 kW heat is transferred to the wastewater stream with a flow rate of 53.5 kg. s^{-1} at 15°C and increases the temperature to 35 °C. This temperature is sufficient for mesophilic thermal pre-treatment in the anaerobic digestion reactor.

The net electrical efficiency of this system is 56.4%, and 8,060 kW electric power is generated (Table 5-6). The overall SOFC system efficiency is increased to around 87.8% by considering the heat transferred to the wastewater stream (4.47 MW). The net exergy efficiency of the system is 52.7%. The exergy efficiency of the SOFC stack ($W/(Ex_{in}-Ex_{out})$) is 87%, and 8% of the total exergy loss takes place in the fuel cell stack.

The exergy loss in all heat exchangers is around 1940 kW, which is 13% of the total exergy (Figure 5-16). The heat exchangers' exergy losses mostly occur in the heat exchanger #401 by 8% of the total exergy. This is due to the high temperature-gradient between the hot and cold airflow. The exergy transferred to the wastewater stream (for thermal pre-treatment) is mostly destructed in the heat exchanger #409 due to the low water temperature in the outlet (35°C). Moreover, 623 kW exergy is transferred to the exhaust (apparatus #601), equal to 4.2% of the mixed fuel exergy.

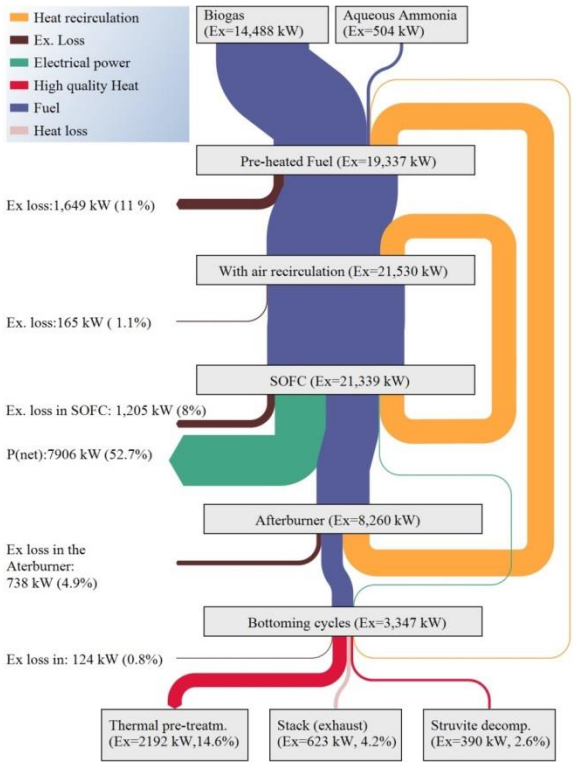

Figure 5-16: Distribution of exergy in the system fuelled with the gas composition G.

5.6.3.2. Aqueous Ammonia (25 mol.%)-biogas fuel

The previous section, calculations were based on the assumption that ammonia is stored after struvite decomposition with an ammonia concentration of 14 mol.%. This section assumes that the ammonia concentration is increased to 25 mol.% and again stored at atmospheric pressure and ambient temperature (the same as commercial aqueous ammonia storage conditions). In this case, the mixing ratio has to be changed in order to satisfy the O/C ratio required for the safe operating condition at the inlet of SOFC. The fuel mixture ratio (aqueous Ammonia/biogas) is increased to 0.48 to keep the O/C ratio at 1.16. The mixed fuel composition is similar to the Gas composition H in this chapter's experimental section. Therefore, the total inlet flow rate of fuel is again 1 $kg.s^{-1}$, similar to the previous model, but the aqueous ammonia flow rate is increased to 0.238 $kg.S^{-1}$. The biogas flow rate in this system decreased to 0.762 $kg.S^{-1}$.

The power generation increases to 8134 kW at the same operating conditions (fuel utilization, cell operating temperature, and cell resistance). The operating cell

voltage slightly decreases to 0.687 V at the current density of 2367 $A.m^{-2}$. The net energy and exergy efficiencies of the system increase to 58.2% and 55.4%, respectively (Table 5-6).

The air recirculation for the cathode side is around 50%. Based on this ratio, oxygen utilization is around 27%. The air to fuel ratio in the afterburner is λ=7.6, which is slightly higher than the previous model. This happens because of the higher airflow rate on the cathode side compared to the system fuelled with gas composition G. In this model, the concentration of water in the fuel decreased compared to the previous model fuelled with aqueous ammonia with 14 mol.% ammonia. This increases the airflow required for SOFC stack cooling.

In the bottoming cycle, the heat required (to produce this flow rate) in the decomposition reactor is increased accordingly to 1130 kW. Then, 4107 kW heat is transferred to the wastewater stream in the thermal pre-treatment process. This is less than the heat transfer in the system fuelled with aqueous ammonia with 14 mol.% ammonia. Moreover, 595 kW heat is also transferred for aqueous ammonia evaporation. Increasing the ammonia concentration increases the heat required for heating up the ammonia-water stream due to the higher Cp of ammonia.

The exergy flow diagram of this system is shown in Figure 5-17. The net exergy efficiency of this system is 55.43%, which increased by 1.7% compared to the previous system. The main reason is that the exergy transferred to the struvite decomposition reactor increased by 2%, increasing the net exergy efficiency. Additionally, the exergy efficiency of the SOFC stack increases to 91.2%. However, the exergy transferred to the thermal pre-treatment process decreases. The total input exergy slightly decreases because of the lower flow rate of biogas in this system. The exergy loss in the SOFC is attributed to operating at a lower cell voltage, which increases losses and decreases the stack's electrical efficiency. However, due to a higher current density of the cells, the power generation increases. Therefore, increasing the concentration of ammonia in the fuel increases the energy and exergy efficiencies of this system.

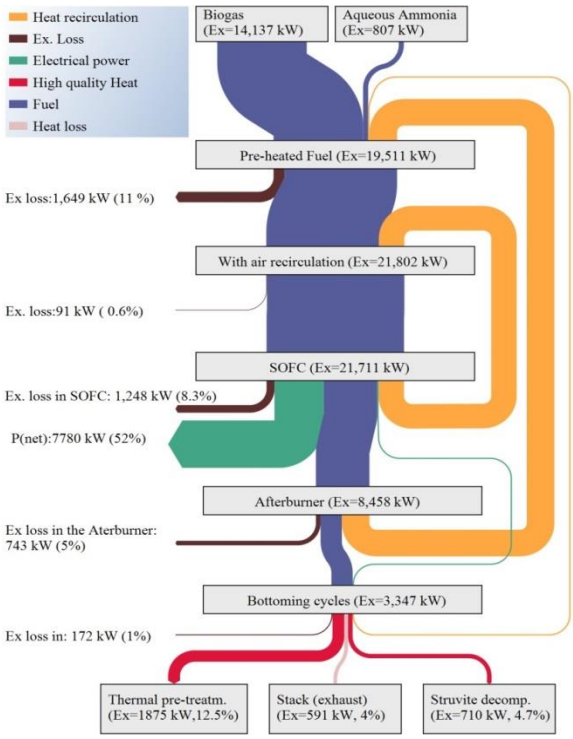

Figure 5-17: Distribution of exergy in the system fuelled with gas composition H.

5.6.3.3. Aqueous ammonia (14 mol.%)-biogas with higher S/C ratio

In the two previous sections, the system operation with two different gas compositions with an S/C ratio of 0.6 were studied. In this section, it is assumed that the aqueous ammonia from the decomposition reactor with an ammonia concentration of 14 mol.% is directly mixed with biogas. In this model, the mixing NH_3/CH_4 ratio is increased to 0.2, which increases the S/C ratio to 1.23 (O/C=1.54), similar to gas composition *L* in the experimental section. The fuel mixture ratio (aqueous ammonia/biogas) increased to 0.56, while the total inlet flow rate of fuel is kept constant (1 $kg.s^{-1}$). This increases the concentration of steam in the SOFC's inlet (up to 40 mol.%) compared to the models described in the previous sections.

In this system, the operating conditions are similar to the previous models. However, due to a higher steam concentration in the inlet fuel, the airflow required for the stack's cooling decreased to 7.75 $kg.s^{-1}$, which is 23% less than the reference model. This results in a lower air/fuel ratio (λ=6.6) in the afterburner. The air recirculation is also around 50%, and oxygen utilization increased to 30%.

The gas composition at the fuel cell stack's inlet and outlet were shown in the following table for the different fuel gas compositions. The steam concentration in the exhaust gas for gas composition *L* is more than two other gas compositions. On the other hand, the concentration of CO_2 decreases. However, the overall concentration of steam and CO_2 at the outlet is more than two other gas compositions, making the fuel more dilute. This influences the stack operating cell voltage. Due to the higher steam concentration at the inlet, the steam reforming reaction contributes more than dry reforming in methane conversion. This results in a higher H_2/CO ratio, as seen in Table 5-5.

Table 5-5: The gas compositions (mol.%) at the inlet and outlet of fuel cell stack for the different fuels.

Gas composition		CH_4	CO_2	NH_3	H_2O	N_2	H_2	CO	H_2/CO
G	Inlet	42.0	28.0	4.2	25.8	0	0	0	-
	Outlet	0	32.0	0	53.0	1.1	8.7	5.2	1.67
L	Inlet	32.3	21.5	6.5	39.7	0	0	0	-
	Outlet	0	27.6	0	58.4	1.9	8.3	3.9	2.13
H	Inlet	40.5	27.0	8.1	24.3	0	0	0	-
	Outlet	0.0	30.7	0	53.4	2.1	8.8	5.0	1.76

Both the cell area and fuel utilization were kept constant for all three fuel mixtures. Due to the different inlet gas composition, the stack operating conditions changed in this system. The cell voltage is higher (V=0.709) than the two previous models at fuel utilization of 85%. Because of the higher operating cell voltage, the net system efficiency increases to 60.3%. On the other hand, a lower current density was achieved in this system, which decreased the power generation and power density to 7053 kW and 1.41kW.m^{-2}, respectively. This is around 13% less than the reference model. This implies that a larger system (more cell area) should be applied to produce the same power as the system fuelled with gas composition *G*. The main reason is that the low heating value (LHV) of the gas composition *L* is less than two other fuel mixtures. A comparison between the results of these three models was shown in the following table.

Table 5-6: The system operating results with different gas compositions.

Gas	Energy efficiency (%)	Exergy efficiency (%)	Cell Voltage (V)	Current density (A.m^{-2})	Power density (kw.m^{-2})	After-burner (λ)	Wastewater flow (kg.s^{-1})
G	56.4	53.7	0.689	2,341	1.61	7.19	53.5
L	60.3	57.4	0.709	1,989	1.41	6.58	34.4
H	58.2	55.4	0.687	2,367	1.63	7.60	49.1

The heat transferred to the reactor is increased to 870 kW because of the higher flow rate of aqueous ammonia in the ammonia decomposition reactor. The heat transferred to the wastewater pre-thermal treatment process is 2963 kW. This is sufficient to heat 35.4 $kg.s^{-1}$ of wastewater flow, which is less than the system Fuelled with gas composition *G* and *H*, as shown in Table 5-6.

The exergy analysis of this system is carried out, and the flow diagram is shown in Figure 5-18. The system's net exergy efficiency fuelled with gas composition *L* is 57.4%, which is higher than the exegy efficiency of the system fuelled with the two other fuels. As explained before, the exergy of this fuel mixture (12755 kW) is less than the two other fuels. However, the exergy efficiency of the system operating with gas composition L is more than the two previous fuel mixtures. The exergy loss in the SOFC stack is 7.6% of the total exergy, and the exergy efficiency of the SOFC stack itself is 90.9%. This is mainly because of a higher stack operating voltage, which decreases the losses.

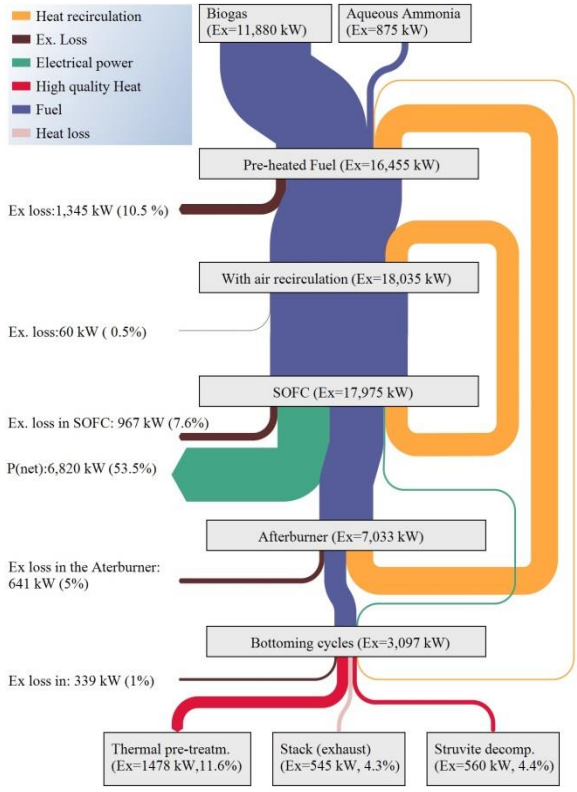

Figure 5-18: Distribution of exergy in the system fuelled with gas composition L.

5.7. Energy flow of the SOFC system fuelled with aqueous ammonia-biogas mixture

In this section, the energy flow in the SOFC system fuelled with biogas and aqueous ammonia (with 14 mol. % ammonia) is assessed. Since the system's energy efficiency fuelled with the gas composition L was maximum, only the energy flow of the system operating with this gas composition was evaluated in this section. The energy flow diagram of this system was shown in Figure 5-19. The LHV of the biogas stream (0.64 kg/s) is 11320 kW. Due to the high water concentration in the aqueous ammonia stream and the temperature of the aqueous ammonia stream (15 °C), the LHV of this fuel stream is zero. However, after evaporating the aqueous ammonia and pre-heating the ammonia-steam mixture, the ammonia cracks to hydrogen and nitrogen in the SOFC stack. In this case, hydrogen improves the performance of SOFC by increasing cell voltage. The net electrical power of this system is 6820 kW, which indicates an electrical efficiency of 60.3%.

To preheat the cathode air, 3600 kW heat is provided by the afterburner. Then, the cathode air recirculation provides 1420 kW heat to increase the cathode air inlet temperature to 650°C. Biogas and aqeous ammonia streams are also heated by 1165 kW heat supplied by the afterburner. Then, in the heat recovery section (bottoming cycle) of this system, 870 kW heat is transferred to the decomposition reactor, and 2900 kW is conveyed to the wastewater stream for thermal pre-treatment. This results in a thermal efficiency of 33.3%, and only 730 kW heat is transferred to the environment.

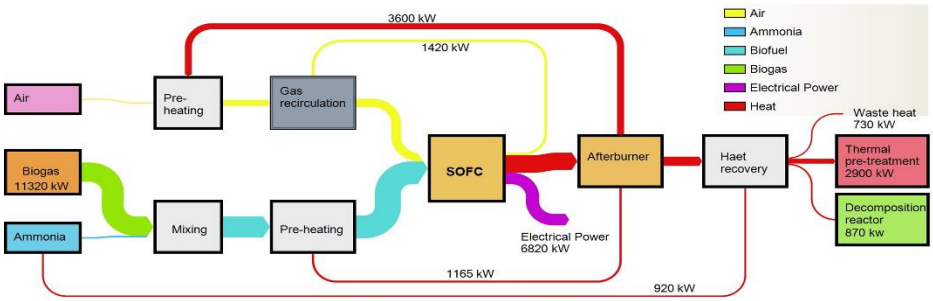

Figure 5-19: Energy flow diagram of the SOFC system fuelled with gas composition L.

5.8. Conclusions

Methane reforming is crucial in biogas fuelled SOFC in WWTPs to prevent carbon deposition on the anode. Therefore, an extra reforming agent like steam is

required to be mixed with biogas. On the other hand, there is a potential to recover ammonia from the wastewater stream in the form of aqueous ammonia with a high water concentration (>70%). Aqueous ammonia (after evaporation) can be mixed with biogas and used in SOFCs. The steam in the ammonia-steam mixture acts as a reforming agent to convert methane to H_2 and CO. The presence of ammonia might influence the internal methane reforming, which was not experimentally investigated. This study aimed to assess the impact of ammonia cracking on the internal methane reforming taking place in the anode of Ni-GDC SOFCs.

First, biogas steam reforming is explored to identify the required S/C ratio to prevent carbon deposition in the absence of ammonia. Results showed that the cell performance with an S/C ratio of 0.6 at 850°C was stable, and no cell voltage degradation was observed. An internal methane conversion of 97% was obtained at a CD of 1000 A m^{-2}. Three series of experiments were performed with different mixtures of ammonia-steam and biogas. Adding ammonia increase the cell voltage, and no negative impact on the internal methane reforming is observed. Adding 8% ammonia increased the cell power density by 8%. Moreover, the results showed that adding ammonia decreased the required S/C ratio in suppressing carbon deposition. By adding 6% ammonia to biogas fuelled SOFC, the required S/C ratio decreased to 0.5. Therefore, in the given conditions, the optimum ammonia to methane (A/C) ratio of 0.17 was identified to maximise the SOFC power density when an ammonia-steam mixture with 25 mol.% ammonia is mixed with biogas.

The system modelling results showed that the biogas-ammonia mixture is a promising fuel for a SOFC system. A model of the SOFC system is developed operating with three different biogas-ammonia mixtures. The net electrical system efficiency was above 56% for all the fuel mixtures. The heat generated in the SOFC stack and the afterburner is sufficient for air and fuel preheating, including the heat required for the struvite decomposition and aqueous ammonia evaporation. Moreover, the remaining heat can be used in a thermal pre-treatment of wastewater to improve the biogas production rate. Although using aqueous ammonia with 14 mol.% increases the system efficiency to 60.3%, on the other hand, the power density of the system drops by 14%. Generally, the system modelling study illustrates that the SOFC based power plant in wastewater treatment sites brings an opportunity to supply heat and power required for different processes.

Chapter 6

Developing an SOFC system at a groundwater plant

This chapter aims to investigate the feasibility of electricity production in a solid oxide fuel cell using methane recovered from groundwater as fuel. Methane must be removed from groundwater for the production of drinking water. Instead of releasing methane into the atmosphere, methane can be recovered by vacuum stripping and served as fuel. However, the electrical efficiency of currently used combustion-based technologies fuelled with methane-rich gas is limited due to the power derating because of the presence of CO_2 (25 mol.%). Moreover, the gas internal combustion engines are not practically viable in small-scale plants. The performance of SOFC fuelled by recovered methane is experimentally investigated. Additionally, a system modelling study is carried out to determine the optimum operating conditions of this system. The results are used to design an SOFC pilot plant at Spannenburg, the Netherlands.

Parts of this chapter have been published in Journal of cleaner production,125877 (2021)

6.1. Introduction

Vitens is the largest drinking water company in the Netherlands, supplying 330 million m^3 of drinking water per year to 5.7 million customers. Several groundwater sources Vitens abstracts water from containing dissolved methane gas with concentrations of up to 45 milligrams per liter. Because methane is a carbon and energy source for aerobic microbiology, it has to be removed from the water to prevent biofouling and water quality problems in the treatment plant and distribution network.

Conventional treatment involving intensive air stripping using tower or plate aerators costs a lot of energy and vents methane to the atmosphere. As methane is a powerful greenhouse gas, up to 24 times as potent as carbon dioxide, the venting of methane is the single most significant contributor to the climate footprint of Vitens.

At the Spannenburg treatment plant, the biggest treatment plant of Vitens with the most methane-rich groundwater, a vacuum degassing system is currently used to extract 1.3 million kilograms of methane from the water per year. The CH_4-rich recovered gas, consisting of around 70% methane and 25% CO_2, is used as a fuel for an internal combustion engine since the concentration of methane is high enough for efficient combustion. The electrical efficiency of this IC engine is around 35%, producing 550 kW of power that supplies 40% of the electricity demand of the treatment plant.

At Vitens, research is currently being done on a new methane abstraction system involving hollow fiber membranes that allow for CH_4-rich production at smaller treatment plants with a lower groundwater methane content. The resulting gas stream is too small and too diluted (CH_4<50%) with CO_2 and N_2 to be used as fuel for an IC engine. Therefore, the use of Solid Oxide Fuel Cell (SOFC) technology as an alternative is considered.

We propose to use a Solid Oxide Fuel Cell (SOFC) to use the CH_4-rich gas as fuel. SOFCs are fuel-flexible and potentially attain higher electrical efficiencies of up to 60%. To this end, specific gas processing, including cleaning and methane reforming, is required to allow for durable operation in a solid oxide fuel cell. We assessed whether electricity could be generated by a solid oxide fuel cell using methane recovered from a full-scale drinking water treatment plant as a fuel. The groundwater had a methane concentration of 45 $mg \cdot L^{-1}$, and the recovered gas by vacuum towers contained 70 mol.% methane. We used a gas cleaning reactor with

impregnated activated carbon to remove hydrogen sulfide traces from the CH_4-rich gas.

IC engines can be replaced by SOFCs to generate electrical power and high-quality heat. The electrical efficiency of SOFC is much higher than the IC and can be up to 55%. SOFCs are modular and can be installed in different scales (even as small as a 50 kW system) without sacrificing the electrical system efficiency. Another advantage of SOFCs is being fuel-flexible and can operate with a lower methane concentration in comparison to IC engines. However, extensive fuel processing is required. In fuel cell applications, contaminations can strongly influence the performance and the durability of the cells. The produced methane-rich gas contains traces of H_2S (9 ppm), and therefore, a gas cleaning unit needs to be designed to control the concentration of these trace contaminants properly. Furthermore, methane should be reformed to H_2 and CO (either internally or externally) to react with oxygen inside the SOFC electrochemically.

6.1.1. Groundwater as a source of drinking water

Groundwater is the most frequently used source for the production of drinking water in the Netherlands [354]. However, treatment of groundwater is needed to produce drinking water to meet the guidelines for drinking water set by the Drinking Water Directive (Council Directive 98/83/EC) in Europe. The required treatment depends on the specific composition of the groundwater, which amongst others depends on the characteristics of the subsurface. In addition to the conventional removal of natural organic matter, hardness, nitrate, and other geogenous substances, recent trends in drinking water production from groundwater focus on the removal of organic micropollutants [355] and toxic metals such as arsenic [356]. Furthermore, drinking water treatment plants (DWTPs) must minimise their carbon footprint to meet the 2020 Climate and Energy Package and the 2030 Climate and Energy Framework set by the European Union by decreasing the consumption of energy and chemicals and the direct emission of greenhouse gases [357].

6.1.2. Removal of methane from groundwater

Besides the presence of natural organic matter, carbon can be present in groundwater as methane (CH_4), which must be removed to avoid bacterial regrowth during the treatment, transportation, and drinking water distribution. CH_4 becomes present in groundwater as a result of anaerobic degradation of organic matter in the subsurface or the infiltration of CH_4 from natural gas

reservoirs [358]. Traditional treatment of groundwater typically comprises aeration using tower- and plate-aerators and cascades, to add oxygen (O_2) to the water and simultaneously strip undesired gases, such as hydrogen sulphide (H_2S), carbon dioxide (CO_2), and CH_4. However, the application of aeration results in greenhouse gas emissions to the environment because the off-gas containing air and the undesired gases are directly emitted. The emission of CH_4 is undesirable because it has 28 times higher global warming potential than CO_2 [359]. The annual methane emissions by the groundwater treatment global sector was estimated to be 0.53 teragrams which is around 0.2% of global methane emissions [360]. Therefore, the emission of CH_4 during groundwater treatment can contribute significantly to the total carbon footprint of DWTPs.

Besides aeration, CH_4 can be removed from water by vacuum (membrane) stripping [361], through which a gas with a concentration of CH_4 of 60% can be recovered from wastewater effluents [362]. The recovery of CH_4 by vacuum (membrane) stripping allows for flaring of CH_4, resulting in the conversion of CH_4 to CO_2, lowering the carbon footprint. However, the direct emission to the environment and the flaring of CH_4 both ignore the potential to generate energy after the recovery of CH_4.

6.1.3. CH_4 recovered from groundwater during drinking water production

A full-scale DWTP owned by Vitens N.V. produces drinking water from groundwater and has a maximum capacity of 25 million $m^3 \cdot year^{-1}$. The concentration of CH_4 in the groundwater ranges between 35 and 45 $mg \cdot L^{-1}$. The groundwater is pumped from the deep-wells directly to a system of vacuum towers, which remove 90 percent of the dissolved CH_4 using a vacuum depth of 0.2 bar(a). This results in a gas stream with a CH_4 concentration of 65-72 vol%. Subsequent treatment by plate aeration allows for the removal of the remaining 10 percent. Because plate aeration increases the concentration of O_2 in the water, iron is oxidised and iron hydroxide ($Fe(OH)_3$) flocs are formed, which are subsequently removed by media (sand and anthracite) filtration. After the media filtration, tower aeration is used to further remove CO_2 before pellet softening to lower hardness. Finally, any residual suspended solids are removed by another step of media filtration, and colour is removed by anion exchange to produce a final water quality suitable as drinking water. The recovered CH_4-rich gas is currently utilised in a 550 kW (nominal power) gas turbine, which has an electrical efficiency in the order of 35% (

Figure **6-1**).

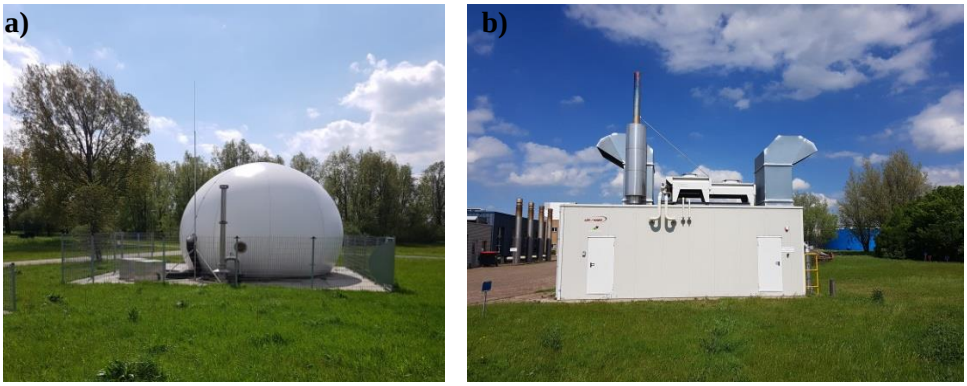

Figure 6-1: Recovered methane storage (a) and internal combustion engine (b) at Spannenburg treatment plant.

6.1.4. Energy generation from recovered methane

Recent efforts to valorise recovered CH_4 from water showed that it is possible to recover CH_4 for energy generation in a (micro) gas turbine [362]. Combustion-based energy conversion technologies, such as gas turbines, are widely applied to generate electricity and heat from (recovered) CH_4. However, combustion-based energy conversion technologies emit a large amount of CO_2 (per kW electrical power generation) and have an electrical efficiency of 20 - 35% [15], while micro-scale systems (< 10 kW_e) only have an electrical efficiency of 20% (Figure 6-2) [363].

On the contrary, electrochemical energy conversion technologies, such as solid oxide fuel cells (SOFCs), are reported to have an electrical efficiency up to 60% when using CH_4 as fuel (Figure 6-2), while the total energy efficiency can go up to 90% when the generated high-grade heat (at high temperature) is used [364, 365]. More specifically, Farhad, Hamdullahpur and Yoo [156] achieved an electrical efficiency of 42% for a 1 kW_e SOFC stack with an external steam reforming, fuelled with biogas (60 mol.% CH_4 and 35 mol.% CO_2) mixed with

anode off-gas. Tjaden, Gandiglio, Lanzini, Santarelli and Järvinen [366] achieved a 57% electrical efficiency for a 25 kW_e SOFC system using biogas fuel. Both studies used biogas containing around 60% CH_4, while Staniforth and Ormerod [132] showed the feasibility of using biogas containing only 45% of CH_4 as a fuel for an SOFC. Furthermore, Yi, Rao, Brouwer and Samuelsen [367] showed that the efficiency of the SOFC decreases only by 1% when shifting from natural gas (CH_4 > 90%) to biogas (with a system efficiency of 51.1%) as the primary source of CH_4. Hence, SOFCs are very flexible with respect to fuel composition in contrast to combustion-based technologies, opening opportunities for more efficient energy generation from fuels recovered from (waste) water.

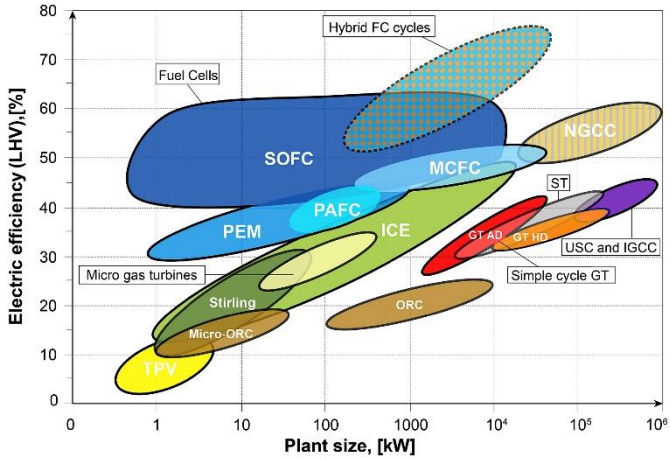

Figure 6-2: Electrical efficiency of power system technologies at different system scales [368].

6.1.5. Removal of contaminants for fuel cell

When CH_4 is recovered from the water, for example, after biogas production during waste (water) treatment, contaminations like H_2S can be present in the recovered fuel. H_2S is a corrosive gas that could form concentrated sulphuric acid, depending on humidity, O_2 concentration and the presence of bio-film. It can lead to the deterioration of pipelines and other metal equipment [369]. Equipment in conventional power generation systems can tolerate H_2S levels around 250 ppm [87]. Contaminants such as H_2S and hydrochloric acids strongly influence the SOFC performance and the durability of the cells [231].

The recovered methane gas at the Spannenburg drinking water plant is relatively clean in comparison to biogas produced via anaerobic digestion or in landfills, where a wide range of harmful constituents is often found in the gas (e.g.,

siloxanes and halogens). At Spannenburg, the only significant contaminant is sulfur in the form of H_2S.

6.1.5.1. Influence on methane reforming

The reforming is carried out in the presence of a nickel-based catalyst, and H_2S is known to react with nickel via the following two reactions [103].

Chemisorption: $H_2S_{(g)} \longleftrightarrow HS_{(ads)} + H(ads/g) \longleftrightarrow S(ads) + H_2\ (ads/g)$ (6-1)

Sulfidation: $Ni + H_2S \longleftrightarrow NiS + H_2$ (6-2)

At lower concentrations, the first reaction is dominant and deactivates the catalyst in the process. Appari et al. [103] have developed a detailed kinetic model for simultaneous dry and steam reforming and have shown the immediate deactivation of the catalyst at the introduction of H_2S due to the occupation of the Ni-surface by sulfur.

6.1.5.2. Influence on SOFC performance

Since the anode of a SOFC is generally Ni-based, the mechanisms that influence the fuel cell performance are not much different from those of the reformer. The effects of sulfur poisoning on the performance of the SOFC can be divided into short-term and long-term effects [107]. The fast chemisorption of the sulfur on the nickel anode causes a rapid decline in performance (cell voltage drop) due to the deactivation of the triple-phase boundary (TPB). Long-term effects include the formation of bulk nickel sulfide and microstructural changes like nickel migration.

H_2S deactivates the nickel catalyst present on the anode by forming nickel sulphide particles on the anode surface. The formation of large and dense nickel sulphide particles decreases in the three-phase boundaries (where the electrochemical reactions take place) [370]. A detailed kinetic model of methane reforming has been developed by Appari et al. [103]. The results showed an immediate deactivation of the catalyst at the introduction of H_2S as a result of the occupation of the Ni-surface by sulfur. The studies of the impact of sulfur poisoning on cell performance of different SOFC anodes have illustrated that Ni/GDC (Gadolinium Doped Ceria) cermet (ceramic-metallic composite) anode has a better performance during exposure to H_2S-containing hydrogen fuels [104]. This is due to the fact that GDC possesses mixed ionic and electronic conductivity.

Ouweltjes et al. [21] studied the influence of sulfur contaminant (2-9 ppm) on the Ni-GDC cell. Results indicated that sulfur mainly impacts the methane reforming

while the effect was negligible for H_2 and CO electrochemical oxidation. Experimental studies on conventional SOFC anode (Ni-SSZ) showed considerable electric potential drops with H_2S impurities higher than 5 ppm in the fuel [135]. Bao et al. [371] have reported a rapid cell voltage drop after exposure to H_2S, which is reversible after short-term exposure to a 1 ppm H_2S. Even though SOFCs are known as the most tolerant fuel cell type to H_2S impurities [99], fuel cleaning should be included to remove H_2S.

6.1.5.3. H_2S removal

One of the most promising technologies for removing H_2S to sub-ppm levels is adsorption on metal oxides. An adsorption media, typically zinc, copper, or iron oxide, is coated on a supporting material [372]. It is reported that the use of a Na–X zeolites fixed bed reactor and zinc oxide guard bed decreased the H_2S Concentration from simulated biogas contaminated with traces of 30 ppm H_2S to 0.07 ppm [107]. Additionally, synthesised adsorbent materials like activated carbon are commonly used for H_2S removal in dry conditions and ambient temperature [373].

Activated carbon (AC) shows great promise for its low cost, durability, and high activity at low concentrations of H_2S [374]. The well-developed pore volume and high surface area of AC's form the base of their excellent performance, however for optimized performance, the AC has to be chemically modified, mainly done by impregnation with suitable chemicals. According to the literature, impregnated AC removes H_2S via both adsorption and catalytic oxidation [374]. These two mechanisms at hand do not strengthen each other. However, even though the impregnation might negatively influence the physical adsorption capacity, the overall performance of impregnated activated carbons is much more excellent.

Most impregnated ACs are impregnated with basic compounds or oxidation-promoting chemicals like KMn04. These impregnated ACs perform best in the presence of small amounts of oxygen and high humidity. Xiao et al. [374] investigated the oxygen's influence by testing two different samples (impregnated and unmodified) under aerobic and anaerobic conditions and have shown a significant difference in performance. These results support the theory that H_2S is removed both by adsorption and by catalytic oxidation.

The dependence on the presence of oxygen and humidity, however, is different for each impregnation. Several commercially available adsorbents were tested by Sisani et al. [375] in an anaerobic environment. The Gas Hourly Space Velocity

(GHSV), defined as the volume flow rate of the gas stream divided by the filter volume, strongly influences the capacity. It is observed that the lower the GHSV, the higher the adsorbent capacity.

6.2. Proof of principle test

To improve the sustainability of drinking water production from CH_4-containing anaerobic groundwater, we propose to use the recovered CH_4-rich gas as a fuel for SOFC and thereby reduce the carbon footprint. However, to our best knowledge, it remains unknown whether CH_4-rich gas from groundwater can be effectively used as fuel in an SOFC. To this end, CH_4-rich gas from a full-scale DWTP was sampled and, analysed and contaminants were removed. Finally, the cleaned CH_4-rich gas was fed to an SOFC to assess the feasibility of energy generation under both dry reforming and steam reforming conditions.

6.2.1. Experimental SOFC set-up

A single cell SOFC test station (Fig. 6-3) was used to conduct the experiments. A planar nickel-coated scandium oxide stabilised zirconia (Ni-ScSZ) electrolyte supported cell (purchased from the Ningbo SOFCMAN Energy Technology Co., Ltd) with an effective surface area of 3.8 cm^2 was used for the experiments. The cell was placed between two Crofer metal plates, and gas tightness was achieved by sealing the cell with mica (thermiculite) sheets. Nickel foam and a gold mesh were used as current collectors at the anode and cathode, respectively. The cell and associated sealing were placed in a furnace to allow for a stable operational temperature.

The supply of synthetic N_2, O_2 and H_2 gas (with purity > 99.99%) was controlled by calibrated mass flow controllers (Bronkhorst High-Tech BV). The CH_4-rich gas was pumped from the sample bags to the anode by a suction pump (Hyco Vakuumtechnik GmbH), and the fuel flow rate was regulated by a calibrated rotameter. The fuel was initially pumped through a 500 mL gas reactor containing 225 grams of impregnated steam activated extruded carbon (Norit® RGM 3) designed to remove low concentrations of sulphur compounds. A sampling point for the fuel was placed after the adsorption media reactor to determine the concentration of H_2S in the fuel after the pre-treatment (Fig. 6-3).

To allow for steam reforming of CH_4, demineralised water was injected into the fuel inlet by a calibrated peristaltic pump, having a flow rate range of 0.006 – 2,300 $mL \cdot min^{-1}$ (Leadfluid Technology Co.). Due to the high temperature of the furnace and the low flow rate (ranging 1.8 - 9.2 $mL \cdot min^{-1}$) of the water, the water

evaporated before reaching the anode. To validate that the supplied gases and steam affected the actual cell temperature, a k-type thermocouple was placed at the anode surface of the cell. The anode off-gas was connected to exhaust tubing, while the cathode off-gas was vented to the air.

Finally, electric measurements were performed by an electrochemical impedance spectroscopy (EIS) device (Gamry FC-350) by simultaneously measuring the electric potential while a variable resistance was set to draw the electric current.

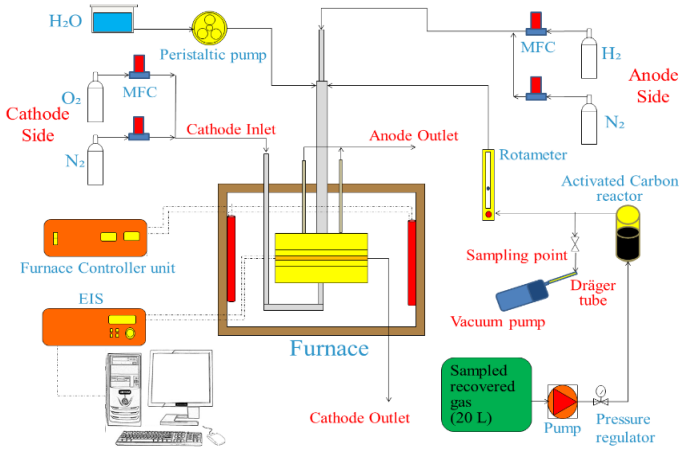

Figure 6-3: Schematic representation of the experimental SOFC set-up.

6.2.2. Experimental method

The CH_4-rich gas produced by the vacuum towers was sampled to conduct the experimental study by this recovered gas in the fuel cell lab. At this DWTP, water vapour in the recovered gas stream is condensed by cooling before the CH_4-rich gas storage. The CH4-rich was sampled in three bags with a volume of 20 litres (each) after the water vapour condensation. The sample bags were filled by connecting the bag to the recovered gas pipeline with a pressure of 22 mbar. The presence of H_2S in the CH_4-rich gas was measured directly after sampling, using a Dräger-Tube. Precipitation reactions of metal salts are the basis of measurement in the Dräger-Tube. Metal salts react with H_2S and form soluble metal sulphides, which have a different colour, and the contaminant level is visible through the shell of the Dräger-Tube. Additionally, the CH_4-rich gas was analysed in an Agilent 490 micro gas chromatograph, containing Molsieve 5A and PoraPLOT U columns. 200 mL of the CH_4-rich gas was used to determine the concentration of CH_4, H_2, O_2, nitrogen (N_2), CO, and CO_2.

After mounting the cell, the furnace was heated up to 850 °C with a ramp of 150 °C per hour. During the furnace heating, N_2 was fed to the anode and cathode at a flow rate of 200 Nml·min^{-1}. Before using the CH_4-rich gas as fuel, the nickel catalyst was reduced because the nickel was initially present as nickel oxide (NiO) on the anode of the cell. The reduction of NiO, and thus the activation of the nickel catalyst, was achieved by feeding hydrogen to the anode at 850 °C. The H_2 flow rate was gradually increased to 200 Nml·min^{-1} while simultaneously, the N_2 flow rate was decreased from 200 to 0 Nml.min^{-1}. Throughout the entire operation of the SOFC air simulated by a controlled mixture of N_2 and O_2 was fed to the cathode at a flow rate of 400 and 110 NmL·min^{-1}, respectively. Subsequently, the cell temperature was decreased to 800 °C. A mixture of H_2 and N_2 was fed to the anode as a reference for the cell performance, at a flow rate of 140 and 60 NmL·min^{-1}, respectively. Subsequently, the CH_4-rich gas was fed to the anode at a flow rate of 200 NmL·min^{-1}, both solely and in combination with steam. After stabilising the electric potential during the feeding of the fuel, the open circuit potential (OCP) was logged. Finally, the electric circuit was closed, and the electric current was drawn stepwise (5 mA.s^{-1}), while logging the electric potential.

6.2.3. Composition and pre-treatment of CH_4-rich gas

The concentration of CH_4 in the gas recovered from the DWTP was 71.4 mol. % (with standard deviation σ =1.83 and number of samples of r = 8). In addition to CH_4, the recovered gas contained 23 mol.% CO_2 and 5 mol.% N_2 and a trace of oxygen and H_2S (average of 9 ppm). The composition of the gas is similar to biogas generated during the anaerobic digestion, which also mainly contains CH_4 and CO_2 in the range of 70 - 45 and 60 - 40%, respectively [25].

The measurement of H_2S in the recovered gas after the pre-treatment indicates that the use of activated carbon as adsorbent was sufficient to decrease the Concentration of H_2S from 9 to below 0.1 ppm, which is an acceptable level for SOFC applications [231]. The residence time of the gas of 150 seconds allowed for sufficient contact time to adsorb the H_2S. Because the H_2S concentration was already below the detection limit, the effectivity of the other adsorbents was not further considered.

6.2.4. Reforming procedure of the CH_4-rich gas

Because the CH_4-rich gas contains a lower fraction of CO_2 compared to CH_4, dry reforming could lead to carbon formation, and thus the addition of steam is

required to reform the CH_4. Adding steam to the CH_4-rich gas fuel leads to a decrease in the concentration of CH_4 at OCP operating condition, as presented in Fig. 6-4a. As explained in 2.3, carbon deposition can be predicted by FactSage.

Fig. 6-4b presents the gas concentrations at equilibrium conditions (at 800 °C) after reforming the CH_4-rich gas mixed with steam (S/C ratio up to 1). When the recovered CH_4 is reformed without steam (S/C ratio = 0), carbon deposition takes place, and there is still 2.3 mol.% CH_4 present, which is not reformed to H_2 and CO. Meanwhile, the CO_2 concentration decreases to 0.7 mol.% due to the dry reforming reaction. By adding steam to the CH_4-rich gas, methane-steam reforming also takes place, and the equilibrium CH_4 concentration decreases to 1.3 mol.%, and only 3.5 mol.% of steam remains at an S/C of 0.6. Moreover, CO_2 in CH_4-rich recovered gas also contributes to the methane dry reforming reaction and WGSR [376], resulting in a decrease of the CO_2 concentration to less than 2 mol.%. Due to the higher concentration of steam at the S/C ratio of 1.0, the steam and CO_2 concentrations in the reformed gas (at equilibrium) increase to 11 and 4.6 mol.%, respectively.

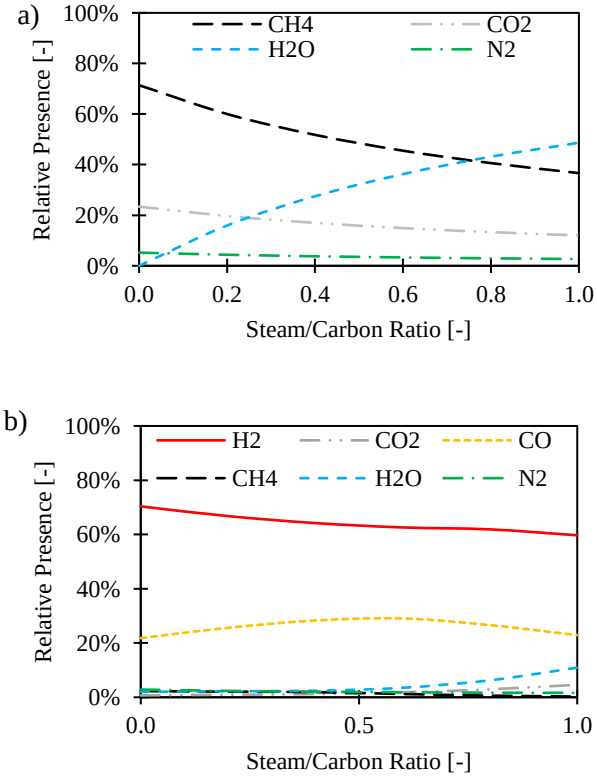

Figure 6-4: (a) The gas composition of fuel at the inlet of SOFC before reforming. (b) The gas composition of reformed fuel, according to equilibrium condition at 800 °C.

6.2.5. Thermodynamic approach

CH_4 must be reformed to H_2 and CO before electricity can effectively be generated in an SOFC. However, the deposition of carbon must be avoided, of which the risk is determined by the fuel gas composition and operating temperature at atmospheric pressure.

FactSage thermochemical simulation software is used to determine the required amount of steam to prevent carbon deposition. FactSage software is mainly based on chemical equilibrium conditions by minimising Gibbs free energy. Carbon-based fuels typically consist of three key elements that are involved in carbon deposition: carbon (C), hydrogen (H) and oxygen (O). Ternary C-H-O phase diagrams are used to identify solid carbon formation regions based on the operating temperature, and the amount of required reforming agent (in this case, steam) can be determined to shift the operating condition with the gas composition to the safe operating region. However, the chemical equilibrium condition cannot be completely achieved.

Several studies have reported significant deviations between the equilibrium calculations and experimental measurements [352]. The deviation might vary based on the anode catalyst types and the size of nickel crystallites [377]. Moreover, the fuel flow rate impacts the internal methane reforming in the SOFC due to the mass transfer effects at different fuel velocities [378]. The anode also impacts the carbon deposition risk in hydrocarbon Fuelled SOFCs. For instance, Takeguchi et al. [379] claimed that the Ni–YSZ cermet structure is favourable for whisker carbon growth. The authors proposed a carbon growth formation mechanism based on the dissolution of adsorbed carbon atoms in the metal crystallite, diffusion of carbon atoms through the metal, and precipitation at the rear of the metal particle.

The carbon deposition threshold for different operating temperatures of SOFCs is visualised in the C–H–O ternary diagram in Fig. 6-5. The gas composition of the CH_4-rich gas is located in the carbon deposition region. Adding steam as a reforming agent moves the operating condition into the safe region by increasing the concentration of H and O elements in the fuel. A steam to carbon (S/C) ratio

of 0.6 is required for the safe operation of SOFC at 800°C. However, local temperature drops due to the endothermic reforming reactions, can still lead to local carbon deposition. Increasing the S/C ratio to 1.0 brings the operating condition to the safe region even at lower cell temperatures (around 700 °C). However, the long-term safe operation should be experimentally investigated for different operating conditions.

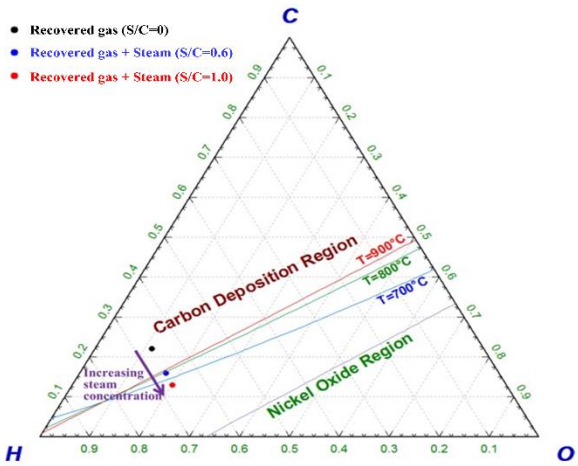

Figure 6-5: The C-H-O ternary diagram indicating solid carbon formation (based on equilibrium calculations) for various S/C ratios and operating temperatures at atmospheric pressure.

Furthermore, increasing the steam concentration of the fuel increases the CH_4 reforming, as presented in Fig. 6-6. At equilibrium conditions at 800°C, the CH_4 conversion increases from 82% (through the dry reforming reaction) to around 98% when instead of only dry reforming, also steam reforming takes place due to the addition of steam. By increasing the S/C ratio to 0.6, carbon deposition is suppressed at equilibrium condition, and this leads to a sudden increase in the CH_4 conversion rate (Fig. 6-6). The concentration of formed solid carbon (graphite) with various S/C ratios at equilibrium conditions is presented in Fig. 6-6.

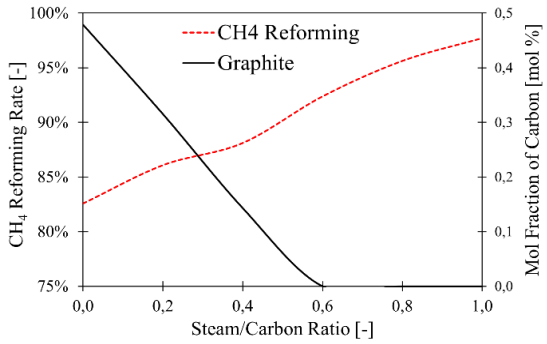

Figure 6-6: The reforming of CH_4 and carbon deposition (graphite formation) at different S/C ratios, according to equilibrium calculations.

However, the increasing contribution of steam reforming in comparison to dry reforming does not necessarily lead to an increase in H_2 concentration (according to the H_2/CO ratios of steam and dry reforming reactions). Increasing steam concentration to S/C of 1.0 increases the concentration of unreacted steam in the reformed gas composition, and this decreases the H_2 and CO concentrations. Moreover, increasing the H_2 concentration shifts the WGSR equilibrium toward the reactants (CO and H_2O), which again leads to a decrease in H_2 concentration. Ultimately, the results of equilibrium calculations (Fig. 6-4b) show that increasing the conversion of CH_4 by increasing the steam concentration does not lead to a higher concentration of H_2 and CO.

Figure 6-7 presents the Nernst potential for different gas compositions with the S/C ratio ranging between 0 and 1.0. When the S/C < 0.6, by increasing S/C, the H_2 concentration decreases. In contrast, the CO concentration increases. Thus, the Nernst voltage does not significantly change. When the S/C ≥ 0.6, due to remaining steam and CO_2 in the reformed gas, both H_2 and CO concentrations decrease. Therefore, the Nernst voltage drops by increasing the S/C. However, despite the lower Nernst potential, increasing the S/C ratio is necessary to prevent carbon deposition.

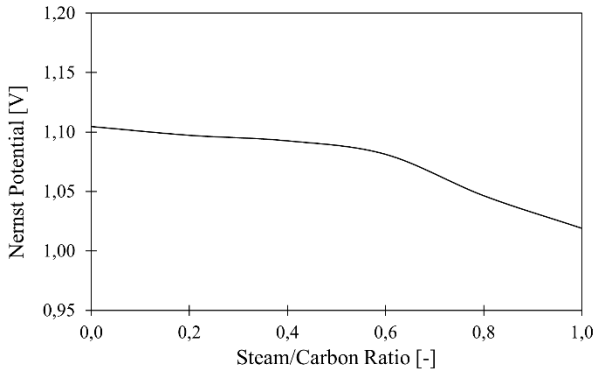

Figure 6-7: The calculated Nernst potential decreases when the S/C ratio increases, because the partial pressure of H_2 and CO decrease due to dilution, and the partial pressure of water increases due to the addition of steam.

6.2.6. Performance of the solid oxide fuel cell on CH4-rich gas

After the reduction of NiO to nickel, the cell performance was tested at 800 °C. A mixture of H_2 (100 NmL·min^{-1}) and N_2 (60 NmL·min^{-1}) was used as a reference for the performance of the cell. The electric potential measurements and I-V characterisation were performed after the stabilisation of temperature and electric potential. The measured OCP with H_2 and N_2 was 1.21 V, which corresponded well with the Nernst potential at 800°C (1.24 V), implying negligible H_2 leakage inside the setup [380]. Figure 6-8 presents the I-V characterisation and shows that the electric potential gradually decreased to 0.65 V at a rate of 5 mA·s^{-1} until an electric current density of 155 mA·cm^{-2} was achieved.

Subsequently, the CH_4-rich gas was fed to the cell, while the flow rate of H_2 was gradually decreased to 0 mL·min^{-1}. The measured OCP was 1.11 V when solely the CH_4-rich gas was fed to the cell, which again corresponded well with the Nernst potential at equilibrium conditions (1.10 V), indicating that the concentrations of H_2 and CO are similar to the equilibrium calculations, and the same (internal dry) CH_4 reforming is achieved. After stabilisation of the electric potential, the I-V characterisation was conducted. By increasing the electric current density, the electric potential dropped to 0.62 V at 150 mA·cm^2. The ohmic resistance (the slope of the curve at high electric current densities) is the same for H_2 and the CH_4-rich gas, as can be seen in Figure 6-8.

According to the equilibrium calculations, operating an SOFC with the CH_4-rich gas composition (CH_4 concentration of 70 mol.%) results in carbon deposition in long-term operation, which was experimentally investigated by Lanzini and

Leone [157]. The OCP decreased from 1.11 V (for dry reforming conditions) to 1.02 V (for steam reforming conditions) by adding steam to allow for steam reforming. The measured OCP was equal to the Nernst potential (1.02 V), again indicating that CH_4 was almost completely reformed to H_2 and CO. Similar results regarding the high CH_4 reforming with the S/C ratio of 0 to 3 has been observed in the study of Timmermann, Fouquet, Weber, Ivers-Tiffée, Hennings and Reimert [381]. However, an electric potential fluctuation (±2 mV) was observed, caused by the non-uniform fuel-steam gas mixture. The I-V characterisation of the cell performance with CH_4-rich gas and steam reforming is presented in Figure 6-8. As a result of the lower OCP, the maximum achieved current density at 0.6 V was 123 $mA \cdot cm^{-2}$, which is lower than the achieved current density with H_2 and the CH_4-rich gas at dry reforming conditions. Due to higher ohmic resistance of electrolyte supported cells, the obtained current densities in this study are lower than the CH_4 fed SOFC with anode supported (Ni-YSZ) cells with the current densities in a range of 500 $mA \cdot cm^{-2}$ [168]. However, the cell resistance in this study is lower than the test carried out by Goula, Kiousis, Nalbandian and Yentekakis [270], who used a button Ni-YSZ cell at dry reforming condition and achieved a current density of 95 $mA \cdot cm^{-2}$. The cell resistance in this study is comparable with the results reported by Timmermann, Fouquet, Weber, Ivers-Tiffée, Hennings and Reimert [381], who reported a current density of 140 $mA \cdot cm^{-2}$ using an S/C ratio of 1.0 with both Ni-YSZ and Ni-GDC anodes, electrolyte supported cell. However, the cell resistance in this study is higher than a test with commercialized electrolyte supported Ni-YSZ cell, achieving a current density of 300 $mA \cdot cm^{-2}$ [157]. Hence, the cell performance in this study might be improved further by selecting a proper cell for this operating condition [9].

The power density curves for the different fuels are calculated (based on the I-V characterisation) and presented in Figure 6-8. Due to a lower OCP, the maximum power generation while using the CH_4-rich gas with steam reforming (72 $mW \cdot cm^{-2}$) was lower than for using H_2 (99 $mW \cdot cm^{-2}$) and CH_4-rich (89 $mW \cdot cm^{-2}$) at dry reforming conditions. Achieving a lower power density implies that a larger SOFC stack should be used for the CH_4-rich gas Fuelled SOFC system with steam reforming, compared to dry reforming. However, the use of steam reforming avoids any risk of carbon deposition, according to the experimental results of Lanzini and Leone [157].

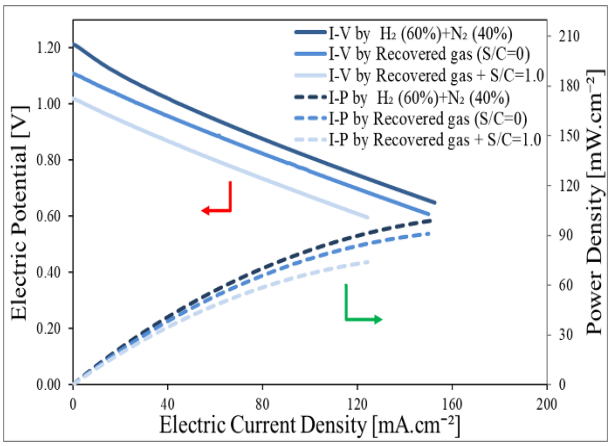

Figure 6-8: The I-V characterisations of the cell and the determination of the peak power density for the various tested fuel compositions.

Using recovered methane from the drinking water treatment plant in SOFC opens up an opportunity to increase the treatment plant's efficiency and decrease the emissions. The experiment results show that it is possible to clean the trace of H2S (10 ppm) by activated carbon with a residence time of 150 S at ambient temperature. However, this should be considered that the residence time plays a vital role in the gas cleaning unit, and this should be optimized.

6.3. Gas cleaning unit design

This section focuses on designing a GCU for the Spannenburg groundwater treatment plant, where a hydrogen sulfide (H_2S) fraction of 10 ppmv is present in the recovered methane. A 4-kW SOFC will be installed at this plant, and a proper gas cleaning unit needs to be designed. Traces of H_2S can be very harmful to metal equipment under some conditions. At lower concentrations (<250 ppm), it forms no direct hazard for pipelines or other robust equipment. However, it can strongly influence the performance of more sensitive equipment like SOFCs. The nickel catalyst in both the external reformer and the anode of the SOFC reacts with H_2S. Therefore, it is essential to implement a gas cleaning unit (GCU) to treat the gas before being fed to the system.

As explained before, the H_2S concentration in the SOFC fuel should be less than 0.5 ppmv. Iron oxide is one of the by-products of the Vitens' groundwater

treatment plant and can be used to adsorb H_2S. The feasibility of H_2S adsorption with Iron (III) oxide (ferric oxide) is studied.

The Iron sulfide will be converted back into Iron oxide (regeneration) by being in contact with oxygen or air through an exothermic reaction. The optimal temperature range for this reaction is between 25–60 °C for iron oxides. It is reported that (under proper operating conditions) iron oxide's sulfur loading capacity can reach 25% (w/w) [382].

6.3.1. Experimental method

At the beginning of this study, a fixed-bed reactor of iron oxide is used to clean a contaminated gas with 50 ppmv H_2S (and balance Nitrogen) at room temperature (20°C) and atmospheric pressure. The schematic of this small gas cleaning unit is shown in Figure 6-9. An MFC controls the gas flow rate. The contaminated gas enters from the bottom of the fixed bed reactor. After cleaning with Iron Oxide, the gas passes through a bubbler to condense the water vapour produced. The height of the fixed-bed was 20 cm with an inner diameter of 3.6 cm. It is considered that the diameter of the reactor should be ten times bigger than the size of adsorbent particles.

The gas can be sampled from the top and bottom of the fixed-bed reactor. A manual pump is used to suck the gas through an H_2S measurement tube. Different types of tubes with different gas detection levels can be used to measure the concentration of H_2S.

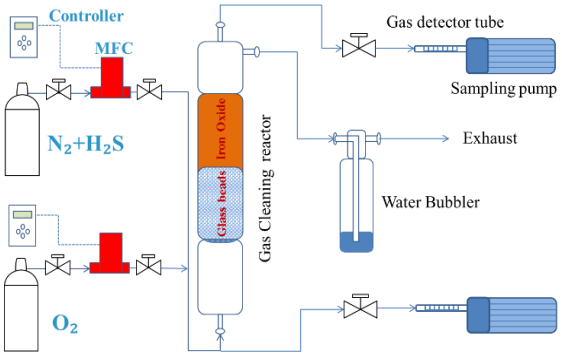

Figure 6-9: Schematic of the experimental gas cleaning unit

The reactor was filled with 177 g (200 cm^3) Iron oxide. During this experiment, the gas flow rate set to 1.0 lN/min, and the outlet gas was sampled every 8 hours. Results showed that the concentration of H_2S at the outlet was below the detection

level (0.2 ppmv). Measurements have been repeated for two days, and no H_2S was detected at the outlet.

After evaluating the feasibility of H_2S removal with Iran Oxide at room temperature, the breakthrough behaviours of H_2S adsorption in a fixed-bed reactor of iron oxide-based adsorbent were studied. This test aims to determine the adsorption capacity of Iron Oxide produced at the Spannenburg groundwater treatment plant.

6.3.2. Breakthrough tests

The same fixed-bed reactor is used, but utilizing a gas bottle with a higher H_2S concentration (300 ppmv) shortens the test period. Moreover, the amount of Iron oxide has been decreased to 100 grams. The reactor was filled with some glass beads to keep the height to diameter ratio (h/D) of the reactor around 6.0. The gas flowrate decreased to 850 Nml/min. The gas hourly space velocity (GHSV=Q/V) is around 500 hr^{-1}, and the superficial gas velocity was around 0.015 m/s. The concentration of H_2S gas at the outlet of the reactor was measured on average every 15 hours. The colour of Iron oxide changed to black starting from the bottom of the reactor.

The results of breakthrough tests have shown in Figure 6-10. The breakthrough took place after 113 hours when the concentration of H_2S increased to 0.75 ppmv at the outlet. The iron oxide adsorbed more than 2.5 grams of H_2S, so the Iron oxide's adsorption capacity is 2.5 g/100gIron oxide. The concentration increased to 100 ppmv after 190 hours test, and more than 4 grams of H_2S was adsorbed through the entire test.

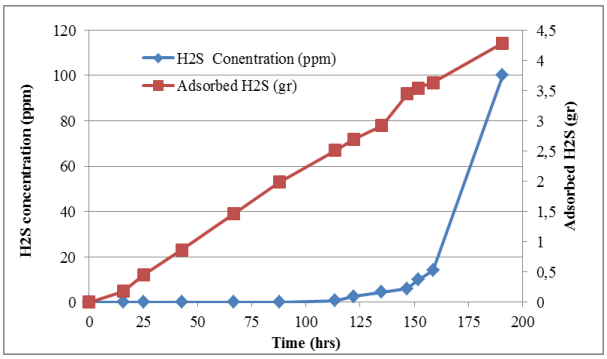

Figure 6-10: Breakthrough test of H_2S with 300 ppmv gas bottle

In order to conduct the second breakthrough test, another reactor is used. This reactor was slightly smaller. The reactor's diameter was 2 cm with the same height

as the previous one (15 cm). In this reactor, the h/D ratio increased to 7.5. First, the reactor was filled with some glass beads (5 cm height) and 25.5 grams of granular Iron oxide (10 cm height). In this test, a gas bottle with 600 ppmv H_2S (balance Nitrogen) is used. The test started with different gas flow rates to test the influence of GHSV on H2S adsorption. The results are shown in the table below.

Table 6-1: Influence of GHSV on Iron Oxide adsorption

Flow rates (Nml/min)	GHSV (1/hr)	H_2S Concentration (ppmv)
274.9	350	0
392.9	500	0
550.0	700	0.75
785.7	1000	2.0

By increasing the GHSV to 700 (1/hr), a trace of H_2S (0.75 ppmv) was detected at the outlet. The H_2S concentration increased to 2 ppmv when the GHSV was 1000 1/hr. Based on these results, a GHSV of 500 1/hr is considered for the breakthrough test with this reactor.

The breakthrough test with a 600 ppmv H_2S bottle was conducted for more than 145 hours (Figure 6-11). The first H_2S breakthrough was observed after 65 hours while more than 1.5 grams of H_2S was adsorbed with Iron oxide. It should be considered that the amount of Iron oxide used in this reactor is 25.5 grams. The H_2S adsorption capacity in Iron oxide with this reactor was around 5.8 g H_2S/100g of Iron oxide. The concentration of H_2S at the outlet was 2 ppmv after 65 hours and increased to 60 ppmv after 145 hours.

The results showed that the reactor design parameters play an essential role in the H_2S adsorption capacity of Iron oxide (Figure 6-11). Increasing the h/D ratio from 6 (in the first reactor) to 7.5 (in the second reactor) increased the adsorption capacity from 2.5 to 5.8 g H_2S/100 g of Iron Oxide.

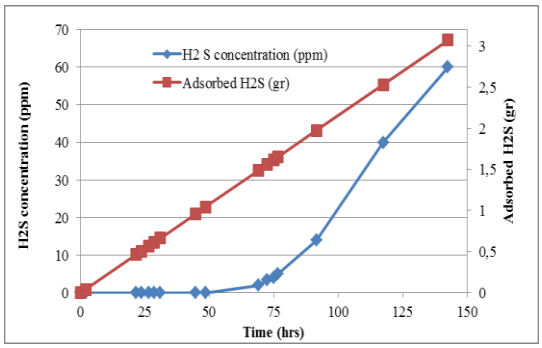

Figure 6-11: Breakthrough test of H_2S with a 600 ppmv gas bottle.

6.4. System modelling study

After the proof of principle test, the use of recovered methane as a fuel for an SOFC system is needed to be investigated. After removing contaminant trance (9-10 ppmv H_2S) through a designed gas cleaning unit, the recovered methane needs to be reformed to a hydrogen-rich gas. Based on the composition of fuel gas, different techniques can be used. The reforming technique and operating conditions should be selected based on optimizing power production. The amount of reforming agent should be properly controlled to optimize power production and prevent carbon deposition.

This section investigates the feasibility of using a 4-kW SOFC system (with CPOX unit) with gas produced at the Spannenburg plant. This SOFC system was modelled with Cycle Tempo software and run with recovered methane gas composition sampled at Spannenburg plant. Then, the optimum operating conditions are defined. Moreover, the other fuel processing method (steam reforming) is also investigated in order to select the optimum methane reforming method. Due to the modularity of SOFC stacks, there is no size limitation, and the design of the 4-kW system can be scaled up. The pilot plant at Spannenburg will be designed based on the modelling results carried out in this section.

6.4.1. Sunfire system description

During the Reinvent the Toilet project, supported by Bill & Melinda Gates Foundation, a 4-kW SOFC system was designed to be integrated with a plasma gasifier [383]. This system consists of a gas conditioning unit and an SOFC stack with 180 cells (Figure 6-12). First, the syngas (roughly 28% H_2 and 24% CO) is cleaned at a high temperature (450 °C) gas cleaning unit, and a catalytic partial oxidation (CPox) unit is applied for syngas conditioning [384]. Oxygen is used to pre-reform hydrocarbons and generates high steam concentration at the SOFC stack inlet. This helps to prevent carbon deposition and increases fuel temperature to 700-800 °C. In this system, the SOFC temperature is controlled by varying the air cathode flow rate and changing the stack fuel utilization.

The 4-kW SOFC system consists of a BoP hot box and a make-up gases panel (Figure 6-12). The hot box is connected to the supply gases (syngas and intake air) and has an exhaust flue gas pipe, which is thermally insulated. The hot box contains the air and fuel pre-heaters (counter-flow plate heat exchangers), CPOX unit, and catalytic afterburner. The pre-heaters are designed to increase the air and fuel temperatures to 650°C and 350°C, respectively. The fuel stream is heated up

further in the CPOX unit to 700°C. In the syngas fuelled SOFC system, the oxygen-to-carbon (O/C) ratio of the CPOX unit is controlled to partially oxidize the remaining hydrocarbons (roughly 4% methane) in order to prevent carbon deposition. The afterburner is used to burn the remaining hydrogen due to operating the SOFC stack on fuel utilizations Uf ≤ 85%.

Forming gas (3% hydrogen in balance nitrogen) is provided during system start-up, and the hydrogen, nitrogen, and air (CPOx air) MFCs are used as shown in Fig. 6-8. Some limiting parameters were defined to ensure that the system operates in a safe condition. This influences the system operating flexibility, especially when different fuels are used.

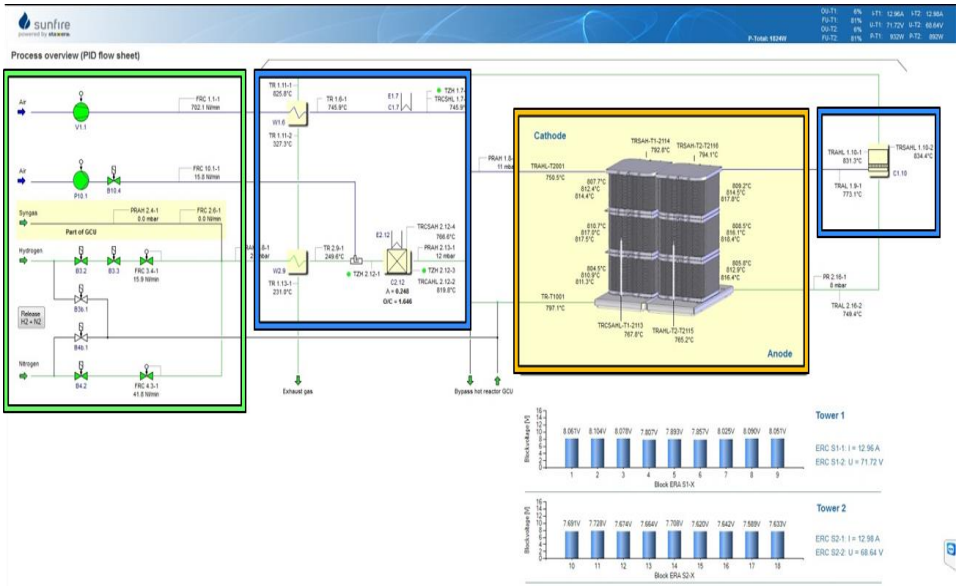

Figure 6-12: The 4-kW SOFC system operating with syngas.

6.4.2. Model description

In order to use this system at the groundwater treatment plant, the gas conditioning process should be assessed when the recovered methane fuel with a high concentration of CH_4 (70%) and CO_2 (25%) is used. Furthermore, other methane reforming techniques (steam/dry/combined reforming) should also be considered to improve the system efficiency.

Cycle Tempo Software is used to evaluate the power cycles thermodynamically. Equilibrium calculations are employed to calculate the fluid properties and energy production/consumption in each apparatus. Mass and energy balance equations

are used to calculate mass flow in each apparatus. The airflow for the cathode side is calculated based on the cooling requirement of the SOFC stack. It should be mentioned that the system efficiency is calculated based on the LHV of the fuel. The gas cleaning unit does not impact the thermodynamics of the system. Therefore, it is not included in the system modelling study (Fig 6-12). This system is operating at atmospheric pressure.

6.4.2.1. Off-design conditions

Based on the experiments conducted with simulated syngas fed-SOFC system [384], an off-designed model was developed to obtain more realistic results. The off-design thermal performance is evaluated based on steady-state monitoring and process simulation. These input data are used for fuel cell and pre-heating heat exchangers. For instance, the cell resistance for the syngas fuelled SOFC was 1.1 $\Omega.cm^2$. The operating temperatures are also inspired by a previous experiment conducted with syngas shown in Fig. 6-11 [384]. It is assumed that the variation in the overall heat transfer coefficient multiplied by the heat transfer surface area is depending on the variation of the mass flow. The following equation calculates the heat transfer coefficient for each gas flow:

$$(U.A)_i = (U.A)_D.\left(\frac{\varphi_{m,i}}{\varphi_{m,D}}\right)^{\eta_{cf}} \qquad (6\text{-}3)$$

Where φ is inlet flow (mol/s) for i: off-design and D: designed operating points, η_{cf} is an exponential correction factor. The UA values and other off-designed data are shown in Table 6-2.

Table 6-2: Input parameters for the SOFC system model in Cycle-tempo.

Parameter		Value
Cell operating temperature		0.6-0.75 V
Fuel utilization (per pass utilization)		76-82%
Current density		1500-2600 $A.m^{-2}$
SOFC temperatures:	Inlet	650-680 °C
	Outlet	775°C
	Operating (reaction)	800°C
Compressor:	Isentropic efficiency	75%
	Mechanical efficiency	98%
Pressure drops:	Fuel Cell	0.005 bars
	Heat Exchanger	0.25 bars

Air heater	$\Phi_{m,D}$= 13.41 kg/s, η_{cf} = 1.45, $(U.A)_D$ = 55.87 W/K
Fuel pre-heater	$\Phi_{m,D}$= 1.4 kg/s , η_{cf} = 0.80, $(U.A)_D$ =3.44 W/K

6.4.2.2. SOFC system with CPOX unit

An SOFC system with the same BOP components (including CPOX unit) as a 4-kW stack system is developed at specific off-design conditions by Cycle-Tempo software (Figure 6-13). The fuel composition is set based on the sampled gas composition at the Spannenburg plant. The air factor (λ) of 0.37 was set to satisfy the O/C ratio of 1.6 and prevent carbon deposition.

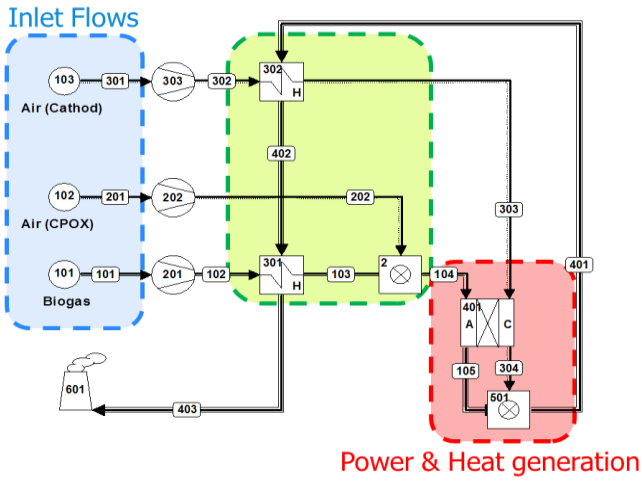

Figure 6-13: System model configuration with a CPOX unit.

6.4.2.3. SOFC system with an external steam reformer

As mentioned in previous chapters regarding the different methane conversion methods, methane steam reforming is considered. COPX unit is replaced by an external steam reformer. This system is shown in Figure 6-14.

The heat produced in the SOFC stack and catalytic afterburner supplies the steam reformer's heat duty of fuel pre-heating and the endothermic steam reforming reaction. After pre-heating cathode air and fuel, the remaining heat is used to generate steam in this system. Three heat exchangers are used to heat up the water stream to the boiling point, evaporation, and superheat the steam stream to 250°C at atmospheric pressure (See Figure 6-14).

The generated steam is mixed with CH_4-rich recovered gas inside the catalytic reformer and hydrogen-rich gas produced at 650°C. The steam to fuel ratio in the reformer (Xsf) is determined to prevent carbon deposition at the operating temperature of external reformer. For instance, the Xsf for CH_4-rich recovered gas with 70% methane is 0.77, which corresponds to the steam to carbon ratio (S/C) of 1.43. The cell voltage is calculated based on Gibbs free energy in equilibrium.

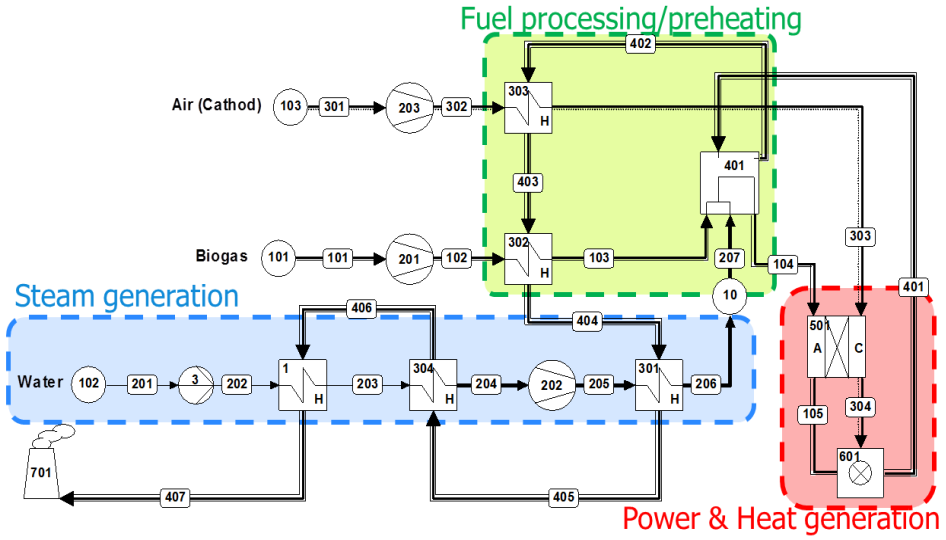

Figure 6-14: System model configuration with an external steam reforming unit.

6.4.2.4. SOFC system with external steam reformer and CO_2 recovery

The CO_2 gas is required to extract methane from groundwater at Spannenburg Plant. On the other hand, there is a possibility to recover CO_2 gas from the SOFC system exhaust gas since the concentration of CO_2 and steam is relatively high in the anode outlet gas. Then steam can be extracted easily with condensation and a CO_2-rich gas can be produced. In this model, the minimum flow rate of oxygen or air is set to burn un-oxidized H_2 and CO in the SOFC outlet gas in the afterburner (Figure 6-15). This prevents the presence of excess oxygen in the exhaust gas. Either oxygen or air can be used in this case. The system modelled with an external steam reformer is considered for integrating with the CO_2 recovery model (Figure 6-15). In this system, the SOFC cathode exhaust flow supplies the heat required for the methane steam reforming reaction and the remaining heat preheats the cathode airflow to 250°C.

The flue gas of the afterburner is used to pre-heat air, fuel, and generate steam. Then, the flue gas stream is passed through a moisture separator to condense the water vapour and increase the concentration of CO_2 in the exhaust gas.

Since oxygen is not available in the Spannenburg plant, air is also considered to be used instead of oxygen in the afterburner. In this case, nitrogen concentration increases in the flue gas and increases the total exhaust flow rate. However, the air factor (λ) is kept constant in this system.

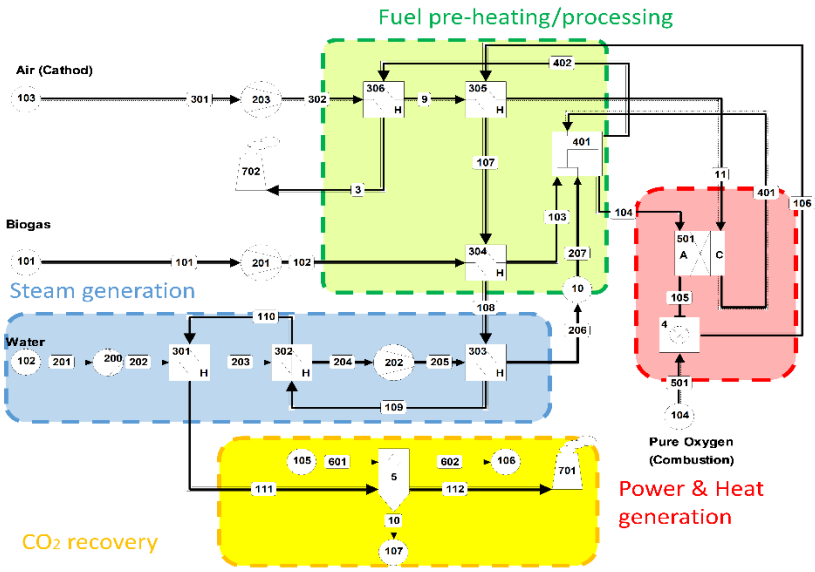

Figure 6-15: SOFC system model with an external steam reforming and CO_2 recovery with oxygen.

6.4.3. System modelling results

6.4.3.1. With CPOX unit

The CH_4-rich recovered gas composition is set based on the sampled gas composition from the groundwater treatment plant. The air factor (λ) of 0.37 was chosen to satisfy the O/C ratio of 1.6 in order to prevent carbon deposition. The gas compositions in different pipes of the system have been shown in Table 6-3.

As shown in the table, the methane is partially oxidized inside the CPOX unit, and the methane concentration is only 2% in the anode inlet (pipe #104 in Figure 6-13). The H_2 and CO concentrations in the SOFC inlet are 22% and 12%,

respectively. The rest of the methane could also be reformed in the SOFC. There is no trace of solid carbon in the pipelines based on equilibrium calculations. After the electrochemical reactions of fuels inside the SOFC, traces of H_2 and CO are still found in the flue gas. This is due to the set fuel utilization of 75%. The concentration of steam and CO_2 at the anode outlet increased to 27% and 18%, respectively. The rest of the fuel is catalytically oxidized inside the afterburner, and no H_2 and CO are in the afterburner flue gas. Due to the high flow rate of air from the cathode side, the concentrations of steam and CO_2 in the flue gas decreased to 5% and 3%, respectively.

Table 6-3: Gas composition of pipelines in the SOFC system with CPOX unit.

Pipe no.	**101**	**201**	**301**	**104**	**105**	**401**
[CH_4]	0.7	-	-	0.02	-	-
[CO_2]	0.25	-	-	0.08	0.18	0.03
[N_2]	0.5	0.77	0.77	0.45	0.45	0.75
[O_2]		0.21	0.21	-	-	0.16
[H_2]	-	-	-	0.22	0.06	-
[CO]	-	-	-	0.12	0.04	-
[H_2O]	-	0.01	0.01	0.08	0.27	0.05

The electrical efficiency of this system with the operating parameters mentioned in Table 6-2 was ηe=29.7 %. This should be mentioned that with the same operating condition, the system efficiency of syngas fuelled 4-kW stack system was ηe=33.7 % at V_{cell}=0.67 [384]. The low system efficiency is attributed to the fact that a high methane partial oxidation rate occurred inside the CPOX unit, which is not as efficient as (H_2 and CO) electrochemical oxidation in the SOFC stack.

The composition of recovered CH_4-rich gas might change by varying the methane recovery system operating conditions, such as the vacuum pressure of degassing vessels. Therefore, it is essential to investigate the influence of methane concentration on the SOFC system performance. This also could help to optimize of whole system's efficiency, including the methane recovered system.

The influence of methane concentration on system performance is studied by changing the methane concentration from 50% to 75%. The concentration of nitrogen (considered as an inert gas) is kept constant. Decreasing the CO_2 concentration increases the oxygen required for the CPOX unit to prevent carbon deposition. So, the λ was increased for higher methane concentration in the recovered gas (note: the minimal step-size for the lambda was 0.01, for this reason some values are used for 2 situations, see Figure 6-16). In this case, by decreasing

the methane concentration to 50% (increasing CO_2 concentration to 45%), the CPOX air factor (λ) decreased to 0.34 (Figure 6-16).

Results illustrate that system efficiency depends on the CPOX air factor, as shown in Figure 6-16. Therefore, a low CH_4 concentration in fuel does not significantly influence the stack efficiency, while the CPOX air factor (λ) plays a more critical role. It is necessary to keep the O/C ratio above 1.6 to prevent carbon formation. However, the λ of CPOX should be kept as low as possible. Lowering the CPOX unit's air factor reduces the exergy and energy losses and improves the system efficiency (around 1%). However, with low methane concentration, the generated power is decreased (around 1.5%), which leads to a lower power density. In this study, the cell resistance and operating current density are assumed to be constant for all gas compositions.

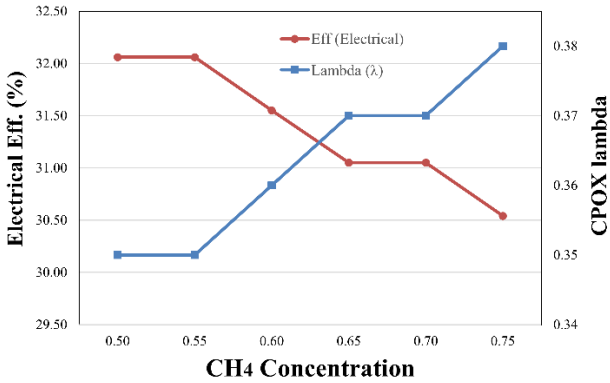

Figure 6-16: Influence of methane concentration on the CPOX air factor (λ) and system efficiency.

The current density (CD) also impacts the system efficiency, as shown in Figure 6-17. Increasing the current density implies that the system operates at lower cell voltage. On the other hand, it should be considered that operating the stack at a low CD (<2000 $A.m^{-2}$) considerably decreases the power density of the system. For instance, decreasing the CD from 2600 to 2000 $A.m^{-2}$ decreases the power production by 15%, while the system efficiency increases by 3%. The operating condition should be chosen to compromise system efficiency and system power density.

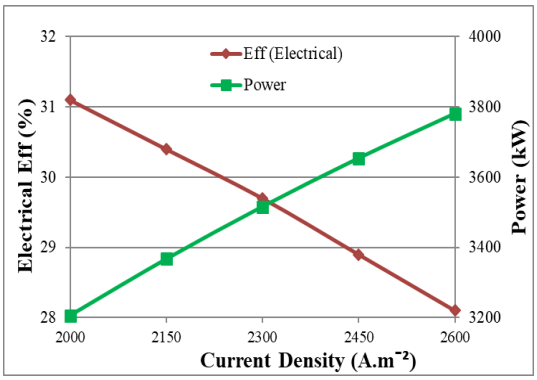

Figure 6-17: Influence of current density on system efficiency.

Based on the sensitivity analysis results, the following operating parameters proposed for the 4-kW SOFC system fuelled with recovered methane fuel:

- U_f=85%
- R=11×10^{-4} Ω.m^{-2}
- CD=2000 A.m^{-2}
- V=0.685 V
- λ=0.37 (O/C=1.6)

Based on these operating conditions, the achieved system efficiency increased to ηe=34.7 %.

6.4.3.2. With external steam reforming

In this section, the steam reforming method is used for methane conversion, and the COPX unit is replaced by an external reformer. Therefore, the CPOX air pump is also replaced by a steam generator. The system model is shown in Figure 6-14. Three heat exchangers are used to heat the water stream to the boiling point, evaporate and superheat the steam stream to 250°C at atmospheric pressure (see Figure 6-18). The generated steam is mixed with recovered CH_4-rich gas inside the catalytic reformer and produced a hydrogen-rich gas at 650°C. The steam to fuel ratio in the reformer (X_{sf}) is determined to prevent carbon deposition. For instance, the X_{sf} for a recovered CH_4-rich gas with 70% methane is 0.77, equal to the steam to carbon ratio (S/C) of 1.43. The system operating parameters are:

- U_f=85%
- R=11×10^{-4} Ω.m^{-2}
- CD=2000 A.m^{-2}
- V= 0.697 V
- Xsf = 0.77

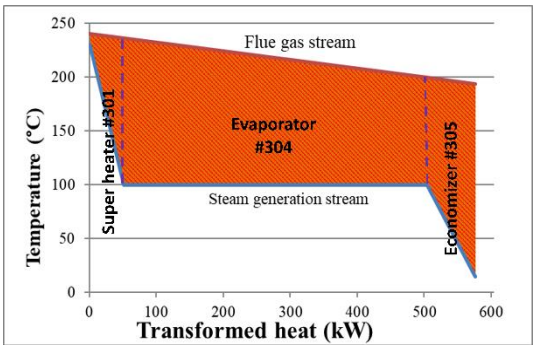

Figure 6-18: The Q-T diagram for three heat exchangers through steam generation.

The system efficiency is ηe=56.1%, which is much higher than the system efficiency with a CPOX unit (ηe=34,7 %). The power density of the system is also increased by 1.3%. This high efficiency is because of the high concentration of hydrogen (50%) at the anode's inlet and a very high H_2/CO ratio (3.55), as shown in Table 6-4. The hydrogen concentration and the H_2/CO ratio for the system with the CPOX unit were around 22% and 2.0, respectively. Moreover, the heat produced in the SOFC stack and afterburner is used in the steam generator. The system exhaust gas temperature was around 180°C, which was less than the one in the system with the CPOX unit (310°C). The cell operating voltage (at CD=2000 $A.m^{-2}$) for the system with the external steam reformer was higher (0.695 V), which resulted in higher system efficiency. Due to a higher cell voltage, it is possible to operate the system at higher current densities, which improves the power density of this system.

Table 6-4**:** Gas compositions of pipelines for the 4kW SOFC system with steam reformer.

Pipe no.	**101**	**201**	**301**	**104**	**105**	**401**
[CH_4]	0.7	-	-	0.077	-	-
[CO_2]	0.25	-	-	0.104	0.243	0.024
[N_2]	0.5	-	0.77	0.017	0.015	0.736
[O_2]		-	0.21	-	-	0.163
[H_2]	-	-	-	0.500	0.088	-
[CO]	-	-	-	0.141	0.035	-
[H_2O]	-	1.0	0.01	0.162	0.619	0.069

As mentioned in the previous section, the CO_2 concentration in fuel depends on the operating condition of the methane recovery system. Due to the presence of CO_2, the set S/C ratio was a bit lower than the reported S/C ratios in literature (based on SOFC operation) with external methane steam reforming. The required

stem is calculated based on the equilibrium condition inside the external steam reformer unit at 630°C.

The effect of methane concentration on system performance is evaluated by changing the methane concentration from 50% to 75%. Increasing the CH_4 concentration increases the required steam. The CO_2 gas in the recovered methane stream also contributes to the reforming to suppress carbon deposition. In this model, the steam to fuel ratio (S/F) decreased to 0.45 by decreasing the methane concentration to 50% (increasing CO_2 concentration to 45%), as shown in Figure 6-19.

Results indicated that the CH_4 concentration also impacted the required S/F ratio, as illustrated in Fig. 6-18. By increasing the methane concentration from 50% to 75%, the required S/F ratio increases to 0.85 and slightly increases the system efficiency by 0.9%. Therefore, increasing the methane concentration did not considerably improve the system efficiency neither the power density of this system.

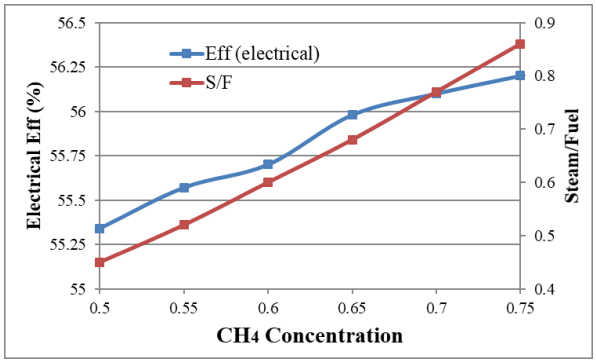

Figure 6-19: System efficiency and steam to fuel ratio for different gas compositions.

6.4.3.3. System with CO_2 recovery process

First, oxygen is considered as an oxidant in the afterburner to catalytically burn the remaining H_2 and CO in the exhaust gas of the SOFC stack. After this system modification, the system efficiency is still as high as ηe=50.6 %. This is around 5% less than the system efficiency without the CO_2 recovery process. The system operating parameters were the same as in the previous section. This should be emphasized that the afterburner's air factor should be controlled precisely to prevent the presence of oxygen in the flue gas.

In this case, the concentration of CO_2 in the exhaust of the afterburner is around 27%. After pre-heating the fuel and supplying the required heat for the steam generation, vapour in the flue gas is condensed inside the moisture separator. The concentration of CO_2 in the system exhaust is as high as 91.7% at ambient operating temperature.

This should be considered that oxygen is not available at the groundwater treatment plant, and oxygen increases the operating costs. However, the CO_2 is purchased and used in the methane recovery system of the Spannenburg plant. The molar ratio of the produced CO_2 to the consumed O_2 is around 2.96, equal to the mass ratio of 1.7. The concentrations of different gas species after the moisture removal have been shown in Table 6-4.

Table 6-5: The gas composition in the exhaust of the system with the CO_2 recovery using oxygen.

Gas species	[CO_2]	[N_2]	[H_2O]	[O_2]	[CO]
Pipe #112	0.914	0.048	0.031	0.004	0.003

The performance of the system is also evaluated using a precise amount of air to be mixed with the flue gas at the afterburner. Using air instead of oxygen did not impact the system efficiency nor the SOFC stack operating conditions. In this case, the CO_2/air ratio was set to 0.43 to meet λ=1.0 in the afterburner. However, the exhaust flow rate increased by 60% compared to the system using O_2 in the afterburner.

Nitrogen concentration in the exhaust flow is higher than that in the system using O_2 in the afterburner (47.8%), as shown in Table 6-6. However, the concentration of CO_2 was still very high (48.5%) after moisture separation. The nitrogen can be separated further using other technologies like using membrane [385]. A techno-economic study should be conducted to determine a cost-effective method for CO_2 recovery in this SOFC system.

Table 6-6: The gas composition in the exhaust of the system with the CO_2 recovery using air.

Gas species	[CO_2]	[N_2]	[H_2O]	[O_2]	[CO]
Pipe #112	0.485	0.478	0.031	0.001	0.001

6.5. Conclusions

The high concentration of CH_4 in groundwater causes high greenhouse gas emissions at the Spannenburg groundwater treatment plant. Technologies such as

vacuum stripping allow for the recovery of CH_4 from groundwater. The recovered CH4-rich gas could be subsequently used as fuel. It was proposed to use SOFC as an efficient energy-conversion technology to improve the sustainability of this DWTP. The feasibility of using CH_4-rich gas recovered from the groundwater was studied through a proof of principle test.

Thermodynamic calculations based on equilibrium conditions showed that using recovered CH_4 directly in SOFCs results in carbon deposition and deactivation of the anode in long-term operation. The fraction of CO_2 in the recovered gas was not sufficient to allow for complete dry reforming of CH_4. Therefore, extra steam should be added to the CH_4-rich gas to increase the CH_4 conversion through steam reforming reaction. Thus, the cell performance was experimentally evaluated at an S/C ratio of 1.0. Additionally, the recovered gas contained 9 ppm of H_2S, which can influence the SOFC performance. H_2S was effectively removed (< 0.1 ppm) with impregnated activated carbon with a residence time of 150 seconds at ambient temperature.

The system modelling study is carried out for a 4kW-SOFC system based on off-designed conditions (taken from conducted syngas experiments) to simulate the actual operating conditions. The influence of operating parameters such as the composition of the CH_4-rich gas, cell voltage, and fuel utilization on system efficiency were investigated. System configuration plays a vital role in improving system efficiency. Using an external steam reformer instead of the CPOX unit could improve the system efficiency by above 20% in the considered system fuelled with the recovered CH_4-rich gas. Changing the methane concentration in the recovered gas did not significantly influence the system efficiency (<2%). However, a considerable effect on system power density was observed. It is possible to recover a CO_2–rich (91.4%) flue gas from the SOFC system by precisely controlling the amount of oxygen in the afterburner.

Chapter 7

Conclusions and Recommendations

This final chapter summarizes the conclusions drawn in this thesis in view of the scope of the research stated in Chapter 1. Furthermore, suggestions and recommendations are given for future research.

7.1. Conclusions

In line with the objectives of this dissertation, as stated in Chapter 1:

- The extra amount of CO_2 required to prevent carbon deposition for biogas fuelled SOFCs has been investigated for a Ni-GDC electrolyte supported single cell, and the influence of the cell temperature and current density on methane internal dry reforming have been studied.
- Ammonia cracking has been assessed in ammonia fuelled SOFC, and the influence of steam concentration (from aqueous ammonia) on the cell performance has been investigated. Moreover, an ammonia SOFC system integrated with the ammonia removal (precipitation) process has been developed by Cycle-Tempo software.
- Biogas internal combined (dry and steam) reforming has been studied for Ni-GDC anode, and the safe operating condition has been determined in terms of required steam, operating temperature, and current density. Additionally, the influence of ammonia cracking on methane reforming has been identified.
- A conceptual design for a CH_4-rich gas fuelled SOFC system has been developed in an existing groundwater treatment plant (Spannenburg, the Netherlands). A gas cleaning unit has been designed in order to remove a trace of H_2S in the recovered CH_4-rich gas. The optimized methane gas processing method has been determined based on electrical system efficiency.

The main findings contained in this dissertation may be summarized as follows:

In Chapter 3, internal dry reforming of biogas in Ni-GDC electrolyte-supported SOFCs has been studied at different operating conditions, including the CO_2 concentration, operating temperature, and current density. Results showed the feasibility of methane internal reforming in biogas fuelled SOFC. Steam produced through hydrogen electrochemical reaction (close circuit) contributed into internal methane reforming and increased methane conversion. Methane conversion significantly (20%) increased by raising the cell operating temperature from 800°C to 900°C at open circuit condition. However, the effect of operating temperature on methane conversion was negligible (< 5%) at a current density of 2000 $A.m^{-2}$.

The main goal was to determine the minimum amount of CO_2 required to obtain maximum power density while carbon deposition was prevented. The cell performance (more than 215 hrs) under a current density of 2000 $A.m^{-2}$ has been monitored for different gas compositions at 850°C. The high degradation rate has

been observed with simulated biogas (with 60 mol.% methane) fed SOFC at a current density of 2000 $A.m^{-2}$ and 850°C. The cell degradation might be due to carbon deposition. Stable cell performance (in terms of voltage) has been observed when the R ratio (CH_4/CO_2) was less than one ($R \leq 1$). The maximum power was achieved with the gas composition C with equmolar CH_4 and CO_2 (R=1) and the degradation was minimized. However, the power density of biogas-fuelled SOFC cell was around 19% less than hydrogen-fuelled one.

Chapter 4 experimentally investigated the feasibility of operating an SOFC fuelled with ammonia-steam mixtures with different ammonia concentrations (14.3 mol.% to 85 mol.%). Results showed that ammonia was fully cracked in SOFC at an operating temperature of 800°C. Increasing ammonia concentration from 14% to 85% increased the current density of the cell by 50%. The experimental results were used in a system modelling study.

A Cycle-Tempo model was developed to simulate the integration of an SOFC system into an ammonia removal (struvite precipitation) process. The ammonia concentration (in the ammonia-steam mixture) produced from aqueous ammonia in the precipitation process is very low (14.3 mol.%). The energy efficiency of an ammonia-steam mixture fuelled SOFC system with 14.3 mol.% ammonia was around 48.5%. However, the required heat for struvite decomposition could not be generated by the SOFC system (stack and afterburner). Therefore, a heat pump-assisted distillation tower could be integrated to increase the ammonia concentration in the ammonia-steam mixture stream to 90 mol.%. Besides, the heat pump supplied the heat demand of the struvite decomposition reactor from the condenser of the distillation tower. By increasing the ammonia concentration to 90 mol.%, the net energy efficiency of the ammonia-SOFC system was increased to 53.1%. The net energy efficiency (LHV based) of the whole integrated SOFC system with the heat pump-assisted distillation tower was around 39%. Moreover, the SOFC stack supplies the power demand of the heat pump. Therefore, the sustainability of conventional WWTP might be improved by developing such an SOFC system.

In Chapter 5, the amount of steam required to prevent carbon deposition in the biogas fuelled SOFCs has been investigated. The experimental studies were performed with a Ni-GDC (anode), electrolyte-supported cell at an operating temperature of 850°C. Results showed that a minimum S/C ratio of 0.6 was required to prevent carbon deposition at 850°C. Methane conversion with this S/C ratio was higher than 96% at different current densities. Increasing steam

concentration increased methane conversion. However, it decreased the cell voltage. The steam required for preventing carbon deposition could be supplied by adding an ammonia-steam mixture (from struvite decomposition) stream to biogas stream (from anaerobic digestion).

A series of experiments was also performed to investigate the internal reforming of methane for a biogas-ammonia fuelled SOFC. First, the impact of adding ammonia to the biogas-steam mixture (S/C=0.6) was investigated. The results showed that ammonia cracked in the SOFC and did not decrease the methane conversion. Moreover, hydrogen produced through ammonia cracking increased the cell voltage at OCV and high current densities. By adding 8 mol.% of ammonia to the biogas-steam mixture with an S/C of 0.6 increased the power density of the cell by 10%. Moreover, the influence of the mixing ratio of ammonia-steam to biogas on methane reforming and cell performance was studied. It was assumed that the ammonia concentration in ammonia-steam mixture is 25 mol.% and methane concentration in biogas is 60 mol.%. The best cell performance in terms of power production has been achieved with an ammonia-steam/biogas ratio of 0.48. The results were used in developing an SOFC system fuelled by biogas and ammonia-steam mixture.

The system modelling results showed that the net electrical system efficiency of an SOFC system fuelled with aqueous ammonia and biogas was up to 56%. An exergy analysis was performed to evaluate the thermodynamic losses in the SOFC stack and BoP components to identify exergy losses and potentially improve system efficiency. Moreover, the results illustrated that the heat generated in the SOFC stack and afterburner was sufficient for air and fuel (biogas and ammonia-steam mixture) preheating and struvite decomposition. The remaining heat could also be used in thermal pre-treatment of wastewater to improve biogas production.

Chapter 6 presented a conceptual design of a 4-kW SOFC system for a groundwater treatment plant at Spannenburg, the Netherlands. A CH_4-rich gas with a methane concentration of 70 mol.% was recovered, while the gas contained a 9-ppm trace of H_2S. First, the feasibility of operating SOFC fuelled with recovered CH_4-rich gas sampled from the groundwater plant was demonstrated with an experimental study. A gas cleaning unit (GCU) was needed to remove the H_2S trace from recovered CH_4-rich gas. A series of experiments has been conducted to design the GCU with a reactor filled with iron oxide (Fe_2O_3). Using iron oxide could improve the sustainability of the groundwater treatment plant because iron oxide is one of the by-products of this plant. The H_2S adsorption

capacity of 5.8 g H_2S/100 g of iron oxide was achieved through the breakthrough tests. Additionally, the other GCU design parameters, such as the h/D ratio of reactor and GHSV of the fuel stream, were determined.

A system modelling study was carried out to identify the most suitable fuel processing method for an SOFC fuelled with the recovered CH_4-rich gas. An off-design model was developed based on the results of experiments carried out with a syngas-fuelled system. The results showed the possibility of operating the 4-kW SOFC equipped by a CPOX unit with the CH_4-rich gas recovered from the groundwater treatment plant. The net electrical efficiency of the system fuelled with 50% CH_4, 50% CO_2, and 5% N_2 was around 33%. The electrical system efficiency was improved to 55% by replacing the CPOX unit with an external steam reformer in this model. Adding a CO_2 capture process to the model decreased the system efficiency by 5%. The CO_2 captured could be reused in the methane removal process of the groundwater treatment.

7.2. Recommendations for future Research

The research work investigated in this dissertation left many open issues of interest for future research.

7.2.1. Experimental studies

- Despite the research on the effect of contaminants like H_2S and siloxane on SOFC performance, there is no comprehensive report investigating the effect of these contaminants on the dry reforming reaction in biogas fuelled SOFCs.
- The literature mostly focused on the kinetics of steam reforming of methane, and more studies are still needed to investigate the kinetics of methane dry reforming in biogas fuelled SOFCs. Moreover, the influence of ammonia cracking on the kinetics of methane reforming also has not been studied.
- Experimental studies of biogas-SOFC at the stack level are required to have a better understanding of SOFC system performance.
- Anode gas recirculation is an alternative to avoid the use of additional reforming agents in biogas-SOFC system. Integrated system modelling (steady-state) investigations have been performed on biogas-SOFC with AGR. However, to the best of the author's knowledge, no experimental studies have been reported on biogas-SOFC with the AGR system.

7.2.2. Modelling studies

- Developing biogas-SOFC dynamic models is also highly encouraged in order to predict the performance and limitations of biogas-SOFC systems operating under different electrical power demands.
- Integration of natural gas-fuelled SOFC with gas or steam turbine already showed very high efficiencies. This might be an interesting approach for developing the Biogas-SOFC systems as well.

References

[1] S. Kirschke, P. Bousquet, P. Ciais, M. Saunois, J.G. Canadell, E.J. Dlugokencky, P. Bergamaschi, D. Bergmann, D.R. Blake, L. Bruhwiler, Three decades of global methane sources and sinks, Nature Geoscience, 6 (2013) 813-823.

[2] UNFCCC, COP21 Final Draft, https://unfccc.int/resource/docs/2015/cop21/eng/da02.pdf, (2015).

[3] O. Ellabban, H. Abu-Rub, F. Blaabjerg, Renewable energy resources: Current status, future prospects and their enabling technology, Renewable and Sustainable Energy Reviews, 39 (2014) 748-764.

[4] L. Appels, J. Baeyens, J. Degrève, R. Dewil, Principles and potential of the anaerobic digestion of waste-activated sludge, Progress in Energy and Combustion Science, 34 (2008) 755-781.

[5] R.Y. Surampalli, S.K. Banerji, J. Chen, Microbiological stabilization of sludge by aerobic digestion and storage, Journal of Environmental Engineering, 119 (1993) 493-505.

[6] P.L. McCarty, J. Bae, J. Kim, Domestic Wastewater Treatment as a Net Energy Producer-Can This be Achieved?, Environmental Science & Technology, 45 (2011) 7100-7106.

[7] M. Edison, Bio-methane generation from organic waste. A review, in: Proceedings of the World Congress on Engineering and Computer Science (WCECS). San Francisco, USA, 2014.

[8] R.J. Crookes, Comparative bio-fuel performance in internal combustion engines, Biomass and Bioenergy, 30 (2006) 461-468.

[9] S.A. Saadabadi, A. Thallam Thattai, L. Fan, R.E.F. Lindeboom, H. Spanjers, P.V. Aravind, Solid Oxide Fuel Cells fuelled with biogas: Potential and constraints, Renewable Energy, 134 (2019) 194-214.

[10] J. Larminie, A. Dicks, M.S. McDonald, Fuel cell systems explained, Wiley New York, 2003.

[11] V. Cigolotti, E. Massi, A. Moreno, A. Polettini, F. Reale, Biofuels as opportunity for MCFC niche market application, International Journal of Hydrogen Energy, 33 (2008) 2999-3003.

[12] R. Ciccoli, V. Cigolotti, R. Lo Presti, E. Massi, S.J. McPhail, G. Monteleone, A. Moreno, V. Naticchioni, C. Paoletti, E. Simonetti, F. Zaza, Molten carbonate fuel cells fed with biogas: Combating H2S, Waste Management, 30 (2010) 1018-1024.

[13] S.J. McPhail, A. Aarva, H. Devianto, R. Bove, A. Moreno, SOFC and MCFC: Commonalities and opportunities for integrated research, International Journal of Hydrogen Energy, 36 (2011) 10337-10345.

[14] S.-B. Lee, T.-H. Lim, R.-H. Song, D.-R. Shin, S.-K. Dong, Development of a 700W anode-supported micro-tubular SOFC stack for APU applications, International Journal of Hydrogen Energy, 33 (2008) 2330-2336.

[15] A. Trendewicz, R. Braun, Techno-economic analysis of solid oxide fuel cell-based combined heat and power systems for biogas utilization at wastewater treatment facilities, Journal of Power Sources, 233 (2013) 380-393.

[16] J. Van herle, F. Maréchal, S. Leuenberger, Y. Membrez, O. Bucheli, D. Favrat, Process flow model of solid oxide fuel cell system supplied with sewage biogas, Journal of Power Sources, 131 (2004) 127-141.

[17] L. Yingjian, Q. Qi, H. Xiangzhu, L. Jiezhi, Energy balance and efficiency analysis for power generation in internal combustion engine sets using biogas, Sustainable Energy Technologies and Assessments, 6 (2014) 25-33.

[18] M. Gandiglio, A. Lanzini, M. Santarelli, M. Acri, T. Hakala, M. Rautanen, Results from an industrial size biogas-fed SOFC plant (the DEMOSOFC project), International Journal of Hydrogen Energy, 45 (2020) 5449-5464.

[19] J.-Y. Lu, X.-M. Wang, H.-Q. Liu, H.-Q. Yu, W.-W. Li, Optimizing operation of municipal wastewater treatment plants in China: The remaining barriers and future implications, Environment International, 129 (2019) 273-278.

[20] I. Yentekakis, T. Papadam, G. Goula, Electricity production from wastewater treatment via a novel biogas-SOFC aided process, Solid State Ionics, 179 (2008) 1521-1525.

[21] J. Ouweltjes, P. Aravind, N. Woudstra, G. Rietveld, Biosyngas utilization in solid oxide fuel cells with Ni⁄GDC anodes, Journal of fuel cell science and technology, 3 (2006) 495-498.

[22] M. Torrijos, State of Development of Biogas Production in Europe, Procedia Environmental Sciences, 35 (2016) 881-889.

[23] P. Roeleveld, J. Roorda, M. Schaafsma, NEWs: the Dutch roadmap for the WWTP of 2030, STOWA, 2010.

[24] J.P. van der Hoek, A. Struker, J. De Danschutter, Amsterdam as a sustainable European metropolis: integration of water, energy and material flows, Urban Water Journal, 14 (2017) 61-68.

[25] M. Jahn, M. Heddrich, A. Weder, E. Reichelt, R. Lange, Oxidative Dry-Reforming of Biogas: Reactor Design and SOFC System Integration, Energy Technology, 1 (2013) 48-58.

[26] M. Balat, H. Balat, Biogas as a renewable energy source—a review, Energy Sources, Part A, 31 (2009) 1280-1293.

[27] N.S. Siefert, S. Litster, Exergy & economic analysis of biogas fueled solid oxide fuel cell systems, Journal of Power Sources, 272 (2014) 386-397.

[28] M. Ni, Is steam addition necessary for the landfill gas fueled solid oxide fuel cells?, International Journal of Hydrogen Energy, 38 (2013) 16373-16386.

[29] H. Sumi, Y.-H. Lee, H. Muroyama, T. Matsui, K. Eguchi, Comparison between internal steam and CO2 reforming of methane for Ni-YSZ and Ni-ScSZ SOFC anodes, Journal of The Electrochemical Society, 157 (2010) B1118-B1125.

[30] H.C. Patel, A.N. Tabish, F. Comelli, P.V. Aravind, Oxidation of H2, CO and syngas mixtures on ceria and nickel pattern anodes, Applied Energy, 154 (2015) 912-920.

[31] O. Costa-Nunes, R.J. Gorte, J.M. Vohs, Comparison of the performance of Cu–CeO2–YSZ and Ni–YSZ composite SOFC anodes with H2, CO, and syngas, Journal of Power Sources, 141 (2005) 241-249.

[32] N. Mahato, A. Banerjee, A. Gupta, S. Omar, K. Balani, Progress in material selection for solid oxide fuel cell technology: A review, Progress in Materials Science, 72 (2015) 141-337.

[33] J. Staniforth, K. Kendall, Biogas powering a small tubular solid oxide fuel cell, Journal of Power Sources, 71 (1998) 275-277.

[34] K. Girona, J. Laurencin, J. Fouletier, F. Lefebvre-Joud, Carbon deposition in CH4/CO2 operated SOFC: Simulation and experimentation studies, Journal of Power Sources, 210 (2012) 381-391.

[35] X.D. Zhang, H. Spanjers, J.B. van Lier, Potentials and limitations of biomethane and phosphorus recovery from sludges of brackish/marine aquaculture recirculation systems: A review, Journal of Environmental Management, 131 (2013) 44-54.

[36] M. Ferreira, I.P. Marques, I. Malico, Biogas in Portugal: Status and public policies in a European context, Energy Policy, 43 (2012) 267-274.

[37] R.B. Tranter, A. Swinbank, P.J. Jones, C.J. Banks, A.M. Salter, Assessing the potential for the uptake of on-farm anaerobic digestion for energy production in England, Energy Policy, 39 (2011) 2424-2430.

[38] J.B. Holm-Nielsen, T. Al Seadi, P. Oleskowicz-Popiel, The future of anaerobic digestion and biogas utilization, Bioresource Technology, 100 (2009) 5478-5484.

[39] H. Yoshida, T.H. Christensen, C. Scheutz, Life cycle assessment of sewage sludge management: A review, Waste Management & Research, 31 (2013) 1083-1101.

[40] G. Lettinga, Anaerobic digestion and wastewater treatment systems, Antonie van leeuwenhoek, 67 (1995) 3-28.

[41] K. Rajendran, S. Aslanzadeh, M.J. Taherzadeh, Household Biogas Digesters—A Review, Energies, 5 (2012) 2911.

[42] E. Neyens, J. Baeyens, A review of thermal sludge pre-treatment processes to improve dewaterability, Journal of Hazardous Materials, 98 (2003) 51-67.

[43] S. Verma, Anaerobic digestion of biodegradable organics in municipal solid wastes, in, Columbia University, 2002.

[44] J.C. Young, P.L. McCarty, The anaerobic filter for waste treatment, Journal (Water Pollution Control Federation), (1969) R160-R173.

[45] T. De Mes, A. Stams, J. Reith, G. Zeeman, Methane production by anaerobic digestion of wastewater and solid wastes, Bio-methane & Bio-hydrogen, (2003) 58-102.

[46] H.F. Kaspar, K. Wuhrmann, Kinetic parameters and relative turnovers of some important catabolic reactions in digesting sludge, Applied and Environmental Microbiology, 36 (1978) 1-7.

[47] M. Persson, O. Jönsson, A. Wellinger, Biogas upgrading to vehicle fuel standards and grid injection, in: IEA Bioenergy task, Vol. 37, 2006, pp. 1-34.

[48] R.J. Meesters, H.F. Schröder, Simultaneous determination of 4-nonylphenol and bisphenol A in sewage sludge, Analytical Chemistry, 74 (2002) 3566-3574.

[49] J.B. Van Lier, S. Rebac, G. Lettinga, High-rate anaerobic wastewater treatment under psychrophilic and thermophilic conditions, Water Science and Technology, 35 (1997) 199-206.

[50] S. Rebac, J. Ruskova, S. Gerbens, J.B. Van Lier, A.J. Stams, G. Lettinga, High-rate anaerobic treatment of wastewater under psychrophilic conditions, Journal of fermentation and bioengineering, 80 (1995) 499-506.

[51] C.H. Pham, C.C. Vu, S.G. Sommer, S. Bruun, Factors Affecting Process Temperature and Biogas Production in Small-scale Rural Biogas Digesters in Winter in Northern Vietnam, Asian-Australasian Journal of Animal Sciences, 27 (2014) 1050-1056.

[52] H.M. El-Mashad, G. Zeeman, W.K. Van Loon, G.P. Bot, G. Lettinga, Effect of temperature and temperature fluctuation on thermophilic anaerobic digestion of cattle manure, Bioresource technology, 95 (2004) 191-201.

[53] I.A. Nges, J. Liu, Effects of anaerobic pre-treatment on the degradation of dewatered-sewage sludge, Renewable Energy, 34 (2009) 1795-1800.

[54] A. Hendriks, G. Zeeman, Pretreatments to enhance the digestibility of lignocellulosic biomass, Bioresource technology, 100 (2009) 10-18.

[55] H. Carrère, C. Dumas, A. Battimelli, D.J. Batstone, J.P. Delgenès, J.P. Steyer, I. Ferrer, Pretreatment methods to improve sludge anaerobic degradability: A review, Journal of Hazardous Materials, 183 (2010) 1-15.

[56] A.T.W.M. Hendriks, G. Zeeman, Pretreatments to enhance the digestibility of lignocellulosic biomass, Bioresource Technology, 100 (2009) 10-18.

[57] C. Bougrier, J.P. Delgenes, H. Carrere, Effects of thermal treatments on five different waste activated sludge samples solubilisation, physical properties and anaerobic digestion, Chemical Engineering Journal, 139 (2008) 236-244.

[58] S.I. Perez-Elvira, M. Fdz-Polanco, F. Fdz-Polanco, Increasing the performance of anaerobic digestion: Pilot scale experimental study for thermal hydrolysis of mixed sludge, Frontiers of Environmental Science & Engineering in China, 4 (2010) 135-141.

[59] R. Alvarez, G. Lidén, The effect of temperature variation on biomethanation at high altitude, Bioresource Technology, 99 (2008) 7278-7284.

[60] M. Climent, I. Ferrer, M.d.M. Baeza, A. Artola, F. Vázquez, X. Font, Effects of thermal and mechanical pretreatments of secondary sludge on biogas production under thermophilic conditions, Chemical Engineering Journal, 133 (2007) 335-342.

[61] W. Qiao, X.Y. Yan, J.H. Ye, Y.F. Sun, W. Wang, Z.Z. Zhang, Evaluation of biogas production from different biomass wastes with/without hydrothermal pretreatment, Renewable Energy, 36 (2011) 3313-3318.

[62] L. Appels, J. Degrève, B. Van der Bruggen, J. Van Impe, R. Dewil, Influence of low temperature thermal pre-treatment on sludge solubilisation, heavy metal release and anaerobic digestion, Bioresource Technology, 101 (2010) 5743-5748.

[63] C. González-Fernández, B. Sialve, N. Bernet, J.P. Steyer, Thermal pretreatment to improve methane production of Scenedesmus biomass, Biomass and Bioenergy, 40 (2012) 105-111.

[64] F. Passos, J. García, I. Ferrer, Impact of low temperature pretreatment on the anaerobic digestion of microalgal biomass, Bioresource Technology, 138 (2013) 79-86.

[65] R.T. Haug, D.C. Stuckey, J.M. Gossett, P.L. McCarty, Effect of thermal pretreatment on digestibility and dewaterability of organic sludges, Journal (Water Pollution Control Federation), (1978) 73-85.

[66] T. Noike, Upgrading of anaerobic digestion of waste activated sludge by thermal pretreatment, Water Science and Technology, 26 (1992) 857-866.

[67] H.N. Gavala, U. Yenal, I.V. Skiadas, P. Westermann, B.K. Ahring, Mesophilic and thermophilic anaerobic digestion of primary and secondary sludge. Effect of pre-treatment at elevated temperature, Water Research, 37 (2003) 4561-4572.

[68] J. Kim, C. Park, T.-H. Kim, M. Lee, S. Kim, S.-W. Kim, J. Lee, Effects of various pretreatments for enhanced anaerobic digestion with waste activated sludge, Journal of bioscience and bioengineering, 95 (2003) 271-275.

[69] A. Valo, H. Carrere, J.P. Delgenes, Thermal, chemical and thermo-chemical pre-treatment of waste activated sludge for anaerobic digestion, Journal of Chemical Technology and Biotechnology, 79 (2004) 1197-1203.

[70] T.Y. Jeong, G.C. Cha, S.S. Choi, C. Jeon, Evaluation of methane production by the thermal pretreatment of waste activated sludge in an anaerobic digester, Journal of Industrial and Engineering Chemistry, 13 (2007) 856-863.

[71] M. Climent, I. Ferrer, M. del Mar Baeza, A. Artola, F. Vázquez, X. Font, Effects of thermal and mechanical pretreatments of secondary sludge on biogas production under thermophilic conditions, Chemical Engineering Journal, 133 (2007) 335-342.

[72] J. Lu, H.N. Gavala, I.V. Skiadas, Z. Mladenovska, B.K. Ahring, Improving anaerobic sewage sludge digestion by implementation of a hyper-thermophilic prehydrolysis step, Journal of Environmental Management, 88 (2008) 881-889.

[73] A. Donoso-Bravo, S. Pérez-Elvira, E. Aymerich, F. Fdz-Polanco, Assessment of the influence of thermal pre-treatment time on the macromolecular composition and anaerobic biodegradability of sewage sludge, Bioresource technology, 102 (2011) 660-666.

[74] J. Ma, T.H. Duong, M. Smits, W. Verstraete, M. Carballa, Enhanced biomethanation of kitchen waste by different pre-treatments, Bioresource Technology, 102 (2011) 592-599.

[75] X. Liu, W. Wang, X. Gao, Y. Zhou, R. Shen, Effect of thermal pretreatment on the physical and chemical properties of municipal biomass waste, Waste Management, 32 (2012) 249-255.

[76] C.J. Banks, M. Chesshire, S. Heaven, R. Arnold, Anaerobic digestion of source-segregated domestic food waste: Performance assessment by mass and energy balance, Bioresource Technology, 102 (2011) 612-620.

[77] M. Lübken, M. Wichern, M. Schlattmann, A. Gronauer, H. Horn, Modelling the energy balance of an anaerobic digester fed with cattle manure and renewable energy crops, Water Research, 41 (2007) 4085-4096.

[78] I. Bohn, L. Björnsson, B. Mattiasson, The energy balance in farm scale anaerobic digestion of crop residues at 11–37 °C, Process Biochemistry, 42 (2007) 57-64.

[79] M. Berglund, P. Börjesson, Assessment of energy performance in the life-cycle of biogas production, Biomass and Bioenergy, 30 (2006) 254-266.

[80] M. Pöschl, S. Ward, P. Owende, Evaluation of energy efficiency of various biogas production and utilization pathways, Applied Energy, 87 (2010) 3305-3321.

[81] H. Bouallagui, O. Haouari, Y. Touhami, R. Ben Cheikh, L. Marouani, M. Hamdi, Effect of temperature on the performance of an anaerobic tubular reactor treating fruit and vegetable waste, Process Biochemistry, 39 (2004) 2143-2148.

[82] E. Porpatham, A. Ramesh, B. Nagalingam, Investigation on the effect of concentration of methane in biogas when used as a fuel for a spark ignition engine, Fuel, 87 (2008) 1651-1659.

[83] S. Bari, Effect of carbon dioxide on the performance of biogas/diesel duel-fuel engine, Renewable Energy, 9 (1996) 1007-1010.

[84] E. Porpatham, A. Ramesh, B. Nagalingam, Effect of hydrogen addition on the performance of a biogas fuelled spark ignition engine, International Journal of Hydrogen Energy, 32 (2007) 2057-2065.

[85] P.F. HENSHAW, T. D'ANDREA, K.R. MANN, D.S.-K. TING, Premixed ammonia-methane-air combustion, Combustion science and technology, 177 (2005) 2151-2170.

[86] P. Weiland, Biogas production: current state and perspectives, Applied Microbiology and Biotechnology, 85 (2010) 849-860.

[87] N. Abatzoglou, S. Boivin, A review of biogas purification processes, Biofuels, Bioproducts and Biorefining, 3 (2009) 42-71.

[88] V. Scholz, J. Ellner, Use of biogas in fuel cells-current R&D', Journal of Sustainable Energy & Environment Special Issue, 11 (2011) 15.

[89] Y. Chen, J.J. Cheng, K.S. Creamer, Inhibition of anaerobic digestion process: A review, Bioresource Technology, 99 (2008) 4044-4064.

[90] V. O'Flaherty, T. Mahony, R. O'Kennedy, E. Colleran, Effect of pH on growth kinetics and sulphide toxicity thresholds of a range of methanogenic, syntrophic and sulphate-reducing bacteria, Process Biochemistry, 33 (1998) 555-569.

[91] D. Schieder, P. Quicker, R. Schneider, H. Winter, S. Prechtl, M. Faulstich, Microbiological removal of hydrogen sulfide from biogas by means of a separate biofilter system: experience with technical operation, Anaerobic Digestion of Solid Wastes III, 48 (2003) 209-212.

[92] L. Frare, M. Vieira, M. Silva, N. Pereira, M. Gimenes, Hydrogen sulfide removal from biogas using Fe/EDTA solution: gas/liquid contacting and sulfur formation, Environmental progress & sustainable energy, 29 (2010) 34-41.

[93] S.S. Kapdi, V.K. Vijay, S.K. Rajesh, R. Prasad, Biogas scrubbing, compression and storage: perspective and prospectus in Indian context, Renewable Energy, 30 (2005) 1195-1202.

[94] N. Tippayawong, P. Thanompongchart, Biogas quality upgrade by simultaneous removal of CO2 and H2S in a packed column reactor, Energy, 35 (2010) 4531-4535.

[95] W. Yuan, T.J. Bandosz, Removal of hydrogen sulfide from biogas on sludge-derived adsorbents, Fuel, 86 (2007) 2736-2746.

[96] J. Krischan, A. Makaruk, M. Harasek, Design and scale-up of an oxidative scrubbing process for the selective removal of hydrogen sulfide from biogas, Journal of Hazardous Materials, 215–216 (2012) 49-56.

[97] Y. Belmabkhout, G. De Weireld, A. Sayari, Amine-bearing mesoporous silica for CO2 and H2S removal from natural gas and biogas, Langmuir, 25 (2009) 13275-13278.

[98] K. Sasaki, K. Haga, T. Yoshizumi, D. Minematsu, E. Yuki, R.-R. Liu, C. Uryu, T. Oshima, S. Taniguchi, Y. Shiratori, Impurity poisoning of SOFCs, ECS Transactions, 35 (2011) 2805-2814.

[99] P. Hofmann, K.D. Panopoulos, P.V. Aravind, M. Siedlecki, A. Schweiger, J. Karl, J.P. Ouweltjes, E. Kakaras, Operation of solid oxide fuel cell on biomass product gas with tar levels >10 g Nm−3, International Journal of Hydrogen Energy, 34 (2009) 9203-9212.

[100] A. Norheim, I. Waernhus, M. Brostrom, J.E. Hustad, A. Vik, Experimental studies on the influence of H2S on solid oxide fuel cell performance at 800 degrees C, Energy & Fuels, 21 (2007) 1098-1101.

[101] L. Aguilar, S. Zha, Z. Cheng, J. Winnick, M. Liu, A solid oxide fuel cell operating on hydrogen sulfide (H2S) and sulfur-containing fuels, Journal of Power Sources, 135 (2004) 17-24.

[102] K. Sasaki, K. Susuki, A. Iyoshi, M. Uchimura, N. Imamura, H. Kusaba, Y. Teraoka, H. Fuchino, K. Tsujimoto, Y. Uchida, N. Jingo, H2S poisoning of solid oxide fuel cells, Journal of the Electrochemical Society, 153 (2006) A2023-A2029.

[103] S. Appari, V.M. Janardhanan, R. Bauri, S. Jayanti, Deactivation and regeneration of Ni catalyst during steam reforming of model biogas: An experimental investigation, International Journal of Hydrogen Energy, 39 (2014) 297-304.

[104] L. Zhang, S.P. Jiang, H.Q. He, X. Chen, J. Ma, X.C. Song, A comparative study of H2S poisoning on electrode behavior of Ni/YSZ and Ni/GDC anodes of solid oxide fuel cells, International Journal of Hydrogen Energy, 35 (2010) 12359-12368.

[105] A.L. da Silva, N.C. Heck, Thermodynamics of sulfur poisoning in solid oxide fuel cells revisited: The effect of H2S concentration, temperature, current density and fuel utilization, Journal of Power Sources, 296 (2015) 92-101.

[106] Y. Shiratori, T. Oshima, K. Sasaki, Feasibility of direct-biogas SOFC, International Journal of Hydrogen Energy, 33 (2008) 6316-6321.

[107] D. Papurello, R. Borchiellini, P. Bareschino, V. Chiodo, S. Freni, A. Lanzini, F. Pepe, G.A. Ortigoza, M. Santarelli, Performance of a Solid Oxide Fuel Cell short-stack with biogas feeding, Applied Energy, 125 (2014) 254-263.

[108] B. Tansel, S.C. Surita, Oxidation of siloxanes during biogas combustion and nanotoxicity of Si-based particles released to the atmosphere, Environmental Toxicology and Pharmacology, 37 (2014) 166-173.

[109] D.-G. Wang, W. Norwood, M. Alaee, J.D. Byer, S. Brimble, Review of recent advances in research on the toxicity, detection, occurrence and fate of cyclic volatile methyl siloxanes in the environment, Chemosphere, 93 (2013) 711-725.

[110] M. Ajhar, M. Travesset, S. Yüce, T. Melin, Siloxane removal from landfill and digester gas – A technology overview, Bioresource Technology, 101 (2010) 2913-2923.

[111] T. Matsui, S. Imamura, Removal of siloxane from digestion gas of sewage sludge, Bioresource technology, 101 (2010) S29-S32.

[112] M. Schweigkofler, R. Niessner, Removal of siloxanes in biogases, Journal of Hazardous Materials, 83 (2001) 183-196.

[113] M. Yu, H. Gong, Z. Chen, M. Zhang, Adsorption characteristics of activated carbon for siloxanes, Journal of Environmental Chemical Engineering, 1 (2013) 1182-1187.

[114] P. Gislon, S. Galli, G. Monteleone, Siloxanes removal from biogas by high surface area adsorbents, Waste Management, 33 (2013) 2687-2693.

[115] K. Haga, Y. Shiratori, K. Ito, K. Sasaki, Chemical Degradation and Poisoning Mechanism of Cermet Anodes in Solid Oxide Fuel Cells, ECS Transactions, 25 (2009) 2031-2038.

[116] H. Madi, A. Lanzini, S. Diethelm, D. Papurello, J. Van herle, M. Lualdi, J. Gutzon Larsen, M. Santarelli, Solid oxide fuel cell anode degradation by the effect of siloxanes, Journal of Power Sources, 279 (2015) 460-471.

[117] K. Haga, S. Adachi, Y. Shiratori, K. Itoh, K. Sasaki, Poisoning of SOFC anodes by various fuel impurities, Solid State Ionics, 179 (2008) 1427-1431.

[118] N. de Arespacochaga, C. Valderrama, C. Mesa, L. Bouchy, J.L. Cortina, Biogas deep clean-up based on adsorption technologies for Solid Oxide Fuel Cell applications, Chemical Engineering Journal, 255 (2014) 593-603.

[119] S. Rasi, J. Läntelä, J. Rintala, Trace compounds affecting biogas energy utilisation – A review, Energy Conversion and Management, 52 (2011) 3369-3375.

[120] D.J. Randall, T.K.N. Tsui, Ammonia toxicity in fish, Marine Pollution Bulletin, 45 (2002) 17-23.

[121] H.B. Nielsen, I. Angelidaki, Strategies for optimizing recovery of the biogas process following ammonia inhibition, Bioresource Technology, 99 (2008) 7995-8001.

[122] M. Walker, K. Iyer, S. Heaven, C.J. Banks, Ammonia removal in anaerobic digestion by biogas stripping: An evaluation of process alternatives using a first order rate model based on experimental findings, Chemical Engineering Journal, 178 (2011) 138-145.

[123] F. Abouelenien, W. Fujiwara, Y. Namba, M. Kosseva, N. Nishio, Y. Nakashimada, Improved methane fermentation of chicken manure via ammonia removal by biogas recycle, Bioresource Technology, 101 (2010) 6368-6373.

[124] X. Lei, N. Sugiura, C. Feng, T. Maekawa, Pretreatment of anaerobic digestion effluent with ammonia stripping and biogas purification, Journal of Hazardous Materials, 145 (2007) 391-397.

[125] B. Molinuevo, M.C. García, D. Karakashev, I. Angelidaki, Anammox for ammonia removal from pig manure effluents: Effect of organic matter content on process performance, Bioresource Technology, 100 (2009) 2171-2175.

[126] J. Wendt, C. Sternling, Effect of ammonia in gaseous fuels on nitrogen oxide emissions, Journal of the Air Pollution Control Association, 24 (1974) 1055-1058.

[127] K. Arrhenius, U. Johansson, Characterisation of contaminants in biogas before and after upgrading to vehicle gas, SGC Rapport, 246.

[128] P. Aravind, J. Ouweltjes, N. Woudstra, G. Rietveld, Impact of biomass-derived contaminants on SOFCs with Ni/Gadolinia-doped ceria anodes, Electrochemical and Solid-State Letters, 11 (2008) B24-B28.

[129] A. Klerke, C.H. Christensen, J.K. Nørskov, T. Vegge, Ammonia for hydrogen storage: challenges and opportunities, Journal of Materials Chemistry, 18 (2008) 2304-2310.

[130] R. Lan, S. Tao, Ammonia as a suitable fuel for fuel cells, Frontiers in Energy Research, 2 (2014).

[131] A. Afif, N. Radenahmad, Q. Cheok, S. Shams, J.H. Kim, A.K. Azad, Ammonia-fed fuel cells: a comprehensive review, Renewable and Sustainable Energy Reviews, 60 (2016) 822-835.

[132] J. Staniforth, R.M. Ormerod, Running solid oxide fuel cells on biogas, Ionics, 9 (2003) 336-341.

[133] T. Papadam, G. Goula, I.V. Yentekakis, Long-term operation stability tests of intermediate and high temperature Ni-based anodes' SOFCs directly fueled with simulated biogas mixtures, International Journal of Hydrogen Energy, 37 (2012) 16680-16685.

[134] A. Fuerte, R.X. Valenzuela, M.J. Escudero, L. Daza, Ammonia as efficient fuel for SOFC, Journal of Power Sources, 192 (2009) 170-174.

[135] K. Sasaki, S. Adachi, K. Haga, M. Uchikawa, J. Yamamoto, A. Iyoshi, J.-T. Chou, Y. Shiratori, K. Itoh, Fuel impurity tolerance of solid oxide fuel cells, ECS Transactions, 7 (2007) 1675-1683.

[136] V. Lazarova, K.-H. Choo, P. Cornel, Water-energy interactions in water reuse, IWA Publishing, 2012.

[137] F. Ishak, I. Dincer, C. Zamfirescu, Energy and exergy analyses of direct ammonia solid oxide fuel cell integrated with gas turbine power cycle, Journal of Power Sources, 212 (2012) 73-85.

[138] M.B. Beck, A. Speers, 2nd IWA Leading-Edge on Sustainability in Water-Limited Environments, Water Intelligence Online, 4 (2005) 9781780402871.

[139] M. Maurer, P. Schwegler, T. Larsen, Nutrients in urine: energetic aspects of removal and recovery, Water Science and Technology, 48 (2003) 37-46.

[140] K.D. Panopoulos, L.E. Fryda, J. Karl, S. Poulou, E. Kakaras, High temperature solid oxide fuel cell integrated with novel allothermal biomass gasification, Journal of Power Sources, 159 (2006) 570-585.

[141] A. Kelaidopoulou, A. Siddle, A. Dicks, A. Kaiser, J. Irvine, Methane Electro-Oxidation on a Y0. 20Ti0. 18Zr0. 62O1. 90 Anode in a High Temperature Solid Oxide Fuel Cell, Fuel cells, 1 (2001) 219-225.

[142] J.-M. Klein, Y. Bultel, S. Georges, M. Pons, Modeling of a SOFC fuelled by methane: from direct internal reforming to gradual internal reforming, Chemical Engineering Science, 62 (2007) 1636-1649.

[143] P. Ferreira-Aparicio, M. Benito, J. Sanz, New trends in reforming technologies: from hydrogen industrial plants to multifuel microreformers, Catalysis Reviews, 47 (2005) 491-588.

[144] J. Xuan, M.K.H. Leung, D.Y.C. Leung, M. Ni, A review of biomass-derived fuel processors for fuel cell systems, Renewable & Sustainable Energy Reviews, 13 (2009) 1301-1313.

[145] C.M. Finnerty, R.M. Ormerod, Internal reforming over nickel/zirconia anodes in SOFCS oparating on methane: influence of anode formulation, pre-treatment and operating conditions, Journal of Power Sources, 86 (2000) 390-394.

[146] J.-M. Lavoie, Review on dry reforming of methane, a potentially more environmentally-friendly approach to the increasing natural gas exploitation, Frontiers in chemistry, 2 (2014).

[147] Y. Shiratori, T. Ijichi, T. Oshima, K. Sasaki, Internal reforming SOFC running on biogas, International Journal of Hydrogen Energy, 35 (2010) 7905-7912.

[148] A. Dominguez, Y. Fernandez, B. Fidalgo, J.J. Pis, J.A. Menendez, Biogas to syngas by microwave-assisted dry reforming in the presence of char, Energy & Fuels, 21 (2007) 2066-2071.

[149] S.-K. Ryi, S.-W. Lee, J.-W. Park, D.-K. Oh, J.-S. Park, S.S. Kim, Combined steam and CO2 reforming of methane using catalytic nickel membrane for gas to liquid (GTL) process, Catalysis Today, 236, Part A (2014) 49-56.

[150] Y. Takahashi, Y. Shiratori, S. Furuta, K. Sasaki, Thermo-mechanical reliability and catalytic activity of Ni–Zirconia anode supports in internal reforming SOFC running on biogas, Solid State Ionics, 225 (2012) 113-117.

[151] J. Gao, Z. Hou, H. Lou, X. Zheng, Chapter 7 - Dry (CO2) Reforming, in: D. Shekhawat, J.J.S.A. Berry (eds.) Fuel Cells: Technologies for Fuel Processing, Elsevier, Amsterdam, 2011, pp. 191-221.

[152] N. Laosiripojana, S. Assabumrungrat, Catalytic dry reforming of methane over high surface area ceria, Applied Catalysis B: Environmental, 60 (2005) 107-116.

[153] W. Zhu, S. Deevi, A review on the status of anode materials for solid oxide fuel cells, Materials Science and Engineering: A, 362 (2003) 228-239.

[154] J. Xuan, M.K.H. Leung, D.Y.C. Leung, M. Ni, A review of biomass-derived fuel processors for fuel cell systems, Renewable and Sustainable Energy Reviews, 13 (2009) 1301-1313.

[155] P. Piroonlerkgul, N. Laosiripojana, A.A. Adesina, S. Assabumrungrat, Performance of biogas-fed solid oxide fuel cell systems integrated with membrane module for CO2 removal, Chemical Engineering and Processing: Process Intensification, 48 (2009) 672-682.

[156] S. Farhad, F. Hamdullahpur, Y. Yoo, Performance evaluation of different configurations of biogas-fuelled SOFC micro-CHP systems for residential applications, International Journal of Hydrogen Energy, 35 (2010) 3758-3768.

[157] A. Lanzini, P. Leone, Experimental investigation of direct internal reforming of biogas in solid oxide fuel cells, International Journal of Hydrogen Energy, 35 (2010) 2463-2476.

[158] I.V. Yentekakis, T. Papadam, G. Goula, Electricity production from wastewater treatment via a novel biogas-SOFC aided process, Solid State Ionics, 179 (2008) 1521-1525.

[159] J. Xu, W. Zhou, Z. Li, J. Wang, J. Ma, Biogas reforming for hydrogen production over a Ni–Co bimetallic catalyst: Effect of operating conditions, International Journal of Hydrogen Energy, 35 (2010) 13013-13020.

[160] M. Pillai, Y. Lin, H. Zhu, R.J. Kee, S.A. Barnett, Stability and coking of direct-methane solid oxide fuel cells: Effect of CO 2 and air additions, Journal of Power Sources, 195 (2010) 271-279.

[161] J. Staniforth, R.M. Ormerod, Implications for using biogas as a fuel source for solid oxide fuel cells: internal dry reforming in a small tubular solid oxide fuel cell, Catalysis letters, 81 (2002) 19-23.

[162] M. Santarelli, F. Quesito, V. Novaresio, C. Guerra, A. Lanzini, D. Beretta, Direct reforming of biogas on Ni-based SOFC anodes: Modelling of heterogeneous reactions and validation with experiments, Journal of Power Sources, 242 (2013) 405-414.

[163] C. Guerra, A. Lanzini, P. Leone, M. Santarelli, N.P. Brandon, Optimization of dry reforming of methane over Ni/YSZ anodes for solid oxide fuel cells, Journal of Power Sources, 245 (2014) 154-163.

[164] E.P. Murray, T. Tsai, S. Barnett, A direct-methane fuel cell with a ceria-based anode, Nature, 400 (1999) 649-651.

[165] S. Ahmed, M. Krumpelt, Hydrogen from hydrocarbon fuels for fuel cells, International Journal of Hydrogen Energy, 26 (2001) 291-301.

[166] P. Piroonlerkgul, S. Assabumrungrat, N. Laosiripojana, A.A. Adesina, Selection of appropriate fuel processor for biogas-fuelled SOFC system, Chemical Engineering Journal, 140 (2008) 341-351.

[167] J. Van herle, F. Maréchal, S. Leuenberger, D. Favrat, Energy balance model of a SOFC cogenerator operated with biogas, Journal of Power Sources, 118 (2003) 375-383.

[168] P. Leone, A. Lanzini, M. Santarelli, M. Calì, F. Sagnelli, A. Boulanger, A. Scaletta, P. Zitella, Methane-free biogas for direct feeding of solid oxide fuel cells, Journal of Power Sources, 195 (2010) 239-248.

[169] W. Wang, C. Su, Y. Wu, R. Ran, Z. Shao, Progress in solid oxide fuel cells with nickel-based anodes operating on methane and related fuels, Chemical reviews, 113 (2013) 8104-8151.

[170] S.-G. Wang, Y.-W. Li, J.-X. Lu, M.-Y. He, H. Jiao, A detailed mechanism of thermal CO 2 reforming of CH 4, Journal of Molecular Structure: THEOCHEM, 673 (2004) 181-189.

[171] N. Gokon, Y. Osawa, D. Nakazawa, T. Kodama, Kinetics of CO 2 reforming of methane by catalytically activated metallic foam absorber for solar receiver-reactors, International Journal of Hydrogen Energy, 34 (2009) 1787-1800.

[172] E.S. Hecht, G.K. Gupta, H. Zhu, A.M. Dean, R.J. Kee, L. Maier, O. Deutschmann, Methane reforming kinetics within a Ni–YSZ SOFC anode support, Applied Catalysis A: General, 295 (2005) 40-51.

[173] G. Brus, R. Nowak, J.S. Szmyd, Y. Komatsu, S. Kimijima, An experimental and theoretical approach for the carbon deposition problem during steam reforming of model biogas, Journal of Theoretical and Applied Mechanics, 53 (2015) 273-284.

[174] M.H. Park, B.K. Choi, Y.H. Park, D.J. Moon, N.C. Park, Y.C. Kim, Kinetics for steam and CO2 reforming of methane over Ni/La/Al2O3 catalyst, Journal of nanoscience and nanotechnology, 15 (2015) 5255-5258.

[175] A.L. da Silva, N.C. Heck, Oxide incorporation into Ni-based solid oxide fuel cell anodes for enhanced sulfur tolerance during operation on hydrogen or biogas fuels: A comprehensive thermodynamic study, International Journal of Hydrogen Energy, 40 (2015) 2334-2353.

[176] K. Eguchi, K. Tanaka, T. Matsui, R. Kikuchi, Reforming activity and carbon deposition on cermet catalysts for fuel electrodes of solid oxide fuel cells, Catalysis Today, 146 (2009) 154-159.

[177] K. Ke, A. Gunji, H. Mori, S. Tsuchida, H. Takahashi, K. Ukai, Y. Mizutani, H. Sumi, M. Yokoyama, K. Waki, Effect of oxide on carbon deposition behavior of CH4 fuel on Ni/ScSZ cermet anode in high temperature SOFCs, Solid State Ionics, 177 (2006) 541-547.

[178] P.K. Cheekatamarla, C.M. Finnerty, J. Cai, Internal reforming of hydrocarbon fuels in tubular solid oxide fuel cells, International Journal of Hydrogen Energy, 33 (2008) 1853-1858.

[179] D.L. Trimm, Coke formation and minimisation during steam reforming reactions, Catalysis Today, 37 (1997) 233-238.

[180] T. Horita, K. Yamaji, T. Kato, N. Sakai, H. Yokokawa, Design of metal/oxide interfaces for the direct introduction of hydrocarbons into SOFCs, Journal of Power Sources, 131 (2004) 299-303.

[181] Z. Alipour, M. Rezaei, F. Meshkani, Effects of support modifiers on the catalytic performance of Ni/Al 2 O 3 catalyst in CO 2 reforming of methane, Fuel, 129 (2014) 197-203.

[182] P. Vernoux, E. Djurado, M. Guillodo, Catalytic and electrochemical properties of doped lanthanum chromites as new anode materials for solid oxide fuel cells, J. Am. Ceram. Soc., 84 (2001) 2289-2295.

[183] R.J. Gorte, S. Park, J.M. Vohs, C. Wang, Anodes for direct oxidation of dry hydrocarbons in a solid-oxide fuel cell, Advanced Materials, 12 (2000) 1465-1469.

[184] J.H. Edwards, A.M. Maitra, The chemistry of methane reforming with carbon dioxide and its current and potential applications, Fuel Processing Technology, 42 (1995) 269-289.

[185] J. Kuhn, O. Kesler, Carbon deposition thresholds on nickel-based solid oxide fuel cell anodes II. Steam:carbon ratio and current density, Journal of Power Sources, 277 (2015) 455-463.

[186] J. Kuhn, O. Kesler, Carbon deposition thresholds on nickel-based solid oxide fuel cell anodes I. Fuel utilization, Journal of Power Sources, 277 (2015) 443-454.

[187] K. Girona, J. Laurencin, M. Petitjean, J. Fouletier, F. Lefebvre-Joud, SOFC Running on Biogas: Identification and Experimental Validation of" Safe" Operating Conditions, ECS Transactions, 25 (2009) 1041-1050.

[188] J. Van herle, Y. Membrez, O. Bucheli, Biogas as a fuel source for SOFC co-generators, Journal of Power Sources, 127 (2004) 300-312.

[189] J. Malzbender, E. Wessel, R.W. Steinbrech, Reduction and re-oxidation of anodes for solid oxide fuel cells, Solid State Ionics, 176 (2005) 2201-2203.

[190] M. Ettler, H. Timmermann, J. Malzbender, A. Weber, N. Menzler, Durability of Ni anodes during reoxidation cycles, Journal of Power Sources, 195 (2010) 5452-5467.

[191] M. Pihlatie, A. Kaiser, M. Mogensen, Redox stability of SOFC: Thermal analysis of Ni–YSZ composites, Solid State Ionics, 180 (2009) 1100-1112.

[192] D. Waldbillig, A. Wood, D.G. Ivey, Thermal analysis of the cyclic reduction and oxidation behaviour of SOFC anodes, Solid State Ionics, 176 (2005) 847-859.

[193] V. Vedasri, J. Young, V. Birss, A possible solution to the mechanical degradation of Ni–yttria stabilized zirconia anode-supported solid oxide fuel cells due to redox cycling, Journal of Power Sources, 195 (2010) 5534-5542.

[194] A. Baldinelli, L. Barelli, G. Bidini, A. Di Michele, R. Vivani, SOFC direct fuelling with high-methane gases: Optimal strategies for fuel dilution and upgrade to avoid quick degradation, Energy Conversion and Management, 124 (2016) 492-503.

[195] A. Lanzini, P. Leone, M. Pieroni, M. Santarelli, D. Beretta, S. Ginocchio, Experimental investigations and modeling of direct internal reforming of biogases in tubular solid oxide fuel cells, Fuel cells, 11 (2011) 697-710.

[196] S. Wongchanapai, H. Iwai, M. Saito, H. Yoshida, Performance evaluation of a direct-biogas solid oxide fuel cell-micro gas turbine (SOFC-MGT) hybrid combined heat and power (CHP) system, Journal of Power Sources, 223 (2013) 9-17.

[197] Y. Membrez, O. Bucheli, Biogas as a fuel source for SOFC co-generators, Journal of Power Sources, 127 (2004) 300-312.

[198] K.J. Chae, A. Jang, S.K. Yim, I.S. Kim, The effects of digestion temperature and temperature shock on the biogas yields from the mesophilic anaerobic digestion of swine manure, Bioresource Technology, 99 (2008) 1-6.

[199] D.-W. Gao, X.-L. Huang, Y. Tao, Y. Cong, X.-l. Wang, Sewage treatment by an UAFB–EGSB biosystem with energy recovery and autotrophic nitrogen removal under different temperatures, Bioresource Technology, 181 (2015) 26-31.

[200] A. Choudhury, H. Chandra, A. Arora, Application of solid oxide fuel cell technology for power generation—A review, Renewable and Sustainable Energy Reviews, 20 (2013) 430-442.

[201] X. Zhang, S.H. Chan, G. Li, H.K. Ho, J. Li, Z. Feng, A review of integration strategies for solid oxide fuel cells, Journal of Power Sources, 195 (2010) 685-702.

[202] B. Tjaden, M. Gandiglio, A. Lanzini, M. Santarelli, M. Jarvinen, Small-scale biogas-SOFC plant: technical analysis and assessment of different fuel reforming options, Energy & Fuels, 28 (2014) 4216-4232.

[203] H.C. Patel, T. Woudstra, P.V. Aravind, Thermodynamic Analysis of Solid Oxide Fuel Cell Gas Turbine Systems Operating with Various Biofuels, Fuel Cells, 12 (2012) 1115-1128.

[204] R. Bove, S. Ubertini, Modeling solid oxide fuel cells: methods, procedures and techniques, Springer Science & Business Media, 2008.

[205] S. Kakaç, A. Pramuanjaroenkij, X.Y. Zhou, A review of numerical modeling of solid oxide fuel cells, International Journal of Hydrogen Energy, 32 (2007) 761-786.

[206] E. Vakouftsi, G. Marnellos, C. Athanasiou, F.A. Coutelieris, A detailed model for transport processes in a methane fed planar SOFC, Chemical Engineering Research and Design, 89 (2011) 224-229.

[207] L. Fan, L. van Biert, A. Thallam Thattai, A.H.M. Verkooijen, P.V. Aravind, Study of Methane Steam Reforming kinetics in operating Solid Oxide Fuel Cells: Influence of current density, International Journal of Hydrogen Energy, 40 (2015) 5150-5159.

[208] T. Nishino, J.S. Szmyd, Numerical analysis of a cell-based indirect internal reforming tubular SOFC operating with biogas, Journal of Fuel Cell Science and Technology, 7 (2010) 051004.

[209] E. Vakouftsi, G.E. Marnellos, C. Athanasiou, F. Coutelieris, CFD modeling of a biogas fuelled SOFC, Solid State Ionics, 192 (2011) 458-463.

[210] F. Elizalde-Blancas, I.B. Celik, V. Rangel-Hernandez, A. Hernandez-Guerrero, J.M. Riesco-Avila, Numerical modeling of SOFCs operating on biogas from biodigesters, International Journal of Hydrogen Energy, 38 (2013) 377-384.

[211] T. Ogura, K. Wakamatsu, Three Dimensional Temperature Distribution Analysis in Directly Internal Reforming SOFC Fuelled by Methane, ECS Transactions, 68 (2015) 3075-3081.

[212] N.Q. Minh, Solid oxide fuel cell technology—features and applications, Solid State Ionics, 174 (2004) 271-277.

[213] M. Lang, C. Auer, P. Jentsch, T. Weckesser, SOFC stacks for mobile applications, in: Materials Science Forum, Vol. 638, Trans Tech Publ, 2010, pp. 1170-1175.

[214] T. Aicher, B. Lenz, F. Gschnell, U. Groos, F. Federici, L. Caprile, L. Parodi, Fuel processors for fuel cell APU applications, Journal of Power Sources, 154 (2006) 503-508.

[215] K. Föger, R. Donelson, R. Ratnaraj, Demonstration of anode supported cell technology in kW class stack, in: Proceedings of 6th International Symposium on Solid Oxide Fuel Cells (SOFC VI), Vol. 99, The Electrochemical Society Honolulu, Hawaii, 1999, pp. 95-100.

[216] F.J. Gardner, M.J. Day, N.P. Brandon, M.N. Pashley, M. Cassidy, SOFC technology development at Rolls-Royce, Journal of Power Sources, 86 (2000) 122-129.

[217] M. Gariglio, F. De Benedictis, M. Santarelli, M. Calì, G. Orsello, Experimental activity on two tubular solid oxide fuel cell cogeneration plants in a real industrial environment, International Journal of Hydrogen Energy, 34 (2009) 4661-4668.

[218] L. Mastropasqua, S. Campanari, P. Iora, M.C. Romano, Simulation of Intermediate-Temperature SOFC for 60%+ Efficiency Distributed Generation, in: ASME 2015 13th International Conference on Fuel Cell Science, Engineering and Technology collocated with the ASME 2015 Power Conference, the ASME 2015 9th International Conference on Energy Sustainability, and the ASME 2015 Nuclear Forum, American Society of Mechanical Engineers, 2015, pp. V001T005A003-V001T005A003.

[219] life+, ENERGY SELF-SUSTAINING AND ENVIRONMENTAL FOOTPRINT REDUCTION ON WASTEWATER TREATMENT PLANTS VIA FUEL CELLS (BIOCELL), (2012).

[220] N. de Arespacochaga, C. Valderrama, C. Peregrina, C. Mesa, L. Bouchy, J. Cortina, Evaluation of a pilot-scale sewage biogas powered 2.8 kW e Solid Oxide Fuel Cell: Assessment of heat-to-power ratio and influence of oxygen content, Journal of Power Sources, 300 (2015) 325-335.

[221] SOFCOM, SOFC CCHP with POLY-FUEL: Operation and Maintenance, (2011).

[222] M. Gandiglio, A. Lanzini, M. Santarelli, P. Leone, Design and balance-of-plant of a demonstration plant with a solid oxide fuel cell fed by biogas from waste-water and exhaust carbon recycling for algae growth, Journal of Fuel Cell Science and Technology, 11 (2014) 031003.

[223] M. Santarelli, DEMOSOFC project to install first European plant to produce clean energy from waste water, Fuel Cells Bulletin, 2015 (2015) 14-15.

[224] B. Andresen, A. Norheim, J. Strand, Ø. Ulleberg, A. Vik, I. Wærnhus, BioZEG–Pilot Plant Demonstration of High Efficiency Carbon Negative Energy Production, Energy Procedia, 63 (2014) 279-285.

[225] P. Habermeyer, A. Sánchez, Optimization of the intermittent aeration in a full-scale wastewater treatment plant biological reactor for nitrogen removal, Water environment research, 77 (2005) 229-233.

[226] K. Hemmes, P. Luimes, A. Giesen, A. Hammenga, P. Aravind, H. Spanjers, Ammonium and phosphate recovery from wastewater to produce energy in a fuel cell, Water Practice and Technology, 6 (2011) wpt20110071.

[227] P. Aravind, A. Cavalli, H.C. Patel, M. Recalde, A. Saadabadi, A. Tabish, G. Botta, A.T. Tattai, A. Teodoru, Y. Hajimolana, Opportunities and Challenges in Using SOFCs in Waste to Energy Systems, ECS Transactions, 78 (2017) 209-218.

[228] TU Delft-Global Initiative Project-Biogas-SOFC energy system for rural energy supply, https://www.tudelft.nl/global/, (2018).

[229] NWO, N2kWh Project- from Pollutant to Power, http://www.stw.nl/nl/content/n2kwh-pollutant-power, (2016).

[230] S. Pipatmanomai, S. Kaewluan, T. Vitidsant, Economic assessment of biogas-to-electricity generation system with H2S removal by activated carbon in small pig farm, Applied Energy, 86 (2009) 669-674.

[231] D.D. Papadias, S. Ahmed, R. Kumar, Fuel quality issues with biogas energy – An economic analysis for a stationary fuel cell system, Energy, 44 (2012) 257-277.

[232] B. Paulsrud, K. Nedland, Operation of Municipal Wastewater Treatment Plants, (1995).

[233] V. Larsson, Energy savings with a new aeration and control system in a mid-size Swedish wastewater treatment plant, in, 2011.

[234] G.D. Zupančič, M. Roš, Aerobic and two-stage anaerobic–aerobic sludge digestion with pure oxygen and air aeration, Bioresource technology, 99 (2008) 100-109.

[235] T.A. Larsen, W. Gujer, Separate management of anthropogenic nutrient solutions (human urine), Water Science and Technology, 34 (1996) 87-94.

[236] M. Strous, J.J. Heijnen, J.G. Kuenen, M.S.M. Jetten, The sequencing batch reactor as a powerful tool for the study of slowly growing anaerobic ammonium-oxidizing microorganisms, Applied Microbiology and Biotechnology, 50 (1998) 589-596.

[237] N. Morales, M.A. Boehler, S. Buettner, C. Liebi, H. Siegrist, Recovery of N and P from urine by struvite precipitation followed by combined stripping with digester sludge liquid at full scale, Water, 5 (2013) 1262-1278.

[238] I. Martin, M. Pidou, A. Soares, S. Judd, B. Jefferson, Modelling the energy demands of aerobic and anaerobic membrane bioreactors for wastewater treatment, Environmental technology, 32 (2011) 921-932.

[239] K.H. Hansen, I. Angelidaki, B.K. Ahring, Anaerobic digestion of swine manure: inhibition by ammonia, Water research, 32 (1998) 5-12.

[240] O. Yenigün, B. Demirel, Ammonia inhibition in anaerobic digestion: a review, Process Biochemistry, 48 (2013) 901-911.

[241] A. Serna-Maza, S. Heaven, C.J. Banks, Ammonia removal in food waste anaerobic digestion using a side-stream stripping process, Bioresource Technology, 152 (2014) 307-315.

[242] L. Zhang, Y.-W. Lee, D. Jahng, Ammonia stripping for enhanced biomethanization of piggery wastewater, Journal of Hazardous Materials, 199 (2012) 36-42.

[243] S. Montalvo, L. Guerrero, R. Borja, E. Sánchez, Z. Milán, I. Cortés, M. Angeles de la la Rubia, Application of natural zeolites in anaerobic digestion processes: A review, Applied Clay Science, 58 (2012) 125-133.

[244] L. Xu, F. Dong, H. Zhuang, W. He, M. Ni, S.-P. Feng, P.-H. Lee, Energy upcycle in anaerobic treatment: Ammonium, methane, and carbon dioxide reformation through a hybrid electrodeionization–solid oxide fuel cell system, Energy Conversion and Management, 140 (2017) 157-166.

[245] L. Lin, S. Yuan, J. Chen, Z. Xu, X. Lu, Removal of ammonia nitrogen in wastewater by microwave radiation, Journal of Hazardous Materials, 161 (2009) 1063-1068.

[246] M. Mondor, L. Masse, D. Ippersiel, F. Lamarche, D. Masse, Use of electrodialysis and reverse osmosis for the recovery and concentration of ammonia from swine manure, Bioresource technology, 99 (2008) 7363-7368.

[247] V.K. Gupta, H. Sadegh, M. Yari, R. Shahryari Ghoshekandi, B. Maazinejad, M. Chahardori, Removal of ammonium ions from wastewater: A short review in development of efficient methods, Global Journal of Environmental Science and Management, 1 (2015) 149-158.

[248] X. Wang, X. Zhang, Y. Wang, Y. Du, H. Feng, T. Xu, Simultaneous recovery of ammonium and phosphorus via the integration of electrodialysis with struvite reactor, Journal of Membrane Science, 490 (2015) 65-71.

[249] A.K. Luther, J. Desloover, D.E. Fennell, K. Rabaey, Electrochemically driven extraction and recovery of ammonia from human urine, Water research, 87 (2015) 367-377.

[250] W. Verstraete, P. Van de Caveye, V. Diamantis, Maximum use of resources present in domestic “used water”, Bioresource Technology, 100 (2009) 5537-5545.

[251] A. Mulder, The quest for sustainable nitrogen removal technologies, Water Science and Technology, 48 (2003) 67-75.

[252] Y.-q. Chen, J.-j. Tang, W.-l. Li, Z.-h. Zhong, J. Yin, Thermal decomposition of magnesium ammonium phosphate and adsorption properties of its pyrolysis products toward ammonia nitrogen, Transactions of Nonferrous Metals Society of China, 25 (2015) 497-503.

[253] A. Gunay, D. Karadag, I. Tosun, M. Ozturk, Use of magnesit as a magnesium source for ammonium removal from leachate, Journal of Hazardous Materials, 156 (2008) 619-623.

[254] C.K. Chauhan, M.J. Joshi, In vitro crystallization, characterization and growth-inhibition study of urinary type struvite crystals, Journal of Crystal Growth, 362 (2013) 330-337.

[255] A. Sarkar, Hydration/dehydration characteristics of struvite and dittmarite pertaining to magnesium ammonium phosphate cement systems, Journal of materials science, 26 (1991) 2514-2518.

[256] J.D. Seader, E.J. Henley, D.K. Roper, Separation process principles, (1998).

[257] B. Metcalf Eddy, Wastewater Engineering: Treatment Disposal Reuse, 1980.

[258] M.K. Ghose, Complete physico-chemical treatment for coke plant effluents, Water Research, 36 (2002) 1127-1134.

[259] S.E. Hosseini, M.A. Wahid, Feasibility study of biogas production and utilization as a source of renewable energy in Malaysia, Renewable and Sustainable Energy Reviews, 19 (2013) 454-462.

[260] N. Scarlat, J.-F. Dallemand, F. Fahl, Biogas: Developments and perspectives in Europe, Renewable Energy, 129 (2018) 457-472.

[261] V.G. Gude, Energy and water autarky of wastewater treatment and power generation systems, Renewable & Sustainable Energy Reviews, 45 (2015) 52-68.

[262] Y. Shen, J.L. Linville, M. Urgun-Demirtas, M.M. Mintz, S.W. Snyder, An overview of biogas production and utilization at full-scale wastewater treatment plants (WWTPs) in the United States: Challenges and opportunities towards energy-neutral WWTPs, Renewable and Sustainable Energy Reviews, 50 (2015) 346-362.

[263] F. Maréchal, S. Leuenberger, Y. Membrez, O. Bucheli, D. Favrat, Process flow model of solid oxide fuel cell system supplied with sewage biogas, Journal of Power Sources, 131 (2004) 127-141.

[264] S. Farhad, Y. Yoo, F. Hamdullahpur, Effects of fuel processing methods on industrial scale biogas-fuelled solid oxide fuel cell system for operating in wastewater treatment plants, Journal of Power Sources, 195 (2010) 1446-1453.

[265] L. Barelli, A. Ottaviano, Solid oxide fuel cell technology coupled with methane dry reforming: A viable option for high efficiency plant with reduced CO2 emissions, Energy, 71 (2014) 118-129.

[266] D. Papurello, A. Lanzini, L. Tognana, S. Silvestri, M. Santarelli, Waste to energy: Exploitation of biogas from organic waste in a 500 Wel solid oxide fuel cell (SOFC) stack, Energy, 85 (2015) 145-158.

[267] R.M. Ormerod, Solid oxide fuel cells, Chemical Society Reviews, 32 (2003) 17-28.

[268] E.A. Liese, R.S. Gemmen, Performance comparison of internal reforming against external reforming in a solid oxide fuel cell, gas turbine hybrid system, J. Eng. Gas Turbines Power, 127 (2005) 86-90.

[269] V. Chiodo, A. Galvagno, A. Lanzini, D. Papurello, F. Urbani, M. Santarelli, S. Freni, Biogas reforming process investigation for SOFC application, Energy conversion and management, 98 (2015) 252-258.

[270] G. Goula, V. Kiousis, L. Nalbandian, I.V. Yentekakis, Catalytic and electrocatalytic behavior of Ni-based cermet anodes under internal dry reforming of CH4+CO2 mixtures in SOFCs, Solid State Ionics, 177 (2006) 2119-2123.

[271] I.V. Yentekakis, Open-and closed-circuit study of an intermediate temperature SOFC directly fueled with simulated biogas mixtures, Journal of Power Sources, 160 (2006) 422-425.

[272] A. Lanzini, P. Leone, C. Guerra, F. Smeacetto, N.P. Brandon, M. Santarelli, Durability of anode supported Solid Oxides Fuel Cells (SOFC) under direct dry-reforming of methane, Chemical Engineering Journal, 220 (2013) 254-263.

[273] W.S. Jablonski, S.M. Villano, A.M. Dean, A comparison of H2S, SO2, and COS poisoning on Ni/YSZ and Ni/K2O-CaAl2O4 during methane steam and dry reforming, Applied Catalysis A: General, 502 (2015) 399-409.

[274] G.B. Johnson, P. Hjalmarsson, K. Norrman, U. Ozkan, A. Hagen, Biogas Catalytic Reforming Studies on Nickel-Based Solid Oxide Fuel Cell Anodes, Fuel Cells, 16 (2016) 219-234.

[275] T. Chen, W.G. Wang, H. Miao, T. Li, C. Xu, Evaluation of carbon deposition behavior on the nickel/yttrium-stabilized zirconia anode-supported fuel cell fueled with simulated syngas, Journal of Power Sources, 196 (2011) 2461-2468.

[276] D. Mogensen, J.-D. Grunwaldt, P.V. Hendriksen, K. Dam-Johansen, J. Nielsen, Internal steam reforming in solid oxide fuel cells: Status and opportunities of kinetic studies and their impact on modelling, Journal of Power Sources, 196 (2011) 25-38.

[277] L. Fan, Z. Qu, M. Pourquie, A. Verkooijen, P. Aravind, Computational studies for the evaluation of fuel flexibility in solid oxide fuel cells: a case with biosyngas, Fuel Cells, 13 (2013) 410-427.

[278] H. Madi, S. Diethelm, N. Petigny, Effect of Steam-to-Carbon Ratio on Degradation of Ni-YSZ Anode Supported Cells, ECS Transactions, 57 (2013) 1517-1525.

[279] Y. Jiao, L. Zhang, W. An, W. Zhou, Y. Sha, Z. Shao, J. Bai, S.-D. Li, Controlled deposition and utilization of carbon on Ni-YSZ anodes of SOFCs operating on dry methane, Energy, 113 (2016) 432-443.

[280] W.Y. Lee, J. Hanna, A.F. Ghoniem, On the predictions of carbon deposition on the nickel anode of a SOFC and its impact on open-circuit conditions, Journal of The Electrochemical Society, 160 (2012) F94.

[281] X. Jacques-Bédard, T. Napporn, R. Roberge, M. Meunier, Performance and ageing of an anode-supported SOFC operated in single-chamber conditions, Journal of Power Sources, 153 (2006) 108-113.

[282] J. Laurencin, V. Roche, C. Jaboutian, I. Kieffer, J. Mougin, M. Steil, Ni-8YSZ cermet re-oxidation of anode supported solid oxide fuel cell: From kinetics measurements to mechanical damage prediction, International Journal of Hydrogen Energy, 37 (2012) 12557-12573.

[283] W. Mo, Q. Zhang, Energy–nutrients–water nexus: Integrated resource recovery in municipal wastewater treatment plants, Journal of Environmental Management, 127 (2013) 255-267.

[284] M. MosayebNezhad, A.S. Mehr, M. Gandiglio, A. Lanzini, M. Santarelli, Techno-economic assessment of biogas-fed CHP hybrid systems in a real wastewater treatment plant, Applied Thermal Engineering, 129 (2018) 1263-1280.

[285] W. Verstraete, P.V. de Caveye, V. Diamantis, Maximum use of resources present in domestic "used water", Bioresource Technology, 100 (2009) 5537-5545.

[286] B. Wett, K. Buchauer, C. Fimml, Energy self-sufficiency as a feasible concept for wastewater treatment systems, in: IWA Leading Edge Technology Conference, Singa-pore: Asian Water, 2007, pp. 21-24.

[287] S. Sengupta, T. Nawaz, J. Beaudry, Nitrogen and phosphorus recovery from wastewater, Current Pollution Reports, 1 (2015) 155-166.

[288] E. Grönlund, Sustainable wastewater treatment, (2014).

[289] R. Howarth, H.W. Paerl, Coastal marine eutrophication: Control of both nitrogen and phosphorus is necessary, Proceedings of the National Academy of Sciences, 105 (2008) E103-E103.

[290] P.D. Jenssen, L. Vråle, O. Lindholm, Sustainable wastewater treatment, in: Proceedings of International Conference on Natural Resources and Environmental Management and Environmetal Safety and Health, Kuching, Malaysia, Vol. 2729, 2007.

[291] B. Oram, Ammonia in groundwater, runoff, surface water, lakes and streams, Water Research Center, na, (2015).

[292] J. Serralta, J. Ribes, A. Seco, J. Ferrer, A supervisory control system for optimising nitrogen removal and aeration energy consumption in wastewater treatment plants, Water Science and Technology, 45 (2002) 309-316.

[293] D.J. Kinnear, M.-L. Pellegrin, T.B. Cross, M.J. Condran, T. Kochaba, C.M. Haney, Comparing membrane bioreactors and conventional activated sludge processes for low nutrient limits, Proceedings of the Water Environment Federation, 2010 (2010) 18-29.

[294] C. Zamfirescu, I. Dincer, Using ammonia as a sustainable fuel, Journal of Power Sources, 185 (2008) 459-465.

[295] R. Michalsky, A. Avram, B. Peterson, P.H. Pfromm, A. Peterson, Chemical looping of metal nitride catalysts: low-pressure ammonia synthesis for energy storage, Chemical science, 6 (2015) 3965-3974.

[296] L.F. Razon, Life cycle analysis of an alternative to the haber-bosch process: Non-renewable energy usage and global warming potential of liquid ammonia from cyanobacteria, Environmental Progress & Sustainable Energy, 33 (2014) 618-624.

[297] D. Frattini, G. Cinti, G. Bidini, U. Desideri, R. Cioffi, E. Jannelli, A system approach in energy evaluation of different renewable energies sources integration in ammonia production plants, Renewable energy, 99 (2016) 472-482.

[298] W.T. Mook, M.H. Chakrabarti, M.K. Aroua, G.M.A. Khan, B.S. Ali, M.S. Islam, M.A. Abu Hassan, Removal of total ammonia nitrogen (TAN), nitrate and total organic carbon (TOC) from aquaculture wastewater using electrochemical technology: A review, Desalination, 285 (2012) 1-13.

[299] M. Ni, M.K. Leung, D.Y. Leung, Ammonia-fed solid oxide fuel cells for power generation—A review, International Journal of Energy Research, 33 (2009) 943-959.

[300] A. Chellappa, C. Fischer, W. Thomson, Ammonia decomposition kinetics over Ni-Pt/Al 2 O 3 for PEM fuel cell applications, Applied Catalysis A: General, 227 (2002) 231-240.

[301] G.G.M. Fournier, I.W. Cumming, K. Hellgardt, High performance direct ammonia solid oxide fuel cell, Journal of Power Sources, 162 (2006) 198-206.

[302] G. Cinti, U. Desideri, D. Penchini, G. Discepoli, Experimental analysis of SOFC fuelled by ammonia, Fuel Cells, 14 (2014) 221-230.

[303] N.J.J. Dekker, G. Rietveld, Highly efficient conversion of ammonia in electricity by solid oxide fuel cells, Journal of Fuel Cell Science and Technology, 3 (2006) 499-502.

[304] R. Lan, S. Tao, Ammonia as a suitable fuel for fuel cells, Frontiers in Energy Research, 2 (2014) 35.

[305] L. Zhang, W. Yang, Direct ammonia solid oxide fuel cell based on thin proton-conducting electrolyte, Journal of Power Sources, 179 (2008) 92-95.

[306] K. Xie, Q. Ma, B. Lin, Y. Jiang, J. Gao, X. Liu, G. Meng, An ammonia fuelled SOFC with a BaCe0.9Nd0.1O3−δ thin electrolyte prepared with a suspension spray, Journal of Power Sources, 170 (2007) 38-41.

[307] G.Y. Meng, C.R. Jiang, J.J. Ma, Q.L. Ma, X.Q. Liu, Comparative study on the performance of a SDC-based SOFC fueled by ammonia and hydrogen, Journal of Power Sources, 173 (2007) 189-193.

[308] L.M. Liu, K.N. Sun, X.Y. Wu, X.K. Li, M. Zhang, N.Q. Zhang, X.L. Zhou, Improved performance of ammonia-fueled solid oxide fuel cell with SSZ thin film electrolyte and Ni-SSZ anode functional layer, International Journal of Hydrogen Energy, 37 (2012) 10857-10865.

[309] M. Ni, M.K.H. Leung, D.Y.C. Leung, Ammonia-fed solid oxide fuel cells for power generation-A review, International Journal of Energy Research, 33 (2009) 943-959.

[310] Q. Ma, R. Peng, Y. Lin, J. Gao, G. Meng, A high-performance ammonia-fueled solid oxide fuel cell, Journal of Power Sources, 161 (2006) 95-98.

[311] Q. Ma, R. Peng, L. Tian, G. Meng, Direct utilization of ammonia in intermediate-temperature solid oxide fuel cells, Electrochemistry Communications, 8 (2006) 1791-1795.

[312] S. Farhad, F. Hamdullahpur, Conceptual design of a novel ammonia-fuelled portable solid oxide fuel cell system, Journal of Power Sources, 195 (2010) 3084-3090.

[313] M. Rokni, Thermodynamic analysis of SOFC (solid oxide fuel cell)–Stirling hybrid plants using alternative fuels, Energy, 61 (2013) 87-97.

[314] E. Baniasadi, I. Dincer, Energy and exergy analyses of a combined ammonia-fed solid oxide fuel cell system for vehicular applications, International Journal of Hydrogen Energy, 36 (2011) 11128-11136.

[315] F. Leucht, W.G. Bessler, J. Kallo, K.A. Friedrich, H. Müller-Steinhagen, Fuel cell system modeling for solid oxide fuel cell/gas turbine hybrid power plants, Part I: Modeling and simulation framework, Journal of Power Sources, 196 (2011) 1205-1215.

[316] S. Chan, H. Ho, Y. Tian, Multi-level modeling of SOFC–gas turbine hybrid system, International Journal of Hydrogen Energy, 28 (2003) 889-900.

[317] N. Dekker, G. Rietveld, Highly efficient conversion of ammonia in electricity by solid oxide fuel cells, Journal of fuel cell science and technology, 3 (2006) 499-502.

[318] A.K. Jana, Advances in heat pump assisted distillation column: A review, Energy Conversion and Management, 77 (2014) 287-297.

[319] H. Li, N. Russell, V. Sharifi, J. Swithenbank, Techno-economic feasibility of absorption heat pumps using wastewater as the heating source for desalination, Desalination, 281 (2011) 118-127.

[320] D.J. Batstone, T. Hülsen, C.M. Mehta, J. Keller, Platforms for energy and nutrient recovery from domestic wastewater: A review, Chemosphere, 140 (2015) 2-11.

[321] P.L. McCarty, J. Bae, J. Kim, Domestic wastewater treatment as a net energy producer–can this be achieved?, in, ACS Publications, 2011.

[322] M. Strous, J. Heijnen, J.G. Kuenen, M. Jetten, The sequencing batch reactor as a powerful tool for the study of slowly growing anaerobic ammonium-oxidizing microorganisms, Applied microbiology and biotechnology, 50 (1998) 589-596.

[323] N. de Arespacochaga, C. Valderrama, C. Peregrina, A. Hornero, L. Bouchy, J.L. Cortina, On-site cogeneration with sewage biogas via high-temperature fuel cells: Benchmarking against other options based on industrial-scale data, Fuel Processing Technology, 138 (2015) 654-662.

[324] K. Lee, S. Kang, K.-Y. Ahn, Development of a highly efficient solid oxide fuel cell system, Applied Energy, 205 (2017) 822-833.

[325] S. Majerus, D. Lauinger, Taking advantage of the vastly underused European biogas potential: break-even conditions for a fuel cell and an engine as biogas converters, Journal of Electrochemical Energy Conversion and Storage, 15 (2018) 031006.

[326] J. Lackey, P. Champagne, B. Peppley, Use of wastewater treatment plant biogas for the operation of Solid Oxide Fuel Cells (SOFCs), Journal of Environmental Management, 203 (2017) 753-759.

[327] J. Smitshuijzen, J. Pérez, O. Duin, M.C.M.v. Loosdrecht, A simple model to describe the performance of highly-loaded aerobic COD removal reactors, Biochemical Engineering Journal, 112 (2016) 94-102.

[328] Y.-Y. Choi, S.-R. Baek, J.-I. Kim, J.-W. Choi, J. Hur, T.-U. Lee, C.-J. Park, B.J. Lee, Characteristics and biodegradability of wastewater organic matter in municipal wastewater treatment plants collecting domestic wastewater and industrial discharge, Water, 9 (2017) 409.

[329] Y. Sun, Z. Chen, G. Wu, Q. Wu, F. Zhang, Z. Niu, H.-Y. Hu, Characteristics of water quality of municipal wastewater treatment plants in China: implications for resources utilization and management, Journal of Cleaner Production, 131 (2016) 1-9.

[330] D. Martinez-Sosa, B. Helmreich, T. Netter, S. Paris, F. Bischof, H. Horn, Anaerobic submerged membrane bioreactor (AnSMBR) for municipal wastewater treatment under mesophilic and psychrophilic temperature conditions, Bioresource Technology, 102 (2011) 10377-10385.

[331] C. Bougrier, C. Albasi, J.-P. Delgenès, H. Carrère, Effect of ultrasonic, thermal and ozone pre-treatments on waste activated sludge solubilisation and anaerobic biodegradability, Chemical Engineering and Processing: Process Intensification, 45 (2006) 711-718.

[332] C. Bougrier, J.P. Delgenès, H. Carrère, Effects of thermal treatments on five different waste activated sludge samples solubilisation, physical properties and anaerobic digestion, Chemical Engineering Journal, 139 (2008) 236-244.

[333] A. Valo, H. Carrere, J.P. Delgenes, Thermal, chemical and thermo-chemical pre-treatment of waste activated sludge for anaerobic digestion, Journal of Chemical Technology & Biotechnology: International Research in Process, Environmental & Clean Technology, 79 (2004) 1197-1203.

[334] A. Lanzini, H. Madi, V. Chiodo, D. Papurello, S. Maisano, M. Santarelli, Dealing with fuel contaminants in biogas-fed solid oxide fuel cell (SOFC) and molten carbonate fuel cell (MCFC) plants: degradation of catalytic and electro-catalytic active surfaces and related gas purification methods, Progress in Energy and Combustion Science, 61 (2017) 150-188.

[335] M. Altinbaş, C. Yangin, I. Ozturk, Struvite precipitation from anaerobically treated municipal and landfill wastewaters, Water Science and Technology, 46 (2002) 271-278.

[336] J.H. Ahn, S. Kim, H. Park, B. Rahm, K. Pagilla, K. Chandran, N2O emissions from activated sludge processes, 2008− 2009: results of a national monitoring survey in the United States, Environmental Science & Technology, 44 (2010) 4505-4511.

[337] M.S.M. Jetten, S.J. Horn, M.C.M. van Loosdrecht, Towards a more sustainable municipal wastewater treatment system, Water Science and Technology, 35 (1997) 171-180.

[338] N. van Linden, G.L. Bandinu, D.A. Vermaas, H. Spanjers, J.B. van Lier, Bipolar membrane electrodialysis for energetically competitive ammonium removal and dissolved ammonia production, Journal of Cleaner Production, (2020) 120788.

[339] S.S. Gill, G.S. Chatha, A. Tsolakis, S.E. Golunski, A.P.E. York, Assessing the effects of partially decarbonising a diesel engine by co-fuelling with dissociated ammonia, International Journal of Hydrogen Energy, 37 (2012) 6074-6083.

[340] A. Van Nieuwenhuijzen, M. Havekes, B. Reitsma, P. De Jong, Wastewater treatment plant Amsterdam West: new, large, high-tech and sustainable, Water Practice and Technology, 4 (2009).

[341] S. Saadabadi, H. Patel, T. Woudstra, P. Aravind, Thermodynamic Analysis of Solid Oxide Fuel Cell Integrated System Fuelled by Ammonia from Struvite Precipitation Process, Fuel Cells, (2020).

[342] R. Van Kempen, J. Mulder, C. Uijterlinde, M. Loosdrecht, Overview: full scale experience of the SHARON® process for treatment of rejection water of digested sludge dewatering, Water science and technology, 44 (2001) 145-152.

[343] M. Türker, I. Celen, Removal of ammonia as struvite from anaerobic digester effluents and recycling of magnesium and phosphate, Bioresource technology, 98 (2007) 1529-1534.

[344] A. Lanzini, H. Madi, V. Chiodo, D. Papurello, S. Maisano, M. Santarelli, J. Van herle, Dealing with fuel contaminants in biogas-fed solid oxide fuel cell (SOFC) and molten carbonate fuel cell (MCFC) plants: Degradation of catalytic and electro-catalytic active surfaces and related gas purification methods, Progress in Energy and Combustion Science, 61 (2017) 150-188.

[345] N. Chatrattanawet, D. Saebea, S. Authayanun, A. Arpornwichanop, Y. Patcharavorachot, Performance and environmental study of a biogas-fuelled solid oxide fuel cell with different reforming approaches, Energy, 146 (2018) 131-140.

[346] L. van Biert, K. Visser, P.V. Aravind, A comparison of steam reforming concepts in solid oxide fuel cell systems, Applied Energy, 264 (2020) 114748.

[347] H. Madi, S. Diethelm, D. Constantin, Biogas-fed SOFC: Performance Investigation with Variable CH4/CO2 Composition, A11, A12.

[348] G. Fournier, I. Cumming, K. Hellgardt, High performance direct ammonia solid oxide fuel cell, Journal of Power Sources, 162 (2006) 198-206.

[349] L. Liu, K. Sun, X. Wu, X. Li, M. Zhang, N. Zhang, X. Zhou, Improved performance of ammonia-fueled solid oxide fuel cell with SSZ thin film electrolyte and Ni-SSZ anode functional layer, International Journal of Hydrogen Energy, 37 (2012) 10857-10865.

[350] G. Cinti, U. Desideri, SOFC fuelled with reformed urea, Applied energy, 154 (2015) 242-253.

[351] W. Wang, R. Ran, C. Su, Y. Guo, D. Farrusseng, Z. Shao, Ammonia-mediated suppression of coke formation in direct-methane solid oxide fuel cells with nickel-based anodes, Journal of Power Sources, 240 (2013) 232-240.

[352] Y. Haseli, Criteria for chemical equilibrium with application to methane steam reforming, International Journal of Hydrogen Energy, 44 (2019) 5766-5772.

[353] J. Aboudi, M. Vafaeezadeh, Efficient and reversible CO2 capture by amine functionalized-silica gel confined task-specific ionic liquid system, Journal of advanced research, 6 (2015) 571-577.

[354] Vewin, Drinking water fact sheet 2019, in, Den Haag, the Netherlands, 2019.

[355] D.J. Lapworth, N. Baran, M.E. Stuart, R.S. Ward, Emerging organic contaminants in groundwater: A review of sources, fate and occurrence, Environmental Pollution, 163 (2012) 287-303.

[356] A. Ahmad, P. van der Wens, K. Baken, L. de Waal, P. Bhattacharya, P. Stuyfzand, Arsenic reduction to <1 μg/L in Dutch drinking water, Environment International, 134 (2020) 105253.

[357] EurEau, Reducing the Energy Footprint of the Water Sector, in, EurEau, Brussels, 2019.

[358] S.G. Osborn, A. Vengosh, N.R. Warner, R.B. Jackson, Methane contamination of drinking water accompanying gas-well drilling and hydraulic fracturing, Proceedings of the National Academy of Sciences of the United States of America, 108 (2011) 8172-8176.

[359] T.F. Stocker, D. Qin, G.-K. Plattner, M. Tignor, S.K. Allen, J. Boschung, A. Nauels, Y. Xia, V. Bex, P.M. Midgley, Climate change 2013: The physical science basis, Contribution of working group I to the fifth assessment report of the intergovernmental panel on climate change, 1535 (2013).

[360] J.T. Kulongoski, P.B. Mcmahon, Methane emissions from groundwater pumping in the USA, npj Climate and Atmospheric Science, 2 (2019) 1-8.

[361] P. Velasco, V. Jegatheesan, M. Othman, Recovery of Dissolved Methane From Anaerobic Membrane Bioreactor Using Degassing Membrane Contactors, Frontiers in Environmental Science, 6 (2018).

[362] W. Rongwong, K. Goh, T.-H. Bae, Energy analysis and optimization of hollow fiber membrane contactors for recovery of dissolve methane from anaerobic membrane bioreactor effluent, Journal of Membrane Science, 554 (2018) 184-194.

[363] R. Mikalsen, Y.D. Wang, A.P. Roskilly, A comparison of Miller and Otto cycle natural gas engines for small scale CHP applications, Applied Energy, 86 (2009) 922-927.

[364] A.B. Stambouli, E. Traversa, Solid oxide fuel cells (SOFCs): a review of an environmentally clean and efficient source of energy, Renewable and Sustainable Energy Reviews, 6 (2002) 433-455.

[365] T.M. Gür, Comprehensive review of methane conversion in solid oxide fuel cells: Prospects for efficient electricity generation from natural gas, Progress in Energy and Combustion Science, 54 (2016) 1-64.

[366] B. Tjaden, M. Gandiglio, A. Lanzini, M. Santarelli, M. Järvinen, Small-Scale Biogas-SOFC Plant: Technical Analysis and Assessment of Different Fuel Reforming Options, Energy & Fuels, 28 (2014) 4216-4232.

[367] Y. Yi, A.D. Rao, J. Brouwer, G.S. Samuelsen, Fuel flexibility study of an integrated 25kW SOFC reformer system, Journal of Power Sources, 144 (2005) 67-76.

[368] S. Campanari, L. Mastropasqua, M. Gazzani, P. Chiesa, M.C. Romano, Predicting the ultimate potential of natural gas SOFC power cycles with CO2 capture – Part A: Methodology and reference cases, Journal of Power Sources, 324 (2016) 598-614.

[369] C. Zhou, S. Zheng, C. Chen, G. Lu, The effect of the partial pressure of H2S on the permeation of hydrogen in low carbon pipeline steel, Corrosion Science, 67 (2013) 184-192.

[370] K. Sasaki, K. Haga, T. Yoshizumi, D. Minematsu, E. Yuki, R.-R. Liu, C. Uryu, T. Oshima, S. Taniguchi, Y. Shiratori, K. Ito, Impurity Poisoning of SOFCs, ECS Transactions, 35 (2011) 2805-2814.

[371] J. Bao, G.N. Krishnan, P. Jayaweera, K.-H. Lau, A. Sanjurjo, Effect of various coal contaminants on the performance of solid oxide fuel cells: Part II. ppm and sub-ppm level testing, Journal of Power Sources, 193 (2009) 617-624.

[372] P. Cherosky, Y. Li, Hydrogen sulfide removal from biogas by bio-based iron sponge, Biosystems engineering, 114 (2013) 55-59.

[373] I. Isik-Gulsac, Investigation of impregnated activated carbon properties used in hydrogen sulfide fine removal, Brazilian Journal of Chemical Engineering, 33 (2016) 1021-1030.

[374] Y. Xiao, S. Wang, D. Wu, Q. Yuan, Catalytic oxidation of hydrogen sulfide over unmodified and impregnated activated carbon, Separation and purification technology, 59 (2008) 326-332.

[375] E. Sisani, G. Cinti, G. Discepoli, D. Penchini, U. Desideri, F. Marmottini, Adsorptive removal of H2S in biogas conditions for high temperature fuel cell systems, International Journal of Hydrogen Energy, 39 (2014) 21753-21766.

[376] Y. Jiang, A.V. Virkar, Fuel composition and diluent effect on gas transport and performance of anode-supported SOFCs, Journal of the Electrochemical Society, 150 (2003) A942-A951.

[377] J.R. Rostrup-Nielsen, Equilibria of decomposition reactions of carbon monoxide and methane over nickel catalysts, Journal of Catalysis, 27 (1972) 343-356.

[378] N. Laosiripojana, S. Assabumrungrat, Catalytic dry reforming of methane over high surface area ceria, Applied Catalysis B: Environmental, 60 (2005) 107-116.

[379] T. Takeguchi, Y. Kani, T. Yano, R. Kikuchi, K. Eguchi, K. Tsujimoto, Y. Uchida, A. Ueno, K. Omoshiki, M. Aizawa, Study on steam reforming of CH4 and C2 hydrocarbons and carbon deposition on Ni-YSZ cermets, Journal of Power Sources, 112 (2002) 588-595.

[380] R. Li, X. Liang, X. Wang, W. Zeng, J. Yang, D. Yan, J. Pu, B. Chi, J. Li, Improvement of sealing performance for Al2O3 fiber-reinforced compressive seals for intermediate temperature solid oxide fuel cell, Ceramics International, 45 (2019) 21953-21959.

[381] H. Timmermann, D. Fouquet, A. Weber, E. Ivers-Tiffée, U. Hennings, R. Reimert, Internal reforming of methane at Ni/YSZ and Ni/CGO SOFC cermet anodes, Fuel Cells, 6 (2006) 307-313.

[382] H. Wang, D.M. Wang, K.T. Chuang, A sulfur removal and disposal process through H2S adsorption and regeneration: Breakthrough behaviour investigation, Process Safety and Environmental Protection, 89 (2011) 53-60.

[383] P. Aravind, M. Liu, L. Fan, E. Promes, S. Giraldo, T. Woudstra, Biomass gasifier–SOFC systems: from electrode studies to the development of integrated systems and new applications, ECS Transactions, 57 (2013) 2893.

[384] A. Fernandes, J. Brabandt, O. Posdziech, A. Saadabadi, M. Recalde, L. Fan, E.O. Promes, M. Liu, T. Woudstra, P.V. Aravind, Design, construction, and testing of a gasifier-specific solid oxide fuel cell system, Energies, 11 (2018) 1985.

[385] A. Brunetti, F. Scura, G. Barbieri, E. Drioli, Membrane technologies for CO2 separation, Journal of Membrane Science, 359 (2010) 115-125.

List of Publications

- **Solid Oxide Fuel Cells fuelled with biogas: Potential and constraints**, **S.A. Saadabadi**, A. Thallam Thattai, L. Fan, R.E.F. Lindeboom, H. Spanjers, P.V. Aravind, , Renewable Energy, 134 (2019) 194-214.

- **Thermodynamic Analysis of Solid Oxide Fuel Cell Integrated System Fuelled by Ammonia from Struvite Precipitation Process**, **S.Ali Saadabadi,** Hrishikesh Patelb, Theo Woudstraa, P. V. Aravind, Fuel Cells 20 (2), 143-157

- **A solid oxide fuel cell fuelled by methane recovered from groundwater,** **S. Ali Saadabadi**, N. van Linden, A. Heinsbroek, P.V. Aravind, Journal of Cleaner Production 291, 125877

- **Direct internal methane reforming in biogas fuelled SOFC; the influence of operating parameters,** **S.A. Saadabadi**, Biju Illathukandy, P.V. Aravind, accepted in the Journal of Energy science & engineering (2021).

- **Design and construction of a fully integrated SOFC power system fed by bio-syngas: from modeling to real system,** A. Fernandes, J. Brabandt, O. Posdziech, **A. Saadabadi**, M. Recalde, L. Fan, E.O. Promes, M. Liu, T. Woudstra, P.V. Aravind, Energies, 11 (2018) 1-17.

- **Infiltration of commercially available, anode supported SOFC's via inkjet printing,** T. B. Mitchell-WilliamsEmail ,R. I. Tomov, **S. A. Saadabadi**, M. Krauz, P. V. Aravind, B. A. Glowacki, R. V. Kumar, J. Materials for Renewable and Sustainable Energy, (2017) 6:12

- **Opportunities and Challenges in using SOFCs in Waste to Energy Systems,** P. V. Aravinda , A. Cavallia , H. C. Patela , M. Recaldea , **A. Saadabadia** , A. N. Tabisha,b , G. Bottaa , A. T. Thattaia , A. Teodorua , S. Hajimolanaa , P. Chundrua , T. Woudstra, ECS Transactions, 78 (1) 209-218 (2017)

Acknowledgment

This is the end of my Ph.D. journey. I am so grateful that I had this opportunity to contribute to ongoing research in accelerating the penetration of renewable energy into the electricity supply. I am also profoundly thankful to meet such great people on this journey. They have always been helpful and supportive in all of my academic work and personal life. I would like to express my appreciation for some of them who helped me to accomplish this work.

I would first like to thank my promoter, **Prof. P.V. Aravind**, for giving me this opportunity to start this journey and for his valuable supervision and guidance. I enjoyed our technical discussion and really liked your approach to different aspects of problems. I also would like to express my gratitude to **Prof. B.J. Boersma** for his valuable advice. I admire you for being compassionate and caring about the people working with you. I want to thank my dissertation committee, **Prof. A.J.M. van Wijk**, **Prof. M. van der Kreuk**, **Prof. M. Santarelli**, **Prof. M. A. van den Broek**, and **Dr. Ralph Lindeboom**, for their supports and inputs to my dissertation.

Special thanks to **Theo Woudstra** for his valuable recommendations and stimulating discussions on thermodynamics. You are a nice person, and I am deeply grateful for being in contact with you during this period. I also want to thank **Maarten de Groot** for sharing the latest fuel cell/hydrogen news. I really enjoy your company. I would like to thank the P&E Lab/workshop team, **Michel**, **Jaap**, **Martijn**, **Gerard**, **Daniel**, and **Bas,** for providing the required facilities to conduct the experimental studies. I would like to acknowledge the Vitens team, **Abel**, **Jan**, **Peter**, and **Anne Bart**, for providing a pleasant atmosphere during our collaboration and support in conducting the experimental study at the Spannenburg plant. **Prof. Henri Spanjers** and **Niels,** thank you for the cooperation, all scientific discussions, and for giving me a chance to know more about wastewater treatment technologies.

My greatest gratitude goes to my colleagues, **Liyuan**, **Hrishikesh**, **Eva**, **Aditya**, **Alvaro**, **Giulia**, **Alessandro**, **Tabish**, **Mayra**, **Rashi**, **Lindert**, **Jelle**, **Vincent**, **Faruk**, **Henry**, **Biju, Ming, Vikrant**, **Ana**, and **Yashar**. After moving to the Netherlands, I was very fortunate to have you as colleagues. You made me feel at home. I enjoyed working with you, and I learned a lot from you. I could not have completed this dissertation without your help. **Shahram** and **Davood,** thank you for all the conversation during our coffee breaks and the happy moments we shared. All my **volleyball friends** (both the Rijswijk team and Ashayere Den Haag team), I cannot mention your names here, even though I spent incredible times with you guys. That helped me a lot to release my stress and gain energy again.

Hassan and **Ami**, it was not possible to reach this point without you. You are always there for me and I never felt alone although I was far away from my family. Specially, thank you for bringing **Sam** to my life who woke up my inner-child and reminded me how to say "dooda dooda" again. Sam, it is such an honour to be a part of your rescue team.

And finally, my dear family, I am so blessed to have you beside me. **Baba**, you are always my role model. You thought me to be ambitious and encouraged me to follow my dreams and try out new things in my life. **Maman** your kindness is immense and endless. You are always at my side when I needed this makes me so calm and confident. My beloved sister, **Atefeh**, I am really proved of having such a wise, supportive and cheerful person in my life. I hope to be able to spend more time with you in the future and meet you more often.

About the author

He was born on 30 Jun 1984 in Neyshabour, Iran. He obtained his bachelor's degree in Mechanical engineering at the Shahrood University of Technology in June 2008. He became an M.Sc. student in Tehran Azad University in Mechanical Engineering, Energy Conversion. He obtained his M.Sc. degree in the work entitled "*Determining the optimum tilt angle and orientation of flat-plate solar collector*" in June 2011.

He joined as a Ph.D. candidate to the Fuel cell group at the Process & Energy department of 3mE, Delft University of Technology, in September 2014. He started working on a Solid Oxide Fuel Cell (SOFC) based power systems fuelled with biogas and ammonia from the wastewater streams under the supervision of Prof. dr. ir. P.V. Aravind and Prof. dr. ir. B.J. Boersma. Experimental and system modelling studies have been carried out to determine the optimum operating conditions of SOFC systems fed with biogas-ammonia mixtures. The results have been published in the International Journal of Renewable Energy, Journal of Fuel Cells, Energy science & engineering, and Journal of Cleaner Production.